

# **Thermo-Hydro-Mechanical Behaviour of Kaolin Clay**

by

**Ali Haghghi**

Submitted for the degree of Doctor of Philosophy in

**Geotechnical Engineering**

Heriot-Watt University

School of the Built Environment

October 2011

The copyright in this thesis is owned by the author. Any quotation from the thesis or use of any of the information contained in it must acknowledge this thesis as the source of the quotation or information.

## **ABSTRACT**

The need for an improved understanding of the effects of temperature on the hydro-mechanical behaviour of compacted clays is important in many applications, such as disposal of high level nuclear wastes, burial of high voltage cables, drilling of deep offshore wells, and clay liners used on landfills. In this thesis, a study of the thermo-hydro-mechanical (THM) behaviour of kaolin clay under different conditions is presented. A series of experimental unsaturated tests was carried out, including temperature and suction controlled oedometer tests, and suction measurements to obtain the soil water retention curves at different temperatures. In order to describe the dependency of the soil water retention curves on temperature, the influences of temperature on the contact angle of menisci and the microstructure of the soil samples were studied. Moreover, Environmental Scanning Electron Microscopy was employed for studying the microstructure of the soil at certain conditions of interest. A new suction and temperature controlled oedometer cell was designed, developed and calibrated for investigating THM behaviour of kaolin clay. The oedometer was used to examine the combined effects of suction and temperature on compressibility and collapse behaviour of the soil. In this thesis, special attention was given to the filter paper methodology for suction measurements at different temperatures. The calibration curve of Whatman No. 42 filter paper was determined at 10, 25 and 50°C using the vapour equilibrium technique with sodium chloride solutions at different concentrations and the axis translation technique. Based on the experimental data, a unique calibration equation was proposed; taking into account the effect of temperature. The experimental results showed that temperature has a relevant influence on filter paper suction measurement and that misleading results can be obtained if temperature is not taken into account in the calibration equation.

Dedicated to my parents, Fereidoon and Manijeh  
and my brother, Hooman

## **ACKNOWLEDGMENTS**

This thesis is submitted in partial fulfilment of the requirements for the Ph.D. degree at Heriot-Watt University. This work has been conducted at the School of the Built Environment from October 2007 to October 2011 under supervision of Dr. Gabriela Medero and Professor Peter Woodward.

I would like to thank my first supervisor, Dr. Gabriela Medero for providing me the opportunity to work with such a scientifically interesting and challenging research project, and would like to express my sincere gratitude for her help and guidance throughout this work. Special thanks go to Professor Peter Woodward for all his continuous help and support, and his huge enthusiasm during the time we worked together. Also in this regard, I would like to thank Professor Fernando Marinho for his close collaboration and fruitful discussions. Additionally, I greatly appreciate the help from Mr. Alastair MacFarlane and all the members of the Laboratory of Soil Mechanics for providing me with any help needed.

At the end but not at the least, I am grateful to my parents. Words can not express how much I thank them for their continuous support through my graduate research. It was not easy for them seeing their son leave Iran for another country far away.

Ali Haghighi

# ACADEMIC REGISTRY

## Research Thesis Submission



Name:	Ali Haghighi		
School/PGI:	School of the Built Environment		
Version: <i>(i.e. First, Resubmission, Final)</i>	Final	Degree Sought (Award <b>and</b> Subject area)	PhD

### **Declaration**

In accordance with the appropriate regulations I hereby submit my thesis and I declare that:

- 1) the thesis embodies the results of my own work and has been composed by myself
- 2) where appropriate, I have made acknowledgement of the work of others and have made reference to work carried out in collaboration with other persons
- 3) the thesis is the correct version of the thesis for submission and is the same version as any electronic versions submitted\*.
- 4) my thesis for the award referred to, deposited in the Heriot-Watt University Library, should be made available for loan or photocopying and be available via the Institutional Repository, subject to such conditions as the Librarian may require
- 5) I understand that as a student of the University I am required to abide by the Regulations of the University and to conform to its discipline.

\* Please note that it is the responsibility of the candidate to ensure that the correct version of the thesis is submitted.

Signature of Candidate:		Date:	
-------------------------	--	-------	--

### **Submission**

Submitted By <i>(name in capitals)</i> :	Ali Haghighi
Signature of Individual Submitting:	
Date Submitted:	

### **For Completion in the Student Service Centre (SSC)**

Received in the SSC by <i>(name in capitals)</i> :			
Method of Submission <i>(Handed in to SSC; posted through internal/external mail):</i>			
E-thesis Submitted <i>(mandatory for final theses)</i>			
Signature:		Date:	

# TABLE OF CONTENTS

<b>TABLE OF CONTENTS</b>	<b>i</b>
<b>LISTS OF TABLES</b>	<b>iv</b>
<b>LISTS OF FIGURES</b>	<b>v</b>
<b>LIST OF PUBLICATIONS BY THE CANDIDATE</b>	<b>x</b>
<b>Chapter 1 INTRODUCTION</b>	<b>1</b>
1.1 Background	1
1.2 Objectives and outlines	2
<b>Chapter 2 LITERATURE REVIEW</b>	<b>5</b>
2.1 Introduction	5
2.2 Soil physics relevant to the study of unsaturated soils	5
2.2.1 The concept of soil suction	5
2.2.2 Soil water retention behaviour	11
2.2.3 Microstructural behaviour	14
2.3 Mechanical behaviour of unsaturated soils	20
2.3.1 Stress state variables	20
2.3.2 Volume change behaviour	22
2.3.3 Shear strength behaviour	26
2.3.4 Development of elasto-plastic models	29
2.3.5 Effects of temperature on mechanical behaviour	32
2.4 Experimental techniques for testing unsaturated soils	37
2.4.1 Suction measurement methods	37
(a) Filter paper method	38
(b) Tensiometer	42
(c) Thermal conductivity sensor (TCS)	43
(d) Dew point sensor	46
2.4.2 Suction control techniques	47
(a) Axis translation technique	47
(b) Osmotic technique	50
(c) Relative humidity technique	52
2.5 Chapter summary	53

<b>Chapter 3</b>	<b>EXPERIMENTAL PROGRAMME</b>	<b>56</b>
3.1	Introduction	56
3.2	Characteristics of the material	56
3.3	Experimental test programme	58
3.3.1	Filter paper calibration test using vapour equilibrium technique	58
3.3.2	Filter paper calibration test using axis translation technique	59
3.3.3	Soil water retention curves	62
3.3.4	Collapse behaviour	65
3.3.5	Temperature and suction controlled oedometer	67
	(a) Calibration of the Oedometer	69
3.3.6	Microstructural analysis	73
3.3.7	Thermal hysteresis is soil water retention curves	74
3.4	Chapter summary	76
<b>Chapter 4</b>	<b>TEMPERATURE EFFECTS ON SUCTION MEASUREMENTS USING THE FILTER PAPER TECHNIQUE</b>	<b>77</b>
4.1	Introduction	77
4.2	Filter paper calibration curves	78
4.2.1	Background	78
4.2.2	Calibration curves	82
	(a) Accuracy and performance	84
4.3	Soil water retention curves	86
4.3.1	Background	86
4.3.2	Experimental results	87
	(a) Accuracy of suction measurement	92
4.4	Shrinkage behaviour	93
4.5	Chapter summary	95
<b>Chapter 5</b>	<b>THERMAL EFFECTS ON THE COLLAPSE BEHAVIOUR OF KAOLIN CLAY</b>	<b>96</b>
5.1	Introduction	96
5.2	Sample preparation	96
5.3	Experimental results and analysis	98
5.3.1	Compressibility behaviour	101
5.3.2	Collapse behaviour	107
5.4	Chapter summary	110

<b>Chapter 6</b>	<b>TEMPERATURE AND SUCTION INFLUENCES ON OEDOMETER BEHAVIOUR OF KAOLIN CLAY</b>	<b>112</b>
6.1	Introduction	112
6.2	Sample preparation and experimental set-up	112
6.3	Experimental test results and analysis	113
6.4	Chapter summary	119
<b>Chapter 7</b>	<b>EXPERIMENTAL AND THEORETICAL STUDY OF THERMAL EFFECTS ON SOIL WATER RETENTION CURVES</b>	<b>120</b>
7.1	Introduction	120
7.2	Microstructural analysis	121
7.3	Temperature-induced changes in contact angle	125
7.4	Thermal hysteresis in soil water retention curves	128
7.5	Chapter summary	131
<b>Chapter 8</b>	<b>CONCLUSIONS AND RECOMMENDATIONS</b>	<b>133</b>
8.1	Conclusions	133
8.2	Recommendations for future work	136
<b>Chapter 9</b>	<b>REFERENCES</b>	<b>137</b>



## LISTS OF TABLES

<b>Table 2.1</b> Comparison of different techniques for control of suction.	54
<b>Table 2.2</b> Comparison of different suction measurement techniques.	55
<b>Table 3.1</b> Physical properties of kaolin clay used in this study.	56
<b>Table 3.2</b> Mineralogy of the studied kaolin clay.	58
<b>Table 3.3</b> Initial condition of the soil specimens.	62
<b>Table 3.4</b> List of tests performed in this thesis.	76
<b>Table 5.1</b> List of tests in temperature controlled oedometer apparatus ( $e_0 = 1.5$ ).	97
<b>Table 5.2</b> List of tests in temperature controlled oedometer apparatus ( $e_0 = 2$ ).	97
<b>Table 5.3</b> Maximum collapse potential of samples at different temperatures.	109
<b>Table 6.1</b> Initial condition of soil samples.	112
<b>Table 6.2</b> Initial and final condition of soil samples.	113
<b>Table 6.3</b> Comparison of reduction in void ratio when imposing suction/wetting the samples.	115
<b>Table 6.4</b> Compressibility parameters obtained for different tests.	118
<b>Table 7.1</b> Comparison of height of water in a capillary tube at different temperatures.	127

## LISTS OF FIGURES

<b>Figure 2.1</b> Surface tension (a) intermolecular forces acting in a liquid (b) capillary phenomenon (c) pressures and surface tension acting on a two-dimensional surface (Fredlund and Rahardjo, 1993).	7
<b>Figure 2.2</b> (a) Water in an unsaturated soil, subjected to capillary and adsorption (after Hillel, 1998) (b) Diffuse Double Layer.	8
<b>Figure 2.3</b> Influence of external stress and suction on interparticle forces (Wheeler and Karube, 1995).	9
<b>Figure 2.4</b> SWRC showing the regions of desaturation (after McQueen and Miller, 1974).	11
<b>Figure 2.5</b> Hysteresis of soil water retention curve (after Wheeler et al., 2003).	12
<b>Figure 2.6</b> SWRC at different temperatures for MX80 bentonite (Tang and Cui, 2005).	14
<b>Figure 2.7</b> SWRC at different temperatures for FEBEX bentonite (Villar and Lloret, 2004).	14
<b>Figure 2.8</b> Pore size distribution at two different temperatures (Romero and Li, 2005).	16
<b>Figure 2.9</b> Intra-aggregate and inter-aggregate pores (Lamande et al., 2003).	17
<b>Figure 2.10</b> SEM micrographs of Jossigny silt compacted (a) on the dry side of optimum (b) the wet side of optimum (Cui, 1993).	18
<b>Figure 2.11</b> PSD of a compacted bentonite to different dry densities (Lloret et al., 2003).	19
<b>Figure 2.12</b> Different criteria for to distinguish the intra-aggregate pores from inter-aggregate pores (a) from water retention curves at different void ratios, (b) from PSD of as-compacted samples, (3) from separation between constricted and non-constricted porosity (Romero et al., 2011).	20
<b>Figure 2.13</b> Wetting induced swelling and collapse in kaolin, under a mean net stress of 40 kPa (Sivakumar, 1993).	23
<b>Figure 2.14</b> (a) Volume change under suction-controlled isotropic loading, (b) Stress-strain curves at different suctions (Cui and Delage, 1999).	24
<b>Figure 2.15</b> (a) Volume change during the suction-controlled triaxial compression tests, (b) Yield points in suction-controlled isotropic compression tests (Rampino et al., 1999).	24
<b>Figure 2.16</b> Variation of void ratio with applied suction (Yong et al., 1971).	25
<b>Figure 2.17</b> Schematic representation of different stages of shrinkage.	26
<b>Figure 2.18</b> Failure envelope for unsaturated soils (Fredlund et al., 1978).	27
<b>Figure 2.19</b> Influence of suction on shear strength.	28
<b>Figure 2.20</b> Critical state lines for kaolin at different suctions (Wheeler and Sivakumar, 1995).	29

<b>Figure 2.21</b> Yield surface in q-p-s space (after Alonso et al., 1990).	30
<b>Figure 2.22</b> Loading Collapse yield curve (after Alonso et al., 1990).	31
<b>Figure 2.23</b> Temperature effects on the preconsolidation pressure (Sultan et al., 2005).	34
<b>Figure 2.24</b> Thermal volumetric strain of kaolin clay during drained heating from 22 to 90°C (Cekerevac and Laloui, 2004).	34
<b>Figure 2.25</b> Effect of the dry density and the external vertical stress on the swelling and/or collapse behaviour upon wetting. Compacted boom clay (Romero et al., 2003): (a) Collapse of loose soil ( $\gamma_d=13.7 \text{ kN/m}^3$ ); (b) Swelling of dense soil ( $\gamma_d=16.7 \text{ kN/m}^3$ ).	35
<b>Figure 2.26</b> Effect of temperature on the maximum deviatoric stress observed upon triaxial shearing. (a) Kaolin clay (Cekerevac, 2003); (b) MC clay (Kuntiwattanakul et al., 1995).	36
<b>Figure 2.27</b> Phase diagram for a simple substance (from Lu and Likos, 2004).	38
<b>Figure 2.28</b> Filter paper calibration curves presented for total and matric suction measurements.	39
<b>Figure 2.29</b> Total suction calibration test configuration.	40
<b>Figure 2.30</b> Wetting and drying calibration curves presented by Bulut et al. (2001).	41
<b>Figure 2.31</b> Theoretical relationship between total suction and relative humidity.	41
<b>Figure 2.32</b> Wykeham Farrance-Durham University high capacity tensiometer – Stainless steel housing dimensions: 14mm diameter and 35mm long (after Lourenco et al., 2008).	42
<b>Figure 2.33</b> Fredlund thermal conductivity sensor (after Fredlund and Wang, 1989).	44
<b>Figure 2.34</b> Hysteresis curves for thermal conductivity sensors (Feng et al., 2002).	45
<b>Figure 2.35</b> Schematic of chilled mirror dew point hygrometer (after Leong et al., 2003).	47
<b>Figure 2.36</b> Schematic diagram of the axis translation device used by Fredlund (1989) for measuring matric suction (typical size of a soil sample: 50mm diameter and 20mm height).	48
<b>Figure 2.37</b> Water menisci in the pores of the ceramic HAEV ceramic disc.	50
<b>Figure 2.38</b> Schematic of the suction-controlled oedometer device using osmotic solutions (Cuisinier and Masrouri, 2005).	51
<b>Figure 2.39</b> Imposing suction in a desiccator (Tang and Cui, 2005), 1. Soil sample, 2. Desiccator, 3. Glass cup, 4. Support, 5. Salt solution.	53
<b>Figure 2.40</b> Suction measurement ranges of various methods.	54
<b>Figure 3.1</b> Particle size distribution of the studies material obtained by hydrometer test.	57
<b>Figure 3.2</b> Compaction curve of kaolin clay obtained following BS 1377 (Standard Proctor).	57

<b>Figure 3.3</b> X-ray diffraction pattern of kaolin clay.	58
<b>Figure 3.4</b> The designed pressure plate cell.	60
<b>Figure 3.5</b> The pressure plate cell dimensions.	60
<b>Figure 3.6</b> Schematic diagram of the pressure plate apparatuses.	61
<b>Figure 3.7</b> Arrangement of the soil samples and filter papers.	63
<b>Figure 3.8</b> Experimental procedure of the filter paper suction measurements (1) cutting the filter papers to the correct size (2) using tweezers for sandwiching the filter papers (3) taping two pieces of soil samples together (4) placing the arrangement of samples and filter papers in glass jars (5) sealing the glass jars (6) samples ready to be placed inside the temperature chamber.	64
<b>Figure 3.9</b> Typical results from double oedometer test.	66
<b>Figure 3.10</b> Typical results from single point oedometer test.	66
<b>Figure 3.11</b> Schematic diagram of the suction-controlled oedometer cell.	68
<b>Figure 3.12</b> The suction-controlled oedometer cell dimensions.	68
<b>Figure 3.13</b> (a) The designed suction-controlled oedometer cell (b) Details of the cell.	69
<b>Figure 3.14</b> Arrangement of static calibration for diaphragm pressure.	70
<b>Figure 3.15</b> Calibration test results of suction-controlled oedometer cell.	71
<b>Figure 3.16</b> Results of repetition of the calibration test.	72
<b>Figure 3.17</b> High resolution microscope used for recording contact angle in a capillary tube.	74
<b>Figure 4.1</b> Comparison of filter paper calibration curves (temperatures between 21 and 25°C).	79
<b>Figure 4.2</b> Comparison of equilibrium time for filter paper calibration curves using the vapour equilibrium technique (Chao, 2007).	81
<b>Figure 4.3</b> Change in RH with temperature for different solutions (Tang and Cui, 2005).	82
<b>Figure 4.4</b> Filter paper calibration curves at different temperatures.	83
<b>Figure 4.5</b> Error in total suction due to temperature gradient (Agus, 2005).	85
<b>Figure 4.6</b> Calibration data for different batches of Whatman No. 42 filter paper (Likos and Lu, 2002).	86
<b>Figure 4.7</b> Drying paths of the SWRC at different temperatures.	88
<b>Figure 4.8</b> Wetting paths of the SWRC at different temperatures.	89
<b>Figure 4.9</b> Comparison of drying paths of SWRCs at 10 and 25°C.	90

<b>Figure 4.10</b> Effect of temperature on capillary suction through change in surface tension.	91
<b>Figure 4.11</b> SWRC at 10 and 25°C with error bars.	93
<b>Figure 4.12</b> Relationship between volume change, suction and degree of saturation.	94
<b>Figure 4.13</b> Main wetting and drying curves and scanning lines.	95
<b>Figure 5.1</b> Compression curves (samples with $e_0 = 1.5$ and $w_0 = 7\%$ , obtained at 20 and 50°C).	98
<b>Figure 5.2</b> Compression curves (samples with $e_0 = 1.5$ and $w_0 = 18\%$ , obtained at 20 and 50°C).	99
<b>Figure 5.3</b> Compression curves (samples with $e_0 = 2$ and $w_0 = 7\%$ , obtained at 20 and 50°C).	99
<b>Figure 5.4</b> Compression curves (samples with $e_0 = 2$ and $w_0 = 18\%$ , obtained at 20 and 50°C).	100
<b>Figure 5.5</b> Comparison of compression curves for samples compacted at different initial water content (a) samples with initial void ratio of 1.5 (b) samples with initial void ratio of 2.	101
<b>Figure 5.6</b> As-compacted compression curves at 20 and 50°C for samples with initial void ratio of 1.5 and initial water-content of 18%.	102
<b>Figure 5.7</b> As-compacted compression curves at 20 and 50°C for samples with initial void ratio of 2 and initial water content of 18%.	103
<b>Figure 5.8</b> As-compacted compression curves at 20 and 50°C for samples with initial void ratio of 1.5 and initial water-content of 7%.	103
<b>Figure 5.9</b> As-compacted compression curves at 20 and 50°C for samples with initial void ratio of 2 and initial water content of 7%.	104
<b>Figure 5.10</b> Variation of yield stress with temperature.	104
<b>Figure 5.11</b> Influence of initial water-content on compression behaviour, As-compacted compression curves at 20°C.	105
<b>Figure 5.12</b> Influence of initial water-content on compression behaviour, As-compacted compression curves at 50°C.	106
<b>Figure 5.13</b> Influence of initial void ratio on compression behaviour at 20°C (a) Samples with initial water content of 18% (b) Samples with initial water content of 7%.	106
<b>Figure 5.14</b> Wetting-induced deformation under loading.	108
<b>Figure 6.1</b> Oedometer compression curves (at 10°C) for suctions of 100, 300, and 500 kPa.	114
<b>Figure 6.2</b> Oedometer compression curves (at 50°C) for suctions of 100, 300, and 500 kPa.	114

<b>Figure 6.3</b> Suction-controlled compression curves for suctions of 100, 300, 500 kPa (a) at 10°C (b) at 50°C.	116
<b>Figure 6.4</b> Suction-controlled compression curves at 10 and 50°C (a) for suction of 100 kPa (b) for suction of 300 kPa (c) for suction of 500 kPa.	117
<b>Figure 6.5</b> Variation of yield stress with respect to suction.	118
<b>Figure 6.6</b> Variation of yield stress with respect to temperature.	119
<b>Figure 7.1</b> PSD of kaolin clay determined from desorption path of the SWRCs at 10 and 25°C.	123
<b>Figure 7.2</b> ESEM micrograph, drying path ( $w = 17\%$ and $s = 1000$ kPa) - compacted on the wet side of optimum.	124
<b>Figure 7.3</b> ESEM micrograph, wetting path ( $w = 12\%$ and $s = 1000$ kPa) - compacted on the dry side of optimum.	124
<b>Figure 7.5</b> Analysis of pores in ESEM micrographs (a) wetting path (b) drying path.	125
<b>Figure 7.6</b> Capillary water at the air-water interface at 16, 28 and 35°C.	126
<b>Figure 7.7</b> (a) Capillary tubes showing the air-water interface at different temperatures (b) effect of temperature on angle of contact between two identical particles.	127
<b>Figure 7.8</b> Capillary water at the air-water interface at 14, 35 and 40°C.	128
<b>Figure 7.9</b> (a) Capillary pressure of a coarse sand presented by Gardner (1955), (b) Capillary pressure of a loam soil measured by Faybishenko (1983).	128
<b>Figure 7.10</b> (a) Variation of sample water-content by temperature (b) Measured suction values in a cycle of heating and cooling.	130

## LISTS OF PUBLICATIONS BY THE CANDIDATE

**Haghighi, A.**, Medero, G., Marinho, F.A.M., Mercier, B., and Woodward, P.K. 2012. Temperature effects on suction measurement using the filter paper technique. *ASTM Geotechnical Testing Journal*, **35**(1), in press.

**Haghighi, A.**, Medero, G., Marinho, F.A.M., and Woodward, P. Discussion of ‘Critical review of the methodologies employed for suction measurement’. *ASCE International Journal of Geomechanics*, in press.

**Haghighi, A.**, Medero, G., Marinho, F.A.M., and Woodward, P. 2011. Discussion of ‘Measurements of suction versus water content for bentonite-sand mixtures’. *Canadian Geotechnical Journal*, **48**(2), 336-337.

**Haghighi, A.**, Medero, G., Woodward, P., and Laloui, L. 2010. Effect of temperature on collapse potential of kaolin clay. Published and presented in the 5<sup>th</sup> International Conference on Unsaturated Soils, Barcelona, Spain, 543-548.

**Haghighi, A.**, Gatmiri, B., De Gennaro, V., and Sultan, N. 2008. Numerical analysis of PiezoCone Penetrometer Testing in partially saturated marine sediments. Published and presented in the 1<sup>st</sup> European Conference on Unsaturated Soils, Durham, UK, 841-846.

# CHAPTER 1 – INTRODUCTION

## 1.1 Background

Over the past few decades, geotechnical researchers have become very interested in the study of the thermo-hydro-mechanical (THM) behaviour of unsaturated soils. One of the main reasons for this is due to the interest in storage and disposal of high level nuclear wastes. Heavily compacted clays surrounding waste disposal are subjected to long-term elevated temperature and this can significantly affect the physical and mechanical properties of clay (Romero et al., 2003; Delage et al., 2006; Tang et al., 2008; François and Laloui, 2008). The need for an improved understanding of the effects of elevated temperature on soil behaviour is important in many other applications, such as burial of high voltage cables, drilling of deep offshore wells and foundations subjected to temperature changes. Temperature effects are also relevant in the case of compacted clay used as a hydraulic barrier in landfills in order to keep the waste confined and to minimise the escape of contaminants into the groundwater and the surrounding area (Yesiller et al., 2005; Bouazza et al., 2008). Clay liners on landfills may be subjected to a temperature of up to 70°C as a result of biological decomposition of waste containment (Rowe, 2005; Bouazza et al., 2006). To achieve this understanding it is necessary to incorporate the effect of temperature into the current knowledge of soil behaviour.

Studying the effects of temperature on the hydro-mechanical behaviour of unsaturated soils, in general, appears to be relatively complex in comparison to those of fully saturated soils. This is due to the larger number of physical phenomena involved in unsaturated soils: for instance, hydraulic hysteresis during wetting/drying cycles, thermal hysteresis during heating/cooling cycles and hydration of clay minerals. In recent years, much research has been undertaken to study the effects of temperature on the behaviour of unsaturated soils; however, there are still many uncertainties surrounding this subject. For example, the influence of temperature on suction measurement techniques, and thermal hysteresis during heating/cooling cycles are still controversial and little data are available on the thermal collapsibility of soils. Therefore, further experimental research is required for a better understanding of the influence of temperature on soil behaviour.



## **1.2 Objectives and outlines**

The general objective of this study was to investigate the effects of temperature on the hydro mechanical behaviour of kaolin clay. The choice of kaolin clay was motivated by the fact that kaolin clay has been widely investigated and much research has been conducted experimentally and numerically on this material (e.g. Al-Tabbaa and Wood, 1987; Wheeler and Sivakumar, 1995; Cekerevac and Laloui, 2004; Fleureau et al., 2004; Hird and Srisakthivel, 2005; Prashant and Penumadu, 2007; François and Laloui, 2008) thereby allowing comparison of results. Another advantage of studying kaolin clay is that its hydro-mechanical behaviour is sensitive to temperature, therefore it is easier to observe the effects of changing temperature than in some other soils. The results obtained from this study are compared with data available in the literature for isothermal cases at the same temperature, and are discussed further in this thesis. A brief review of each chapter is given as below:

### ***Chapter 2 Literature review***

A review is given in this chapter of the main features of the mechanical behaviour of unsaturated soils, the experimental techniques required for testing them, and the effects of temperature on the behaviour of soil. This chapter provides the necessary background for the subsequent chapters.

### ***Chapter 3 Experimental programme***

In this chapter, the physical characteristics of the material studied and the experimental tests performed in this research are presented. Sample preparation methods, design and calibration of apparatus, experimental techniques and procedures that were adopted in this study are presented.

### ***Chapter 4 Filter paper method***

In this chapter, the effect of temperature on filter paper calibration curves has been studied. The calibration curve for Whatman No. 42 filter paper was obtained at 10, 25 and 50°C using the vapour equilibrium technique and the axis translation technique. Using the experimental data, a calibration equation was proposed taking into account the effect of temperature. As sufficient time is given to reach equilibrium, the proposed calibration equation can be used for both matric and total suction measurements. The proposed calibration equation was used to obtain the soil water retention curves of kaolin clay at different temperatures. Changes in the rate of suction with increasing

temperature was analysed and compared with those reported in the literature. In this chapter, the shrinkage behaviour of the material is also studied.

### ***Chapter 5 Collapse behaviour***

In this chapter, the effect of temperature and initial suction on the collapse behaviour of kaolin clay has been studied. A series of single point and double oedometer tests was conducted on samples with different initial dry densities and suction values. The oedometer apparatus was modified in order to be placed in a temperature chamber. The proposed filter paper calibration curve was used to determine the initial suction of the samples at different temperatures. The influence of temperature, initial water-content and initial void ratio on the compressibility and collapse behaviour of the material are also studied.

### ***Chapter 6 Temperature and suction controlled oedometer tests***

This chapter contains a description of the design, development and calibration of a new suction controlled oedometer cell, which was used to examine the combined effects of suction and temperature on the mechanical behaviour of kaolin clay under controlled conditions. The axis translation technique was used for imposing different matric suction values in soil samples. Isothermal suction controlled oedometer tests ( $s$ : 100, 300, 500 kPa) were performed at 10 and 50°C. The effects of temperature and suction on the preconsolidation pressure, slope of the normal consolidation lines, yield surface and collapse behaviour were investigated.

### ***Chapter 7 Effects of temperature on soil water retention curves***

In this chapter, the temperature dependence of the water retention capacity of kaolin clay was determined by using the vapour equilibrium and the axis translation techniques. The experimental results revealed that the influence of temperature on the water retention capacity of the material is greater than would be predicted only from the temperature dependence of the surface tension at the air-water interface. Therefore, the influence of temperature on additional factors was studied in order to describe the dependency of matric suction on temperature. The factors investigated were temperature induced changes in contact angle and the microstructure of the sample. Furthermore, the influence of temperature changes on suction was analysed in a cycle of heating and cooling of a compacted kaolin clay sample. In this chapter, it was aimed to investigate the presence of thermal hysteresis in a cycle of heating and cooling of samples.

## ***Chapter 8 Conclusions***

This chapter summarises the conclusions drawn from various parts of the thesis. Recommendations for future investigations in this area are given.

## CHAPTER 2 – LITERATURE REVIEW

### 2.1 Introduction

In recent years, geotechnical researchers have become very interested in the study of the effects of temperature on the hydro-mechanical behaviour of unsaturated soils, but there are still many uncertainties surrounding this subject. For instance, the effects of temperature on soil strength and on suction measurement techniques are still controversial, and little data are available on the thermal collapsibility of soils. A review is given in this chapter of the main features of the hydro-mechanical behaviour of unsaturated soils, the experimental techniques required for testing them and the effects of temperature on the behaviour of soil. The necessary background for the subsequent content of the thesis is presented. This chapter commences with a brief review of the concepts of soil suction, hydraulic behaviour (water retention properties), and microstructural behaviour of unsaturated soils. An overview of the previous studies concerning the effect of temperature on the hydro-mechanical behaviour of unsaturated soils is discussed. Finally, the most relevant techniques for testing unsaturated soils are described and the advantages and limitations of each technique are discussed.

### 2.2 Soil physics relevant to the study of unsaturated soils

#### 2.2.1 The concept of soil suction

Suction is one of the most important parameters in unsaturated soils, as it has a significant influence on the mechanical behaviour of the soil. Soil suction can generally be expressed as the potential of the soil for water attraction. Total suction is commonly referred to as the energy required for removing unit volume of water from the soil matrix to a reference reservoir of pure liquid water at atmospheric pressure. Under equilibrium conditions, total suction can be related to the relative humidity of a gas phase in direct contact with the pure water by Kelvin's equation:

$$\psi = \frac{RT_s}{v} \ln\left(\frac{P}{P_0}\right) \quad (2.1)$$

where  $\psi$  refers to total suction,  $R$  is universal gas constant ( $8.314 \text{ J mol}^{-1} \text{ K}^{-1}$ ),  $T_s$  is the absolute temperature,  $v$  is the molecular volume of water vapour ( $0.01802 \text{ m}^3 \text{ mol}^{-1}$ ),  $P/P_0$  is relative humidity,  $P$  is partial pressure of pore-water vapour, and  $P_0$  is saturation

pressure of water vapour over a flat surface of deionised water at the same temperature. From the equation it can be understood that total suction changes because of a change in the relative humidity of the gas phase within an unsaturated soil, if temperature is kept constant. The total suction ( $\psi$ , Equation 2.2) consists of two components: matric suction ( $u_a - u_w$ ) and osmotic suction ( $\pi$ , Equation 2.2). The osmotic suction arises from dissolved salts within the *bulk water* which is defined as the free water (described in section 2.2.3 below), whereas the matric suction is the result of both capillary and adsorption effects.

$$\psi = (u_a - u_w) + \pi \quad (2.2)$$

The matric suction is generally defined as the difference between the external gas pressure ( $u_a$ ) acting on the water's surface and the pore water pressure ( $u_w$ ) within an element of soil. According to Fredlund and Rahardjo (1993), if no drainage of pore-water is allowed, an increase in the amount of external gas pressure surrounding a soil sample results in an increase in the pore-water pressure by the same amount, so that the matric suction in the soil remains constant. The matric suction is the result of both adsorbed and capillary forces between the pore fluid and soil matrix.

The study of capillary phenomena is directly related to the surface tension of water which is temperature dependent. The surface tension is caused by the unbalanced intermolecular forces acting on molecules at the air-water interface, which is known as the contractile skin. A water molecule within the contractile skin experiences inward molecular forces by other molecules deeper inside, which is balanced by the water resistance to compression. In order for the contractile skin to be in equilibrium condition, a tensile pull is generated along it. The tensile pull is tangential to the contractile skin surface. The contractile skin under influence of surface tension behaves like a stretched elastic curved membrane (see Figure 2.1). In unsaturated soils, pores with small radii act as capillary tubes and cause the soil water to rise above the water table. The smaller the tube radius, the greater the curvature, and the higher the capillary rise. The water pressure inside the capillary tube is less than the air pressure, which is generally atmospheric. In the capillary tube, the pressure difference between pore air and pore water pressure can be calculated by using the Young-Laplace equation:

$$u_a - u_w = \frac{2T_s \cos \beta}{r_s} \quad (2.3)$$

In this equation  $T_s$  refers to the surface tension,  $\beta$  is the contact angle between water and tube, and  $r_s$  is radius of the tube.

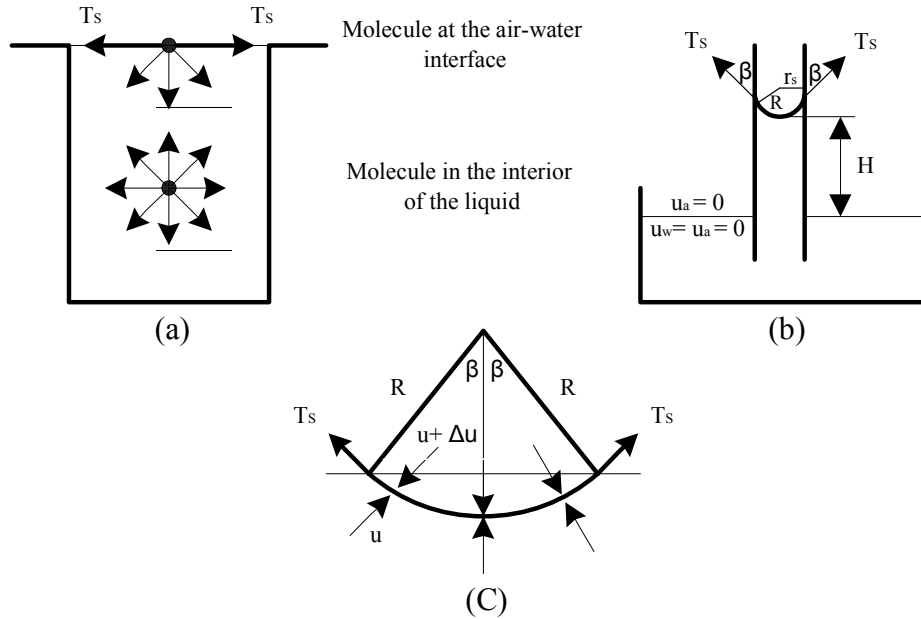


**Figure 2.1** Surface tension (a) intermolecular forces acting in a liquid (b) capillary phenomenon (c) pressures and surface tension acting on a two-dimensional surface (Fredlund and Rahardjo, 1993).

Soil particles, especially in the case of clay minerals, present a net charge imbalance more evidently along the particle surfaces. In this situation, water molecules will be strongly attracted and adsorbed onto the clay particles due to their electrical polarity. This adsorbed water forms a hydration envelope that covers the whole surface area of the particles, as shown in Figure 2.2(a). This is an important phenomenon, as the mechanical behaviour of clayey soils is significantly influenced by the degree of hydration of its clay particles. The attractive force between water molecules and the clay particles decreases with increasing thickness of the hydration, up to a point at which there is no attraction force between the water molecules and the soil particles. The positively charged cations in the soil solution and polar water molecules attracted to the clay surface form an electrical double layer or the Diffuse Double Layer (DDL). The double layer refers to two parallel layers of charge surrounding the clay particles, as shown schematically in Figure 2.2(b). According to Mitchell (1993), an increase in temperature should cause an increase in the diffuse double layer thickness and a decrease in the surface potential for a constant surface charge. However, an increase in temperature also results in a decrease in the dielectric constant of the pore-fluid. As a

result, the change in temperature does not significantly influence the thickness of the diffuse double layer. Temperature also influences the surface tension of water. It is well known that the surface tension of water decreases with increasing temperature, which results in a decrease in the matric suction of soil (Liu and Dane, 1993; Bachmann et al., 2002; Tang and Cui, 2005).

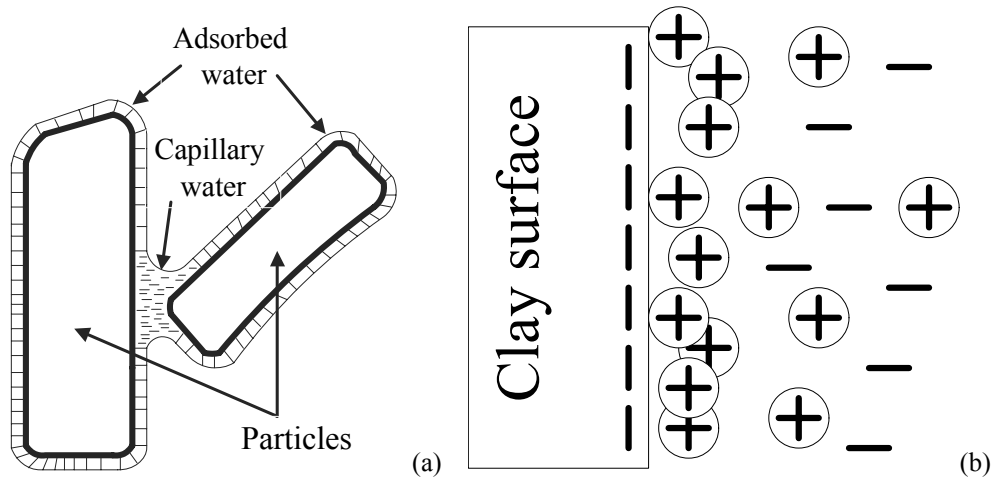


**Figure 2.2** (a) Water in an unsaturated soil, subjected to capillary and adsorption (after Hillel, 1998) (b) Diffuse Double Layer.

According to Hillel (1998), in reality capillary and adsorbed water cannot be considered separately, since the capillary and adsorbed effects are usually intermixed. The author noted that in a situation of hydraulic equilibrium, the capillary and adsorbed water will be at the same potential and thus cannot be distinguished. It was therefore concluded that the value of the measured matric suction, especially if the soil contains a significant amount of clay minerals, denotes the total effect resulting from capillary and adsorption together. As noted by Hillel (1998), for low values of matric suction (0-100 kPa), the amount of pore water retained within the soil matrix will depend primarily on capillary effects. With increasing matric suction, however, the dominant effect controlling the amount of water within the soil matrix will increasingly become adsorption, with capillarity reducing in importance.

The soil pores which are not completely filled with water present water menisci at the particle contact points. The influence of such water menisci on the overall response of the soil has been discussed by several authors (Fisher, 1926; Jennings and Burland, 1962; Burland, 1965; Wheeler and Karube, 1995), who have considered an idealised model, as shown in Figure 2.3. The presence of water menisci at interparticle contacts results in an additional interparticle force, normal to the interparticle contact. This additional normal force improves the stability of an unsaturated soil. The water menisci

can be considered to act as bonds holding the soil particles together, similar in effect to a confining stress. The soil's resistance to compression and swelling increases due to presence of this interparticle bonding. The removal of the interparticle bonds between particles by wetting the soil may result in particle slippage and collapse of the structure.

Figure 2.3 shows the idealised case of the two equal-size spherical particles with a water meniscus at their contact point and associated interparticle forces. An increase in total stress applied to the boundary of a soil will produce both normal ( $N_\sigma$ ) and tangential ( $T_\sigma$ ) forces at particle contacts. If the external stress increases until  $T_\sigma/N_\sigma$  exceed the interparticle friction coefficient, the particles will slip relative to each other. In contrast, the matric suction within the meniscus will result in only an additional normal force ( $N_s$ ) at the contact point. This additional force will improve the stability of the soil particles against slippage, and therefore compressibility of the soil decreases. As Wheeler and Karube (1995) pointed out, the influence of an increase in matric suction can be considered equivalent to an increase in the value of effective stress in a fully saturated soil, since the normal inter-particle force increases. Alternatively, the same suction increase will be like a reduction in the effective stress, because it reduces the possibility of particle slippage and yielding (a decrease of suction is required to induce collapse). The influence of water menisci on the overall stability of an unsaturated soil is important, since it prevents the use of a single effective stress variable for describing the soil response (Jennings and Burland, 1962). This is because matric suction and externally applied stresses have a qualitatively different effect on the stability of the soil structure and, therefore, it is not possible to model a soil response in a realistic manner with a single stress variable (as described in more detail in section 2.3.1).

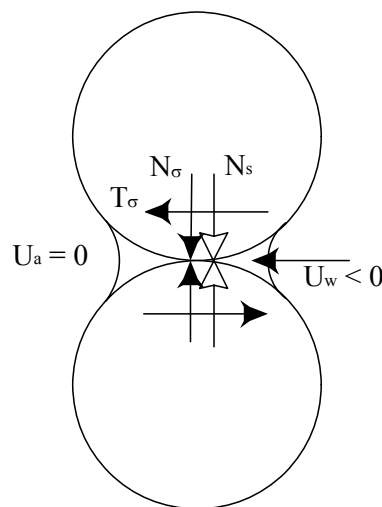


**Figure 2.3** Influence of external stress and suction on interparticle forces (Wheeler and Karube, 1995).



According to Wheeler et al. (2003), the additional normal force caused by a water meniscus increases slightly with increasing suction. It was therefore concluded by the authors that the important parameter for the overall stability of the soil skeleton is the number of interparticle contacts affected by meniscus water lenses rather than the value of matric suction. Due to increase of suction, more voids become air-filled and the number of interparticle contacts influenced by meniscus water increases.

The osmotic suction is a measure of the additional energy required for removing unit volume of water from the water phase due to the presence of dissolved salts, and is defined as the difference between the total suction and matric suction. The presence of dissolved salts contained within the soil-water results in an increase in the energy required to extract a water molecule from the water phase and, therefore, the equilibrium value of vapour pressure in the space above the air-water interface reduces. This reduction in vapour pressure is related to the type and concentration of the salt solution. The osmotic suction of soils can also be determined by measuring the electrical conductivity of soil pore-water (squeezing technique). The squeezing technique for measuring osmotic suction has been used by many authors including Krahn and Fredlund (1972), Leong et al. (2003), Peroni and Tarantino (2005) and Arifin and Schanz (2009). In this technique, a squeezer will be used to extract the macropore water, and the osmotic suction will be calculated using a calibration curve, which is an empirical relationship between electrical conductivity and osmotic pressure. A simple method for the extraction of pore water from soil samples is to apply a compressive pressure on the soil (Nitrogen gas) inside a closed chamber. A thin rubber membrane applies pressure to the sample, while preventing the air from passing through the sample and evaporating an unknown quantity of pore water. The main problem related to the squeezing technique is that the magnitude of the squeezing pressure for extracting pore water influences the results (Iyer, 1990; Fredlund and Rahardjo, 1993; Sacchi et al., 2001). Iyer (1990) found that concentrations of cations of the squeezed water at pressures less than 20 MPa remained approximately constant, which is representative of the macro-porosity and the outer double layer. At higher squeezing pressures, salt concentration decreased due to the mixing of the free pore water with water in the double layer. Iyer (1990) suggested that this threshold squeezing pressure should be established for each soil.

### 2.2.2 Soil water retention behaviour

The soil water retention curve (SWRC) for a soil is defined as the relationship between soil suction and water-content. The water-content represents the amount of water contained within the pores of the soil. The amount of water contained can also be expressed in terms of degree of saturation or volumetric water-content for describing the SWRC. According to Sillers and Fredlund (2001), the SWRC can also be defined as the water storage capacity of an unsaturated soil as it is subjected to various values of suction. McQueen and Miller (1974) provided a conceptual model based on experimental results for describing the general behaviour of SWRCs. As illustrated in Figure 2.4, it was suggested that any SWRC can consist of three different saturation stages: capillary saturation where the soil remains fully saturated, de-saturation or transition stage and residual saturation. The general description of residual saturation available in the literature is that at this condition, the liquid phase is discontinuous and isolated with thin films of water surrounding the soil particles (Vanapalli et al., 1998). It is often essential to define the residual water-content in order to predict the shear strength of unsaturated soil. The residual water-content and its corresponding value of soil suction have been defined in a number of ways in the literature. A consistent way to define the residual water-content is shown in Figure 2.4. Figure 2.4 shows a typical SWRC along a drying path. A tangent line is drawn through the point of maximum slope of the curve. The curve in the high-suction range can be approximated by another line. The residual water-content can be approximated as the ordinate of the point at which the two lines intersect.

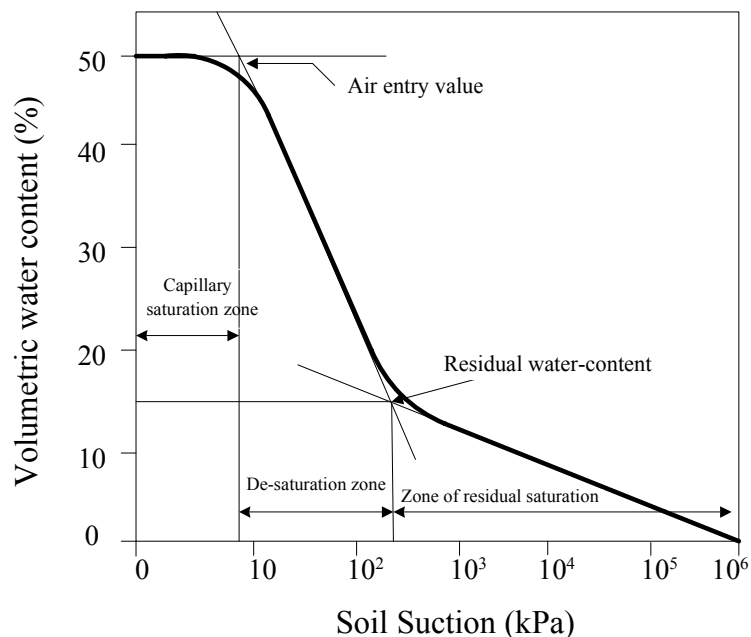


**Figure 2.4** SWRC showing the regions of desaturation (after McQueen and Miller, 1974). Many authors, including Croney and Coleman (1954), have demonstrated the hysteretic nature of the SWRC, as shown schematically in Figure 2.5. This is an important phenomenon as *hydraulic hysteresis* gives rise to different degrees of saturation depending on whether moisture is moving into or out of the soil (wetting/drying paths) at a given suction value. It is also believed that hydraulic hysteresis has an important effect on the mechanical behaviour of unsaturated soils. As noted by Wheeler and Karube (1995), soil undergoing drying generally shows different mechanical behaviour in comparison with the same value of suction during wetting. This is a result of different arrangements of water within the voids and consequently different action of matric suction on the soil skeleton. The hysteresis in the SWRCs can be related to several phenomena including: (1) the *ink-bottle* effect resulting from nonuniformity in shape and size of interconnected pores (2) different liquid-solid contact angles for advancing and reducing water menisci (3) entrapped air in newly wetted soil (4) swelling and shrinking of the soil during wetting and drying processes (Bear, 1979; Lu and Likos, 2004). From Figure 2.5 it can be seen that saturated soil can sustain a significant degree of suction applied to the boundary, which is known as the *air-entry value*, without any drop in the degree of saturation below unity. It is important to emphasise that at suction values smaller than the air-entry value, the soil remains saturated and the stress-strain behaviour of the soil should be represented in terms of the conventional effective stress for saturated soil. On the other hand, the degree of saturation can remain significantly below unity on reducing the applied suction to zero. The air-entry value of a soil is significantly influenced by its structure and is largely dependent on particle size for granular soils and on pore size for clayey soils (Georgiadis, 2003).

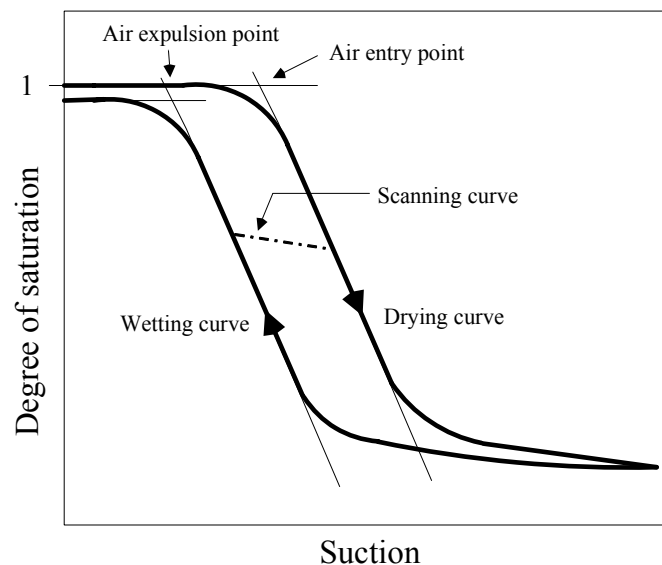


**Figure 2.5** Hysteresis of soil water retention curve (after Wheeler et al., 2003).

Several researchers (e.g. van Genuchten, 1980; Fredlund and Xing, 1994) proposed various mathematical expressions for the SWRCs. However, most of these researchers ignored the hydraulic hysteresis phenomenon and assumed that the SWRC moves along the same curve during drying and wetting. In addition, most mathematical expressions for the SWRC are only capable of representing data up to the residual water-content and tend to overestimate the water-content in the dry range (Sillers and Fredlund, 2001). Therefore, correction factors have been proposed to improve the accuracy of the SWRCs in the dry range by considering zero water-content to a suction of about 1000 MPa (Fredlund and Xing, 1994). Alternatively, other authors, including Mualem (1974, 1977, 1984), have proposed mathematical models which incorporate the influence of the hydraulic hysteresis on SWRCs.

Considerable work has been done on various aspects of the SWRC as a fundamental soil property to investigate the behaviour of unsaturated soils. It is generally known that SWRCs are dependent on temperature (Romero et al., 2001; Salager et al., 2006) and also on dry density of the soil samples; an important effect for high degrees of saturation but a lesser effect for low degrees of saturation (Gallipoli et al., 2003; Salager et al., 2007). Tang and Cui (2005) studied the effect of temperature on water retention behaviour of compacted sodium type bentonite (MX80) using the vapour equilibrium technique (see Figure 2.6). It was found that the retention capacity of the soil decreases with increasing temperature. They concluded that the reduction in water retention was only due to a reduction in the surface tension of water with increasing temperature. However, Romero et al. (2000) and Villar and Lloret (2004) showed that the reduction in water retention capacity as a result of increasing temperature is not only due to a reduction in the surface tension of the water but also due to an alteration of the clay fabric and intra-aggregate fluid chemistry (see Figure 2.7). Kawai et al. (2005) studied the effect of initial void ratio on the soil water retention behaviour of soils. The results of their investigation show that a reduction in the initial void ratio (i.e. the denser soil) gives rise to the higher air-entry value and the higher residual degree of saturation. Vanapalli et al. (1999) and Zhou and Yu (2005) drew attention to the fact that the effect of initial water-content on the soil water retention behaviour should be taken into consideration. The authors indicated that an increase in the initial water-content causes an increase in air-entry value and a steeper slope to the curve.

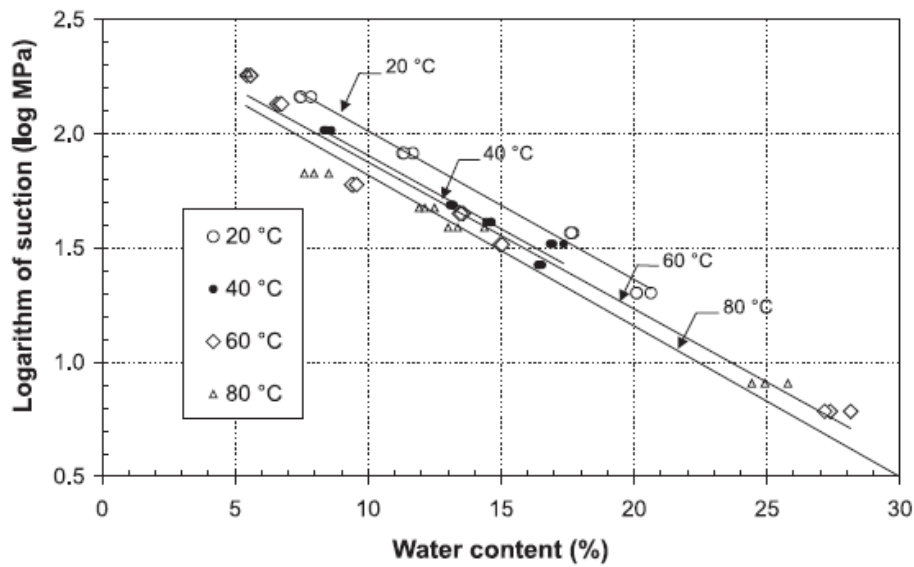


**Figure 2.6** SWRC at different temperatures for MX80 bentonite (Tang and Cui, 2005).

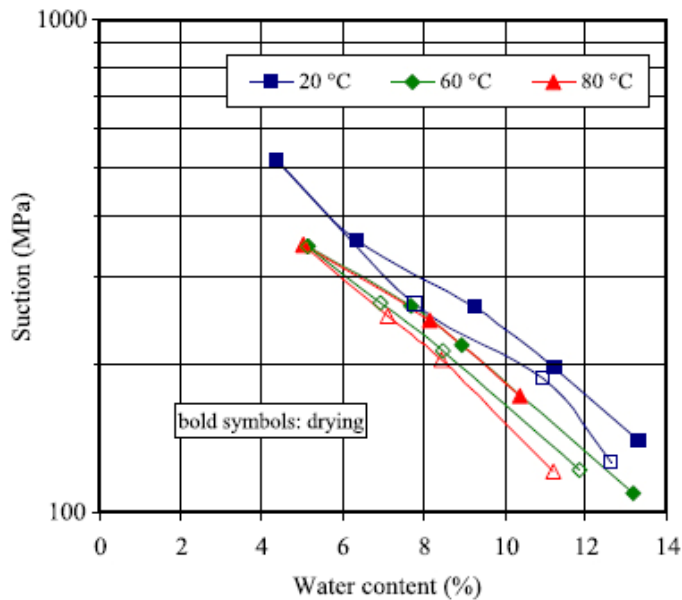


**Figure 2.7** SWRC at different temperatures for FEBEX bentonite (Villar and Lloret, 2004).

### 2.2.3 Microstructural Behaviour

Microstructural studies of soils involve using different techniques for analysing the arrangement and distribution of the particles and pore spaces both within and between the aggregates, inter-connection and connectivity of pores and soil particles (Delage and Lefebvre, 1984; Mitchell, 1993; Delage et al., 1996). The microstructure of clayey soils has an important influence on physical, mechanical and other engineering properties of the soil. The macroscopic soil properties such as strength, permeability and compressibility are often explained in terms of microstructural behaviour (Delage et al., 1996; Djeran-Maigre et al., 1998). Clay microstructure imaging has been used to

illustrate the importance of the arrangement of clay particles and distribution of pores on hydraulic conductivity, compressibility and shrink/swelling behaviour (Hetzel et al., 1994; Pusch and Schomburg, 1999).

Wheeler and Karube (1996) studied different types of pore water in unsaturated soils. They indicated that the pore-water in an unsaturated soil can be classified into three different forms: *bulk water* (or free water) contained in inter-aggregate pores, which is able to flow due to hydraulic gradients, *meniscus water* which exists at the inter-particle contacts, and *adsorbed water* which is tightly bound to the soil particles and acts as an integral part of the particles. Rao and Revanasiddappa (2005) studied the effect of microstructure on matric suction of residual soils. The results of their investigation indicate that in addition to degree of saturation, relative compaction and particle size, microstructure is also expected to influence matric suction of unsaturated soils. The authors used the filter paper method to determine the matric suction of soil samples formed by different processes. It has been observed that there is a considerable difference between matric suction of undisturbed samples from a given location and samples that were statically compacted to the same void ratio and at the same water-content. Given this evidence, it was concluded that microstructure has an important influence on the matric suction of unsaturated soils.

There are various techniques available to study unsaturated soil microstructure, among which mercury intrusion porosimetry (MIP) and environmental scanning electron microscopy (ESEM) are the most commonly used techniques. Romero and Simms (2008) have described the principle of each method with its advantages and limitations. In the MIP technique, an absolute pressure is applied to a non-wetting liquid (mercury) in order to penetrate the empty pores. Assuming the pores in the soil samples are cylindrical flow channels, Jurin's equation is used to determine the pore diameter associated with each mercury pressure increment. It is a simple and quick indirect technique, but it has limitations. The main limitations of the MIP technique are: (a) isolated pores surrounded by solid particles are not measured, (b) the pores that are accessible only through smaller ones are not detected until the smaller pores are penetrated. The MIP test can be conducted using the freeze-drying method, as described by Ahmed et al. (1974). This method involves quick freezing of a soil sample to cryogenic temperatures below  $-130^{\circ}\text{C}$ , to avoid formation of crystalline ice, by direct immersion in liquid nitrogen. Following freezing, the water in the soil sample is removed by sublimation using a vacuum at a temperature between  $-60^{\circ}\text{C}$  and  $-80^{\circ}\text{C}$ .

This process of dehydration prevents formation of water menisci between soil particles as the water is removed. Another technique to obtain pore size distribution of a soil sample is through the desorption path of the SWRCs (Prapaharan et al., 1985; Romero, 1999). In this technique the process of ejection of water from the soil pores by applying external air pressure (desorption path of the SWRC) is considered similar to injection of non-wetting liquid (mercury) to penetrate the empty pores (Mercury Intrusion Porosimetry test). More details about this technique are presented in Chapter 7. ESEM is a newer technique for qualitatively analysing the arrangement of particles and pores in unsaturated soils. The ESEM allows observation of soil sample microstructure under controlled environmental conditions. The main benefit of this technique over conventional SEM is that it allows the examination of wet samples and requires no conductive coating on the specimen.

Romero and Li (2005) studied the effect of temperature on pore size distribution of a clayey-sand mixture. The samples had the same initial water-content of 9%, and they were hydrated at two different temperatures (22°C and 80°C). Figure 2.8 shows the results they obtained. The results of their experiment reveal that the as-compacted specimen shows bimodal pore size distribution (intra-aggregate pores and inter-aggregate pores). It was observed that a decrease in intra-aggregate pores for the specimen saturated at 80°C is significantly larger than that of the specimen saturated at 22°C. A new mode of pore size also emerges in between the inter-aggregate pore and intra-aggregate pore. The peak of new mode of pore size for a specimen saturated at 80°C is significantly larger than that of a specimen saturated at 22°C.

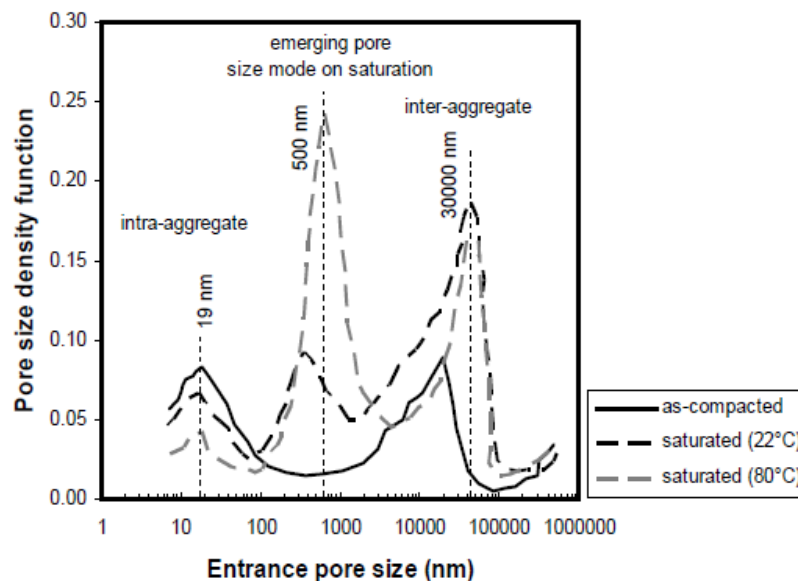


**Figure 2.8** Pore size distribution at two different temperatures (Romero and Li, 2005).

According to Hillel (1998) soil pores can be classified according to their size: micro-pores, capillary pores and macro-pores. Those pores which are smaller than a micron in width are classified as micro-pores, which typically occur in clayey soils. The water held in such narrow pores is subject to adsorptive force and may differ from the water present in wider pores. Such water is referred to as adsorbed water or bound water. Capillary pores may be several microns to a few millimetres in width. In the unsaturated state, such pores exhibit typical air-water menisci. Macro-pores may be several millimetres or even centimetres wide. In strongly aggregated soils, a distinction may be made between the relatively narrow pores within each aggregate (intra-aggregate pores) and the wider cavities between adjacent aggregates (inter-aggregate pores). Figure 2.9 shows a representation of the intra-aggregate and inter-aggregate pores.

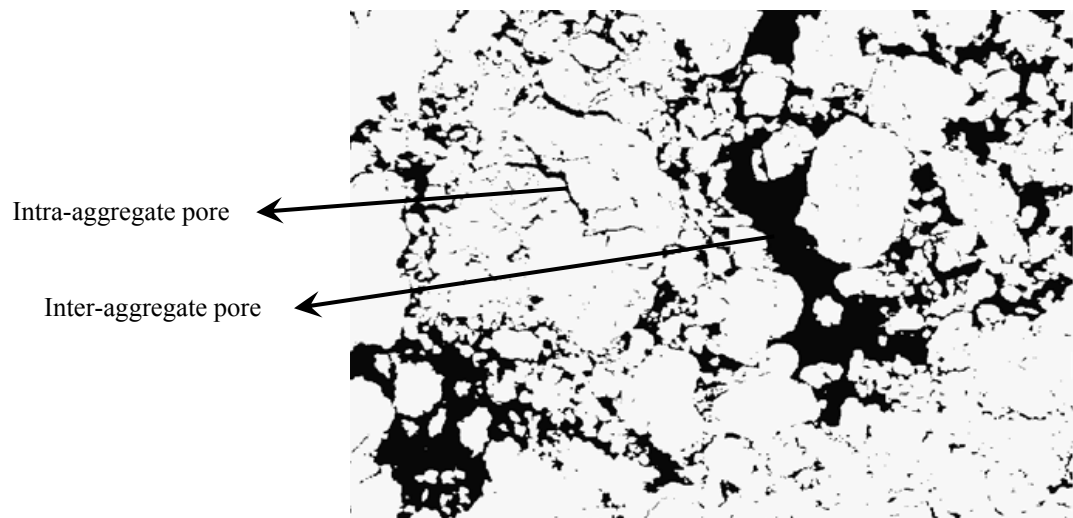


**Figure 2.9** Intra-aggregate and inter-aggregate pores (Lamande et al., 2003).

Clayey soils compacted dry of optimum generally exhibit a fabric made up of aggregates having a bimodal pore size distribution with relatively larger pores, whereas soils compacted wet of optimum tend to show a more homogenous matrix-dominated fabric with a unimodal pore size distribution (Barden and Sides, 1971; Gens and Alonso, 1992; Cui, 1993; Delage et al., 1996). The different fabric of soils compacted on the dry and wet of optimum is shown in Figure 2.10 for the Jossigny silt (Cui, 1993). These structural differences results in a difference in hydraulic characteristics, water retention and stress-strain behaviour of the samples (Seed and Chan, 1959; Elsbury et al., 1990; Wheeler and Sivakumar, 2000). Barden and Sides (1971) performed suction-controlled oedometer tests on samples of West Water clay, compacted at different initial water-contents. They obtained different SWRCs for each compaction water-content. Wheeler and Sivakumar (2000) performed suction controlled triaxial tests on samples of



compacted speswhite kaolin. They observed a significant influence of compaction water-content on the location of the critical state line in the specific volume ( $v$ ) : mean net stress ( $p$ ) plane.

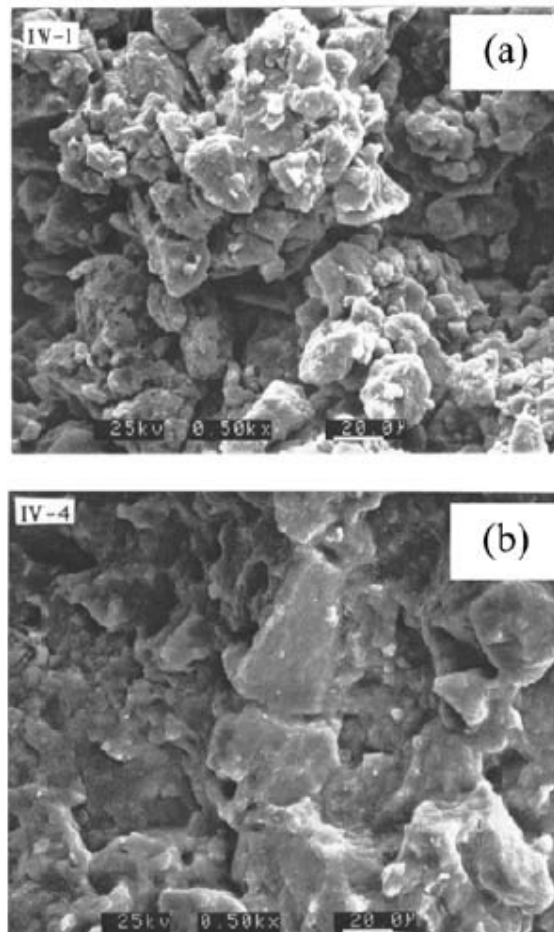


**Figure 2.10** SEM micrographs of Jossigny silt compacted (a) on the dry side of optimum (b) the wet side of optimum (Cui, 1993).

There are different techniques to define the boundary between the micro-pores and macro-pores. Lloret et al. (2003) presented the pore size distribution of a bentonite compacted to different values of dry density,  $1.5 \text{ Mg/m}^3$  and  $1.8 \text{ Mg/m}^3$ . Figure 2.11 shows the results they obtained in terms of incremental pore volume versus pore diameter. The results of their experiment clearly reveal that the compacted specimens show bimodal pore size distribution. The authors reported the boundary between the micro-pores and macro-pores to be around 130 nm, as pores smaller than this magnitude do not appear to be affected by the magnitude of the compaction load. Romero et al. (2011) summarised different criteria to distinguish the intra-aggregate pores from inter-aggregate pores; (1) the intra-aggregate porosity can be estimated from water retention curves at different void ratios (see Figure 2.12a). If the intra-aggregate porosity region

is defined as the domain in which the retention curve is not sensitive to void ratio, the corresponding size can be identified from the Young-Laplace equation; (2) the second method involves using the as-compacted PSD and separating the intra-aggregate porosity from the inter-aggregate porosity by an entrance pore size bounded by the as-compacted dominant modes (see Figure 2.12b); (3) the third method is based on a mercury intrusion/extrusion cycle. During the first intrusion, mercury fills all the accessible and interconnected pore space, thus giving the distribution of the total porosity. On complete releasing of the intrusion pressure, only some mercury will be extruded from the non-constricted pores (Delage and Lefebvre, 1984). Some mercury remains trapped in the constricted pores of the soil. The difference between the intrusion and extrusion branches describes the entrapped (constricted) porosity, which is related to the inter-aggregate pore space. The MIP data presented by Romero et al. (2011) on a compacted Boom clay shows a larger entrance pore size when using the third method in comparison to the two other methods.

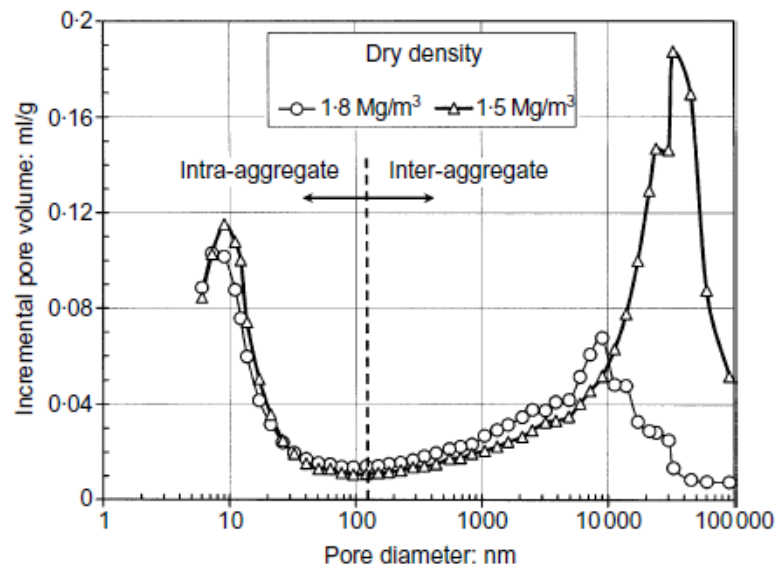


**Figure 2.11** PSD of a compacted bentonite to different dry densities (Lloret et al., 2003).

The PSD of compacted soils change as the soil subjected to drying and wetting. Simms and Yanful (2001) and Cuisinier and Laloui (2004) and investigated the change in PSD upon drying on compacted samples of glacial till and sandy loam, respectively. They observed that the drying process tends to erase the inter-aggregate porosity (capillary suction causes the larger pores to shrink) and that intra-aggregate porosity increases. Monroy et al. (2010) studied the change in PSD of compacted London clay as it is gradually wetted. It was observed that intra-aggregate porosity progressively increases until the inter-aggregate porosity is almost erased. This observation is similar to results

presented by Tarantino and De Col (2008) on PSDs of Speswhite Kaolin compacted at different water contents. Tarantino and De Col (2008) observed that inter-aggregate porosity tends to disappear as water-content increases.

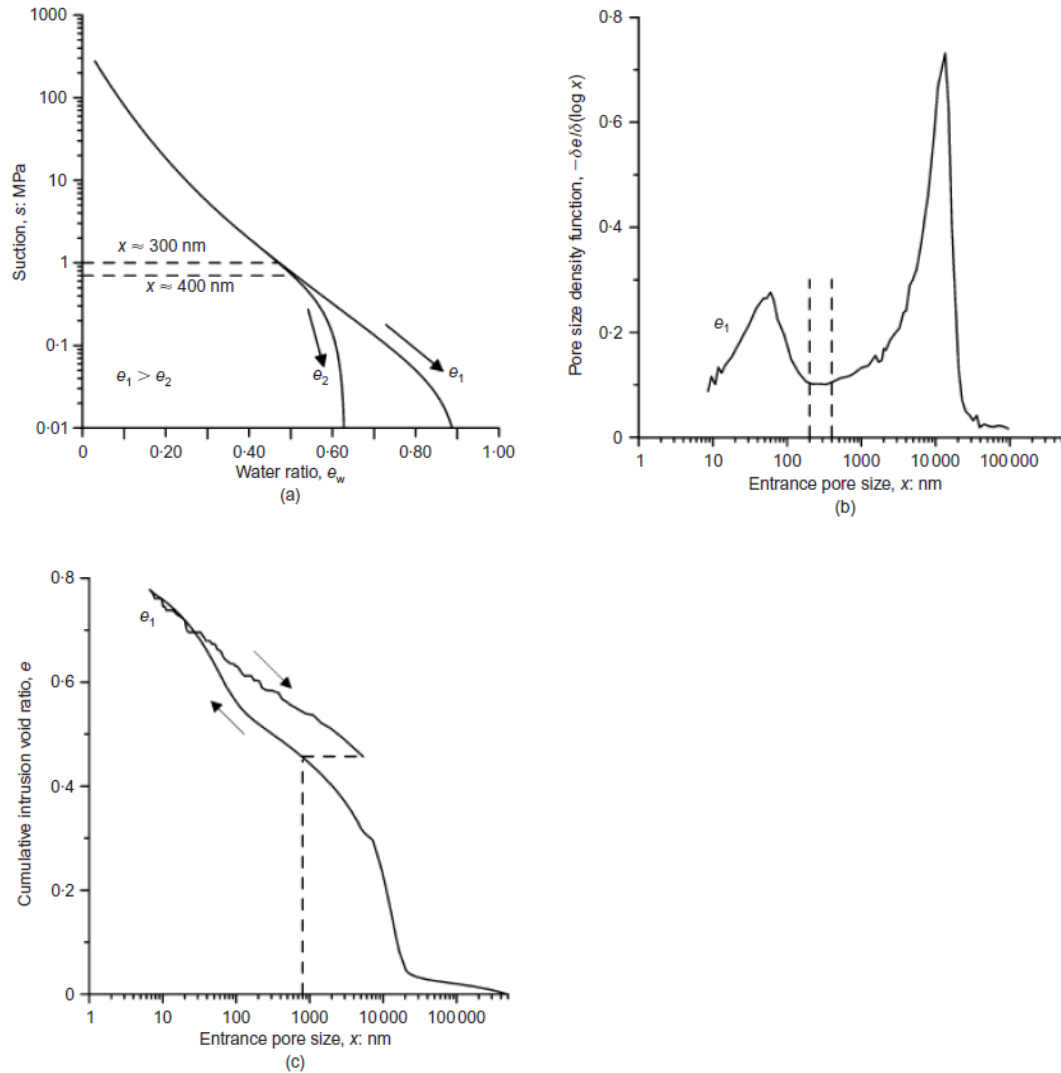


**Figure 2.12** Different criteria for to distinguish the intra-aggregate pores from inter-aggregate pores (a) from water retention curves at different void ratios, (b) from PSD of as-compacted samples, (3) from separation between constricted and non-constricted porosity (Romero et al., 2011).

## 2.3 Mechanical behaviour of unsaturated soils

### 2.3.1 Stress state variables

Classical soil mechanics has been concerned mainly with soil in which the voids between the soil particles are completely filled with water. Terzaghi (1936) introduced the concept of effective stress for saturated soils. The effective stress  $\sigma'$  is defined as the excess of the total applied stress ( $\sigma$ ) over the pore water pressure ( $u$ ), as follows:

$$\sigma' = \sigma - u \quad (2.4)$$

The success of the principle of effective stress in describing the mechanical behaviour of saturated soils led researchers to search for an equivalent single effective stress for unsaturated soils. Bishop (1959) extended the effective stress equation (Equation 2.5) for unsaturated soils to incorporate both pore air pressure ( $u_a$ ) and pore water pressure ( $u_w$ ):

$$\sigma' = (\sigma - u_a) + \chi(u_a - u_w) \quad (2.5)$$

where  $\chi$  is a parameter related the degree of saturation ( $S_r$ ), with zero corresponding to completely dry soil and unity corresponding to fully saturated soil. Terms  $\sigma - u_a$ , and  $u_a - u_w$  define the net stress and matric suction respectively. The important concept behind the single effective stress is that changes in volume and shearing strength of a soil are solely due to changes in the effective stress.

Later on, in a paper presented by Jennings and Burland in 1962, these two authors challenged the validity of Bishop's effective stress equation, considering that it cannot provide explanation for collapse on wetting. The authors showed that during inundation at constant applied stress, samples of silt reduce in volume, even when the effective stress decreases. This reduction in effective stress should, by definition of a saturated soil, induce an increase in void ratio, which is contrary to the experimental observation. Generally, collapse or plastic compression occurs along a wetting path under high values of net stress. Along the same wetting path, reversible swelling can be observed prior to plastic collapse (Escario and Saez, 1973; Wheeler and Sivakumar, 1995). Another example of difficulties in using the single effective stress approach for describing unsaturated soils behaviour is the influence of suction on the interparticle forces. As noted by Jennings and Burland (1962) and many subsequent authors (e.g. Burland, 1965; Wheeler and Karube, 1995), matric suction and externally applied stresses have a qualitatively different effect on the stability of the soil structure (see section 2.2.1) and, therefore, it is not possible to model the soil response in a realistic manner with a single stress variable.

To overcome the inability of the single effective stress approach to explain the mechanical behaviour of unsaturated soils, several researchers including Coleman (1962) and Bishop and Blight (1963) suggested that net stress and matric suction must be considered as independent stress variables with their own separate influences on

stress-strain behaviour. Further work by Fredlund and Morgenstern (1977) indicated that any two of the three independent stress variables among the following  $(\sigma - u_a)$ ,  $(\sigma - u_w)$  and  $(u_a - u_w)$  should be adopted to describe unsaturated soil behaviour. The most common independent stress state variables are net stress and matric suction. This approach was the basis for developments in constitutive modelling of unsaturated soils. Matyas and Radhakrishna (1968) performed suction-controlled compression tests and proposed state surfaces for degree of saturation and void ratio as a function of net stress and suction. The proposed state surface of void ratio presents volume reduction (collapse) on wetting at high value of net stress, and volume expansion (swelling) upon wetting at a low value of net stress. Fredlund (1979), and Lloret and Alonso (1985) suggested mathematical expressions for the state surfaces of void ratio and  $S_r$ . The limitation of elastic models base on the state surface approach is that these models are only valid for the virgin loading conditions (increase of net stress or decrease of suction). The elastic models are unable to describe loading-unloading cycles.

### **2.3.2 Volume change behaviour**

Influence of suction on the volume change behaviour of unsaturated soils has been studied by many authors. It has been found that suction has a fundamental effect on mechanical response of the soil: the yield stress increases with increasing suction; and suction has an important influence on the location and shape of the normal compression line. In order to describe the volume change behaviour of unsaturated soils, it is suitable to employ the following variables: (1) net vertical stress,  $\sigma - u_a$  (for one-dimensional tests) or mean net stress (for isotropic conditions), (2) matric suction,  $u_a - u_w$ . Net stress is the excess of total stress over gas pressure. A review of experimental tests on volume change behaviour of unsaturated soils is given below, including loading/unloading and wetting/drying tests on compacted clays.

Matyas and Radhakrishna (1968) studied the influence of suction on volume change behaviour of a mixture of 80% flint powder and 20% kaolin. They performed suction-controlled compression tests under  $K_0$  and isotropic conditions. Their results showed a lower compressibility at higher suction values. As noted by Jennings and Burland (1962) the presence of water menisci at interparticle contact points results in a normal force in their plane of contact, which improves the stability of the soil structure. Matyas and Radhakrishna (1968) also investigated the volume change behaviour of the samples by wetting them under constant applied vertical stress. They showed that wetting-induced swelling or collapse is dependent on the magnitude of the applied stress. The

authors reported that wetting the soil at a low value of net stress results in an increase of volume (swell), while a decrease in volume (collapse) occurs at high values of net stress. It was also noted that there is a critical vertical stress at which there is no tendency for either swelling or collapse. The authors stated that a reduction in suction has two effects on soil structure: a reduction in interparticle stress and a reduction in the rigidity of the soil structure. Above the critical vertical stress, the volume decrease due to a reduction in rigidity exceeds the volume increase due to a decrease in interparticle stress and therefore collapse occurs. The reverse situation results in swelling below the critical vertical stress. It has been reported by subsequent authors (e.g. Escario and Saez, 1973; El-sohby and Elleboudy, 1987; Sivakumar, 1993) that if the soil is wetted slowly, along a same wetting path swelling can be observed prior to collapse (see Figure 2.13). Matyas and Radhakrishna (1968) suggested that there is a unique state surface relating void ratio to net stress and suction. They also suggested a separate state surface relating degree of saturation to net stress and suction. The limitation of elastic models based on the state surface approach is that these models are only valid for the virgin loading conditions (increase of net stress or decrease of suction). Only virgin loading paths follow a unique normal compression line. For unloading and re-loading paths there are many possible swelling lines.

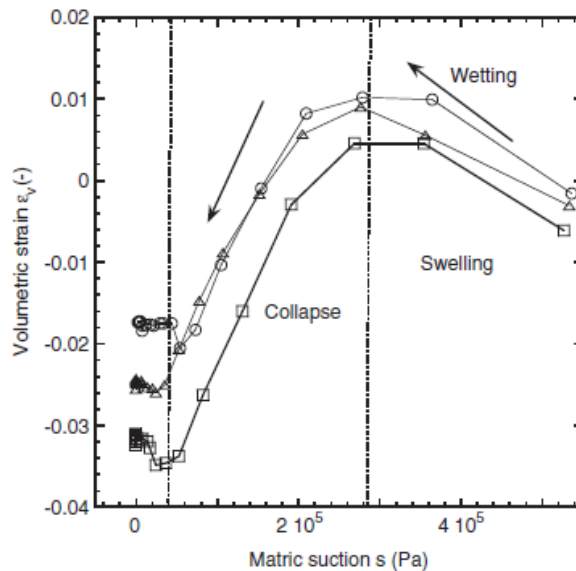


**Figure 2.13** Wetting induced swelling and collapse in kaolin, under a mean net stress of 40 kPa (Sivakumar, 1993).

Many other authors (e.g. Josa et al., 1987; Wheeler and Sivakumar, 1995; Cui and Delage, 1996; Rampino et al., 1999) performed suction-controlled tests in order to investigate the effect of suction on the volumetric behaviour of unsaturated soils. Cui

and Delage (1996) performed a series of suction-controlled triaxial tests on samples of compacted Aeolian silt. The results of their experiments showed that the plastic compressibility of the soil decreases with increasing suction, and that the pressure at which yield occurs increases with suction (Figure 2.14a). Their stress-strain results also showed that initial stiffness of the soil and deviator stress at failure increases with increasing suction (Figure 2.14b). For suction values of above 400 kPa, a more pronounced increase in peak deviator stress was observed at a reducing level of strain, illustrating an increasing fragility of the soil with suction. Rampino et al. (1999) conducted a series of suction-controlled triaxial test on samples of compacted silty sand. The experimental results obtained from isotropic compression test at different values of suction showed that plastic compressibility of the soil decreases with increasing suction (Figure 2.15a). It was observed that the slope of the normal consolidation line decreases with increasing suction. Their results also show that the yield stress increases with increasing suction (Figure 2.15b).

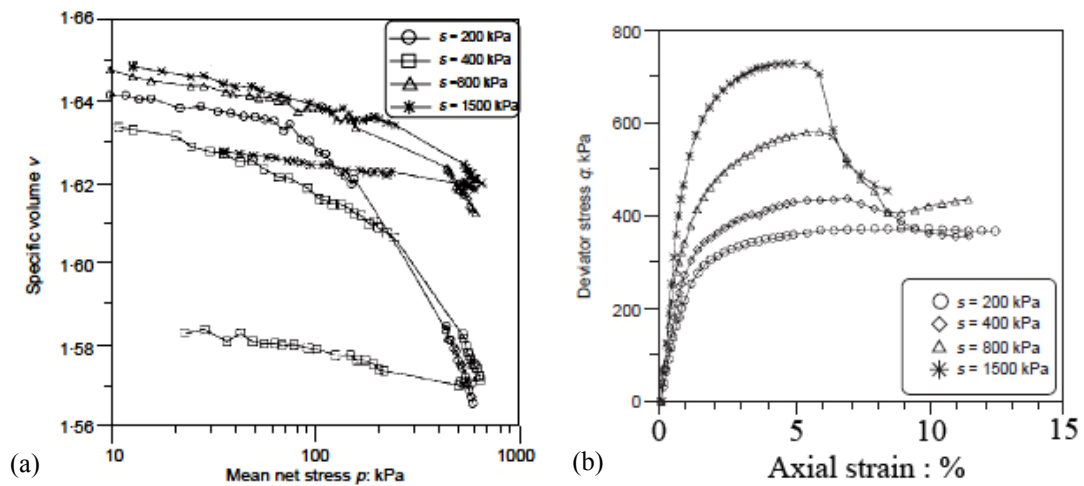


**Figure 2.14** (a) Volume change under suction-controlled isotropic loading, (b) Stress-strain curves at different suctions (Cui and Delage, 1999).

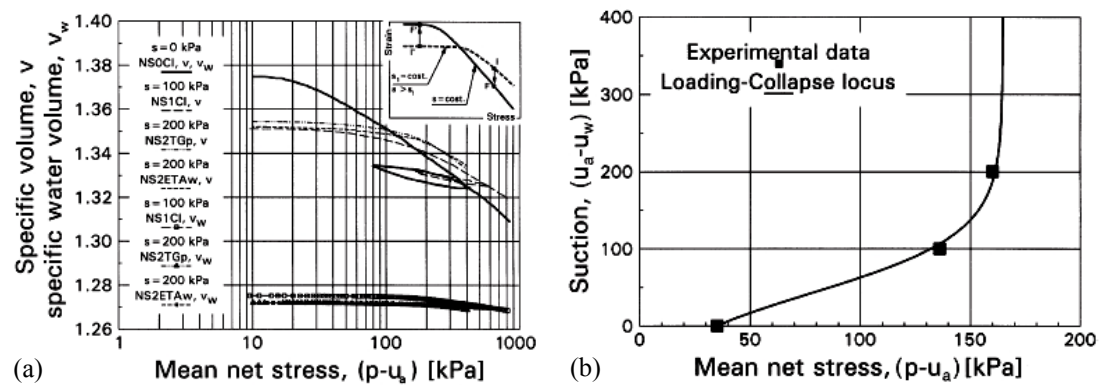


**Figure 2.15** (a) Volume change during the suction-controlled triaxial compression tests, (b) Yield points in suction-controlled isotropic compression tests (Rampino et al., 1999).

Yong et al. (1971) studied the volume change behaviour of kaolinite and Rosalie clay in a cycle of drying and wetting under no external load. Their results show progressive accumulation of irreversible (plastic) deformation along the virgin drying path. A slow accumulation of irreversible expansion was observed along the wetting path (see Figure 2.16). Chu and Mou (1973) also reported the results of cycles of wetting/drying performed on samples of highly expansive clay in a suction-controlled consolidometer. A large irreversible swelling was observed during the first wetting cycle. On the subsequent drying/wetting cycles mainly an elastic behaviour was observed, even though a small accumulation of irreversible swelling was also measured.

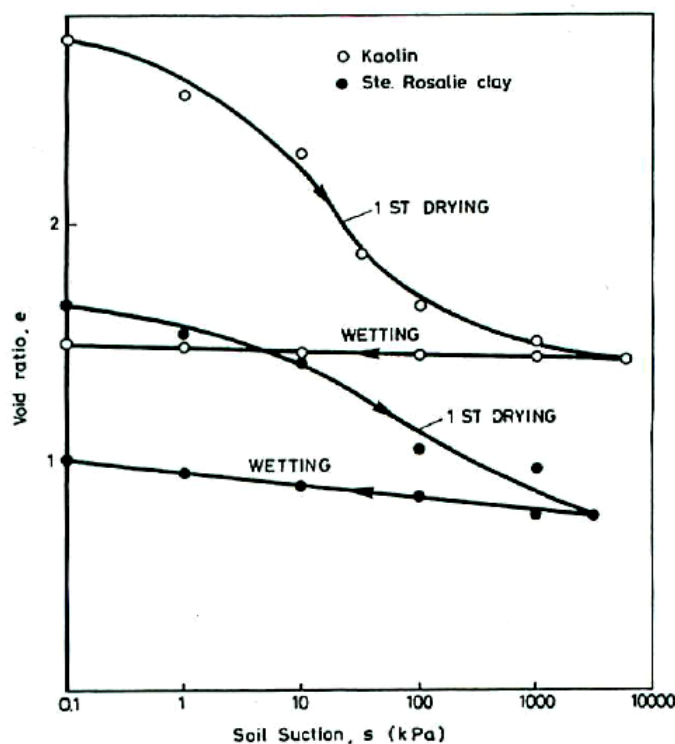


**Figure 2.16** Variation of void ratio with applied suction (Yong et al., 1971).

Clayey soils undergo volume reduction when their water-content is reduced. This reduction in volume of the soil upon drying is a consequence of suction increase and is called shrinkage. The shrinkage of a clay sample is attributed to the surface tension at the contact points of the clay particles created during the drying process. When the soil is saturated, bulk water exists in the soil pores and the effects of surface tension are not significant. As the soil dries and the bulk water is removed from the voids, several menisci are created in the voids. Tensile forces are created at the boundaries between water and air. These forces are accompanied by compressive forces that act on the soil structure. As a consequence of the compressive forces on the soil mass, the volume of



soil decreases during this process. As schematically shown in Figure 2.17, the shrinkage behaviour of an initially saturated soil upon drying can be divided into the following three stages (Haines, 1923); (1) normal shrinkage: in this phase the volume decrease of the soil is equal to water loss, and the soil remains saturated, (2) residual shrinkage: in this phase water loss during drying process is greater than the soil volume decrease (therefore  $S_r$  decreases while drying), (3) zero shrinkage: the soil has reached its maximum density under the drying process, and volume of the sample remains constant with further water extraction. The point separating the saturated phase and the residual phase (Point L in Figure 2.17) corresponds the air entry value of the soil sample. The air entry value of a soil is the matric suction at which air starts to enter the pores in the soil.

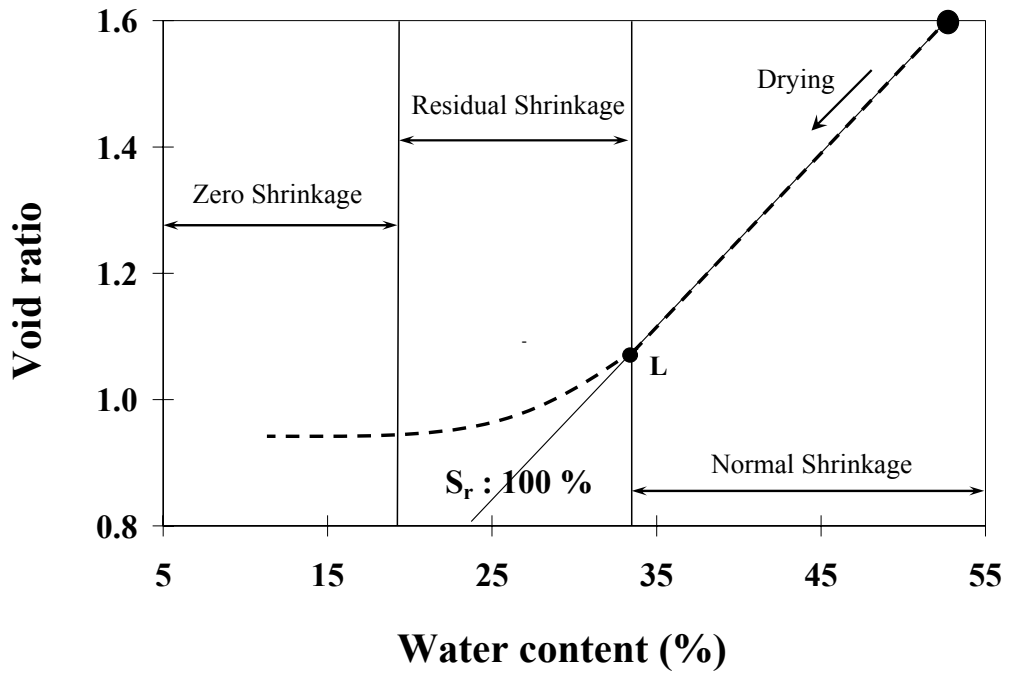


**Figure 2.17** Schematic representation of different stages of shrinkage.

### 2.3.3 Shear strength behaviour

Fredlund et al. (1978) proposed an expression for the shear strength ( $\tau$ ) of unsaturated soils (Equation 2.6), as an extension of the Mohr-Coulomb equation for fully saturated soils:

$$\tau = c' + (\sigma - u_a) \tan \phi' + (u_a - u_w) \tan \phi^b \quad (2.6)$$

where  $c'$  is the effective cohesion intercept,  $\phi'$  is the effective angle of friction,  $\phi^b$  is the slope of the failure surface in the  $\tau : s$  plane. In this approach, it was assumed that  $\phi'$  and  $\phi^b$  are independent of suction. The influence of suction on the shear strength is

therefore equivalent to an increase of the effective cohesion ( $c = c' + (u_a - u_w) \times \tan \phi^b$ ). Figure 2.18 shows a three-dimensional illustration of the failure envelope for unsaturated soils proposed by Fredlund et al. (1978). As shown in Figure 2.18, Equation 2.6 predicts a linear increase of shear strength with suction.

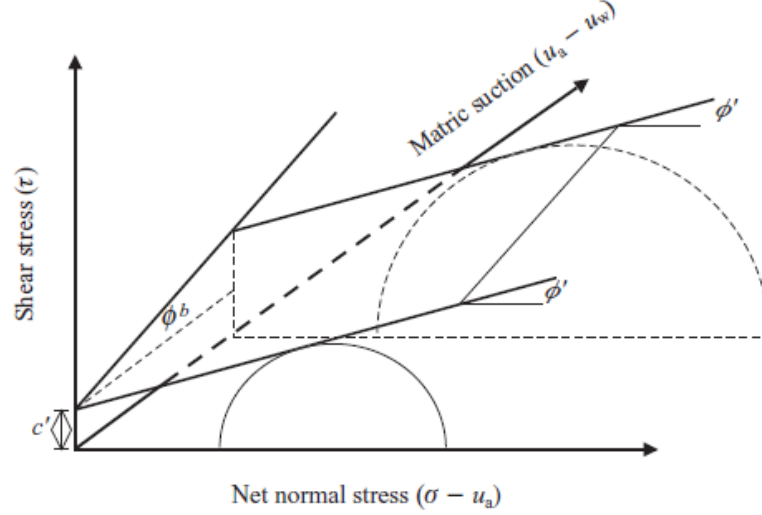


**Figure 2.18** Failure envelope for unsaturated soils (Fredlund et al., 1978).

Many subsequent authors (including Escario and Saez, 1986; Gan et al., 1988; Escario and Juca, 1989) showed that the angle  $\phi^b$  is not constant but changes with suction and it can even become negative at high values of suction, resulting in a decrease in shear strength with increasing suction. At low values of suction  $\phi^b$  is equal to  $\phi'$ . As suction increases tangent value of  $\phi^b$  gradually decreases towards zero. The non-linearity of the relationship between shear strength and suction can be explained by a physical argument. At low values of suction, the soil is almost saturated and the pore water is mainly in the form of bulk water. Therefore in this region  $\phi^b$  is equal to  $\phi'$ , and this makes Equation 2.6 to appear as follows:  $\tau = c' + (\sigma - u_w) \times \tan \phi'$ . As suction increases more voids become air-filled and the number interparticle contacts influenced by meniscus water increases. The shear strength increases with suction because the interparticle normal force (N) increases with increasing suction. However, as suction tends towards infinity  $\Delta N$  reaches a limiting value, and therefore  $\tau$  approaches an asymptotic value, as schematically shown in Figure 2.19. The influence of suction on  $\phi'$  is not certain as some researchers reported that  $\phi'$  is constant with suction for most soils (Escario and Juca, 1989; Ng et al., 2000) while others including Toll (1990) and Toll and Ong (2003) found that  $\phi'$  increases with decreasing degree of saturation, based on triaxial tests on a lateritic gravel and a residual sandy clay. In contrast, Maatouk et al. (1995), Cui and Delage (1996) and Bastos et al. (1998) found that  $\phi'$  decreases with

increasing suction. Given these evidences, it can be recognised that more experimental results are required in order to provide a conclusion regarding the dependency of  $\phi'$  to suction.

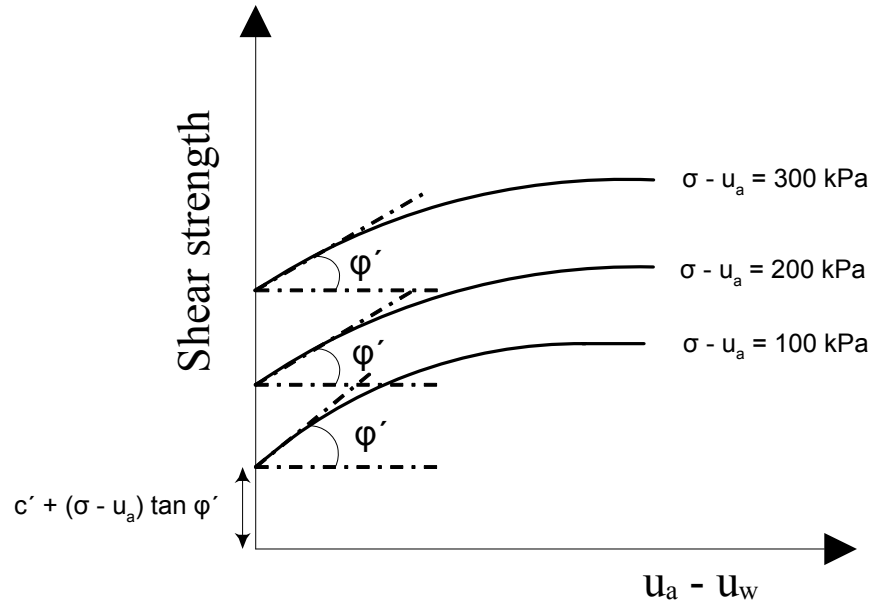


**Figure 2.19** Influence of suction on shear strength.

Fredlund et al. (1995) proposed an empirical relationship between the shear strength and the SWRC. The authors proposed that the component  $(u_a - u_w) \times \tan \phi^b$  can be predicted from the shape of the SWRC. Many subsequent authors (e.g. Vanapalli et al., 1996; Oberg and Salfors, 1997; Toll and Ong, 2003) have proposed similar models for describing the non-linear shear strength relationships in unsaturated soils. Features of the SWRC, including the air entry value and residual water-content, have been used in the formulation of these models. If the shear strength is measured at critical states,  $c' = 0$  and the shear strength relationship can be presented in terms of deviator stress ( $q$ ) and mean net stress ( $p'$ ). For instance, Toll (1990) proposed the following expression for shear strength at critical state:

$$q = M_a \times p' + M_w \times (u_a - u_w) \quad (2.7)$$

where  $M_a$  and  $M_w$  are soil parameters called total stress ratio and suction ratio. These two parameters are functions of  $S_r$ , and represent the contribution of the net stress and suction on the shear strength. Figure 2.20 shows the critical state lines for kaolin at different suctions from Wheeler and Sivakumar (1995).

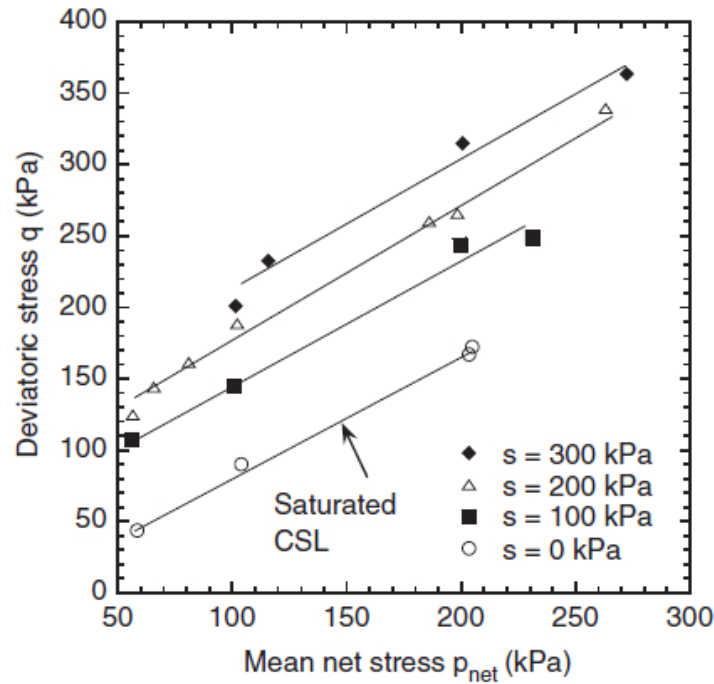


**Figure 2.20** Critical state lines for kaolin at different suctions (Wheeler and Sivakumar, 1995).

Nishimura and Fredlund (2002) studied the influence of wetting and drying process on unconfined compressive strength of a compacted silty soil. It was observed that there is a slight hysteresis in shear strength of the soil under wetting and drying process. The result of their experiment showed that the compressive strength of the soil during wetting is less than that during drying at the same suction value. Khoury and Miller (2010) studied the effect of suction hysteresis on shear strength of a sandy silt soil by using a modified direct shear equipment. The tests are first conducted along the drying path, and compared with tests conducted at same suction but following wetting after drying. The results show that the shear strength obtained from wetting tests are slightly higher than those of drying tests.

#### 2.3.4 Development of elasto-plastic models

Alonso et al. (1987) proposed the first elasto-plastic model for unsaturated soils in a qualitative manner. The model was developed to a full mathematical formulation by Alonso et al. (1990). This model, known as the Barcelona Basic Model (BBM), is based on the well-known Modified Cam Clay (MCC) framework. The BBM is described in terms of four state variables: mean net stress ( $p$ ), deviator stress ( $q$ ), matric suction ( $s$ ) and specific volume ( $v$ ). The main feature of BBM consists of a yield surface which separate elastic and plastic regions, as shown in Figure 2.21. Yield can occur as a result of an increase in the mean net stress or a decrease in matric suction. The BBM assumes

elastic behaviour for stress paths remaining inside a yield surface, with plastic strains commencing once the yield surface is reached.

As shown in Figure 2.21, an increase in the mean net stress, inside a yield surface, causes elastic compression (section AB of stress path ABC) and a decrease in suction causes elastic swelling (section AF of stress path AFG). When the stress state reaches the current location of the yield surface (points B, F, or D), an increase of  $p$  (section BC of stress path ABC), an increase of  $q$  (section DE of stress path ADE), or a reduction of suction (section FG of stress path AFG) results in an expansion of the yield surface. Alonso et al. (1990) defined a LC curve as the intersection of the yield surface with  $q = 0$  plan. LC curve shifts to the right due to any plastic deformations (see Figure 2.22), and as a consequence the elastic region expands. The BBM, similar to MCC framework, is a strain hardening model. The value of  $p_0(0)$  represents the yield stress at zero suction, and it is taken as the hardening parameter.

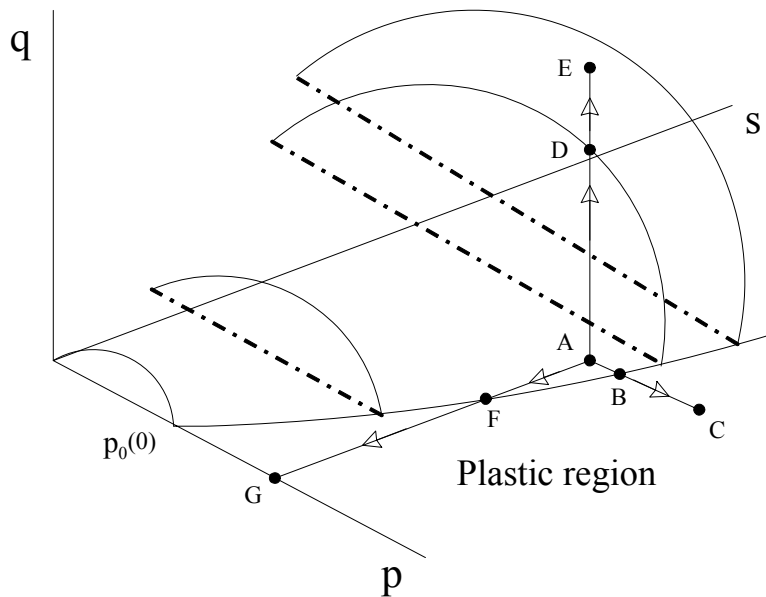


**Figure 2.21** Yield surface in  $q$ - $p$ - $s$  space (after Alonso et al., 1990).

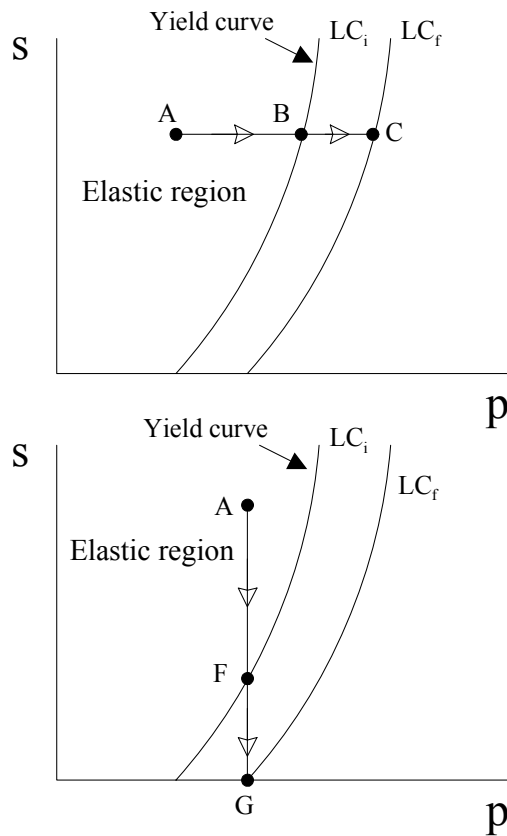


**Figure 2.22** Loading Collapse yield curve (after Alonso et al., 1990).

It should be noted that the model presented by Alonso et al. (1990) assumes that a soil is saturated only when the matric suction equals zero. This assumption is not true in reality. As a soil is gradually dried from a fully saturated condition, the soil remains saturated until the air entry value is exceeded. In this region, the conventional principle of effective stress for saturated soils should be used for representing the stress-strain behaviour of the soil. Alternatively, as a soil is gradually wetted, the soil can still remain unsaturated by reducing suction to zero, and within this region the conventional effective stress principle cannot be used for representing the stress-strain behaviour of the soil. Due to this limitation, subsequent authors (e.g. Gallipoli et al., 2003; Wheeler et al., 2003) proposed new approaches for modelling unsaturated soils. As explained by Wheeler et al. (2003) the mechanical behaviour of an unsaturated soil depends on  $S_r$  even if the suction, net stress and specific volume are kept the same for the soil. Due to presence of the hydraulic hysteresis in the SWRC during drying and wetting, two samples of the same soil subjected to the same value of suction can be at significantly different value of  $S_r$  if one is on a drying path and the other is on a wetting path. The model presented by Wheeler et al (2003) is able to incorporate the effects of variations in  $S_r$  on the stress-strain behaviour. Furthermore, it can also represent the effect of volumetric deformations on the position of the SWRC. A SWRC obtained at a higher

net stress tends to shift towards the higher suction (Ng and Pang, 2000; Gallipoli et al, 2003). This means that the relationship between  $S_r$  and suction depends on net stress. As a soil deforms during loading and its volume decreases, the dimensions of both the voids and all connecting passages will decrease; therefore, a higher value of suction will be required to produce a given  $S_r$ . Alternatively, for a given value of suction, compression will result in an increase in the  $S_r$  of a soil.

The model proposed by Wheeler et al. (2003) is based on two independent stress variables: (1) Bishop's stress ( $\sigma'$ ), as presented in Equation 2.5 and the parameter  $\chi$  replaced by  $S_r$  (2) modified suction ( $s^*$ ), which is given by the expression below:

$$s^* = n(u_a - u_w) \quad (2.8)$$

where  $n$  represents the porosity. The variable  $s^*$  represents the stabilising influence of meniscus water, and Bishop's stress tensors represents the combined contributions of total stress, pore air pressure within air-filled voids and pore water pressure within bulk water. In this model, plastic volumetric deformations during loading are modelled with a LC yield line, similar to the approach followed by Alonso et al (1990). However, Wheeler et al (2003) assume the shape of the LC yield line to be straight and vertical in the  $s^* : \sigma'$  plane. The reason for this is that, whenever there is a meniscus at a particle contact point, the stabilising force is considered to be constant, regardless of the value of the suction prevailing within the meniscus. The stability of the soil structure is derived from the number of inter-particle contacts having menisci and not the actual value of matric suction.

### 2.3.5 Effects of temperature on mechanical behaviour

Many researchers have performed laboratory studies to investigate the influence of temperature on the mechanical behaviour of unsaturated soils (e.g. Baldi et al., 1988; Villar and Lloret, 2004; Romero et al., 2005). A common conclusion from these works is that an increase in temperature on normally consolidated clays causes a reduction in the void ratio. In contrast, it has been observed that heating may induce expansion for overconsolidated clays. It is also believed that the thermal volumetric behaviour of unsaturated soils is strongly affected by suction and over-consolidation ratio. It is important to emphasise that the thermal volume change phenomenon has an important effect on the soil shear strength as the expansion of aggregates reduces the soil shear strength, while thermal contraction hardens the soil and causes an increase in shear strength.

Villar and Lloret (2004) performed a series of single oedometer tests, as part of which a cell was placed in a thermostatic bath with controlled temperature, in order to investigate the influence of temperature on the swelling capacity of a compacted bentonite. The test procedure consisted of incrementally loading a soil sample at constant water-content up to a specified vertical stress and then inundating the sample with water. The results of their investigation indicate that the swelling capacity of clay decreases with increasing temperature. The effect of temperature is, however, less evident as the stress being applied increases. Tang et al. (2008) studied the thermo-mechanical behaviour of compacted unsaturated expansive clays. They performed suction and temperature-controlled isotropic compression tests on samples of compacted bentonite. The results of thermal loading tests at constant pressure showed that at high suction, heating induces a volume expansion under low pressure. In contrast, it was observed that heating tends to induce a contraction under high pressure and low suction. If thermal contraction occurs during heating, this may result in an increase of yield pressure due to a thermal hardening phenomenon. Many authors, including Sultan et al. (2002), have studied the effect of temperature on the preconsolidation pressure of clayey soils (see Figure 2.23). The authors carried out an isotropic compression test on samples of Boom clay at different temperatures. All samples were isotropically loaded up to a specified stress and then heated to 100°C. The samples were cooled to different temperatures and subsequently loaded. The results of their investigation indicate that heating induces a thermal hardening phenomenon which results in an increase of the stress value at which yield occurs. It was shown that a heating-cooling cycle produces over-consolidation behaviour in the material. The authors also studied the effect of over-consolidation ratio on volume change behaviour of a sample heated under a constant load. It was observed that the thermal contraction increases when the over-consolidation ratio decreases.

Cekerevac and Laloui (2004) made similar observations on saturated samples of kaolin clay using a temperature controlled triaxial apparatus. In order to study the effect of overconsolidation ratio and temperature on volume change behaviour of the soil, all samples were consolidated up to a specific value and then unloaded to different values of overconsolidation ratio. The temperature of the samples was subsequently increased under drained testing conditions. The volume change measurement during drained heating was made from the volume of water leaving the saturated samples. It was observed that slightly overconsolidated samples show smaller thermal contraction rather



than normally consolidated samples, while highly overconsolidated samples can show thermal expansion (see Figure 2.24). The results of their research show that the slope of the normal consolidation line and the critical state line can be considered independent of temperature.

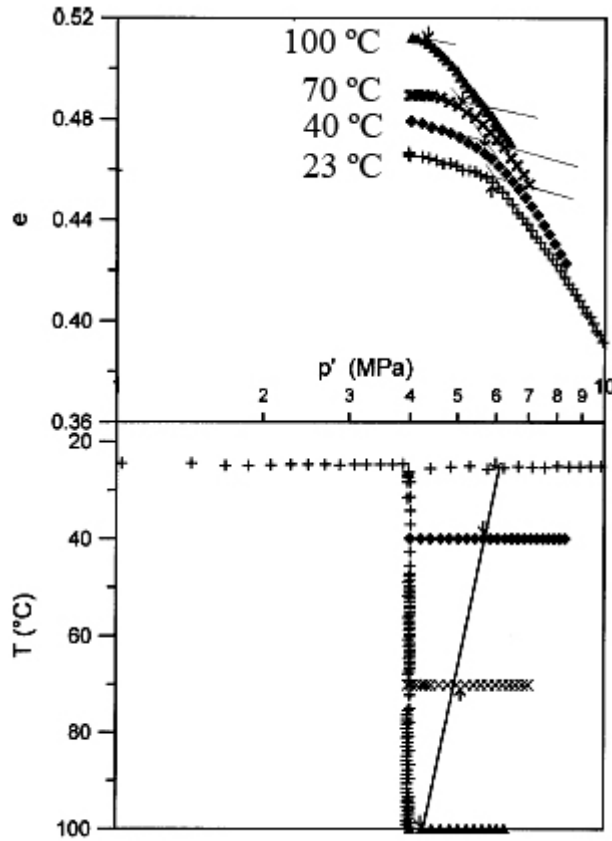


**Figure 2.23** Temperature effects on the preconsolidation pressure (Sultan et al., 2005).

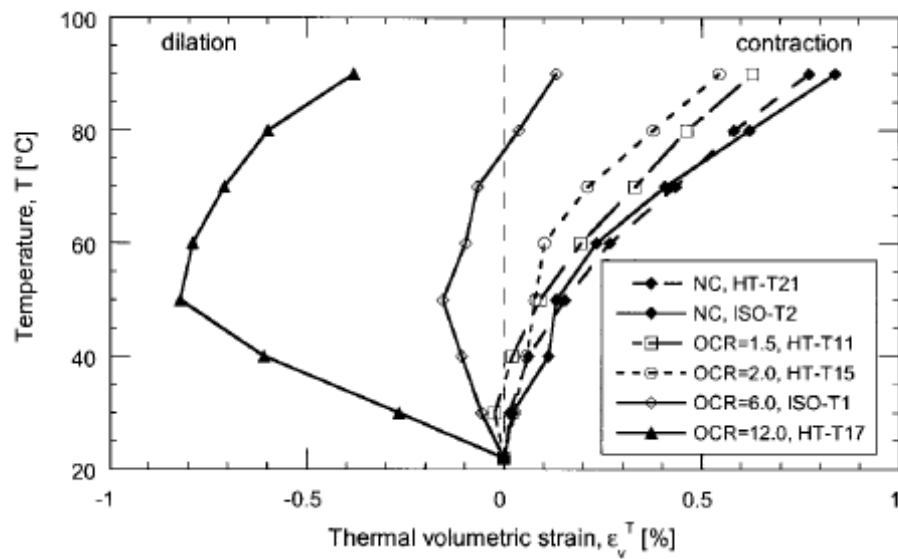


**Figure 2.24** Thermal volumetric strain of kaolin clay during drained heating from 22 to 90°C (Cekerevac and Laloui, 2004).

Tang et al. (2008) demonstrated that the elastic and plastic compressibility parameters are independent of temperature, but affected strongly by suction. The results of their research on bentonite samples show that the value of these two parameters decreases with increasing suction. However, experimental results of controlled suction triaxial tests on samples of compacted Aeolian silt obtained by Cui and Delage (1996) show that the elastic compressibility parameter is suction independent. Cekerevac and Laloui (2004) performed a series of drained triaxial compression shear tests on isotropically consolidated samples of kaolin clay with the same initial states and at different temperatures. The experimental results showed that shear strength increased with increasing temperatures. However, the shear stress obtained at high and low temperatures tended to converge to the same critical state, at large strains. The authors also found that the friction angle at critical state is independent of temperature. Romero et al. (2003) conducted a series of oedometer tests with control of suction and temperature on samples of moderately swelling compacted clay. The results of their research on samples of statically compacted Boom clay show that the loose samples generally develop additional compression upon wetting (collapse), while the denser samples exhibit swelling strains on wetting (see Figure 2.25). It has been observed that the swelling deformation of the high density soil is significantly larger at the higher temperature, especially in the low stress range. In contrast, collapse deformation observed upon wetting of the low-density soil samples appear to be unaffected by temperature.

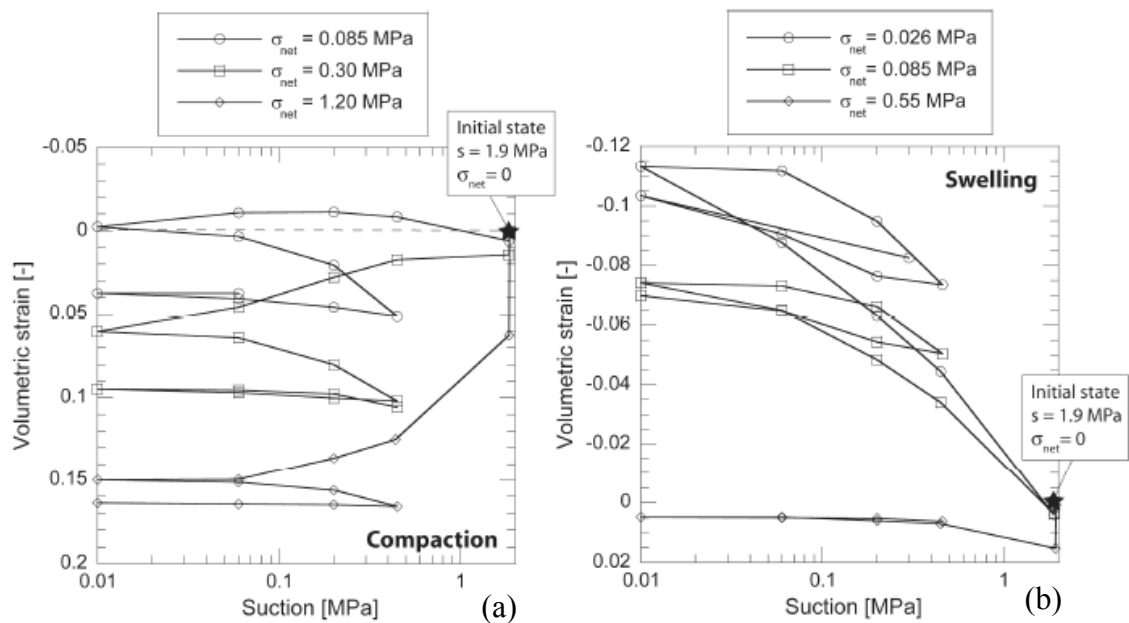


**Figure 2.25** Effect of the dry density and the external vertical stress on the swelling and/or collapse behaviour upon wetting. Compacted boom clay (Romero et al., 2003): (a) Collapse of loose soil ( $\gamma_d = 13.7 \text{ kN/m}^3$ ); (b) Swelling of dense soil ( $\gamma_d = 16.7 \text{ kN/m}^3$ ).

The influence of temperature on the elastic modulus of soils has been investigated by Kuntiwattanakul et al. (1995), Burghignoli et al. (2000), Cekerevac and Laloui (2004), and Abuel-Naga (2005). A common conclusion from these works is that temperature increase has a stiffening effect on the elastic behaviour of soils. The result of an experiment by Cekerevac and Laloui (2004) on kaolin clay shows that soil stiffness is higher at 90°C than at 22°C. Kuntiwattanakul et al. (1995) and Abuel-Naga (2005) noticed a similar increase in stiffness with temperature in kaolin clay and Bangkok clay, respectively. Burghignoli et al. (2000) observed that temperature does not have a significant influence on Tody clay stiffness if that temperature is the highest temperature experienced by the soil. The influence of temperature on shear strength is not certain as some researchers reported that heating results in a reduction of shear strength while others concluded slightly increased strength. This uncertainty could be due to use of different experimental techniques, stress and strain paths and drainage conditions during heating and shearing. Kuntiwattanakul et al. (1995) and Cekerevac (2003) observed that peak strength increases slightly with increasing temperature in kaolin clay and MC clay, respectively (see Figure 2.26). In contrast, Hueckel et al. (1998) reported that a temperature increase from 22° to 120°C results in a decrease of peak strength of a Spanish clay by about 25%. Hueckel and Pellegrini (1989) studied the slope of the friction angle at the critical state for Pontida clay. It was observed that temperature does not have any influence on the friction angle under both drained and undrained shearing. However, the same authors reported that the friction angle of Boom clay increases slightly under undrained shearing.

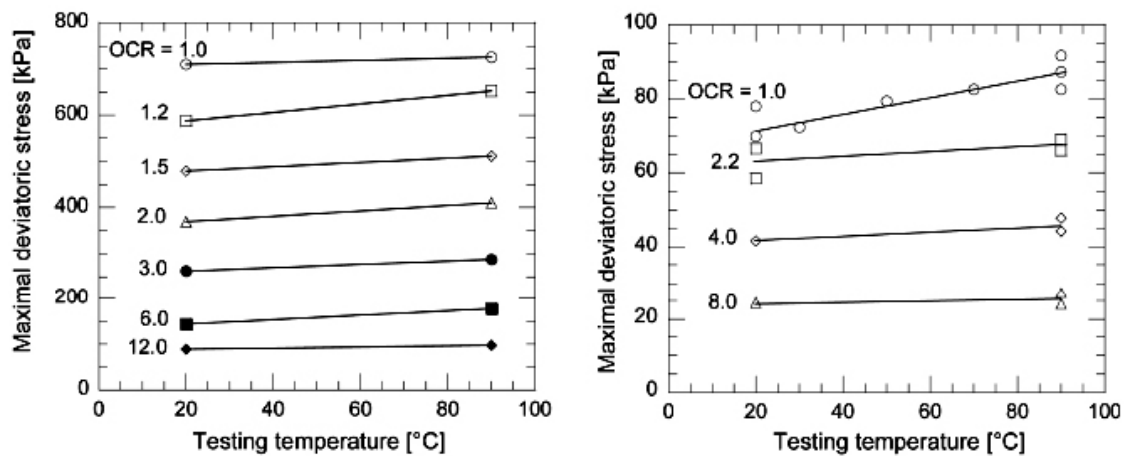


**Figure 2.26** Effect of temperature on the maximum deviatoric stress observed upon triaxial shearing. (a) Kaolin clay (Cekerevac, 2003); (b) MC clay (Kuntiwattanakul et al., 1995).

## **2.4 Experimental techniques for testing unsaturated soils**

Various techniques have been adopted for measuring and controlling suction in a soil specimen during unsaturated soil experiments. A review of the most commonly used techniques for testing unsaturated soils is given here. The advantages and drawbacks of each technique are discussed below.

### **2.4.1 Suction measurement methods**

Suction measurement is an essential issue for testing unsaturated soils due to the key role of suction on the mechanical behaviour of the soil. A review of various methods commonly used for measuring suction is presented here. The most commonly used devices for measuring soil suction include tensiometers, thermal conductivity sensors, dew point sensors, and the filter paper technique. Suction measurements are particularly challenging, when measuring low values of total suction and high values of matric suction. The accuracy of the total suction measurement reduces as total suction decreases. This inaccuracy is due to the long period of time required for suction equalisation as well as isothermal equilibrium between the specimen and vapour space in the closed system. The direct measurement of matric suction requires a separation between the water and air phases, normally by means of a ceramic disk. The maximum value of matric suction that can be measured is limited by the air-entry value of the ceramic disk used. However, cavitation represents another restriction to the technique when used for measuring high matric suctions. Water under tension is in a meta-stable state, which may result in nucleation (formation of vapour cavities). When a soil sample with high suction value is placed in direct contact with the ceramic disc, it will immediately tend to draw water through the porous disk. This can potentially cause cavitation inside the ceramic disc. It is therefore recommended by Romero (1999) to apply high pressures of deaired water to the ceramic disc before opening the drainage lines, in order to dissolve the trapped air inside the disc. Figure 2.27 shows a simple pressure/temperature phase diagram for a simple pure substance.

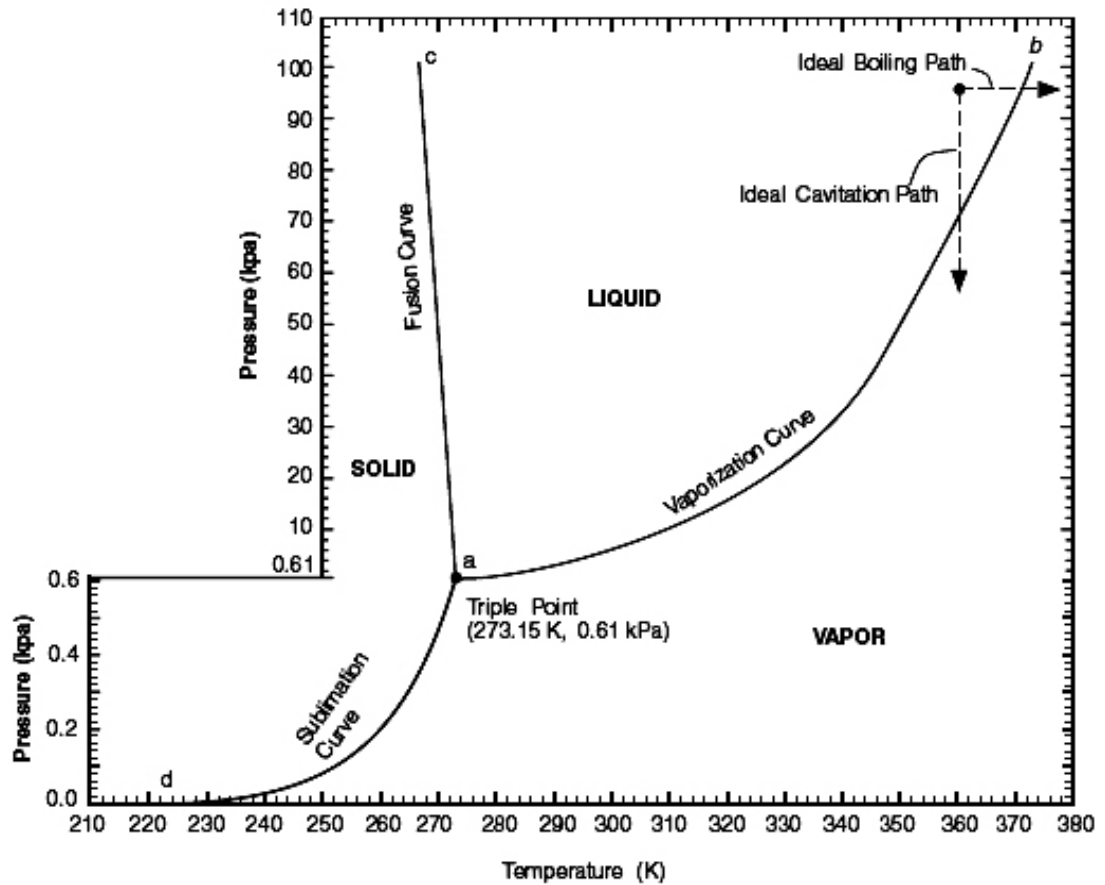


**Figure 2.27** Phase diagram for a simple substance (from Lu and Likos, 2004).

#### (a) Filter paper method

The filter paper method is one of the most widely used techniques for obtaining soil suction due to its simplicity and the fact that it covers a range of suction measurements from almost zero to 100 MPa (Chandler et al., 1992; Houston et al., 1994; Bulut et al., 2001; Leong et al., 2002; Marinho and Oliveira, 2005; Agus et al., 2010). This method consists of placing a piece of standard filter paper against the soil sample whose suction is required. The soil is then placed in an air-tight container at relatively constant temperature in order to reach a state of equilibrium between the soil suction and the filter papers. After equilibrium is established between the filter paper and the soil, a measurement of soil suction can be obtained through the use of suitable calibration curves that relate the water-content in the filter paper to the value of suction. It has been suggested by some authors (e.g. Houston et al., 1994; Leong et al., 2002) that the calibration curve for total suction should differ from the calibration curve for matric suction. Houston et al. (1994) used three different saturated salt solutions (vapour equilibrium technique) and pressure plate (axis translation technique) for calibration of Fisher quantitative coarse filter papers. The authors adopted 7 days equilibration time

and they observed that the filter paper responses are different for total and matric suctions. However, the results of their experiment also show that the total and matric suction calibration curves converge at a suction value of about 1 MPa. It was therefore suggested that at high levels of suction, most of the moisture movement occurs through vapour transfer. Leong et al. (2002) performed a similar study and presented different calibration curves for total suction and matric suction (see Figure 2.28). Marinho (1994b) evaluated the time required for equilibration of Whatman No. 42 filter paper. A range of suctions was generated using solutions of sodium chloride at different concentrations. The author concluded that, given sufficient time for equalization, there is a unique calibration curve for the filter paper regardless of the type of suction.

The vapour equilibrium technique is usually used for calibration of filter papers. In this technique, salt solutions of different concentrations are used as an osmotic potential source for generating ranges of suction values (Bulut et al., 2001). In a closed system and under isothermal conditions, the partial pressure of the water vapour in the air space above the deionised water at equilibrium is equal to the saturated vapour pressure. The partial pressure of the water vapour, and therefore the relative humidity, over a salt solution is less than that over pure water. Total suction values corresponding to each relative humidity can be calculated using Kelvin's equation. The configuration of the calibration setup using the vapour equilibrium technique is shown in Figure 2.29.

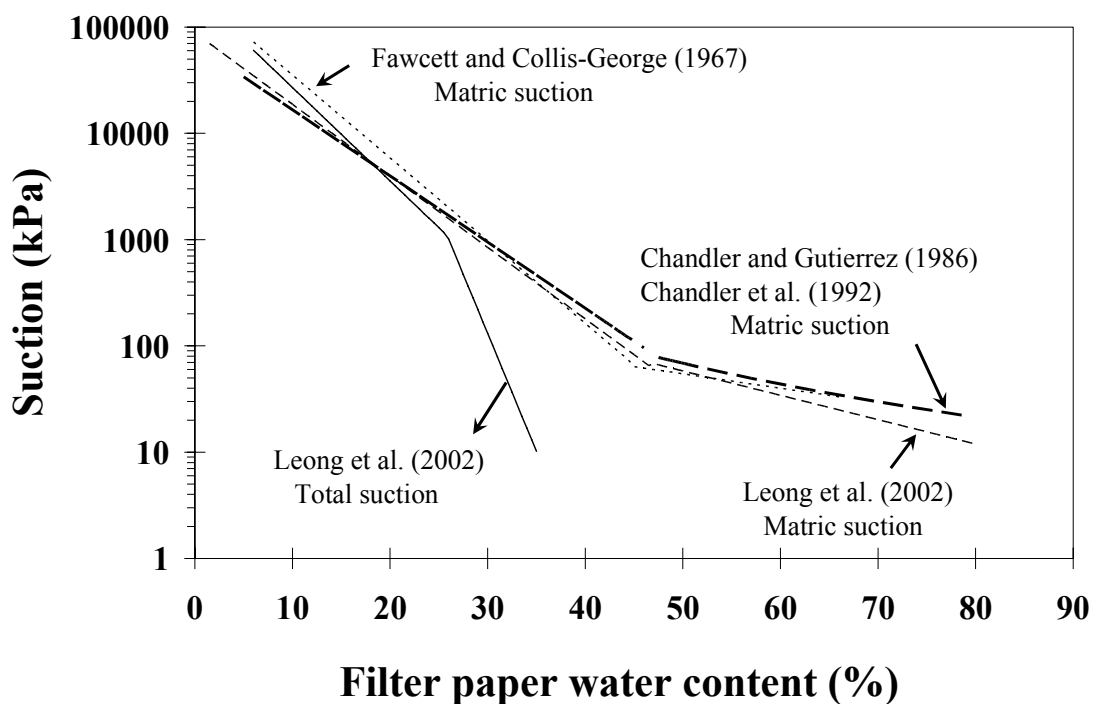


**Figure 2.28** Filter paper calibration curves presented for total and matric suction measurements.

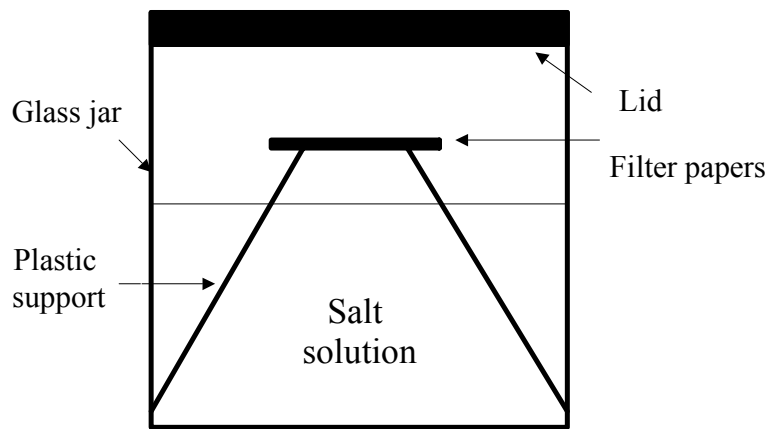


**Figure 2.29** Total suction calibration test configuration.

The filter paper method is capable of measuring both total suction and matric suction. In the case of total suction measurement, the filter papers are placed above the soil sample and therefore the transfer of moisture to the filter papers occurs only through the vapour phase, then both capillary and osmotic gradients exist between the soil and the filter papers. If the filter papers were allowed to absorb water through fluid flow, salt would get into the filter papers and consequently the osmotic gradient would be negligible, then only matric suction is being measured. As a porous medium undergoing drying and wetting processes shows hysteresis, the filter paper would also be expected to exhibit hysteretic behaviour in the drying and wetting process. The hysteresis in the filter paper method has been confirmed by many authors, based on experimental evidence. Therefore, it was suggested to perform soil suction measurement in the same manner as the calibration process to avoid the problem of hysteresis. Bulut et al. (2001) provided two separate equations for wetting and drying calibration curves (see Figure 2.30). Houston et al. (1994), however, reported no measurable difference between the wetting and drying calibration curves for matric suction between 8 and 2500 kPa.

In order to obtain a reliable measurement of total suction using the noncontact filter paper method, the measurements should be limited to a suction range about 1000 kPa to 500 MPa. Figure 2.31 shows a plot of Kelvin's equation at 20°C. From the figure it can be seen that the relationship between total suction and relative humidity becomes very steep at suction values of less than 1000 kPa. Therefore, in this range total suction is very sensitive to relative humidity and, as a consequence, to measure of filter paper water-content. In this range, relative humidity may change significantly due to a small temperature variation. At very high suction values (higher than 500 MP), the filter paper tends to adsorb a smaller amount of water vapour and the accuracy of the measurements

becomes very dependent on equilibration time, isothermal condition and operational procedure.

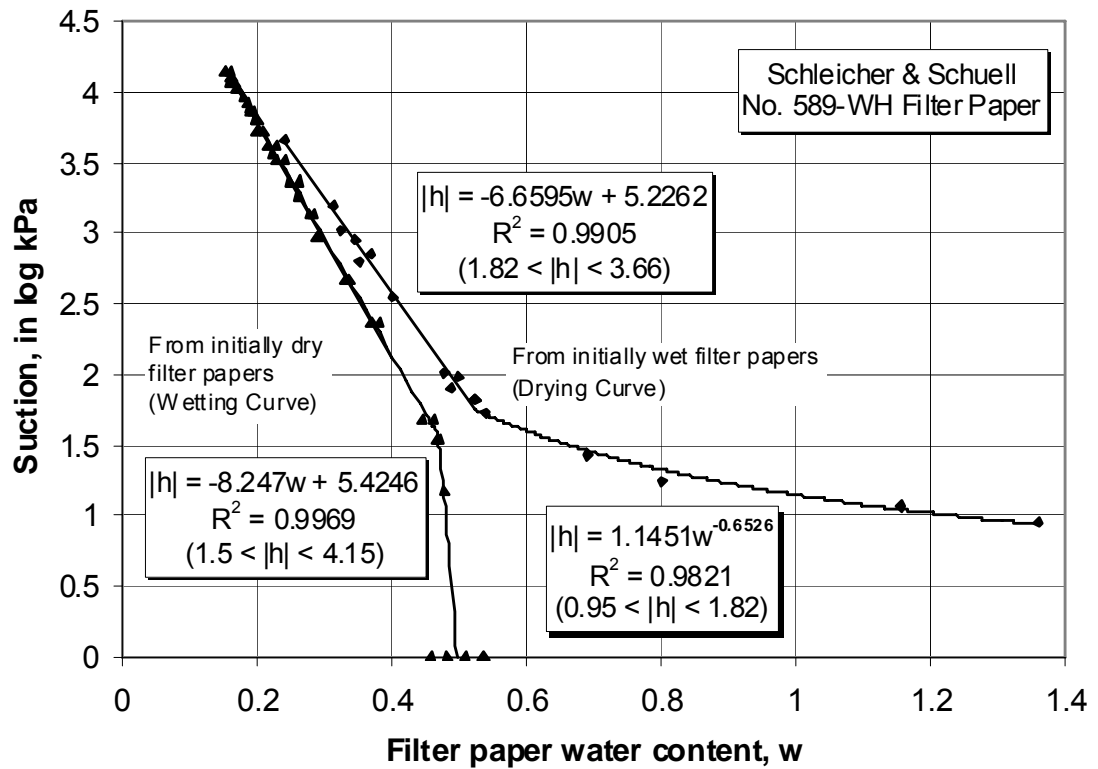


Figure 2.30 Wetting and drying calibration curves presented by Bulut et al. (2001).

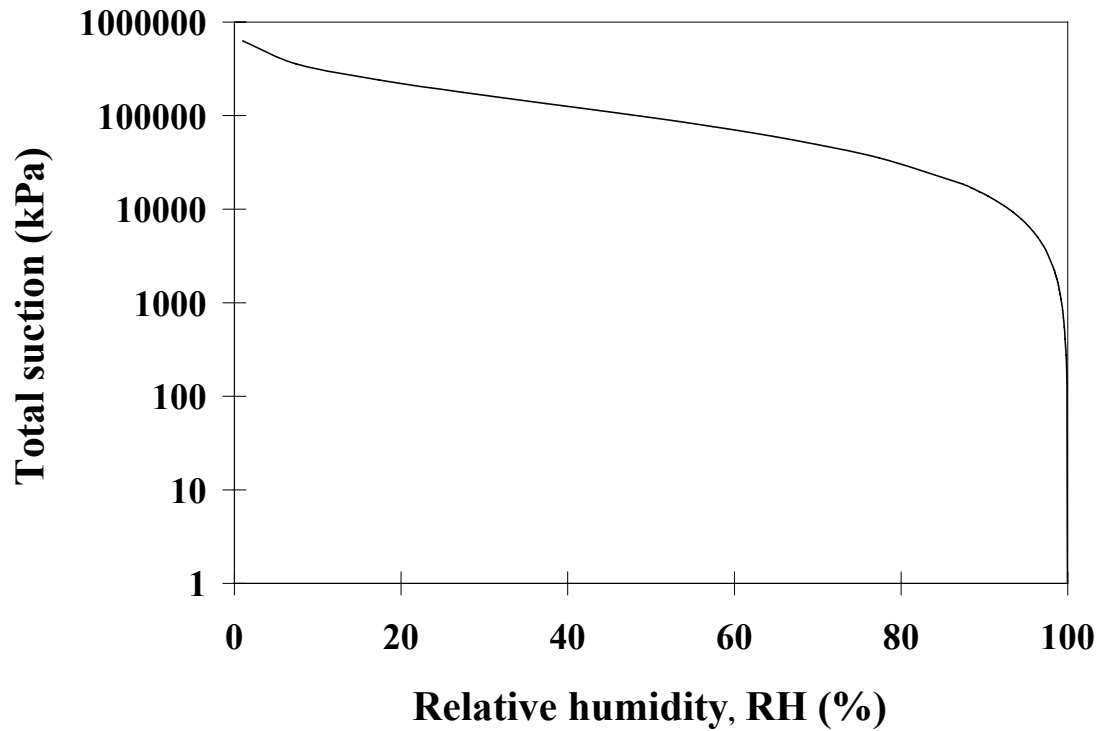


Figure 2.31 Theoretical relationship between total suction and relative humidity.



### (b) Tensiometer

A tensiometer is essentially a piezometer which is specifically designed to measure negative pore water pressure in the soil. A tensiometer mainly consists of a saturated porous ceramic filter, a water reservoir and a pressure measuring device (see Figure 2.327). Tensiometers have been used in unsaturated soils for many applications, including: determination of SWRCs (Toker et al., 2004; Lourenco et al., 2007), direct shear tests (Trantino and Tombolato, 2005), and field suction measurements (Ridley et al., 2003; Mendes et al., 2008).

The tensiometer works by allowing the water to be extracted from the reservoir into the soil across a porous filter. When the negative pore water pressure within the soil and tension in the water reservoir are in equilibrium, there will be no further flow of water, and subsequently soil suction can be measured by an electric transducer. If good contact is made between the tensiometer and the soil pore water, it is the matric suction that is measured by the device. Prior to testing, the tensiometer is saturated with de-aired water, and temporary vacuum maybe applied to remove air bubbles from the system. As noted by Ridley et al. (2003) the main limitation in the use of a conventional tensiometer is that air does eventually form within the water reservoir, when a tension is applied to the water inside a tensiometer at a suction close to the air-entry value of the porous filter. As suggested by the authors, the soil suction that can be measured in a conventional tensiometer is limited within a range of 0 to 100 kPa due to the possibility of cavitation of the water in the tensiometer. Once air is present, suction will not be transmitted efficiently to the measuring device and therefore the pressure measured within the tensiometer will not necessarily be equal to the suction in the soil.

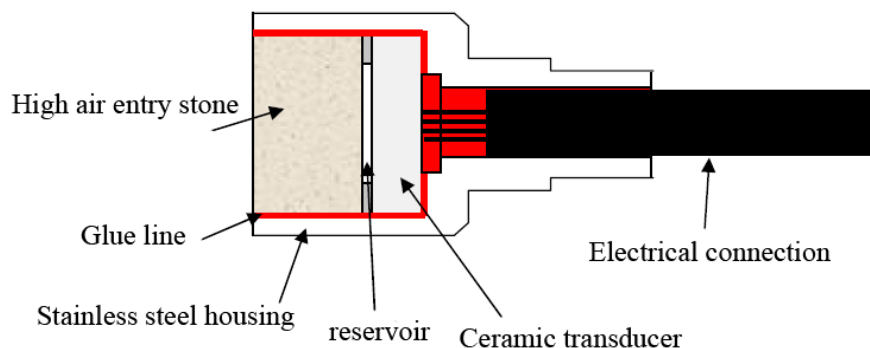


**Figure 2.32** Wykeham Farrance-Durham University high capacity tensiometer – Stainless steel housing dimensions: 14mm diameter and 35mm long (after Lourenco et al., 2008).

Ridley and Burland (1993) introduced a miniature tensiometer to overcome the problem of air formation associated with conventional tensiometers. They extended the suction measurement range of tensiometers by pre-pressuring the water in the reservoir and the filter. The device was made small in order to reduce the compressibility of the system and ease the de-airing procedure. In a further paper, Ridley and Burland (1996) presented a modified version of this device which they named the *suction probe*. The suction probe allows the measurement of soil suction up to 1.5 MPa, corresponding to the air-entry value of the porous filter used. The device consists of an integral strain gauge diaphragm and high air-entry value ceramic filter. The high air-entry porous filter allows passage of water but not air, unless the matric suction exceeds the air entry value. This reduction in the volume of water reservoir was suggested by Ridley et al. (1998) in order to reduce the possibility of cavitation. A smaller reservoir will have a smaller number of imperfections and is less likely to suffer from unpredictable tension breakdowns. The performance of tensiometers depends on their saturation and their accurate calibration. The saturation process of tensiometers has been studied by different authors (e.g. Tarantino and Mongiovi, 2001; Take and Bolton, 2003) who investigated different aspects of the pre-conditioning procedure employed for saturation, such as: magnitude and duration of the positive pre-pressurisation stage and the effect of initial flooding of the tensiometer under vacuum. The calibration of the tensiometers has been studied by Tarantino and Mongiovi (2003) and Lourenco et al. (2008).

### **(c) Thermal conductivity sensor (TCS)**

It has been found that the thermal conductivity of a soil is indicative of its water-content. Shaw and Baver (1939) were the first to use thermal conductivity to measure the water content in a soil. They placed a temperature sensor and a heater directly into a soil in order to measure its thermal conductivity. By using this method, a separate calibration curve is required for different soils in order to relate the measured thermal conductivity to the soil's water-contents. Johnston (1942) suggested that the thermal conductivity sensor can be enclosed in a rigid porous cover with a predetermined calibration curve. If the porous cover is allowed to reach suction equalisation with the soil under consideration, any subsequent change in the suction of the soil results in a corresponding change in the water-content of the porous cover. The thermal conductivity of the porous cover varies as its water-content varies. The water-content of the porous cover is dependent on the matric suction of the surrounding soil. Therefore,

the thermal conductivity of the porous cover can be calibrated with respect to the matric suction of the soil.

A calibrated TCS can therefore measure the matric suction if the sensor placed in the soil and allowed to reach equilibrium with the matric suction of the soil. A TCS consists of a porous block, which contains a miniature heating element and a digital temperature sensor embedded in the centre of the block (see Figure 2.33). The heating element is heated by sending a constant electrical current for a specific time, and the temperature rise is monitored by the temperature sensor located near the heating element. The operation of the sensor depends on the rate of heat dissipation within the porous block. The amount of heat dissipation, which controls the temperature rise, depends on the water-content of the porous block. More heat will be dissipated as the water-content in the porous block increases. The undissipated heat will result in a temperature rise at the centre of the block. The measured temperature rise is expressed in terms of a voltage output.

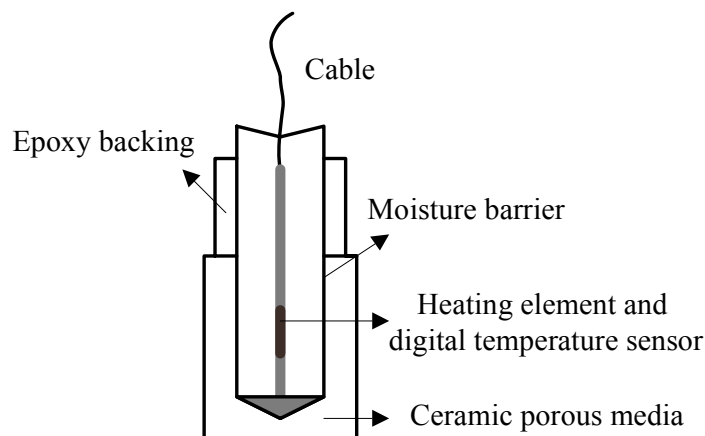
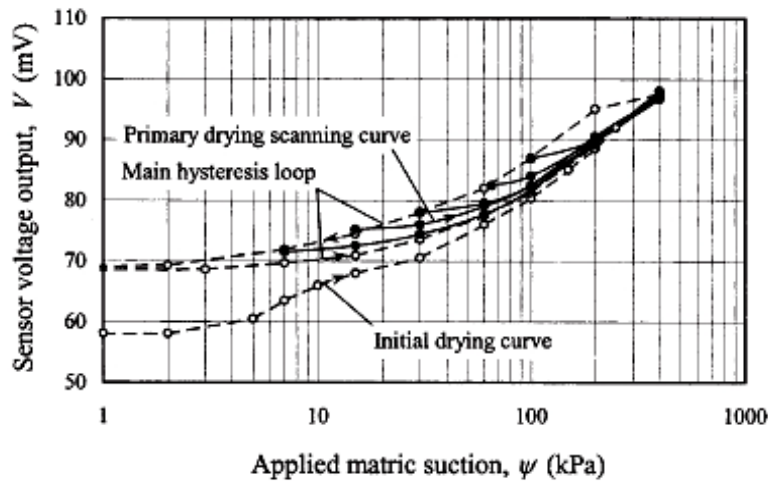


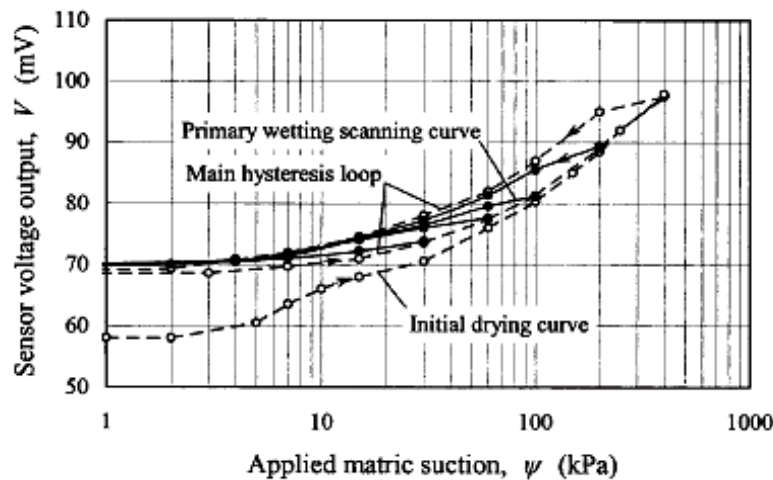
**Figure 2.33** Fredlund thermal conductivity sensor (after Fredlund and Wang, 1989).

Many authors have used TCSs for suction measurements (Phene et al. 1971; Lee and Fredlund, 1984; Rahardjo et al., 1989; Feng et al., 2002; Nichol et al., 2003). Most commercially available TCSs are applicable for suction measurements ranging from about 0 to 300 kPa, with the greatest sensitivity existing for suction less than 175 kPa. Fredlund and Wong (1989) calibrated TCSs using a modified pressure plate apparatus. For suctions above 300 kPa, the calibration curves were found to be highly nonlinear and less accurate. The authors noted that the nonlinear response of the sensors is likely related to the pore size distribution of the ceramic porous block. The TCSs have been

used for both laboratory and field suction measurements by Picornell et al. (1983), van der Raadt et al. (1987), and Sattler and Fredlund (1989). Disadvantages of TCSs include the requirement for a separate calibration curve for each sensor, and potential long-term problems associated with deterioration in the sensor body over time. Advantages include easy set up for automated data acquisition and their relatively low cost. A study by Feng et al. (2002) on the use of TCSs for measuring suction indicates that the TCSs exhibit hysteresis, upon whether water was flowing into the porous block, or out of the porous block. As shown in Figure 2.34, a relatively large gap was found to exist between the initial drying curve and the main hysteresis loop in the low suction range between 1 to 15 kPa. The hysteresis between the water-content of a porous block and matric suction is usually referred to as capillary hysteresis. The effect of hysteresis on calibration curves has to be considered in order to obtain a reliable soil suction measurement.



(a) Primary drying scanning curves



(b) Primary wetting scanning curves

**Figure 2.34** Hysteresis curves for thermal conductivity sensors (Feng et al., 2002).

#### **(d) Dew point sensor**

The dew point sensors measure the dew point and temperature in the vapour space surrounding the soil sample in order to determine the relative humidity (RH) within the closed chamber (Leong et al., 2003; Agus and Schanz, 2003; Agus et al., 2010). Total suction is determined from the measured relative humidity and temperature using Kelvin's equation (Equation 2.1). The dew point is the temperature at which the air can no longer hold all of its water vapour at the same pressure, and some of the water vapour must condense into liquid water. In this technique, two holes are drilled in the soil sample, one for placing the RH sensor and the other one for the temperature sensor (Agus et al., 2010). A PVC pipe is inserted into the hole to accommodate the RH sensor and to prevent direct contact between the sensor and the soil. The RH of salt solutions is usually used for calibration of the RH sensor.

The dew point potentiometer (also known as a chilled-mirror hygrometer) is an instrument for measuring dew point and temperature very accurately in a closed space above the specimen (see Figure 2.35). The dew point potentiometer consists of a mirror and condensation detector with precise temperature sensor inside a sealed chamber. The relative humidity of the air in the chamber is the same as the relative humidity of the specimen at the equilibrium condition. When the first condensation appears on the mirror, the relative vapour pressure (relative humidity) is measured and total suction can be calculated (Leong et al., 2002; Decagon Devices Inc., 2003; Petry and Jiang, 2003; Tang and Cui, 2005; Thakur et al., 2006; Patrick et al., 2007). Due to the rapid suction increase with decreasing relative humidity at low suctions, the dew point potentiometer is considered accurate for suction measurements of above 1000 kPa (Lu and Likos, 2004). In the chilled-mirror hygrometer, isothermal equilibrium between the soil and the vapour space can be maintained accurately since the vapour space is minimised. The device is typically calibrated using standard salt solutions. The difference between dew point and sample temperatures must be kept small. If the sample is cooler than the chamber, equilibration will take longer. If the sample is warmer than the chamber, condensation will occur in the chamber. The accuracy and range of relative humidity measurements by using chilled-mirror hygrometer vary by manufacturer, but are typically in the range 3–99% RH at an accuracy of about  $\pm 3\%$  RH. The main advantages of chilled-mirror hygrometer for soil suction measurement are its simplicity and speed. The suction measurement is automated after placing the sample inside the chamber. The time required for one suction measurement can be as little as 5 min.

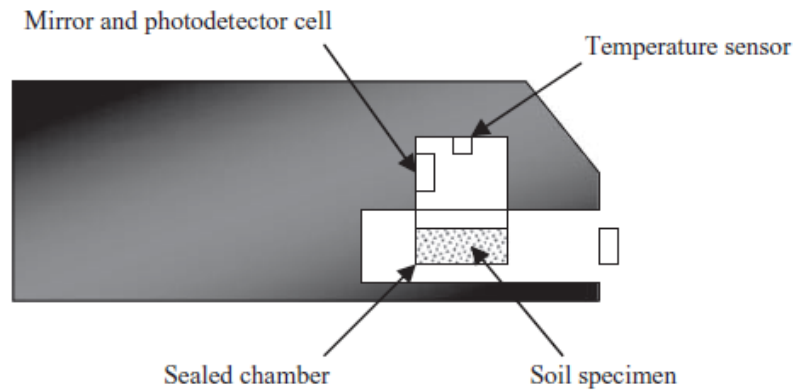


**Figure 2.35** Schematic of chilled mirror dew point hygrometer (after Leong et al., 2003).

#### **2.4.2 Suction control techniques**

Various methods have been adopted for controlling matric or total suction in a soil specimen during unsaturated soil experiments. A brief review of the three methods commonly used for suction control is given here. The description includes axis translation and osmotic techniques for the matric suction control, and the vapour equilibrium technique for the total suction control.

##### **(a) Axis translation technique**

The axis translation technique, or air overpressure technique, is one of the most common techniques for imposing suction. The axis translation technique was first proposed by Hilf (1956) for applying controlled values of suction to a soil sample. The basic principle of this technique is to elevate the pore water pressure and pore air pressure by the same amount so that the matric suction (given by their difference) remains constant; however, the pore water pressure is raised to a positive value and it can be measured using conventional transducers. If the soil is under applied external loads, total stresses must also be elevated by the same amount. As a result of increasing the pore water pressure from a negative to a positive value, the problem of cavitation in the measuring system is prevented. In this technique, both pore water pressure and pore air pressure are controlled and measured independently.

Fredlund (1989) used this technique for the measurement of matric suction in a soil sample. As shown in Figure 2.36, when the soil specimen, with initial negative pore water pressure, is placed on top of the saturated high air-entry disk draws water through the porous disk. This causes the pressure transducer to commence registering a negative value. The test is performed by applying air pressure in the chamber until there is no

further tendency for flow in or out of the soil sample through the high air entry disk. In this way, the water pressure in the measuring system becomes a positive value and the problem of cavitation is prevented. However, it is still possible for air to diffuse into the water through the air-entry filter, as long periods of time are often required for testing unsaturated soils (up to 5 weeks). The diffused air causes an error in either the pore water pressure measurement under undrained testing condition or in the volume change measurement under drained testing conditions.

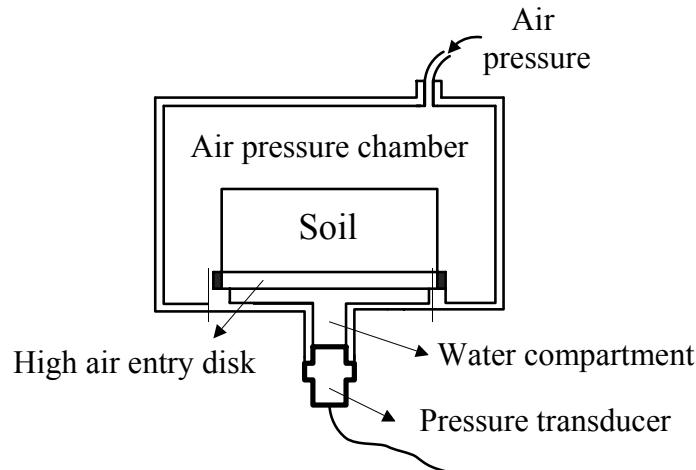


**Figure 2.36** Schematic diagram of the axis translation device used by Fredlund (1989) for measuring matric suction (typical size of a soil sample: 50mm diameter and 20mm height).

The diffused air volume indicator was introduced by Fredlund (1975) in order to flush and measure the volume of the diffused air. The diffused air volume is used to modify the water volume change measurement in drained tests. As noted by Bocking and Fredlund (1980), the main limitation in the use of the axis translation technique is the difficulty of investigating at high degrees of saturation. As the authors pointed out, the axis translation technique can only be used for the soil samples at degrees of saturation less than 80%, beyond which the air phase becomes occluded within the pore water and thus air permeability is effectively zero. In this case, an increase in air pressure results in volumetric strains due to compression of the occluded air bubbles. Dineen and Burland (1995) indicated that the use of the axis translation technique for the soil samples with a degree of saturation in excess of 80% can result in an overestimation of the value of suction prevailing in the soil. When the air phase is discontinuous, control of air pressure is only by diffusion of dissolved air, which is a very slow process. Therefore testing must be very slow if using the axis translation technique for the soil samples with a degree of saturation in excess of 80%.

One of the main problems related to the axis translation technique involves air diffusion through the high air entry value (HAEV) ceramic disc, as long periods of time are often required for testing unsaturated soils. The diffused air bubbles reduce the efficiency of the system and cause a significant error in either the pore-water pressure measurement under undrained testing, or in the volume change measurement under drained testing. To overcome this problem, the air bubbles formed below the HAEV ceramic disc have to be flushed out of the system (Bishop and Donald, 1961; Fredlund et al., 1978; Sivakumar, 1993). The air bubbles (cavity) can grow in a liquid in two ways: slowly or rapidly (Marinho and Chandler, 1995). Slow growth can be as a result of diffusion of dissolved gas into the aqueous phase. Based on Henry's law, air dissolves into water at high air pressure during the saturation process of the HAEV ceramic disc. The pressure in the water below the ceramic disc is a low value, therefore the dissolved air in water diffuses and forms vapour bubbles below the ceramic disc. Rapid air growth (Knapp and Daily, 1970) can be as a result of temperature rise (boiling), or pressure reduction (cavitation).

The axis translation technique has been used by many subsequent researchers (e.g. Cabarkapa et al., 1999; Mohamed et al., 2006; Uchaipichat and Khalili, 2009; François and Laloui, 2010) for testing unsaturated soils. Cabarkapa et al. (1999) used modified triaxial cell for testing unsaturated soils based on the design of Bishop and Wesley's hydraulic triaxial apparatus and using the axis translation technique for applying controlled values of suction to a soil sample. The test was performed by applying air pressure to the top of the specimen at a higher value than pore water pressure applied at the base of the specimen across the HAEV ceramic disk. This enables the top porous disk to be saturated, as water cannot pass into the air line due to the higher pressure of the air. Moreover, air cannot pass into the water line as the HAEV ceramic disk allows only the passage of water but not air. The air pressure will not flow through the pores of the HAEV ceramic disc since they are filled with water. The surface tension of the water in the pores at the air-water interface supports the pressure. The radius of the curvature of the glass-liquid interface decreases when air pressure increases (see Figure 2.37). The maximum air pressure that any given wetted porous ceramic disc can stand before letting air pass through the pore is determined by the diameter of the pores. The smaller the pore size, the higher air pressure will have to be to allow air to pass through. The pressure value that finally breaks down these water menisci is called the air-entry value for the porous ceramic disc.



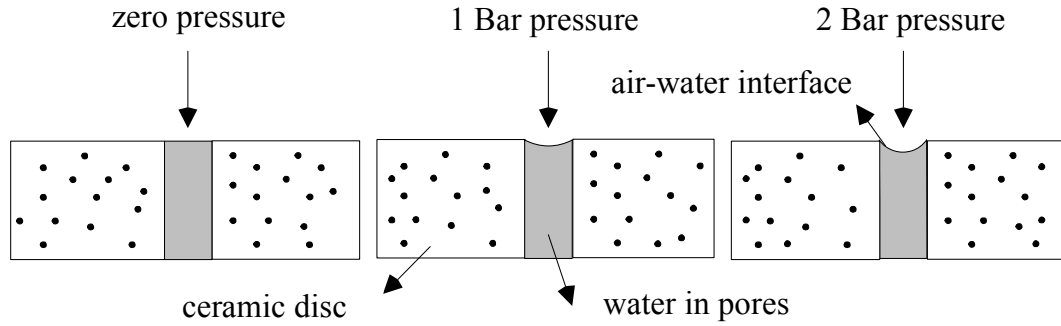


**Figure 2.37** Water menisci in the pores of the ceramic HAEV ceramic disc.

### (b) Osmotic technique

The osmotic technique for applying controlled values of matric suction to a soil sample was first introduced in geotechnical engineering by Kassiff and Ben Shalom (1971), who proposed a new suction controlled oedometer. In this technique, the soil sample is placed in contact with a semi-permeable membrane, behind which a solution of polyethylene glycol (PEG) is circulated. The different concentration of dissolved salts within the soil water and chemical solution results in an osmotic gradient through the membrane. The semi-permeable membrane allows only passage of water but not of the PEG molecules. As a result of the osmotic gradient, water commences to flow from the lower concentration side to the higher concentration side, until equilibrium is established between the matric suction in the soil sample and the osmotic pressure generated by the solution, which is dependent on the concentration of the solution.

The osmotic technique is therefore used to control matric suction rather than osmotic suction and is defined as the difference between the osmotic suction of the chemical solution and the soil water. In order to use the osmotic system, Cui (1993) proposed an empirical relationship between PEG concentration and matric suction, ranging from 0 to 1.5 MPa, as follows:

$$s = 11c^2 \quad (2.9)$$

In this equation  $s$  refers to matric suction in MPa and  $c$  to the concentration of the PEG solution expressed in gram of PEG per gram of water. This empirical relationship is based on the values of matric suction measured directly in the soil, and not on the relative humidity calculations. The osmotic technique has been used by several subsequent researchers, including Delage et al. (1987), Cui and Delage (1996), De Gennaro et al. (2004), Cuisinier and Masrouri (2005) and Monroy et al. (2007), for

testing unsaturated soils. Cuisinier and Masrouri (2005) proposed a modified oedometer testing device, using an osmotic technique for applying controlled values of suction to the soil sample. The test was performed by circulating a PEG solution at a given concentration through the whole bottom surface of the soil sample by means of a pump. A schematic representation of the osmotic oedometer is shown in Figure 2.38. The semi-permeable membrane is introduced between the soil sample and solution to prevent passage of PEG molecules. Using the osmotic technique, a large value of suction up to 12 MPa can be imposed on the samples, with no need for high air and water pressure. One of the problems related to the osmotic technique involves the progressive degradation of the semi-permeable membrane with time which leads to a gradual reduction in suction (Cunningham, 2000). To overcome this problem, the use of a synthetic membrane instead of cellulosic membrane has been proposed. In order to obtain a calibration curve between osmotic pressure and concentration of solution, the authors placed a tensiometer in direct contact with the membrane through a 1 mm layer of kaolin for measuring suction. Different concentrations of solution were circulated underneath the synthetic membrane by means of a peristaltic pump and the response of the tensiometer was recorded. In order to avoid seepage losses around the perimeter of the membrane, the pump was operated in a such a manner as to allow the solution to circulate at a pressure below atmospheric pressure. In addition, the pump flow was reduced to a minimum rate in order to prevent air being drawn into the circulating system.

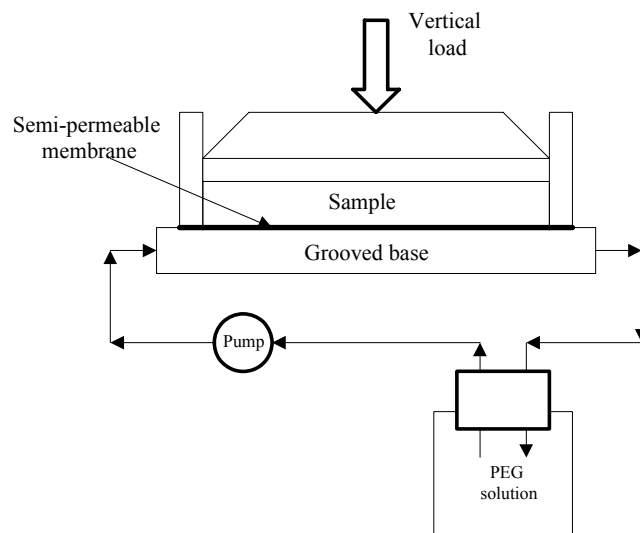


**Figure 2.38** Schematic of the suction-controlled oedometer device using osmotic solutions (Cuisinier and Masrouri, 2005).

Taibi et al. (2005) indicated that the membrane is very sensitive to high temperatures. They observed significant variation in experimental results for tests performed at high

temperatures, therefore a precise calibration equation for different temperatures is needed. The fragility of the semi-permeable membrane, its low mechanical resistance to shearing and its sensitivity to bacterial attack requires a specific experimental test procedure in order to avoid damaging the membrane. Delage et al. (2001) showed that effectiveness of the semi-permeable membrane may be unsatisfactory undergoing wetting process, which leads to inaccurate results.

### **(c) Relative humidity technique**

The relative humidity technique (also called vapour equilibrium technique) has been used by many authors for imposing suction (e.g. Tessier, 1984; Romero, 1999; Delage and Cui, 2000; Villar, 2000). This technique is based on the control of the relative humidity of the air surrounding the soil sample by using a chemical solution (see Figure 2.39). The osmotic potential of the chemical solution forces the air and the soil samples to reach equilibrium in a closed system. If the initial  $S_r$  of the soil sample is less than that required for equilibrium, water vapour will condense to the soil until equilibrium is reached. In this case, the equilibrium  $S_r$  of the soil sample will be on a wetting path of the SWRC. If the initial  $S_r$  of the sample is greater than that required for equilibrium, the pore water evaporates until equilibrium is reached. The equilibrium  $S_r$  of the sample will be on a drying path of the SWRC. There are three different types of chemical solutions typically employed for the constant suction experiments: unsaturated acid solutions, saturated salt solutions and salt solutions at different concentrations. The benefit of using the saturated salt solutions is the consistency of the concentration of the osmotic solution during the equalisation period. The main advantage of the relative humidity technique is that very high suction can be applied using dry atmospheres. The major drawback associated with this technique is that vapour exchange for controlling suction is a very slow process, as a consequence of which very long periods of time are required to reach equilibrium. The time required for suction equalisation depends on the mass of the soil sample, volume of testing chamber, and the difference between initial and equilibrium  $S_r$  of the sample. Kelvin's equation and relative humidity imposed by the saturated saline solution depend on temperature (Delage et al., 1998), therefore special care should be taken to control the accuracy of non-isothermal tests. The relative humidity technique is not suitable for low values of suction, since the relationship between total suction and RH becomes extremely steep at suction values less than 1000 kPa (referring to Figure 2.31). Therefore, the vapour equilibrium technique is often used

in conjunction with other techniques applicable at low values of suction to determine SWRCs over a wide range of suction.

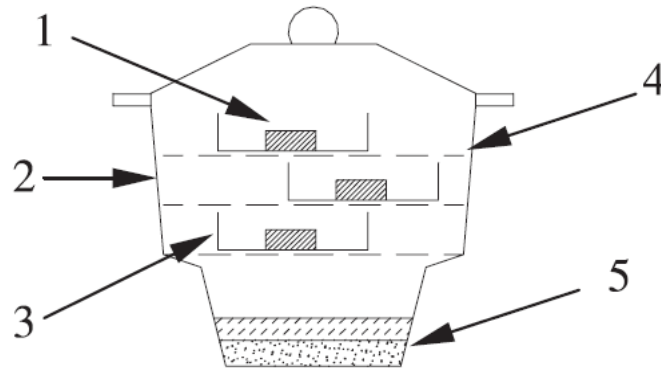


**Figure 2.39** Imposing suction in a desiccator (Tang and Cui, 2005), 1. Soil sample, 2. Desiccator, 3. Glass cup, 4. Support, 5. Salt solution.

## 2.5 Chapter summary

This chapter describes the main features of the thermo-hydro-mechanical behaviour of unsaturated soils and the most relevant testing techniques. Various methods of suction measurement are summarised. Soil suction can be measured by direct or indirect methods. The direct methods measure the suction (i.e. negative pore water pressure) directly, while the indirect methods measure other parameters such as relative humidity, conductivity or water-content and then relate these results to the suction through calibration curves. The direct methods (including tensiometers and the axis translation technique) only measure matric suction. The indirect methods (including filter paper method, thermal conductivity sensors, and dew point sensors) can measure both total and matric suctions, and require isothermal equilibrium between the sensor, soil and the vapour space around the sample. Figure 2.40 shows approximate ranges of various methods used for measuring suction.

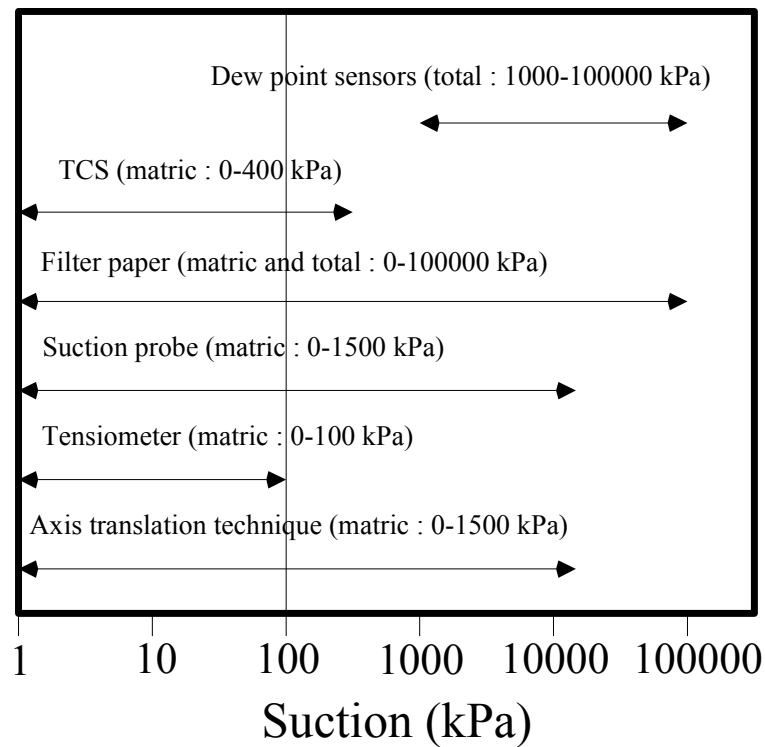


**Figure 2.40** Suction measurement ranges of various methods.

The commonly used techniques (including the axis translation technique, the vapour equilibrium technique and osmotic technique) for control of suction are described in this chapter. Table 2.1 summarises advantages and limitations of each technique.

**Table 2.1** Comparison of different techniques for control of suction.

Method	Axis translation	Vapour equilibrium	Osmotic
<b>Advantage</b>	The main benefit of this technique is the relative simplicity of the method.	The test does not require any special equipment, and is very easy to set up. Very high suction can be applied using dry atmospheres.	A large value of suction up to 12 MPa can be imposed on the samples, with no need for high air and water pressure.
<b>Disadvantage Limit</b>	The maximum matric suction that can be measured is limited by the air-entry value of the ceramic disk used. It is still possible for air to diffuse into the water through the air-entry, as long periods of time are often required for testing unsaturated soils.	Long period of equilibrium time and strict temperature control are required.	Good contact is required between the sample and the membrane. The fragility of the membrane and its sensitivity to bacterial attack and high temperatures require specific attention.

Table 2.2 summarises the advantages and limitations of various techniques for soil suction measurements.

**Table 2.2** Comparison of different suction measurement techniques.

Method	Advantage	Limit / Disadvantage
<b>Filter paper</b>	<ol style="list-style-type: none"> <li>1. Low cost</li> <li>2. Cover entire range of suction measurement</li> </ol>	<ol style="list-style-type: none"> <li>1. Calibration process is sensitive to the equalisation time.</li> <li>2. Precise temperature control is required.</li> </ol>
<b>Tensiometer</b>	<ol style="list-style-type: none"> <li>1. Relatively quick response</li> <li>2. Low cost</li> <li>3. Lab and field measurements</li> </ol>	<ol style="list-style-type: none"> <li>1. Cavitation limits measurement to less than 100 kPa.</li> <li>- Modified version of tensiometers (suction probe) allows the measurement of suction up to 1.5 MPa, corresponding to the air-entry value of the porous filter used. High suction tensiometers have poor sensitivity in the low suction range.</li> </ol>
<b>Thermal conductivity sensor</b>	<ol style="list-style-type: none"> <li>1. Long term automatic measurement</li> <li>2. Lab and field measurements</li> </ol>	<ol style="list-style-type: none"> <li>1. Temperature change influence the accuracy of the thermal conductivity sensors.</li> <li>2. There is hysteresis in the soil suction measurement when using thermal conductivity sensors.</li> </ol>
<b>Dew point sensor</b>	<ol style="list-style-type: none"> <li>1. Accurate method for total suction measurements above 1000 kPa</li> </ol>	<ol style="list-style-type: none"> <li>1. Constant temperature environment</li> <li>2. The difference between dew point and sample temperatures must be kept small</li> <li>3. Generally for lab measurement</li> </ol>
<b>Axis translation</b>	<ol style="list-style-type: none"> <li>1. No cavitation</li> <li>2. High suction measurement</li> </ol>	<ol style="list-style-type: none"> <li>1. Long equilibrium time for high suction values</li> <li>2. Diffusion difficulties</li> <li>3. Only for lab measurement</li> <li>4. Best for suction control than measurement</li> </ol>

## CHAPTER 3 – EXPERIMENTAL PROGRAMME

### 3.1 Introduction

In order to study the effects of temperature on the hydro-mechanical behaviour of kaolin clay, an experimental programme has been designed for testing specimens under controlled conditions. This chapter presents the physical characteristics of the material under study and describes experimental tests performed in this research. The sample preparation methods, experimental techniques and procedures that were adopted in this study are presented. In order to perform the tests at different temperatures, two large temperature-controlled chambers were employed. The chambers maintained the desired temperature within  $\pm 0.1^\circ\text{C}$ .

### 3.2 Characteristics of the material

The soil used in this study is a kaolin clay, with properties shown in Table 3.1. The kaolin clay was supplied by Whitfield & Son Ltd., England. The liquid and plastic limits of the material were obtained following procedures adopted in the British Standard BS 1377. The cone penetrometer method was used to obtain the liquid limit. The specific gravity of the clay was obtained as 2.64, which is consistent with data reported in the literature (e.g. Prashant and Penumadu, 2004). The hydrometer method (BS 1377) was used to determine the distribution of the silt/clay particles. Figure 3.1 presents the particle size distribution of the kaolin, and shows that about 98% by weight is smaller than 0.02 mm and 42% is smaller than 0.002 mm. Figure 3.2 shows the compaction curve obtained following the British Standard BS 1377 (Standard Proctor). From the compaction curve, the optimal water-content was found to be approximately 23.8 % and the maximum dry unit weight was approximately 15.58 kN/m<sup>3</sup>.

**Table 3.1** Physical properties of kaolin clay used in this study.

Property	Value
Liquid limit: %	55.0
Plastic limit: %	31.4
Specific gravity	2.64
Silt fraction: %	58
Clay fraction: %	42
Maximum dry unit weight: kN/m <sup>3</sup>	15.58
Optimum water-content: %	23.8

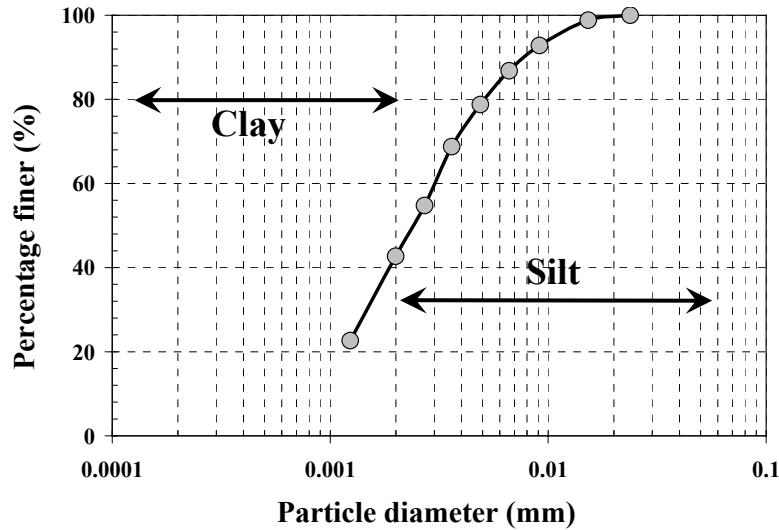


**Figure 3.1** Particle size distribution of the studies material obtained by hydrometer test.

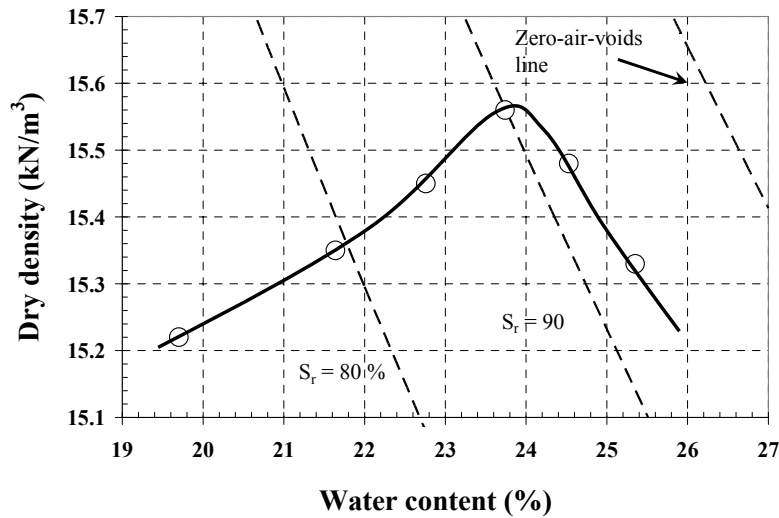


**Figure 3.2** Compaction curve of kaolin clay obtained following BS 1377 (Standard Proctor).

The mineralogical composition of the kaolin was obtained by means of X-ray diffraction. Clay minerals found in the material are summarised in Table 3.2. The equipment used for qualitative characterization of the mineralogical composition of the material was a Bruker Siemens D8 advanced X-ray diffractometer. The X-ray sample was prepared by mixing kaolin clay with deionised water thoroughly to get a homogeneous material, and then statically compacted in the sample holder to reach the desired dry density. The X-ray diffraction test was carried out for  $2\theta$  between  $10^\circ$  to  $80^\circ$  because kaolin clay shows most of its significant peaks within this range (Sachan and Penumadu, 2007). The X-ray diffraction pattern consists of a series of peaks with different intensities and corresponding  $2\theta$  values. The X-ray diffraction pattern of the



sample is given in Figure 3.3. In order to identify the principal clay minerals which exist in the soil sample, the pattern is compared to a large database of mineral patterns.

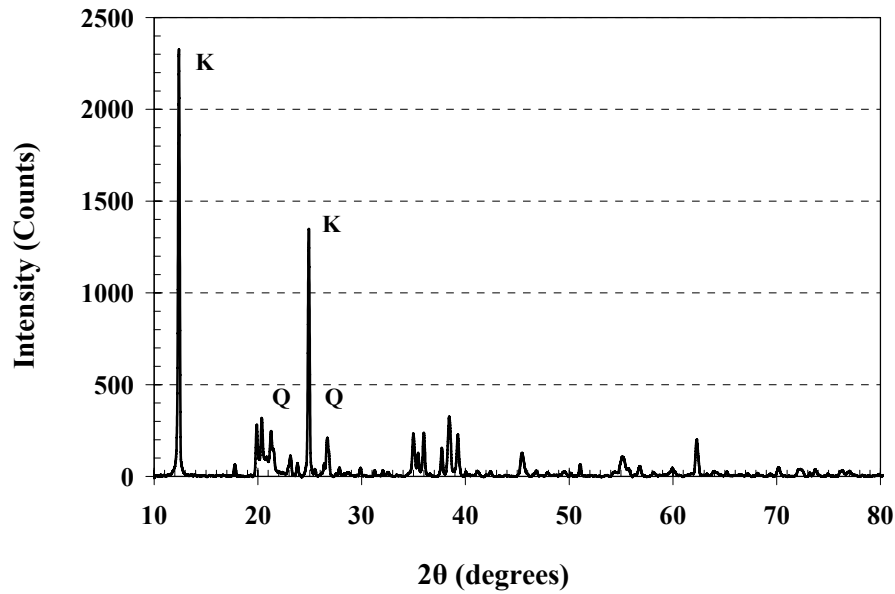


**Figure 3.3** X-ray diffraction pattern of kaolin clay.

**Table 3.2** Mineralogy of the studied kaolin clay.

Minerals	(%)
Kaolinite	82
Quartz	15
Illite and Mica	3

### 3.3 Experimental test programme

#### 3.3.1 Filter paper calibration test using vapour equilibrium technique

The filter paper calibration tests for the Whatman No. 42 filter paper were performed at different temperatures using NaCl salt solutions as an osmotic potential source for suctions above 500 kPa. Ranges of relative humidity were generated using sodium chloride concentrations from 0.001 to 2.1 molar. Aqueous solutions of different salt concentrations used in this work were prepared gravimetrically in the laboratory. The sodium chloride used was of analytical reagent grade, with a reported purity of >99% for anhydrous NaCl. The salt solutions were prepared using deionised water throughout the experimental work.

Two filter papers were simply placed above the salt solutions in sealed glass jars with screw top lids. The filter papers for the calibration test were oven dried, as they needed to be treated against bacterial and fungal growth prior to being placed in contact with

soil samples in order to obtain SWRCs. A PVC support was placed inside glass jars to accommodate the filter papers over the salt solution. As proposed by Houston et al. (1994), the glass jar lids were coated with mineral oil before closing, and then sealed properly with several layers of Parafilm sealing film. Each glass jar (with a 250 ml capacity) was filled with approximately 120 ml of solution with a known concentration of NaCl, leaving an air volume of approximately 80 ml for equilibrium. The distance between the filter papers and the liquid surface was kept to less than 1 cm, as recommended by Marinho (1994b). The glass jars were then placed inside a temperature controlled chamber and tilted 10 to 20° in order to prevent water droplets formed from condensation falling onto the filter papers. The glass jars were left in the temperature chamber for a period of 14 days to ensure that equilibrium was reached. The chamber maintained the desired temperature within  $\pm 0.1^\circ\text{C}$ . After this period, the glass jars were carefully opened and the water-contents of the filter paper were then measured using a scientific balance, weighing accurately to 0.0001g. In order to minimize moisture loss during the weighing process, the filter papers were quickly placed inside plastic containers after removing them from the glass jars.

In a closed system and under isothermal conditions, the partial pressure of the water vapour in the air space above the deionised water at equilibrium is equal to the saturated vapour pressure. The partial pressure of the water vapour, and therefore the relative humidity, over a salt solution is less than that over pure water. Total suction values corresponding to each relative humidity can be calculated using Kelvin's equation (Equation 2.1). In this study, the total suction was obtained using data presented by Clarke and Glew (1985) relating the partial water vapour pressure to the concentration of sodium chloride for a range of temperatures. The relative humidity of the air in equilibrium with sodium chloride solutions was calculated by dividing the water vapour pressure of solutions (with a known amount of salt concentration) by the vapour pressure of pure water at the same temperature. It should be pointed out that a change in temperature will affect the thermodynamic properties of the fluid. Thus, the effect of temperature on molecular volume of water in Kelvin's equation is taken into account in order to obtain a reliable measurement.

### **3.3.2 Filter paper calibration test using axis translation technique**

The filter paper calibration data for suction values of less than 500 kPa were obtained by using the pressure plate apparatus (axis translation technique). Three pressure plate

apparatuses were designed and built in stainless steel. Figures 3.4 and 3.5 show an image of the designed pressure plate cell and the cell dimensions, respectively. The pressure plate apparatuses were employed to work simultaneously in order to impose ranges of suction values. Figure 3.6 shows a schematic of the arrangement of the pressure plates. The water pressure was applied using a GDS digital pressure/volume controller through the HAEV ceramic disc beneath the soil sample. 15 bar HAEV ceramic discs were fixed to the pressure plate cells with a special epoxy resin to avoid water leakage through them. The air pressure was applied by using a compressed air system with air regulators.



**Figure 3.4** The designed pressure plate cell.

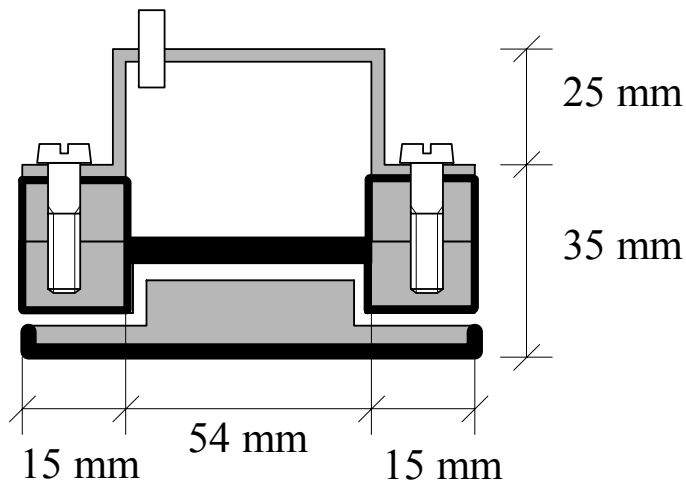


**Figure 3.5** The pressure plate cell dimensions.

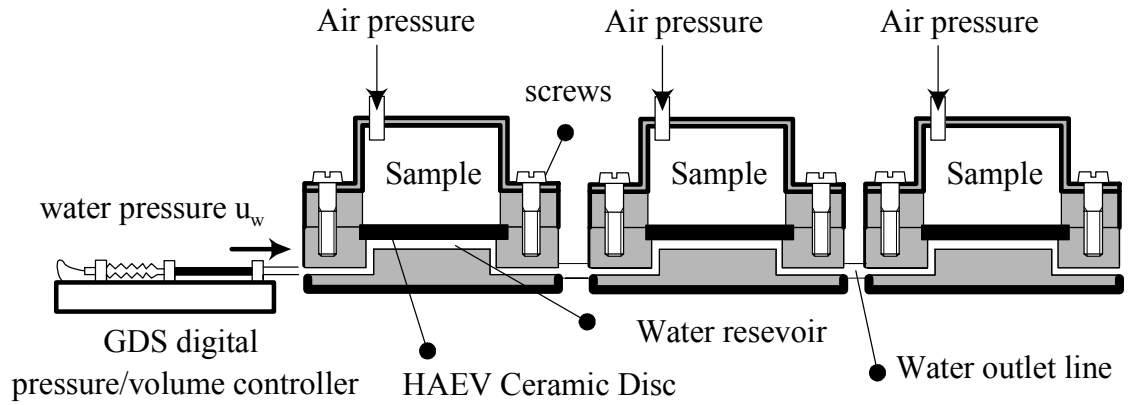


**Figure 3.6** Schematic diagram of the pressure plate apparatuses.

The HAEV ceramic disc was fully saturated before each test. The ceramic disc was used as an interface between the soil sample and pore water pressure system. In order to saturate the HAEV ceramic disc, the pressure plate cell was filled with deaired water and pressurised under constant value of 300 kPa under drained conditions. The procedure used in this research involved three cycles of pressurised water to ensure saturation of the ceramic disc (as suggested by François and Laloui, 2010). The ceramic disc was re-saturated after completing each suction controlled test, particularly under high temperature testing. Prior to each test, the air bubbles which formed below the HAEV ceramic disc were flushed out through the outlet line. Flushing the air bubbles helps to inhibit loss of continuity between the soil pore-water and water in the measuring system. This is particularly important at higher temperatures, as the rate of diffusion increases with temperature. In this research, the volume of diffused air accumulated beneath the ceramic disc was not recorded, as the tests performed in our specific case are not in terms of volume changes.

After saturation of the HAEV ceramic discs, soil samples (50mm diameter and 20mm height) were placed over the ceramic disc in pressure plate apparatuses. The sample preparation method and initial condition of soil samples are presented in section 3.3.3. One filter paper was sandwiched between two larger size filter papers and placed in between the soil samples. The two external papers are to prevent contamination of the middle filter paper by soil. The arrangement of the soil sample and the filter papers were then placed on the HAEV ceramic discs in pressure plate apparatuses. The continuity between soil water and water in the ceramic disc is very important. Therefore, a thin layer of water was left over the HAEV ceramic disc during the setting up process; in this way, the ceramic saturation was ensured thus preventing the possibility of its de-saturation due to air contact, particularly at high temperatures. The pressure plate

apparatus was placed inside the temperature chamber to maintain the desired temperature during the test. Pore-water-pressure was controlled through the ceramic disc beneath the soil sample using a GDS digital pressure/volume controller and air pressure was applied by a compressed air system with air regulators. After 14 days equilibration time, the water-contents of the filter papers and the soil specimens were determined. The relationship between the imposed suction and the water-content of the filter papers represents the filter paper calibration curve.

### 3.3.3 Soil water retention curves

The soil water retention curves (SWRC) for the kaolin clay samples were determined using the filter paper and axis translation techniques. The soil samples were prepared by mixing deionised water thoroughly into the oven-dried soil to obtain a homogenous material, which was then statically compacted into a mould to obtain the desired initial void ratio. Forty-five soil specimens (64mm diameter and 24mm height) were prepared under static compaction with the same void ratio of 1.5 at two different water contents of 9.4% and 51.8% in order to obtain wetting and drying paths of the SWRC. Initial conditions of the soil specimens are presented in Table 3.3. In order to obtain drying and wetting paths, some of these cylindrical samples with the high initial degrees of saturation were dried in the atmosphere and the others, with the low initial degrees of saturation, were wetted in a humidification chamber with 100% relative humidity. After achieving the desired water-content, each sample was wrapped thoroughly with several layers of cling film to equalise for a minimum of three days.

**Table 3.3** Initial condition of the soil specimens.

	$w_0$	$e_0$	$Sr_0$
Wetting Path	9.4 %	1.5	16.5 %
Drying Path	51.8 %	1.5	91.2 %

As mentioned in section 2.2.3, the dry of optimum compacted soils generally tend to exhibit a bimodal PSD; whereas soils compacted wet of optimum tend to show a more homogenous matrix-dominated fabric with a unimodal PSD. The samples compacted wet and dry of optimum may have entirely different fabric and this structural difference results in a difference in hydraulic characteristics, water retention and stress-strain behaviour of the samples. In this thesis therefore, the influence of temperature on drying path of samples compacted wet of optimum ( $w_0 = 51.8\%$ ), and on wetting path of samples compacted dry of optimum ( $w_0 = 9.4\%$ ) is investigated separately.

The procedure used in this research (for filter paper suction measurements) is similar to that proposed by Bulut et al. (2001) and is based on the ASTM D 5298 (1997). Whatman No. 42 filter paper was used in this study. One filter paper was sandwiched between two larger-sized filter papers and placed in between the two soil samples to ensure hydraulic continuity between the soil pore water and the water absorbed in the filter papers. If the filter papers were allowed to absorb water through fluid flow, salt would get into the filter papers and consequently the osmotic gradient would be negligible, then only matric suction would be measured. Prior to sandwiching, the filter papers were treated with 0.02% by weight mercury chloride ( $\text{HgCl}_2$ ) solution (Houston et al., 1994) to avoid fungal and bacterial growth (especially at high temperatures), and then they were oven-dried. In order to measure the total suction of the soil samples, one piece of filter paper was placed above a PVC O-ring on the face of each sample. This is to prevent hydraulic continuity between the filter paper and the soil sample. If the filter paper is allowed to absorb water through the vapour phase, both capillary and osmotic gradients exist between the soil sample and the filter paper, and then total suction is measured. The arrangement of the soil samples and the filter papers, shown schematically in Figure 3.7, was subsequently placed inside a glass jar. The glass jar was sealed and placed inside the constant temperature chamber for 14 days.

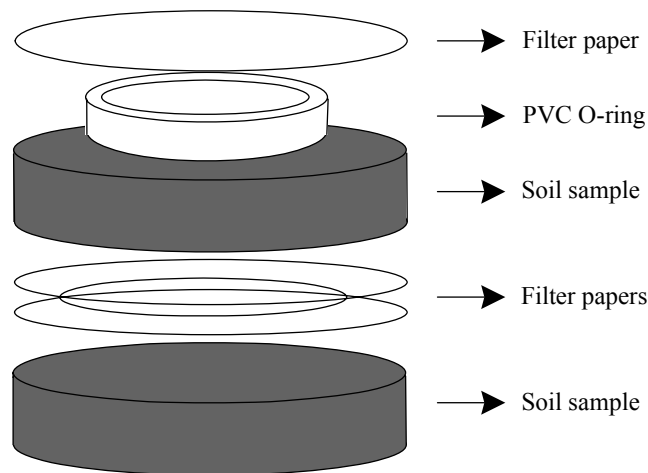


**Figure 3.7** Arrangement of the soil samples and filter papers.

At the end of the equilibration period, the water-contents of each filter paper and the soil specimens were determined by oven-drying at  $105^{\circ}\text{C}$  for 24 hours. When equilibrium is reached a longer time can be taken to remove the filter paper from the soil sample. However, to use a calibration curve obtained at a non-equilibrium condition (such as the calibration equations proposed by Leong et al., 2002) the same time as the calibration

time should be taken during the suction measurement (Haghighi et al., 2011). The suction of the soil samples was calculated from the water-content of the filter papers, using the proposed calibration equation. Figure 3.8 shows the experimental procedure of the filter paper suction measurements performed in this study.

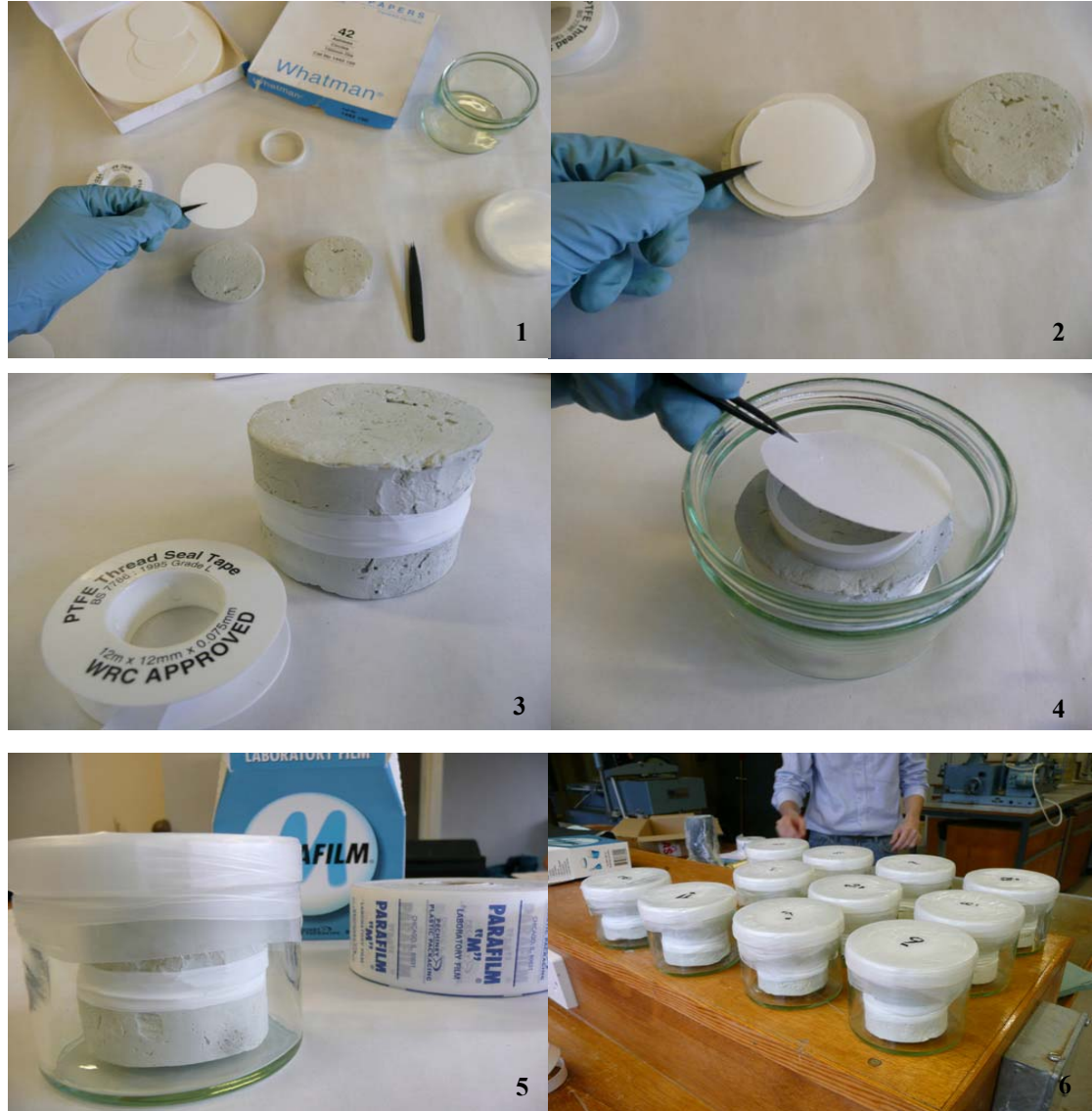


**Figure 3.8** Experimental procedure of the filter paper suction measurements (1) cutting the filter papers to the correct size (2) using tweezers for sandwiching the filter papers (3) taping two pieces of soil samples together (4) placing the arrangement of samples and filter papers in glass jars (5) sealing the glass jars (6) samples ready to be placed inside the temperature chamber.

The SWRC for kaolin clay samples were also determined using the axis translation technique for suction values of less than 500 kPa. The soil samples (50mm diameter and 20mm height) were prepared with the initial conditions presented in Table 3.3. The soil samples were placed over the fully saturated ceramic discs, inside the pressure plate apparatus. The water pressure of 10 kPa was applied through ceramic discs beneath the soil samples using a GDS digital pressure/volume controller. By applying different

values of air pressure (by using air regulators), matric suction ranging between 100 and 300 kPa was imposed and controlled in the soil samples. The pressure plates were placed inside a temperature chamber which allows temperatures to be controlled between  $\pm 0.1^\circ\text{C}$ . An equilibration period of 14 days was used to ensure suction equalisation. At the end of the equilibration time, water-content of the soil samples was determined. The relationship between applied matric suction and the water-content of samples represent the SWRC.

In order to ensure suction equalisation when performing the pressure plate tests, the GDS pressure/volume controller was connected to a computer and water volume movement during the test was recorded after every 20 seconds. It was observed that after seven days the water volume movement through the sample is less than 30 ( $\text{mm}^3/\text{day}$ ). The water volume movement of 30 ( $\text{mm}^3/\text{day}$ ) is equal to 0.03 gram of water per day which is equal to approximately 0.08% change in the soil water-content. This water volume movement is small enough to consider that the sample inside the pressure plate has reached the equilibrium condition.

### 3.3.4 Collapse behaviour

The collapse behaviour of kaolin clay samples has been studied in this experimental programme for a stress level between 5 to 400 kPa, using double and single point oedometer tests. Jennings and Knight (1957) proposed the double oedometer test method which consists of testing two nominally identical samples. One sample is initially saturated with deionised water under a small seating load and allowed to collapse. After equilibrium is reached, the soil sample is loaded according to standard incremental loading procedure. The other sample is tested at the as-compacted water-content using standard incremental loading procedure. The vertical strain difference between the saturated and as-compacted samples was determined as the collapse potential of the sample. Figure 3.9 shows typical results from a double oedometer test. The collapse potentials of the soil samples were found according to the following equation based on the proposition of Jennings and Knight (1975) and defined by ASTM D 5333 (ASTM 2003):

$$\text{Collapse potential} = \frac{e_i - e_f}{1 + e_0} \quad (3.2)$$



In this equation  $e_0$  refers to initial void ratio and  $e_i$  and  $e_f$  are the values of void ratio obtained from the oedometer curves in as-compacted and wetted conditions respectively, under the same applied vertical stress.

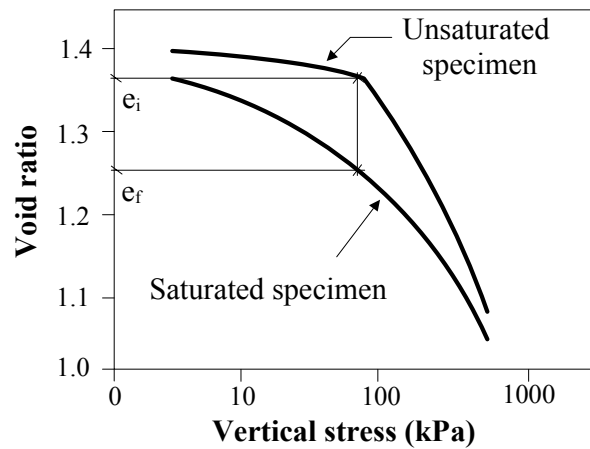


**Figure 3.9** Typical results from double oedometer test.

The collapse potential of the samples was also determined from single-point oedometer test results. The test was performed according to ASTM D 5333. In this method the soil sample was incrementally loaded at its natural water-content until reaching the desired vertical stress; then inundated after which deformation readings were recorded. Water was added until both the specimen and the top cap were fully under water in the cell. The vertical strain difference due to wetting under applied vertical stress after stabilising is determined as the collapse potential of the test specimen. Figure 3.10 shows typical results from a single-point oedometer test.

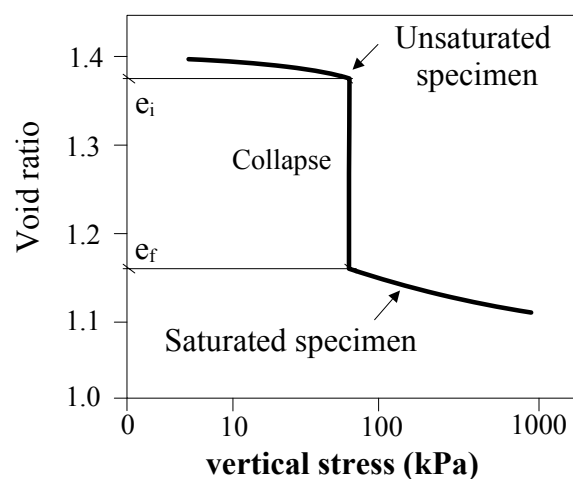


**Figure 3.10** Typical results from single point oedometer test.

The double oedometer test provides a better understanding of the soil behaviour rather than single-point oedometer test, since the volume change behaviour due to wetting is

dependent on net stress level. As mentioned in section 2.3.2, wetting may induce either collapse or swelling strains depending on the stress path. Normally, wetting the soil under a low value of applied net stress results in an increase of volume (swell), while a decrease in volume (collapse) occurs at a high value of net stress. For stress paths remaining inside the yield surface a decrease in suction (i.e. wetting the sample) produce elastic swelling. Once the stress state reaches the yield surface, a further reduction in suction produces plastic compression.

### **3.3.5 Temperature and suction controlled oedometer**

A new suction controlled oedometer cell was designed and built in stainless steel according to the diagram shown in Figure 3.11. Figure 3.12 shows the oedometer cell dimensions. The oedometer cell is cylindrical in shape with a diameter of 100 mm and height of 70 mm. In order to control the temperature during the tests, the cell was placed inside a temperature chamber which allows temperature to be controlled between  $\pm 0.1^{\circ}\text{C}$ . Based on the limitations related to osmotic and vapour equilibrium techniques summarised in Chapter 2, the axis translation technique was chosen as the most suitable technique for imposing suction into the soil samples. Figure 3.13 shows an image of the oedometer cell with all tubing connections. The applied vertical pressure, the pore air pressure and pore water pressure were controlled using three independent devices. The water pressure was controlled through a high air-entry value (HAEV) ceramic disc beneath the soil sample, using a GDS digital pressure/volume controller. The benefit of using a GDS digital pressure/volume controller is measuring the amount of water extracted or injected into the soil sample while applying pressure. The GDS system is designed so that one step of the motor causes the piston to displace  $1\text{ mm}^3$  of volume. Pressure and volume changes are displayed digitally on its control panel.

The pore air pressure was applied to the upper porous stone through a conduit in the loading ram. The air pressure was applied by using a compressed air system with air regulators. Diaphragm pressure was applied by means of pressurised air acting on a loading ram separated by a 1mm thick flexible membrane from the lower chamber. A HAEV (15 bar) ceramic disc with air-entry higher than the maximum applied suction (500 kPa) was fixed to the oedometer cell with a special epoxy resin to avoid water leakage through them and to allow differential expansion between the ceramic disc and the cell with increasing temperature (no fine cracks appear upon heating). The HAEV ceramic disc acts as a link between the soil pore-water and the water in the pressure

controller and avoids passage of free air into the water measuring system. The vertical displacement was measured using an LVDT displacement transducer which was connected on top of the loading ram. A computer continually recorded the vertical displacements. An o-ring groove is formed in the loading cap in order to create an airtight chamber between the loading ram and the membrane.

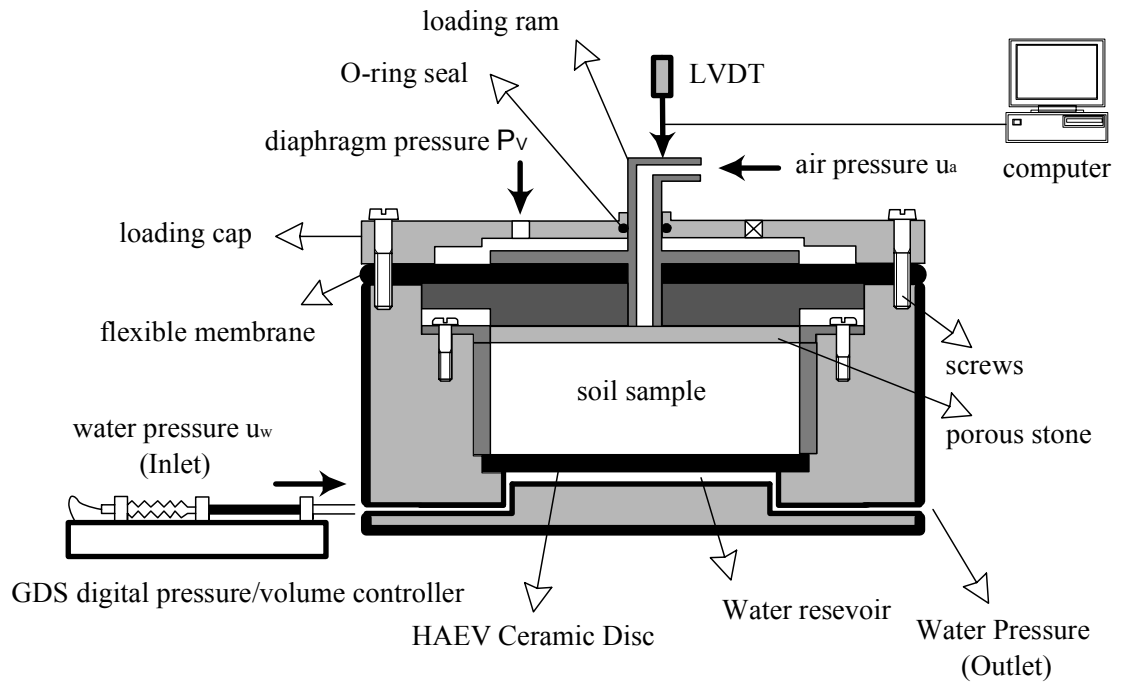


**Figure 3.11** Schematic diagram of the suction-controlled oedometer cell.

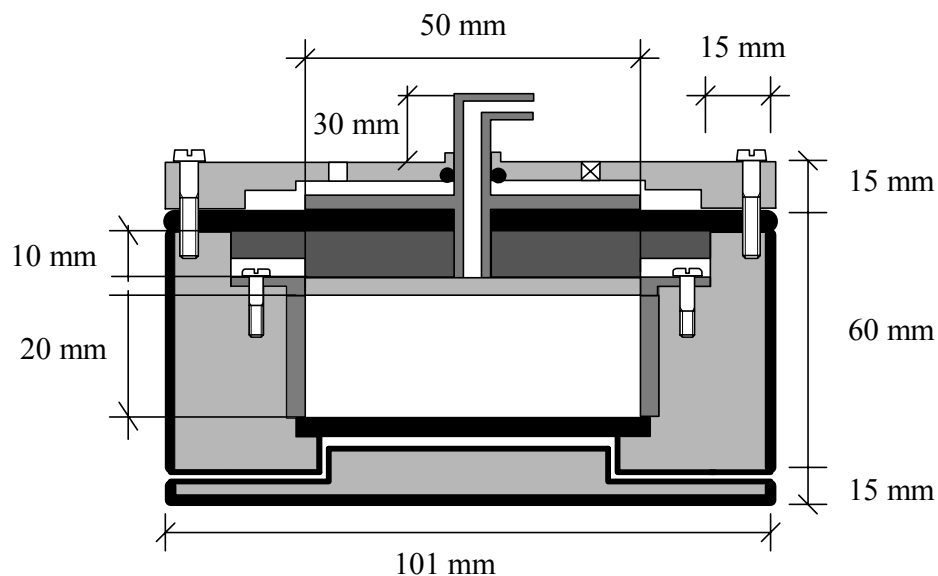


**Figure 3.12** The suction-controlled oedometer cell dimensions.



**Figure 3.13** (a) The designed suction-controlled oedometer cell (b) Details of the cell.

#### **(a) Calibration of the oedometer**

When performing suction-controlled oedometer tests, special care was taken in order to calibrate for vertical load application. The vertical load transmitted by the membrane to the soil sample differs from the pressure applied through the air pressure regulator. This difference is because of the friction occurring between the loading ram and the o-ring seal (see Figure 3.11), and also the gap which exists between the loading platen and the membrane at higher diaphragm deformations. The membrane also takes up some energy during deformation. This difference had to be quantified with respect to the applied vertical pressure during mechanical loading.

Calculated net vertical stress  $(\sigma_v - u_a)_T$  exerted by the diaphragm pressure ( $P_v$ ) in conjunction with applied air pressure ( $u_a$ ) can theoretically be determined by considering vertical equilibrium to the following expression (refer to Figure 3.14):

$$(\sigma_v - u_a)_T = \frac{(A_p - A_r) \times P_v - (A_p - A_a) \times u_a}{A} \quad (3.3)$$

where  $A_p$  is the loading platen or piston area (diameter = 81.70mm),  $A_r$  the ram area (diameter = 12.76mm),  $A_a$  the air pressure conduit area (diameter = 9.24mm), and  $A$  is the coarse porous stone area (diameter = 49.92mm) in contact with the soil sample. Equation 3.3 is adequate if a total contact is ensured between membrane and the loading platen. However, the membrane deforms due to the applied diaphragm pressure, and a certain gap exists between the membrane and the loading platen that affects the net load applied on the soil sample. Figure 3.15 presents the theoretical calculated net vertical stresses (using Equation 3.3) for a range of diaphragm pressure, at different air pressure values. From the figure it can be observed that the calculated theoretical lines are parallel with following equation:

$$(\sigma_v - u_a)_T = 2.61 \times P_v - 2.64 \times u_a \quad (3.4)$$

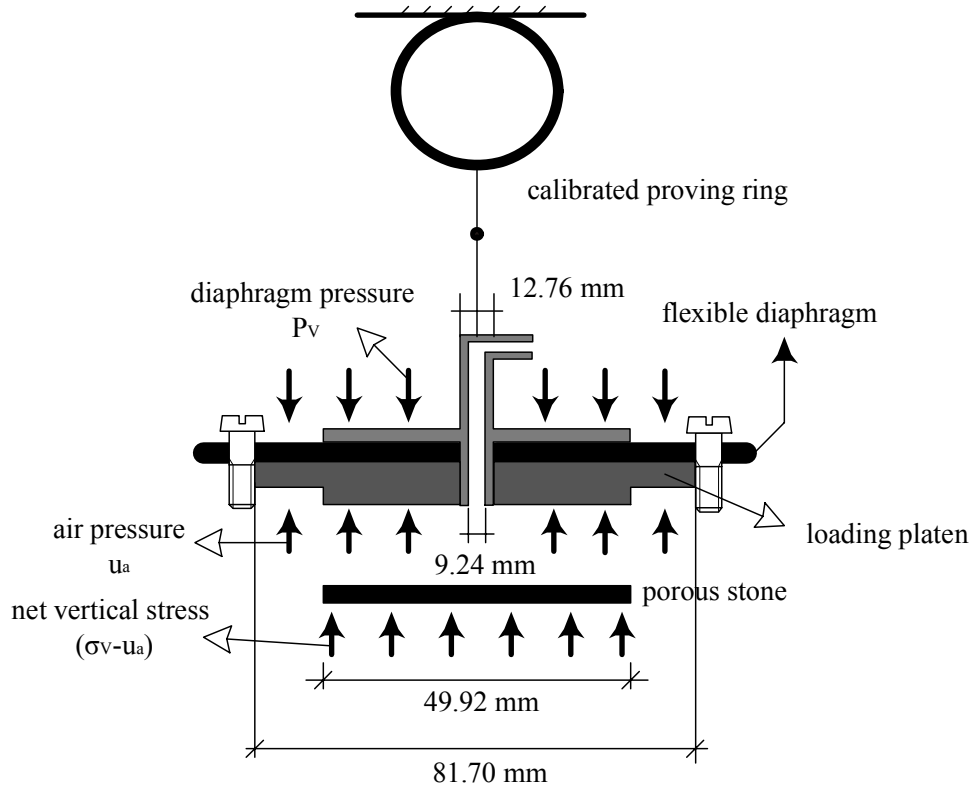


**Figure 3.14** Arrangement of static calibration for diaphragm pressure.

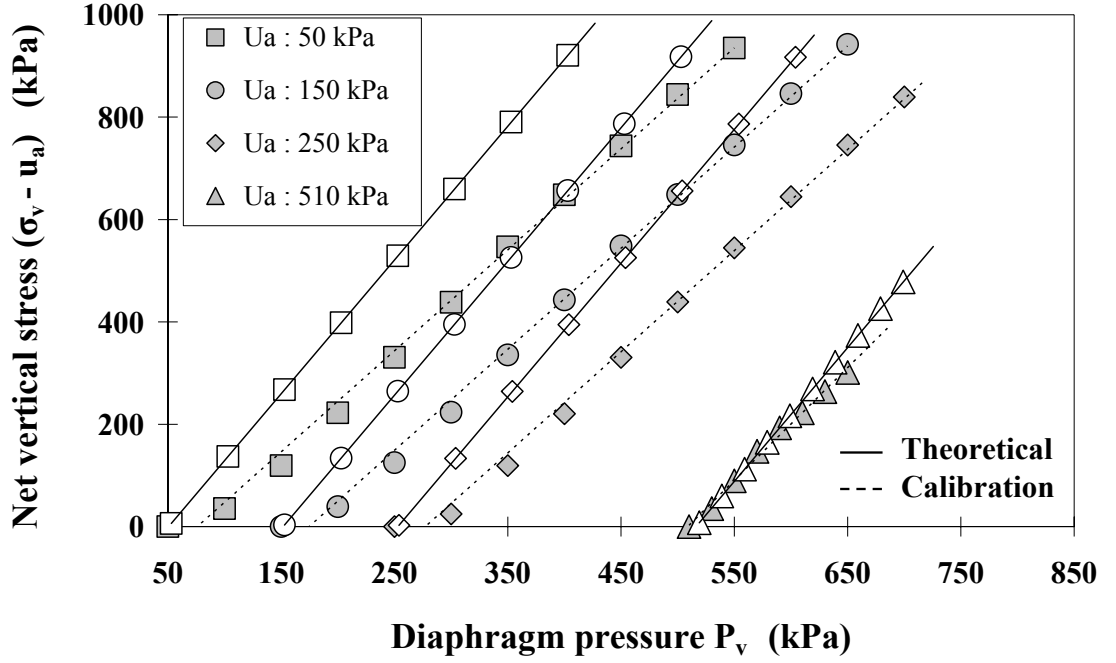


**Figure 3.15** Calibration test results of suction-controlled oedometer cell.

In order to determine the actual load transmitted by the diaphragm and the piston to the soil sample, the oedometer cell was calibrated using a calibrated proving ring. Figure 3.14 shows the arrangement for calibration of the cell. The oedometer cell was fixed to the floor and the loading ram was connected to the proving ring. The force transmitted to the proving ring was measured while applying a range of diaphragm pressure, under constant air pressure inside the cell ( $u_a = 50, 150, 250$ , and  $510$  kPa).

Figure 3.15 presents calibration results to take into account diaphragm effects and the actual geometry of the loading platen on net vertical stress. The relationships obtained between the applied diaphragm pressure ( $P_v$ ) and net vertical stress ( $\sigma_v - u_a$ ) are presented below as linear expressions with the following coefficients:

$$(\sigma_v - u_a) = 1.973P_v - 2.98u_a \quad u_a = 50 \text{ (kPa)} \quad (3.5)$$

$$(\sigma_v - u_a) = 1.975P_v - 2.30u_a \quad u_a = 150 \text{ (kPa)} \quad (3.6)$$

$$(\sigma_v - u_a) = 1.977P_v - 2.19u_a \quad u_a = 250 \text{ (kPa)} \quad (3.7)$$

$$(\sigma_v - u_a) = 2.201P_v - 2.24u_a \quad u_a = 510 \text{ (kPa)} \quad (3.8)$$

From the equations above it can be seen that the coefficient  $(A_p - A_r)/A$  from the actual calibration equations is smaller than the theoretical value, as presented in Equation 3.3. This is due to the fact that the effective value of  $A_p$  is less than the theoretical one, since

there exists a gap between the loading platen and the membrane at higher diaphragm pressures. From the equations above it can also be observed that the coefficient  $(A_p - A_r)/A$  is getting bigger (and getting closer to the theoretical value) with increasing applied air pressure inside the cell. This is because of the gap between the loading platen and the membrane is getting smaller when applying a higher value of air pressure inside the cell. Since the effective value of  $A_p$  is dependent on the applied air pressure inside the cell, the calibration test had to be conducted at different air pressure values. The calibration test has been repeated two times to make sure the repeatability of the calibration equations. Figure 3.16 shows the results of repeating the calibration test for the cell pressure of 50 and 150 kPa. After each set of calibration tests, the diaphragm pressure was completely removed and the test was performed again. From the figure it can be observed that the results are consistent and the obtained calibration equations are reliable.

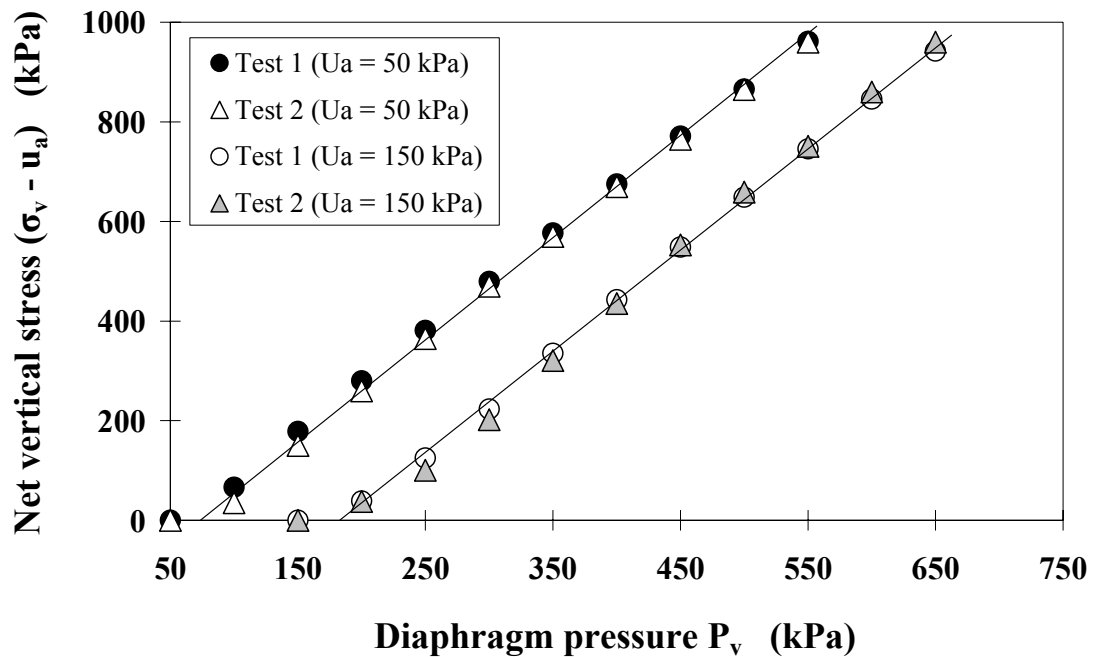


**Figure 3.16** Results of repetition of the calibration test.

As can be seen in Figure 3.15, theoretical net stress is zero when the diaphragm pressure is equal to the applied air pressure. However, the actual net stress (obtained from the calibration test) is zero at a diaphragm pressure slightly higher than the applied air pressure. This is due to the friction occurring between the loading ram and the o-ring seal.

Temperature variation can cause volume changes in all of the constituents of the oedometer cell, especially in the drainage system. When performing non-isothermal

tests it is therefore necessary to consider the effect of water thermal expansion in the tubing. In order to calculate water volume changes, it is essential to quantify this undesired volume change of the drainage system during non-isothermal paths. Mechanical loading causes deformation of the cell, and therefore the measured vertical displacement has to be modified. The deformation caused by the mechanical loading must be subtracted from the total displacement recorded by the LVDT displacement transducer. In order to quantify this effect, an undeformable steel disc was placed inside the sample chamber. Mechanical loads were applied on the disc and the corresponding deformation was recorded using an LVDT displacement transducer. No detectable deformation occurred in the oedometer cell when applying vertical stress up to 400 kPa. Deformability of the cell structure under thermal loading has been neglected in our specific tests, as the compression tests were performed under isothermal conditions.

### **3.3.6 Microstructural analysis**

In order to study the microstructure of kaolin clay samples, an environmental scanning electron microscope (ESEM) type XL30 from Philips was used. ESEM is a relatively new scanning electron microscopy (SEM) technique for qualitative assessment of the microstructure of soil (Delage et al., 1996; Cui et al., 2002; Agus and Schanz, 2005). The main advantage of ESEM over the conventional SEM is that the ESEM does not require the test sample to be under a high vacuum. Therefore, wet samples can be examined in their natural state without modification or special preparation. The sample environment can be varied through a range of pressures, temperatures, gas composition and humidity. The reason for using the ESEM in this research is to gain information about the arrangement of particles and pores in the samples during the wetting and drying. In this study, the influence of temperature on pore size distribution (PSD) of the soil samples was analysed. The PSD of soil samples was determined from the desorption path of the SWRCs. This method has been used by other authors including Prapaharan et al. (1985) and Romero (1999). The details of the method are described in Chapter 7. Furthermore, the temperature dependence of the contact angle at the air-water interface was studied. In order to investigate the influence of temperature on contact angle, the concave curvature of water inside a capillary tube was captured (using a high resolution microscope) while heating the water. The test procedure involved placing a capillary tube (with 0.4mm inside diameter) in deionised water (with initial temperature of 10°C). The water was drawn up in the capillary tube until there was a sufficient mass of water to overcome the intermolecular forces. The water temperature



was increased at a low rate and changes of contact angle at the air water interface were recorded. Figure 3.17 shows the equipment used in the laboratory for studying the temperature dependence of the contact angle. It should be noted that the contact angle of water on a clay surface is clearly different from that on a glass surface; however, this test can give us a general idea of how temperature affects the capillary action in the pores with small radii in unsaturated soils.



**Figure 3.17** High resolution microscope used for recording contact angle in a capillary tube.

### **3.3.7 Thermal hysteresis in soil water retention curves**

Thermal hysteresis in SWRCs was studied by applying a cycle of heating and cooling on compacted kaolin clay samples inside an isolated system, in order to keep the water-content of samples constant. In this study, 20 soil samples (64mm diameter and 24mm height) were prepared with the same initial void ratio of 1.5 and initial water-content of 18%. One filter paper (Whatman No. 42) was sandwiched between two larger-sized filter papers and placed in between two soil samples. The arrangements of the soil samples and the filter papers were placed inside separate sealed glass jars (250 ml capacity) with a screw top lid.

All the glass jars were placed inside a temperature chamber which was maintained at the desired temperature within  $\pm 0.1^{\circ}\text{C}$ . The thermal loading and unloading test was carried out by applying  $25^{\circ}\text{C}$  increments. Starting from  $10^{\circ}\text{C}$ , the temperature was controlled and maintained constant for a period of 14 days at each stage to ensure suction equalisation. At the end of each stage, two glass jars were opened; and the water-content

of the soil samples and the sandwiched filter papers were determined by oven drying them. It should be noted that when the soil samples were placed inside the sealed glass jars, the water-content of the samples decreased to 16.5% (i.e. 1.5% reduction from the initial water-content) due to evaporation, until samples reached an equilibrium state with the air surrounding the samples. The relative humidity (RH) of the air in the laboratory is measured using an RH meter, and was 40% which corresponds to a total suction of 125 MPa (based on Kelvin's equation). While the water-content of the samples decreased due to evaporation, the void ratio of samples decreases accordingly (shrinkage behaviour of the material is studied in Chapter 4). Following the test procedure explained in section 3.3.3, matric suction of the samples was determined at each stage using the filter paper technique.

### 3.4 Chapter summary

In this chapter the physical characteristics of kaolin are described as well as the experimental set-up and testing procedures employed. All tests carried out in this study are summarised in Table 3.4.

**Table 3.4** List of tests performed in this thesis.

Test	Details
<b>Single point and double oedometer</b> (Number of tests: 32)	Isothermal oedometer tests were performed at different temperatures to investigate the influence of temperature and initial water content on the collapse behaviour of the material.
<b>Temperature and suction controlled oedometer</b> (Number of tests: 6) A new suction-controlled oedometer cell was designed, built and calibrated.	Examined the combined effects of suction and temperature on the hydro-mechanical behaviour of kaolin clay.
<b>ESEM microscopy</b> (Number of tests: 2)	Studied the microstructure (arrangement of particles and pores) of samples.
<b>PSD analysis and Temperature induced changes in contact angle</b>	PSD of soil samples were obtained from desorption path of SWRCs. Temperature induced changes in contact angle of water were investigated by capturing the concave curvature of water inside a capillary tube (using a high resolution microscope).
<b>Filter paper calibration</b> Filter paper calibration curves obtained at 10, 25 and 50°C.	Filter paper calibration curves were obtained at different temperatures, using vapour equilibrium and axis translation techniques.
<b>Filter paper suction measurement</b> (Number of tests: 45)	Filter paper method was used to determine the SWRC of the material.
<b>Pressure plate</b> (Number of tests: 10) 3 small pressure plate apparatuses were designed and built.	The pressure plate apparatus (axis translation technique) was used to obtain filter paper calibration data for suction values of less than 400 kPa. This technique was also used to determine the SWRC of the material.
<b>Cycle of heating and cooling</b> 1 cycle of heating and cooling – Total and matric suctions measured for 10 samples.	Thermal hysteresis in SWRCs was studied by applying a cycle of heating and cooling on soil samples.

## **CHAPTER 4 – TEMPERATURE EFFECTS ON SUCTION MEASUREMENTS USING THE FILTER PAPER TECHNIQUE**

### **4.1 Introduction**

The filter paper method has been widely used by many researchers (e.g. Gardner, 1937; Fawcett and Collis-George, 1967; Chandler and Gutierrez, 1986; Houston et al., 1994; Fleureau et al., 2004; Walker et al., 2005) who have investigated different aspects of this method. The filter paper method has several advantages compared to other techniques for soil suction measurements; the method is inexpensive, covers a range of suction values from almost zero to 100 MPa, and the test procedures are simple and do not require any special equipment. Although the filter paper method has several advantages, special care should be taken not only in the test procedure but also in terms of using an appropriate calibration curve to ensure a reliable suction value is obtained. The calibration curves of different filter papers have been studied by many researchers (e.g. Chandler et al., 1992; Houston et al., 1994; Bulut et al., 2001; Leong et al., 2002; Marinho and Oliveira, 2005; Bulut and Wray, 2005; Agus et al., 2010); however, little data are available in the literature on the effect of temperature on the calibration curves. Even though the effect of temperature on SWRCs is an important issue; it is also important to explore how temperature affects the filter paper technique for suction measurement. This chapter aims to show that temperature is an important factor relating to filter paper suction measurement and that misleading results can be obtained if the effect of temperature on the calibration curve is not taken into account. Since suction has a strong influence on the mechanical behaviour of unsaturated soils, its precise measurement is of great importance.

This research presents the results of an experimental study of thermal effects on filter paper calibration curves used to obtain soil suction. When temperature changes are significant, it is essential to consider its influence on the filter paper calibration curves in order to obtain a reliable soil suction measurement. The calibration curve of Whatman No. 42 filter paper was determined at 10, 25 and 50°C using the vapour equilibrium technique with sodium chloride solution at different concentrations and the axis translation technique. The experimental results showed that temperature had a major influence on the filter paper calibration curves. Using the experimental data, a calibration equation was proposed, taking into account the effect of temperature. The

calibration curves were then used to determine the SWRC of kaolin clay, which showed lower retention capacity at higher temperatures.

## **4.2 Filter paper calibration curves**

### **4.2.1 Background**

Many researchers have presented filter paper calibration curves using different methods. Figure 4.1 presents the calibration curves for the Whatman No. 42 filter paper obtained by Fawcett and Collis-George (1967) at 22°C, Chandler and Gutierrez (1986) at 21°C, Chandler et al. (1992) at 21°C, Leong et al. (2002) at 25°C, Agus (2005) at 22°C and also shows the experimental results at 25°C from this current study. The difference in the filter paper calibration curves might be due to factors such as equilibration time, temperature and using different batches of filter paper, as noted by Marinho and Oliveira (2005). The filter paper calibration data at 25°C from this study are very similar to data reported by Marinho and Oliveira (2005) and also to the calibration curve presented by Agus (2005) at 22°C. By assuming that all data presented in Figure 4.1 are at equilibrium condition, the difference between the calibration curves is mainly related to the use of different batches of filter paper.

It has been suggested by some authors (e.g. Houston et al., 1994; Leong et al., 2002) that the calibration curve for total suction should differ from the calibration curve for matric suction. These authors used the vapour equilibrium technique to obtain a calibration curve for total suction measurement, using approximately 7 days equilibration time. They used the axis translation technique and obtained a separate calibration curve for matric suction measurements. Marinho (1994b) studied the time required for equilibration of Whatman No. 42 filter paper. A range of suctions were generated using solutions at different sodium chloride concentrations. The author proved that, given sufficient time for equalisation, there is a unique calibration curve for the filter paper regardless of the type of suction. The results of an experimental investigation by Walker et al. (2005) also confirmed that a unique calibration curve should be used for both matric and total suction measurements, if enough time is allowed for suction equalisation. This fact was also reported by Bulut and Wray (2005) and Haghighi et al. (2011). The study presented here considers equilibrium state and hence the calibration curve can be used for matric or total suction measurement.

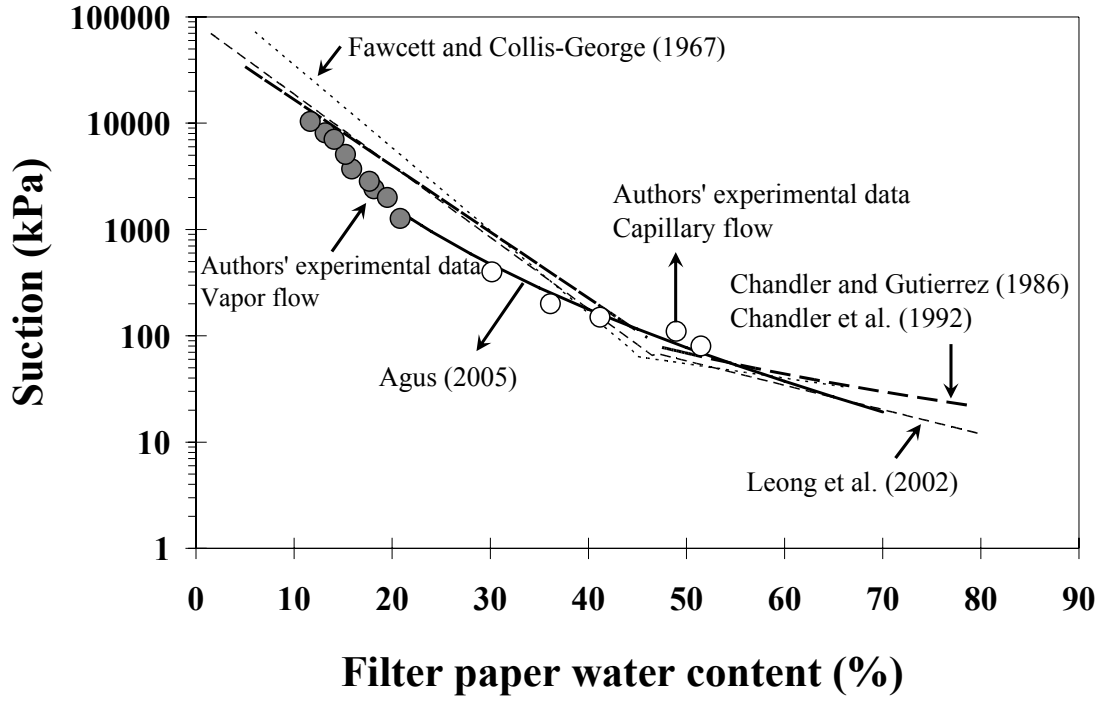


**Figure 4.1** Comparison of filter paper calibration curves (temperatures between 21 and 25°C).

Gourley and Schreiner (1995) performed a series of calibration experiments in order to investigate the influence of temperature and equilibrium time on filter paper calibration curves. The results of their experiments using sodium chloride solutions at 5°C, 15°C and 30°C showed the influence of temperature on the filter paper calibration curve. The authors proposed a time-dependent calibration equation (for filter paper Whatman No. 42) for temperatures between 5 to 30°C:

$$\psi = 10^{5.82 - \frac{T^{0.4}}{15} - 0.096 \times W_f} - \frac{2.2 \times 10^6}{t^{\frac{\ln T - 0.41}{3}} \times W_f^{2 + \frac{t}{82}}} + \frac{500}{t} \times (\sqrt{T} - 3.87) - T^{1.5} \quad (4.1)$$

where  $\psi$  is total suction (in kPa),  $W_f$  is the filter paper water-content (%),  $T$  is temperature (in °C) and  $t$  is equilibrium period in days. The proposed calibration equation by the authors, at 14 days equilibration time, for the same filter paper water-content of 20% gives a suction value equal to 4720.9 kPa at 10°C and 4022.1 kPa at 30°C (i.e. 14.8% reduction in suction by 20°C increase in temperature). The equilibration time required for calibration of the filter papers has been evaluated by various researchers. ASTM D 5298-94 recommends a minimum calibration time of one week for running contact and non-contact filter paper tests. Marinho (1994a) indicated that the equilibration time for calibration of Whatman No. 42 filter paper is dependent

on the imposed level of suction, when using the vapour equilibrium technique. He concluded that the lower the suction, the longer the equilibration time needed to achieve suction equilibrium. The author suggested a period of 15 days equilibration time for total suction measurement ranging between 250 kPa to 1 MPa; and 7 days for the range of 1 MPa to 30 MPa. According to Marinho (1994b), a longer equilibration period of 30 days, and possibly more, is needed when using the vapour equilibrium technique for suctions less than 250 kPa. One of the main problems found when using the vapour equilibrium technique is that reaching a thermal equilibrium between the salt solution and the vapour space above the solution is difficult to achieve. He (1999) calibrated filter papers using the vapour equilibrium technique. The author placed pieces of filter paper inside a desiccator with a salt solution. In order to accelerate the equilibrium condition, the author used a magnetic stirrer to stir the solution. He (1999) explained that the stirring of the salt solution creates a circulation of air in the desiccator, thus enhancing the changes of water molecules leaving the liquid phase and becoming water vapour molecules.

Bulut et al. (2001) adopted an equilibration time of two weeks for Schleicher & Schuell No. 589 filter paper calibration tests. The results of an investigation by Chao (2007) showed that the calibration curve (Whatman No. 42 filter paper) obtained using the vapour equilibrium technique for a period of 2 weeks equilibration time, is in close agreement with the calibration curve obtained for 3 weeks equilibration period (see Figure 4.2). The authors therefore concluded that 2 week equilibration period is sufficient for the calibration of the filter papers. In Figure 4.1, calibration data obtained for a period of 2 weeks equilibration time compared with a calibration curve presented by Agus (2005) after 3 weeks equilibration time; close agreement was observed. In this thesis, it was therefore been concluded that 2 weeks equilibration time is sufficient for a capillary flow of any level and for a vapour flow higher than 500 kPa.

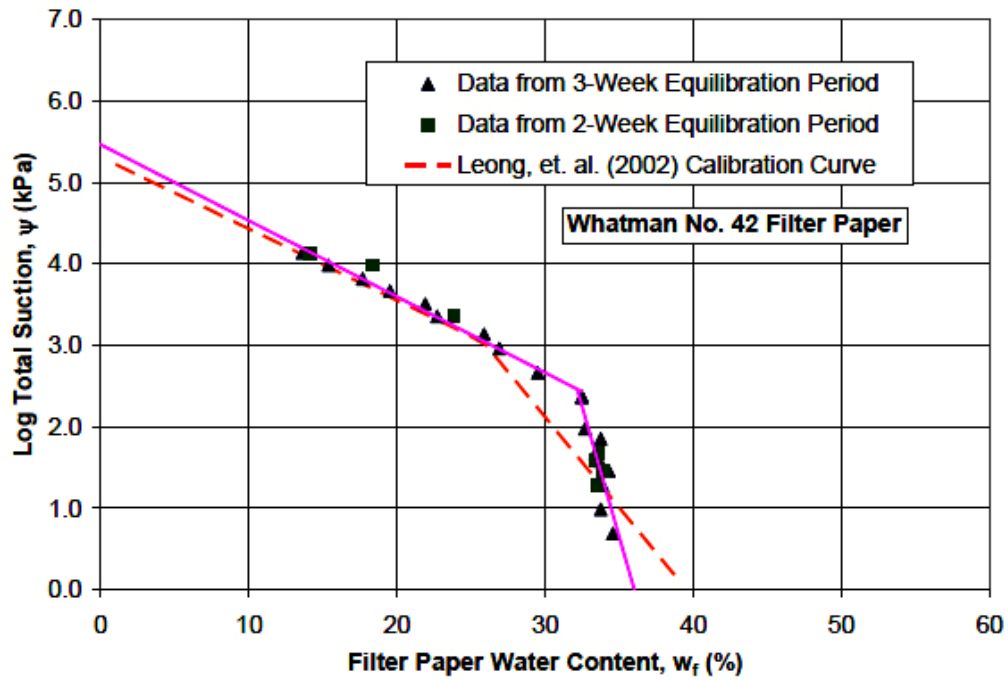


**Figure 4.2** Comparison of equilibrium time for filter paper calibration curves using the vapour equilibrium technique (Chao, 2007).

Tang and Cui (2005) studied the calibration of relative humidity (RH) generated by various saturated saline solutions at different temperatures. They observed that temperature does not have a significant influence on the RH over a sodium chloride solution in a closed system at equilibrium. The results of the experiments showed a very slight increase in RH generated by NaCl solution with increasing temperature (see Figure 4.3). The authors concluded that it could be related to the chemical property of NaCl in terms of solubility changes with temperature. The majority of salts absorb heat when dissolved and they are therefore more soluble at higher temperatures. Other salts release heat when dissolved and consequently solubility decreases with increasing temperature. However, in the case of NaCl solution, heat is neither absorbed nor released so the solubility is almost unaffected by temperature (Getman and Daniels 1943). A similar study by Romero (1999) also showed that relative humidity over NaCl solution is virtually unaffected by temperature. It is then considered that NaCl solution is adequate for studying the effects of temperature on the filter paper calibration curve.



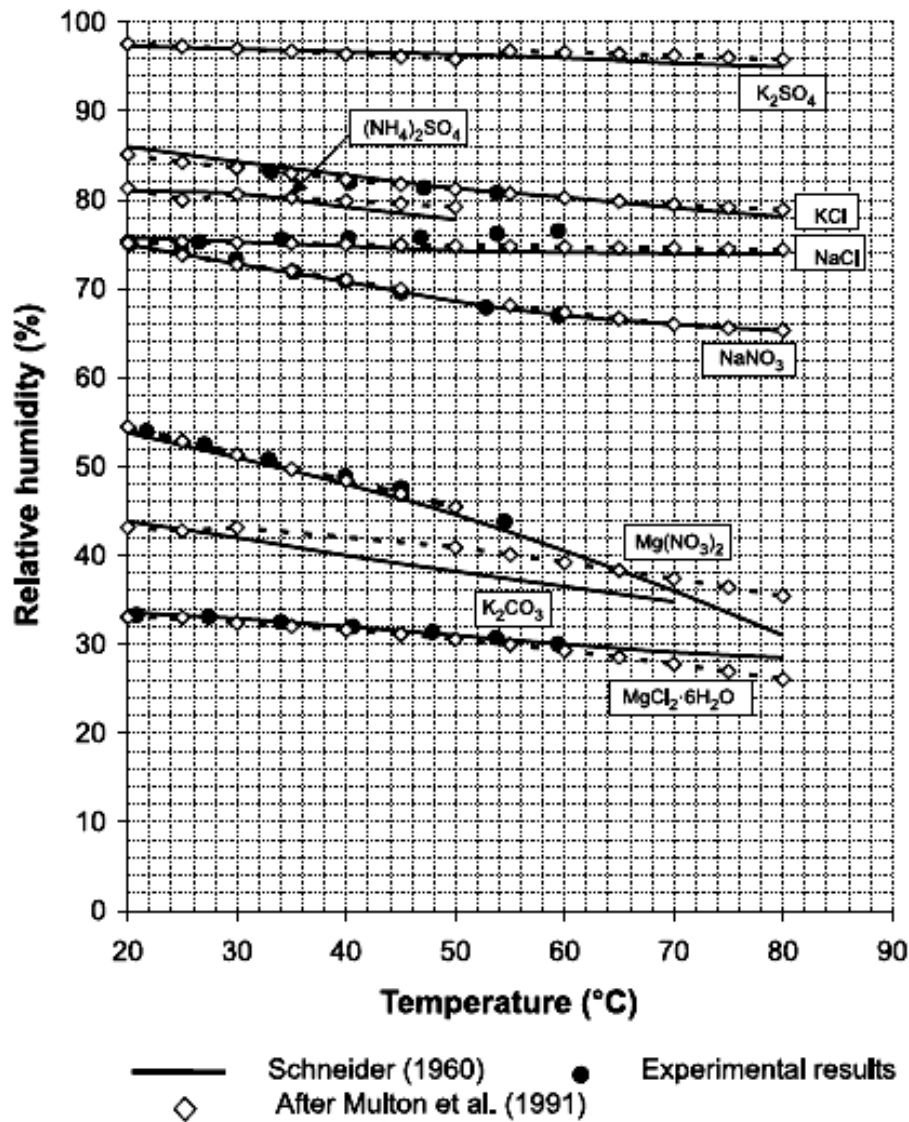


**Figure 4.3** Change in RH with temperature for different solutions (Tang and Cui, 2005).

#### 4.2.2 Calibration curves

The experimental data for filter paper calibration curve at 10, 25, and 50°C is plotted in Figure 4.4. From the figure, it can be observed that the calibration curve shifts downward with increasing temperature. An equilibration period of 14 days was used for all the calibration curves, to ensure equalisation. Using all data obtained from the experiment, a calibration equation is proposed. The mathematical expression developed in this work to achieve a good match between the experimental data and predictions is given below in Equation 4.3. It should be noted that this equation is a best-fit correlation with the experimental data and it does not necessarily provide a physical explanation. This format of the calibration equation has been found to be an accurate way to represent the experimental data in the range of interest of both temperature and filter paper water-content. The average absolute error between the predictions and the

experimental data generated in this work is ~12%. Evaluation of 12% error in suction measurement is presented in the following section. As sufficient time is given to reach equilibrium, the proposed calibration equation will be used for both matric and total suction measurements; it also covers the temperature range from 10 to 50°C:

$$\ln \psi = 33.97 \times W_f^{-0.33} - 4.55 \times T^{0.04} \quad \psi \leq 500 \text{ kPa} \quad (4.2)$$

$$\ln \psi = -1.23 \times (W_f^{0.56} + T^{0.19}) + 16.48 \quad \psi > 500 \text{ kPa}$$

where  $\psi$  is suction (kPa),  $W_f$  is the filter paper water-content (%),  $T$  is temperature (°C). The proposed equation is plotted together with the experimental data in Figure 4.4, demonstrating the reliability of the equation. The contribution of this study, in comparison to previous works in the literature, is that the obtained calibration data are at the equilibrium condition and that the effect of temperature on filter paper calibration is taken into account (covering a wider range of temperatures from 10 to 50°C).

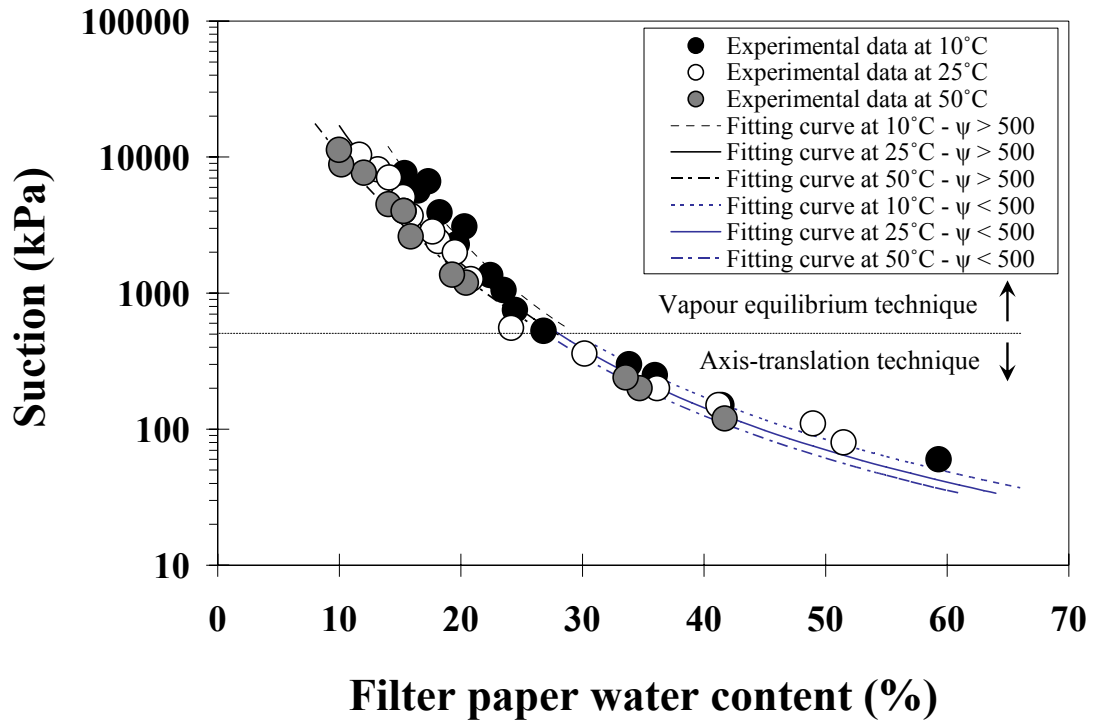


**Figure 4.4** Filter paper calibration curves at different temperatures.

The proposed equation is a relationship between suction, temperature and filter paper water-content. As previously mentioned temperature does not have a significant influence on relative humidity over the NaCl solution; however, the filter paper water-content varies according to temperature for the same suction. From Figure 4.4, it can be observed that the water-storage capacity of the filter paper decreases by increasing the

temperature. The decrease in retention capacity of the filter paper with increasing temperature could be due to temperature induced changes in the surface tension and the contact angle of water within the pores of the filter (Grant and Salehzadeh, 1996). The figure also shows that the influence of temperature on the calibration equation decreases as the filter paper water-content increases. The influence of temperature on filter paper water content is more significant at higher suction values. This could be due to the fact that by using solutions at different concentrations of NaCl for generation of suction, the concentration of the solution varies with respect to temperature. The air above the salt solution can sustain higher water vapour at higher temperature. Therefore, the concentration of salt solution increases with increasing temperature due to evaporation, and consequently the present suction is not equal to the reference suction corresponding to the initial salt molality.

#### **(a) Accuracy and performance**

Accuracy of the filter paper technique for suction measurements is dependent on the accuracy of the calibration curve used. In this study, the filter paper calibration data for suction values of higher than 500 kPa were obtained by using the vapour equilibrium technique. When using the vapour equilibrium technique for imposing suction, the accuracy of the technique depends on how accurate isothermal equilibrium between the salt solution and the vapour space above the solution is maintained. According to Kelvin's equation, total suction is very sensitive to change in RH, particularly for suction values of less than 1000 kPa. A small change in RH (due to a small thermal gradient) can cause a significant change in total suction. The influence of temperature changes in the accuracy of suction measurement has been highlighted by Croney et al. (1952) and Agus (2005). Due to difference in thermal properties of the solution and the air, a small temperature change induces a thermal gradient in the system. Since the amount of water vapour in a closed system is constant, the change in temperature only affects the saturation pressure of water vapour ( $P_0$ ) while the partial pressure of water vapour ( $P$ ) remains constant. Error in suction measurement due to a temperature gradient can be estimated by taking the first derivative of Kelvin's equation with respect to temperature (Croney et al., 1952):

$$\frac{d(\ln \psi)}{dT} = \frac{1}{T} - \frac{1}{P_0 \ln(RH)} \times \frac{d(P_0)}{dT} \quad (4.3)$$

$P_0$  varies with temperature ( $T$ ) and this variation is reported in Lide and Frederikse (1994). By knowing the temperature gradient that may occur in the system, the possible error in the suction measurement can be calculated. Figure 4.5 shows the error in suction measurement due to different values of temperature gradients. Based on this calculation, if the suction measurement error is limited to 10% using the vapour equilibrium technique, the measurement should be limited to a suction of 300 kPa at 0.1°C temperature fluctuation. In this study the suction measurement using the vapour equilibrium technique is limited to a suction of 500 kPa (with temperature accuracy of  $\pm 0.1^\circ\text{C}$ ). Evaluation of 10% error in suction measurement for determination of the influence of temperature on SWRCs is presented in the following section.

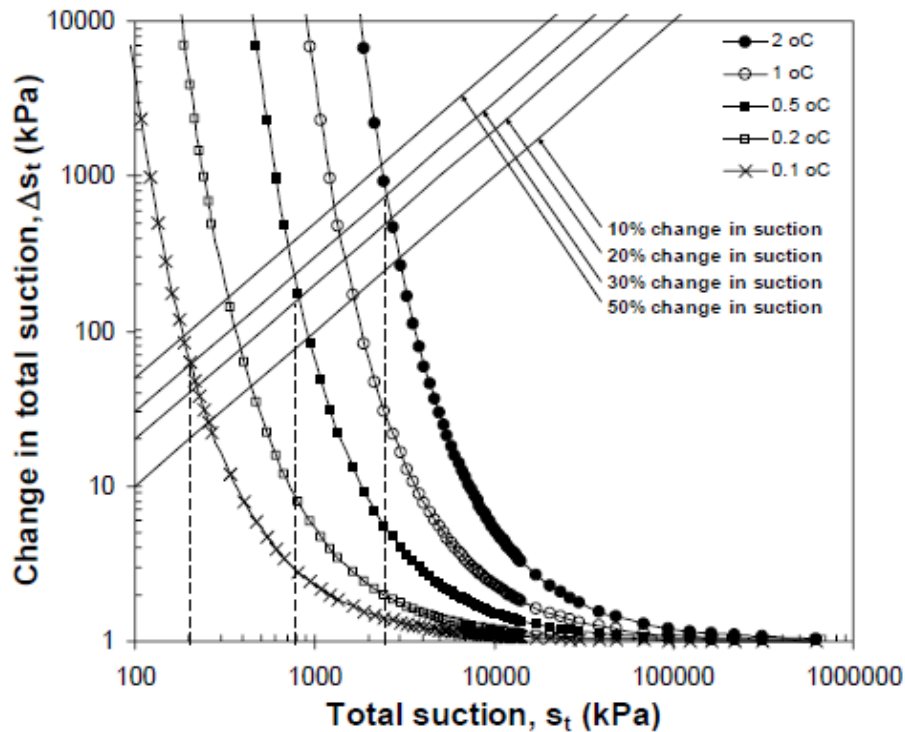


**Figure 4.5** Error in total suction due to temperature gradient (Agus, 2005).

Another important point which has to be emphasised is the influence of using different batches of filter paper on calibration curves. It has been shown that filter paper calibration curves can significantly vary among the same type of filter paper from one researcher to another or among the same type of filter paper from one batch to another (Likos and Lu, 2002; Marinho and Olivera, 2005). Figure 4.6 shows the calibration data for different batches of Whatman No. 42 filter paper. Between the two extreme cases (lot 77743 and lot 812130) there is 11% difference in the measured values of filter paper water content. This difference in terms of total suction corresponds to 92% error. It is

therefore necessary to verify whether a particular batch of filter paper is in agreement with the usual calibration curves (e.g. Fawcett and Collis-George, 1967; Chandler et al., 1992; Leong et al., 2002) or either with those presented by other authors (e.g. Marinho and Olivera, 2005; Agus, 2005; and the calibration curve presented in this study). For this purpose only one point on the curve needs to be obtained to verify the batch-specific calibration.

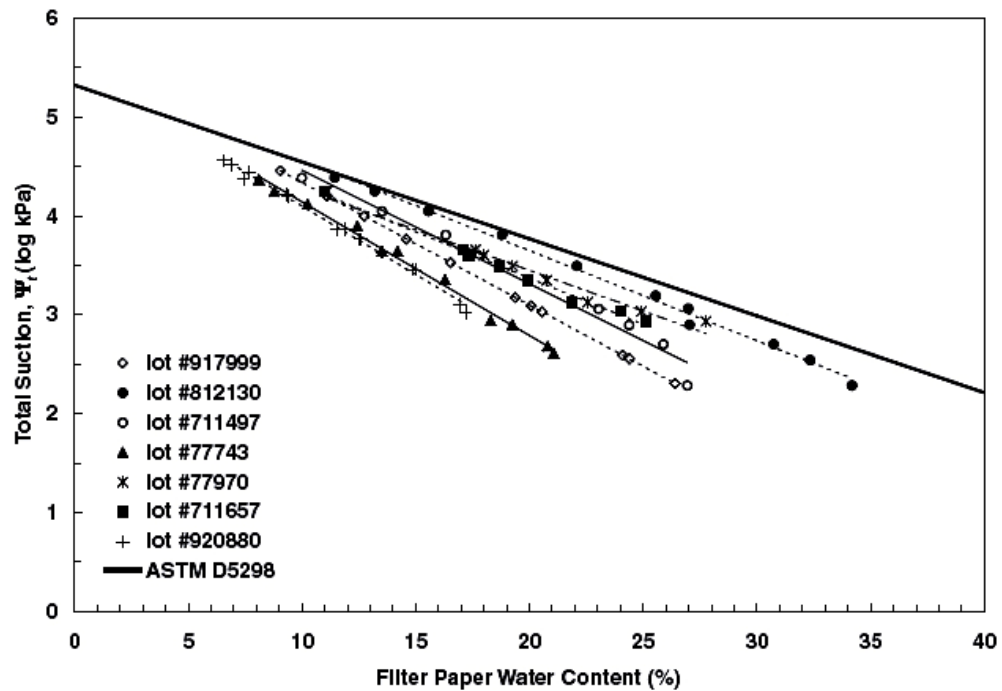


**Figure 4.6** Calibration data for different batches of Whatman No. 42 filter paper (Likos and Lu, 2002).

### 4.3 Soil water retention curves

#### 4.3.1 Background

The effect of temperature on SWRCs has been studied by several authors (e.g. Tang and Cui, 2005; Uchaipichat and Khalili, 2009) and all observed a lower retention capacity at higher temperatures, for the soil samples with the same dry density. A common conclusion from these studies was that at the same suction value, a lower degree of saturation at higher temperatures is only due to lower gravimetric water storage capacity. This is caused by a reduction in the surface tension of water with increasing temperature. However, many experimental results on temperature dependency of soil water retention capacity (e.g. Hopmans and Dane, 1986; Nimmo and Miller, 1986; Liu and Dane, 1993; Bachmann et al., 2002; Villar and Gomez-Espina, 2008) revealed that the influence of temperature on the water retention capacity of soil is several times

greater than would be predicted only from the temperature dependence of the surface tension at the air-water interface. Peck (1960) and Chahal (1965) developed a theoretical model based on the assumption that the volume of entrapped air in the soil increases with temperature. This assumption gives rise to a higher temperature dependence of capillary pressure than predicted only by the variation of the surface tension due to temperature changes. Hopmans and Dane (1986) investigated SWRCs and the corresponding volume of entrapped air at two temperatures and found that the entrapped air volume decreased with increasing temperature. The authors therefore concluded that the observed temperature dependence of capillary pressure cannot be explained by the proposed model by Peck (1960) and Chahal (1965). Liu and Dane (1993) explained the effect of temperature on SWRCs by assuming that the soil water pressure had to be determined by the continuous water phase only and not by the total water-content. Their model supposes that an increase in temperature causes entrapped water to become connected with the continuous water phase, which results in an additional temperature effect on the capillary pressure. Grant and Salehzadeh (1996) studied the SWRCs in soils and a glass-bead sample at different temperatures. The results of their study show that the temperature sensitivity of the contact angle has effects on the retention capacity. She and Sleep (1998) continued the research of Grant and Salehzadeh (1996) on silica sand samples and concluded that contact angle is not only dependent on the temperature but also on the water-content. A similar conclusion was made by Bachmann et al. (2002) when analysing three different soils. According to Romero et al. (2001), in compacted samples of clayey soils, for high water-contents (when capillary effects dominate), temperature dependence of surface tension is the main mechanism affecting the soil water retention capacity. However, in the low water-content regions, the main temperature effects on the water retention capacity are due to changes in the interaction mechanisms between clay particles and water (Romero et al., 2001; Villar and Lloret, 2004; Villar et al., 2005).

#### **4.3.2 Experimental results**

The SWRCs, at different temperatures, in terms of their variation of gravimetric water-content against suction are shown in Figure 4.7 (drying path) and Figure 4.8 (wetting path). The figures show the water retention data obtained through the application of the vapour equilibrium and the axis translation techniques. It should be noted that the samples for wetting and drying paths are compacted at two different water-contents of 9.4% and 51.8% respectively, and therefore they have different soil fabrics. As

mentioned in section 2.2.3, samples compacted dry of optimum generally exhibit a fabric made up of aggregates having a bimodal pore size distribution with relatively larger pores, whereas soils compacted wet of optimum tend to show a more homogenous matrix-dominated fabric with a unimodal pore size distribution. In this study therefore the influence of temperature on wetting curves and drying curves is investigated separately.

From the figures it can be observed that for a given suction, the water-content decreases with increasing temperature. This means that an increase in temperature caused a decrease in water retention capacity of the soil. Similar studies were carried out by other researchers (e.g. Romero et al., 2001; Villar and Lloret, 2004; Olchitzky, 2002; Tang and Cui, 2005; Uchaipichat and Khalili, 2009) on the effect of temperature on the soil water retention behaviour of compacted soils. They all observed a decrease in water retention capacity of soil with increasing temperature. Villar and Lloret (2004) obtained SWRCs of compacted calcium-type bentonite (FEBEX) at 20, 60 and 80°C. The results of their experiments show a reduction in water retention capacity of the soil from 20 to 60°C; however, the difference between the samples tested at 60 and 80°C is minor.

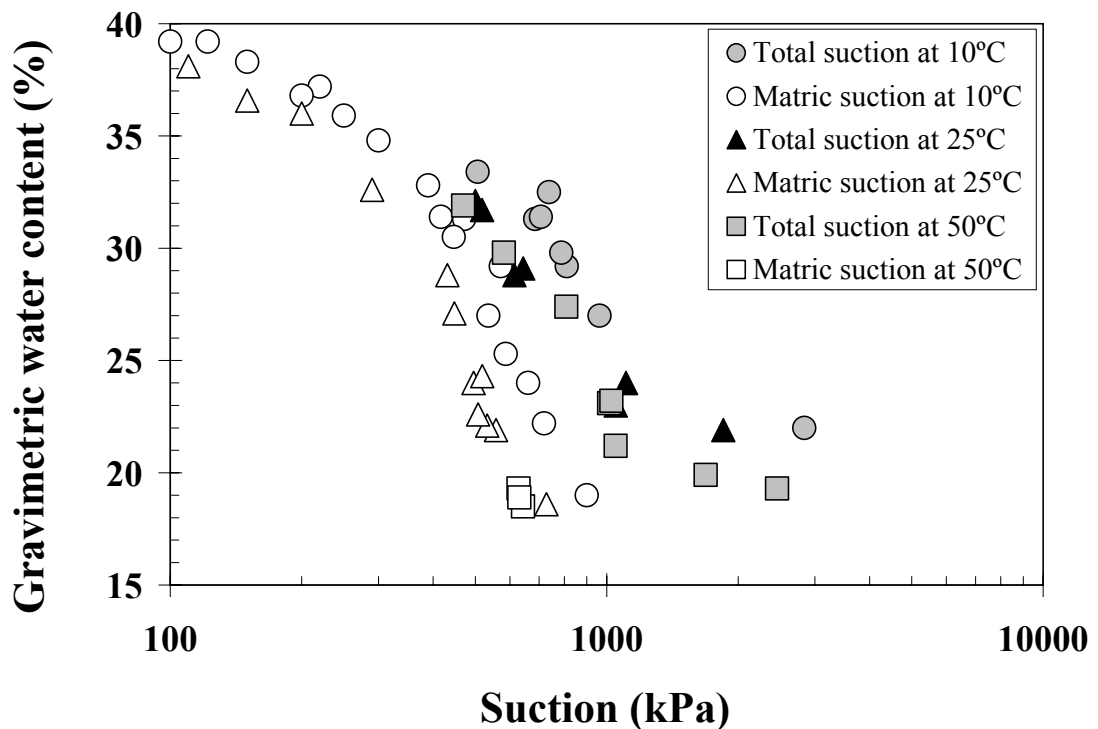


**Figure 4.7** Drying paths of the SWRC at different temperatures.

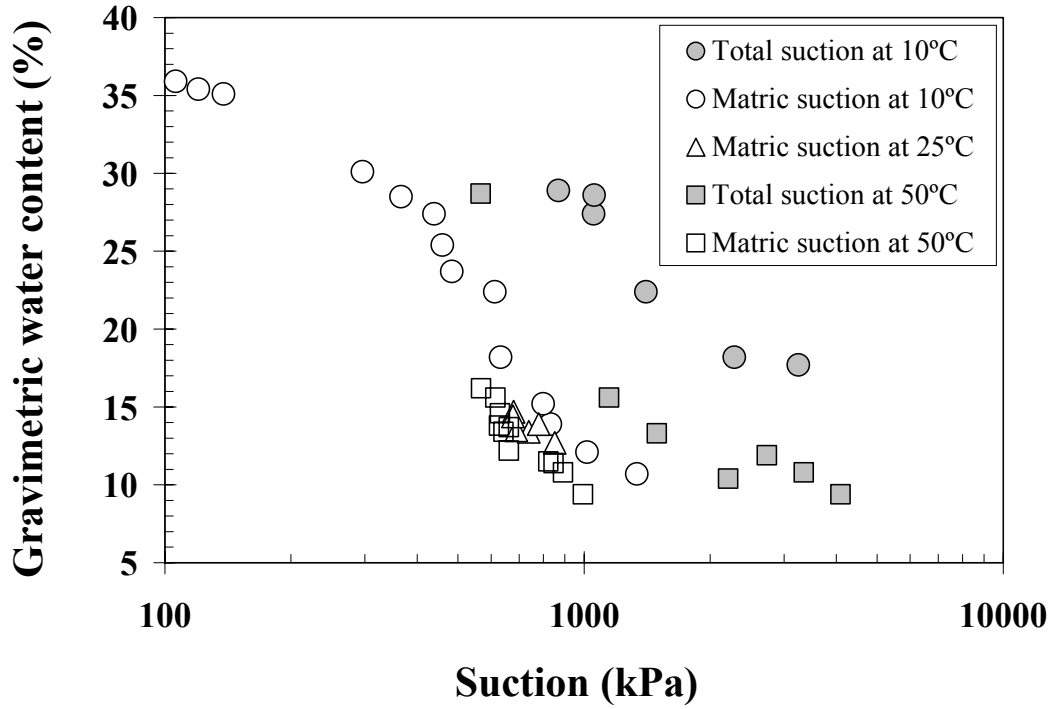


**Figure 4.8** Wetting paths of the SWRC at different temperatures.

The authors (including Villar and Lloret, 2004; Tang and Cui, 2005; Uchaipichat and Khalili, 2009) used different techniques to investigate the effect of temperature on the soil-water retention properties of soils, such as using the axis translation technique in a temperature and suction-controlled triaxial cell, or using a vacuum desiccator with sulphuric acid solution for controlling relative humidity. To the author's knowledge, this thesis presents, for the first time, the SWRCs obtained at different temperatures using the filter paper method. In Figure 4.9, the best fit curves for the experimental data obtained at 10 and 25°C are given, using the empirical equation proposed by van Genuchten (1980). There are many expressions for the SWRC in the literature (e.g. Brooks and Corey 1964; McKee and Bumb 1984; Fredlund and Xing 1994) and each has its advantages and disadvantages when applied to a particular soil. Because the objective of this thesis is not to compare the different SWRC models, it was decided to use the equation (Equation 4.4) proposed by van Genuchten (1980). This model has been successfully applied to fit experimental results for many different soils.

$$\theta_w = \theta_r + \frac{\theta_s - \theta_r}{[1 + a\psi^b]^c} \quad (4.4)$$

where  $\theta_w$  is the volumetric water-content;  $\theta_s$  is the volumetric water-content in saturated conditions;  $\theta_r$  is the volumetric residual water-content, which is the water-content below



which there is negligible change in water-content corresponding to an increase in soil suction,  $\psi$  is the suction; and a, b, c are fitting parameters. The fitting parameters in the equation are optimised to obtain the best fit to the experimental data. In this study, Equation 4.4 was used in terms of gravimetric water-content.

Figure 4.9 compares the drying path of the SWRCs at 10 and 25°C. From the figure it can be observed that the experimental data obtained using the axis translation technique and the vapour equilibrium technique are very similar, even for suctions as low as 100 kPa. This is likely due to the precise temperature control during the tests. Therefore it can be concluded that using the proposed filter paper calibration equation, and adopting two weeks equilibration time, the results obtained from the suction measurements are accurate.

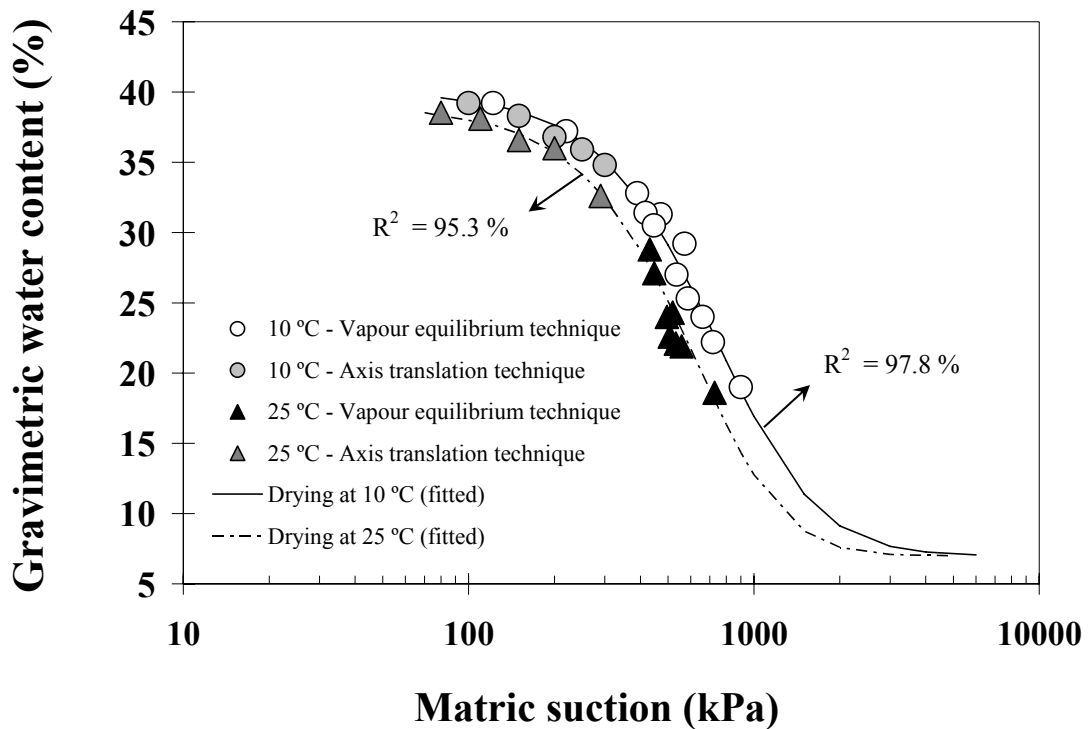


**Figure 4.9** Comparison of drying paths of SWRCs at 10 and 25°C.

From Figure 4.7, the rate of change in suction with increasing temperature ( $\Delta s/\Delta T$ ) was found for the samples compacted with initial water-content of 52% and subsequently dried to water-content of 18%. The amount of  $\Delta s/\Delta T$  is different at different water-contents. The  $\Delta s/\Delta T$  was found at water-content of 18%, since at this water-content the experimental data at 10, 25 and 50°C are presented. The  $\Delta s/\Delta T$  was found equal to approximately -8 (kPa/°C) and from 10°C to 25°C, and -3 (kPa/°C) and from 25°C to 50°C. The  $\Delta s/\Delta T$  obtained from 10°C to 25°C is several times greater than would be

predicted from the temperature dependence of the surface tension alone. The theoretical  $\Delta s/\Delta T$  based on the temperature dependence of the surface tension is calculated using the Young-Laplace equation (Equation 4.5):

$$u_a - u_w = \frac{2T_s \cos \beta}{r_s} \quad (4.5)$$

where  $u_a - u_w$  is the capillary suction,  $T_s$  is the surface tension of water,  $\beta$  is the contact angle (generally assumed to be zero), and  $r_s$  is radius of the equivalent capillary tube.  $T_s$  is a function of temperature,  $T$  ( $^{\circ}\text{C}$ ), and is calculated as follows:

$$T_s(mN / m) = (-2.707 \times 10^{-4}) \times T^2 - 0.142 \times T + 75.69 \quad (4.6)$$

Figure 4.10 plots the capillary suction against pore radius for two values of temperature (at  $10^{\circ}\text{C}$  and  $50^{\circ}\text{C}$ ). This plot is based on the assumption that surface tension is the only temperature dependant parameter in the Young-Laplace equation (i.e. assuming that contact angle and pore radius of the air-water interface remain constant with changing temperature). The  $\Delta s/\Delta T$  (for suctions in the range of 600 to 900 kPa, corresponding to matric suction of samples with water-content of 18% in Figure 4.7) only based on the temperature dependence of the surface tension is approximately  $-2.1$  (kPa/ $^{\circ}\text{C}$ ).

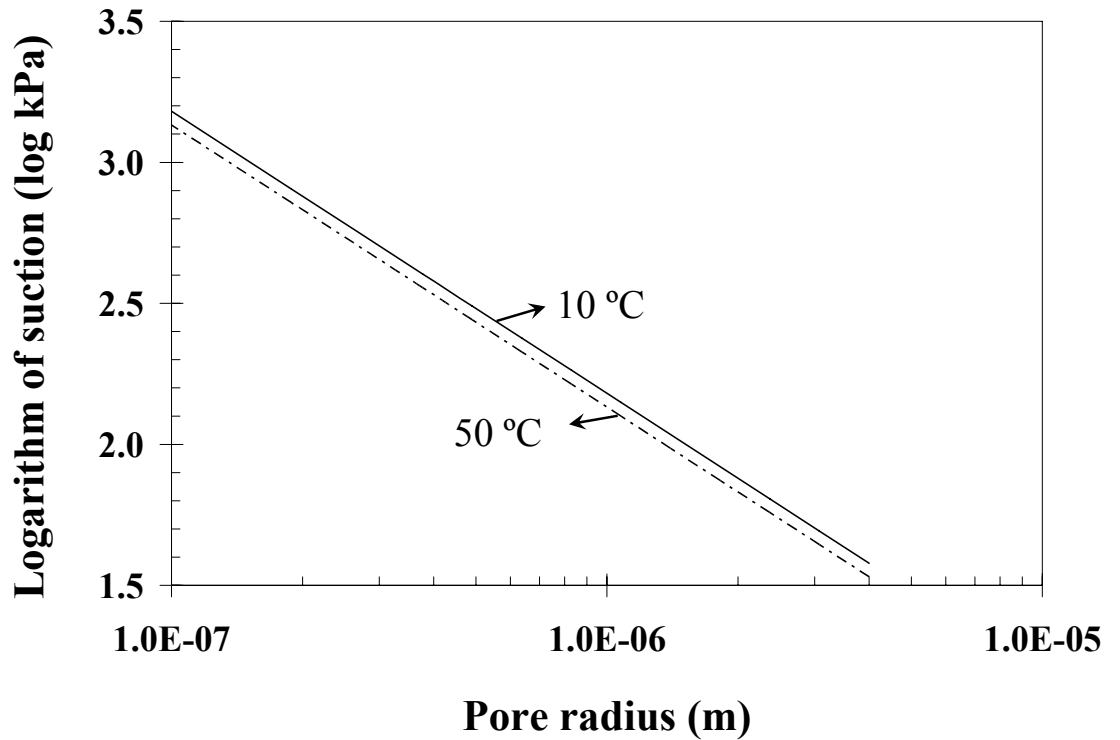


**Figure 4.10** Effect of temperature on capillary suction through change in surface tension.

The  $\Delta s/\Delta T$  obtained for temperature variation from 25°C to 50°C is close to the  $\Delta s/\Delta T$  obtained based only on the temperature dependence of the surface tension. A similar trend was observed from the results of the wetting path. It can therefore be concluded that the influence of temperature variation on water retention capacity of the soil is more significant at lower temperatures. This observation is in agreement with the experimental results reported by Villar and Lloret (2004).

Tang and Cui (2005) obtained the SWRCs of compacted sodium-type bentonite (MX80) at different temperatures by using vapour equilibrium technique. Even though the results of their experiment ( $\Delta s/\Delta T$ ) were twice as large as the calculation using the Young-Laplace equation, they concluded that the reduction of water retention was only due to reduction in surface tension. Many authors (e.g. Liu and Dane, 1993; Grant and Bachmann, 2002; Villar and Gomez-Espina, 2008) reported a higher temperature dependence of capillary pressure than predicted only by variation of the surface tension due to temperature changes. Different alternatives have been suggested to explain the larger than expected changes in the water retention capacity due to temperature changes (including thermal expansion of entrapped air, solute effects on the surface tension of water and temperature-induced changes on contact angle). Romero et al. (2000) and Villar and Lloret (2004) stated that the differences are due to the change in the clay fabric, and the change in the pore water chemistry of the clay. A summary of these suggestions to explain the larger than expected changes in the water retention capacity due to temperature changes is presented in Chapter 7.

#### **(a) Accuracy of suction measurement**

It is important to find out the accuracy of suction measurement when using the filter paper method for determination of the influence of temperature on SWRCs. When using the filter paper method for matric suction measurement, good contact between soil samples and the filter paper has to be ensured. Otherwise, the measured suction could be somewhat in between total and matric suction values. A comparison between the results of matric suction measurement using the filter paper method and the axis translation technique is shown in Figure 4.11. The results from the contact filter paper method agree closely with the pressure plate results.

When using the non-contact filter paper method for total suction measurement, the accuracy of the measurements is dependent on how accurate isothermal equilibrium is maintained. When the suction measurement technique is based on relative humidity

concept, a small temperature fluctuation can result in a significant error in the measurement. In section 4.2.2 it was found that using the proposed calibration equation may result in 12% error in suction measurement. Figure 4.11 shows the matric suction values at 10 and 25°C as well as error bars at each point. The error bars define accuracy range of the experimental data. From the figure it can be observed that the reduction in retention capacity of the soil is bigger than the range of error associated with the measurements. It can therefore be concluded that the proposed calibration equation with the mentioned accuracy is applicable in determination of the influence of temperature on suction measurements.

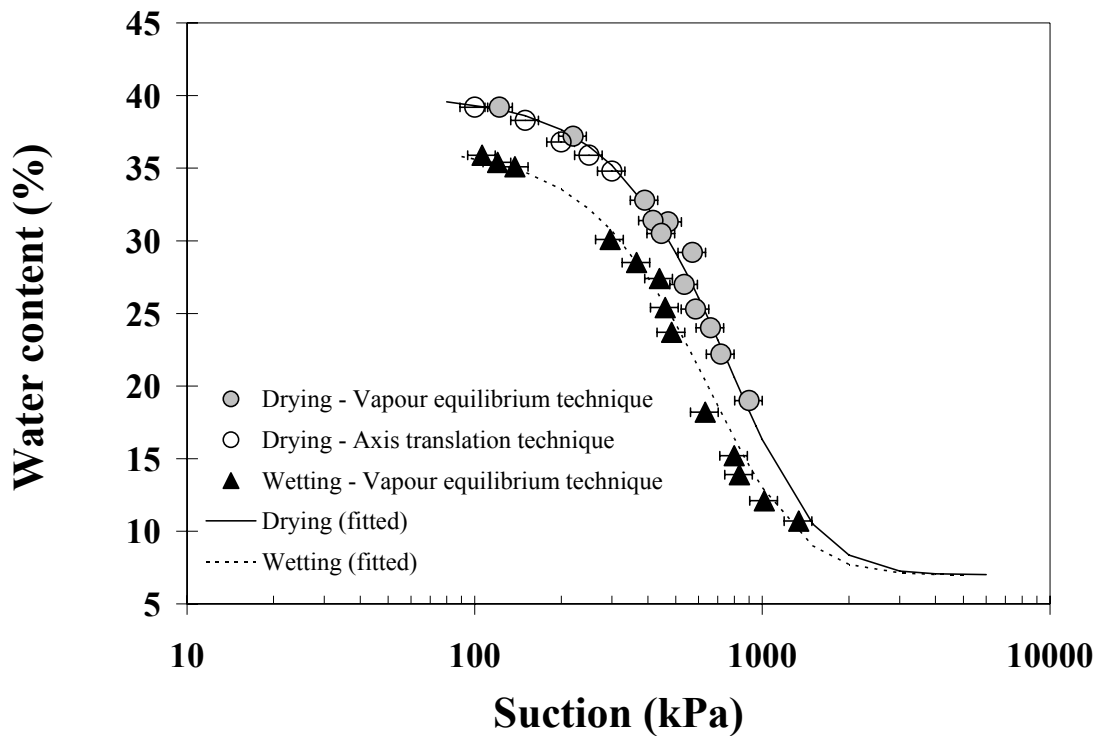
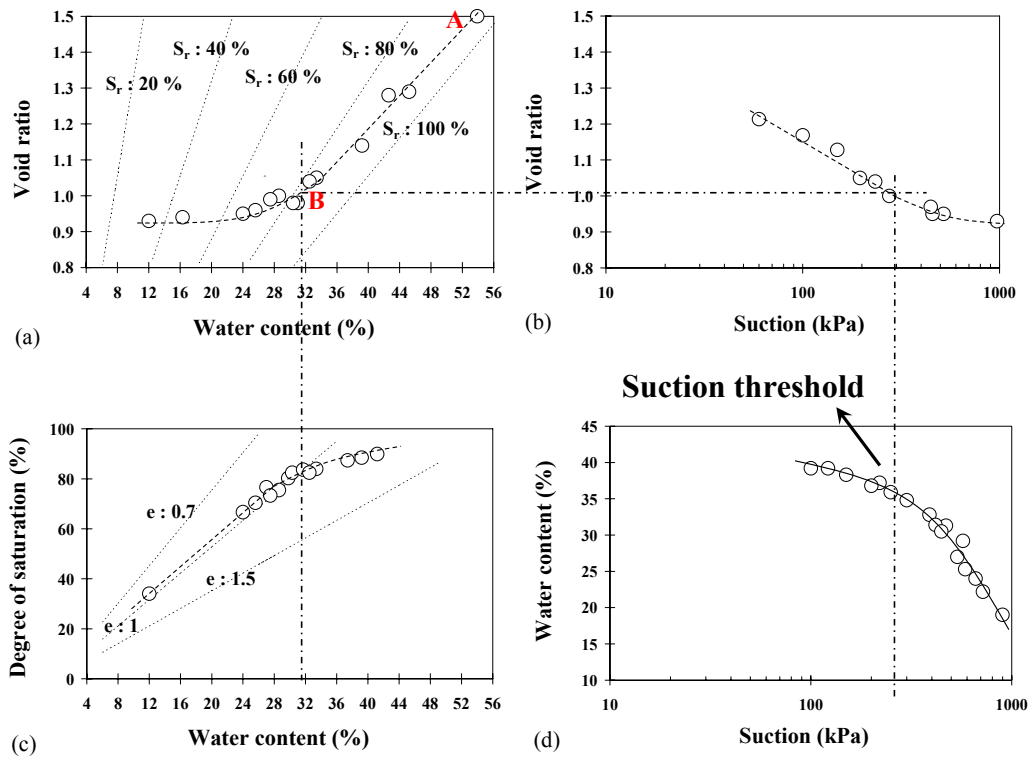


**Figure 4.11** SWRC at 10 and 25°C with error bars.

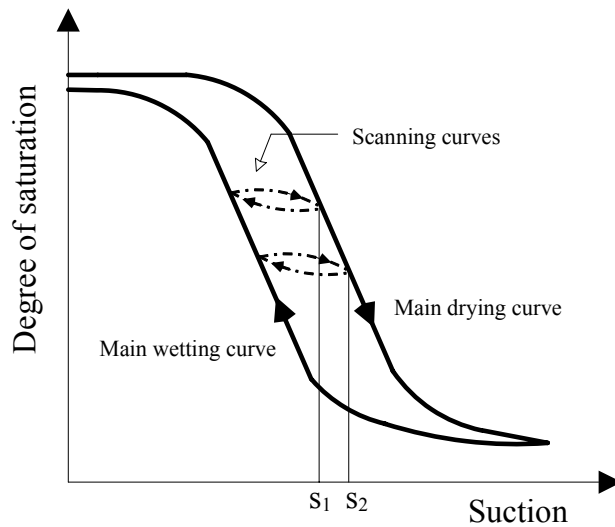
#### 4.4 Shrinkage behaviour

Figure 4.12(a) shows data corresponding to the drying of soil samples used to obtain the SWRC at 10°C, with water-content plotted against void ratio. The void ratio of soil samples was determined by measuring the volume of samples using a vernier calliper (with accuracy of 0.02 mm). As can be observed in Figure 4.12(a), in the initial stage of drying process (from Point A to Point B) degree of saturation of the samples decreases with a small rate. In this phase, the degree of saturation decreases from 91% to about 80% when void ratio of samples decreases from 1.5 to approximately 1. In this study, the samples were prepared with initial  $S_r$  of 91%, therefore they belong to scanning lines. The hysteresis of the SWRC is a typical feature of porous media. Any point in the

plane of degree of saturation versus suction is bounded by two main contours, the main drying curve and the main wetting curve. Any intermediary point located between those curves belongs to a scanning line (see Figure 4.13). A soil sample on a scanning line during drying experience a reversible change in degree of saturation until reach a threshold in suction located on the main drying curve (Point  $s_1$  in Figure 4.13). Above the suction threshold larger irreversible transformations in degree of saturation combined with the shifting the suction threshold (from Point  $s_1$  to Point  $s_2$  in Figure 4.13). As shown in Figure 4.12, Point B corresponds to the suction threshold, after which  $S_r$  of the soil sample starts to decrease rapidly while drying. In this phase ( $S_r$  below 80%); water loss during drying process is much bigger than the soil volume decrease. As can be seen in the figure, in this stage the degree of saturation decreases from 80% to about 20% when void ratio of samples decreases from 1 to approximately 0.9.



**Figure 4.12** Relationship between volume change, suction and degree of saturation.



**Figure 4.13** Main wetting and drying curves and scanning lines.

## 4.5 Chapter summary

A series of filter paper calibration tests was carried out using salt solutions of various concentrations and the axis translation technique at different temperatures. The experimental data in this experiment are in agreement with those published in the literature at the same temperature. The filter paper calibration curve was obtained at 10, 25 and 50°C. Using all data obtained from the experiment at different temperatures, a unique calibration equation was proposed for Whatman No. 42 filter paper. As sufficient time is given to reach equilibrium, the proposed calibration equation can be used for both matric and total suction measurements. The calibration equation, in comparison to previous work presented in the literature, can be considered to be innovative when the fact that the equation is at the equilibrium condition and that the effect of temperature on filter paper calibration is taken into account (covering a wider range of temperature from 10 to 50°C). The SWRC of kaolin clay were obtained at different temperatures using this equation. This thesis presents, for the first time, the SWRCs at different temperatures using the filter paper method. It was observed that water retention capacity of the soil decreases with increasing temperature, however, the rate of suction changes ( $\Delta s/\Delta T$ ) decreases as temperature increases. This chapter also presents the shrinkage behaviour of samples.

## **CHAPTER 5 – THERMAL EFFECTS ON THE COLLAPSE BEHAVIOUR OF KAOLIN CLAY**

### **5.1 Introduction**

In this chapter, the influence of temperature and initial suction on the hydro-mechanical behaviour and collapse potential of kaolin clay samples is examined. A series of temperature controlled oedometer tests were conducted on samples at different initial dry densities and suction values. The filter paper method was used to obtain the initial suction of the soil samples at different temperatures.

### **5.2 Sample preparation**

All the oedometer soil samples were prepared by mixing deionised water thoroughly into the oven dried soil to obtain a homogenous material, which was then statically compacted into the oedometer ring (50mm inner diameter) to obtain the desired initial void ratio. Once each sample was prepared, it was taken with the ring and placed in the oedometer cell. Lower and upper porous stones were dry before placing the ring containing the samples. Possible initial drying of the samples from coming into contact with the dry porous stones was neglected as the porous stones have pores which are too large to be able to sustain capillary forces large enough to draw water from the sample. The oedometer apparatus was modified in order to be used in a temperature chamber. The temperature chamber allows temperature to be controlled between  $\pm 0.1^{\circ}\text{C}$ . Once each specimen was placed in the cell, the upper opening of the cell was wrapped with several layers of cling film in order to minimise evaporation through the porous stones to the atmosphere. It was aimed to maintain the water-content of soil samples constant during the tests; however, some evaporation still occurred, particularly at higher temperatures, as the cling film cannot completely seal the cell. The water-content of soil samples at the beginning and the end of each test is reported in Tables 5.1 and 5.2. It should be noted that in this study  $G_s$  of the soil is assumed to be constant at different temperatures.

Initial matric suction of the soil samples was obtained at  $20^{\circ}\text{C}$  and  $50^{\circ}\text{C}$ , using the filter paper method. The suction measurement test procedures are explained in Chapter 3. The measurement of initial matric suction ( $s_0$ ) was made by placing a piece of Whatman No. 42 filter paper against the soil samples in an air tight glass jar at constant temperature. The soil samples were prepared to the same water-contents and dry densities as the

oedometer tests. The arrangements of the soil samples and the filter papers were placed inside the glass jars. The glass jars were sealed properly and placed inside the constant temperature chamber for a period of 14 days to ensure suction equalisation. After this period, the glass jars were carefully opened and the water-contents of filter papers were measured using a scientific balance weighing accurately to 0.0001g. The suction of the soil samples was calculated from the water-content of filter papers, using the proposed filter paper calibration equation.

**Table 5.1** List of tests in temperature controlled oedometer apparatus ( $e_0 = 1.5$ ).

T (°C)	Initial state					Final state			Test condition
	$e_0$	$\gamma_d$ (kN/m <sup>3</sup> )	$w_0$ (%)	$Sr_0$ (%)	$s_0$ (kPa)	$e_f$	$w_f$ (%)	$Sr_f$ (%)	
20	1.55	10.15	18.4	31.3	658	1.19	16.7	37.0	constant water content
	1.56	10.11	18.6	31.5		0.87	32.3	97.8	wetted at 5 kPa
	1.55	10.15	18.5	31.4		0.87	32.4	98.1	wetted at 100 kPa
	1.55	10.15	18.5	31.4		0.86	31.5	97.3	wetted at 200 kPa
50	1.56	10.11	18.7	31.6	591	1.18	16.1	36.0	constant water content
	1.56	10.11	18.6	31.5		0.88	32.7	98.5	wetted at 5 kPa
	1.56	10.11	18.8	31.8		0.89	-	-	wetted at 100 kPa
	1.55	10.15	18.5	31.4		0.88	32.1	96.4	wetted at 200 kPa
20	1.47	10.48	6.8	12.2	914	1.23	5.8	12.5	constant water content
	1.48	10.44	7.1	12.7		0.84	31.5	98.6	wetted at 5 kPa
	1.47	10.48	6.9	12.3		0.87	-	-	wetted at 100 kPa
	1.47	10.48	6.9	12.3		0.85	31.8	98.8	wetted at 200 kPa
50	1.47	10.48	6.9	12.4	830	1.20	5.9	13.0	constant water content
	1.48	10.44	7.0	12.5		0.84	31.3	97.9	wetted at 5 kPa
	1.47	10.48	6.6	11.9		0.85	31.6	98.1	wetted at 100 kPa
	1.47	10.48	6.6	11.9		0.85	30.7	95.4	wetted at 200 kPa

**Table 5.2** List of tests in temperature controlled oedometer apparatus ( $e_0 = 2$ ).

T (°C)	Initial state					Final state			Test condition
	$e_0$	$\gamma_d$ (kN/m <sup>3</sup> )	$w_0$ (%)	$Sr_0$ (%)	$s_0$ (kPa)	$e_f$	$w_f$ (%)	$Sr_f$ (%)	
20	2.02	8.58	18.7	24.5	671	1.35	16.7	32.5	constant water content
	2.02	8.58	18.7	24.5		1.08	40.1	98.3	wetted at 5 kPa
	2.02	8.57	18.8	24.6		1.07	39.3	96.6	wetted at 100 kPa
	2.02	8.56	18.9	24.7		1.10	40.3	96.4	wetted at 200 kPa
50	2.03	8.54	19.2	25.0	610	1.33	14.4	28.6	constant water content
	2.01	8.59	18.5	24.3		1.05	37.8	95.1	wetted at 5 kPa
	2.01	8.60	18.4	24.2		1.07	37.6	92.4	wetted at 100 kPa
	2.02	8.59	18.6	24.4		1.06	38.4	95.2	wetted at 200 kPa
20	1.99	8.66	7.6	10.1	942	1.37	6.3	12.1	constant water content
	1.98	8.68	7.4	9.9		1.07	39.2	96.7	wetted at 5 kPa
	1.99	8.65	7.7	10.2		1.09	40.1	97.1	wetted at 100 kPa
	1.98	8.69	7.3	9.7		1.08	40.3	98.5	wetted at 200 kPa
50	1.98	8.68	7.4	9.9	864	1.34	3.2	6.3	constant water content
	1.98	8.69	7.2	9.6		1.04	39.1	99.3	wetted at 5 kPa
	1.99	8.65	7.8	10.3		1.04	39.2	99.5	wetted at 100 kPa
	1.99	8.66	7.6	10.1		1.09	40.4	97.8	wetted at 200 kPa



### 5.3 Experimental results and analysis

Figures 5.1 to 5.4 show the results of single and double oedometer tests performed on samples with initial water-contents of 7% and 18%. The figures show the void ratio of the specimens versus vertical pressure (logarithmic scale). Since initial void ratio of the samples varied slightly, the results of individual tests have been adjusted slightly to show all tests starting from the average initial void ratio. From these figures, it can be noticed that the samples are highly collapsible, with significant collapse occurring even on wetting at low vertical stress value of 5 kPa. For the as-compacted samples (the term as-compacted will be used hereinafter to refer to the constant water-content compression tests), the matric suction would be expected to reduce as the void ratio decreases and the degree of saturation increases during each load increment. Based on the compression curves obtained (Figures 5.1 to 5.4), the influences of initial water-content, initial void ratio and temperature are studied on compressibility and collapse behaviour of the material.

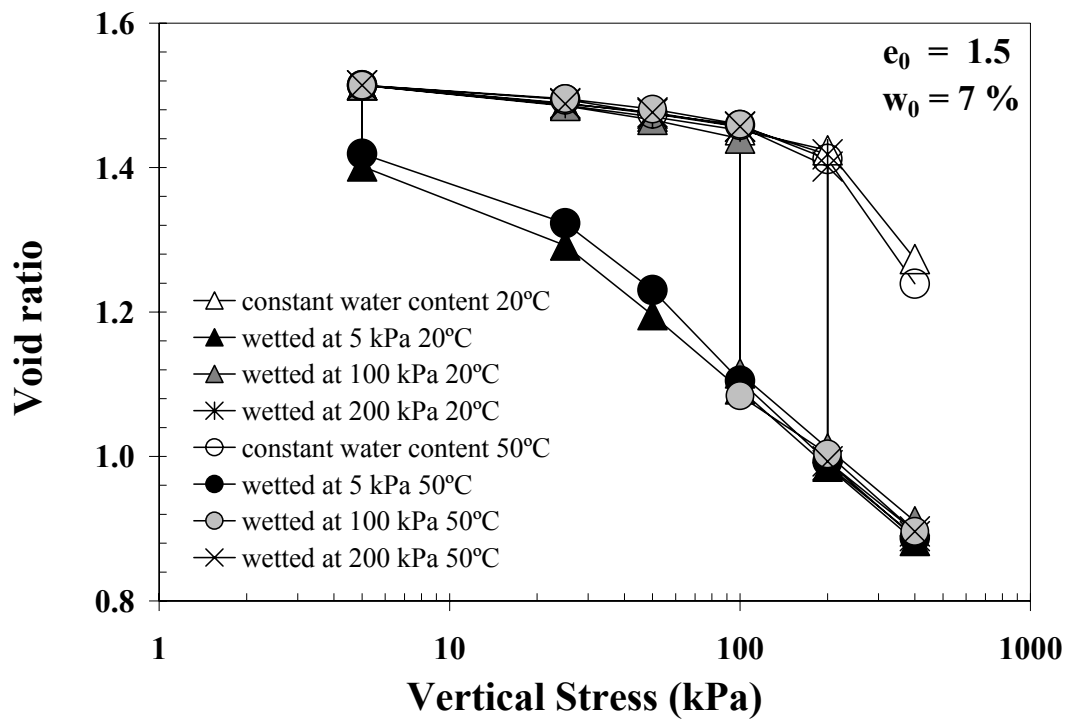


**Figure 5.1** Compression curves (samples with  $e_0 = 1.5$  and  $w_0 = 7\%$ , obtained at 20 and 50°C).

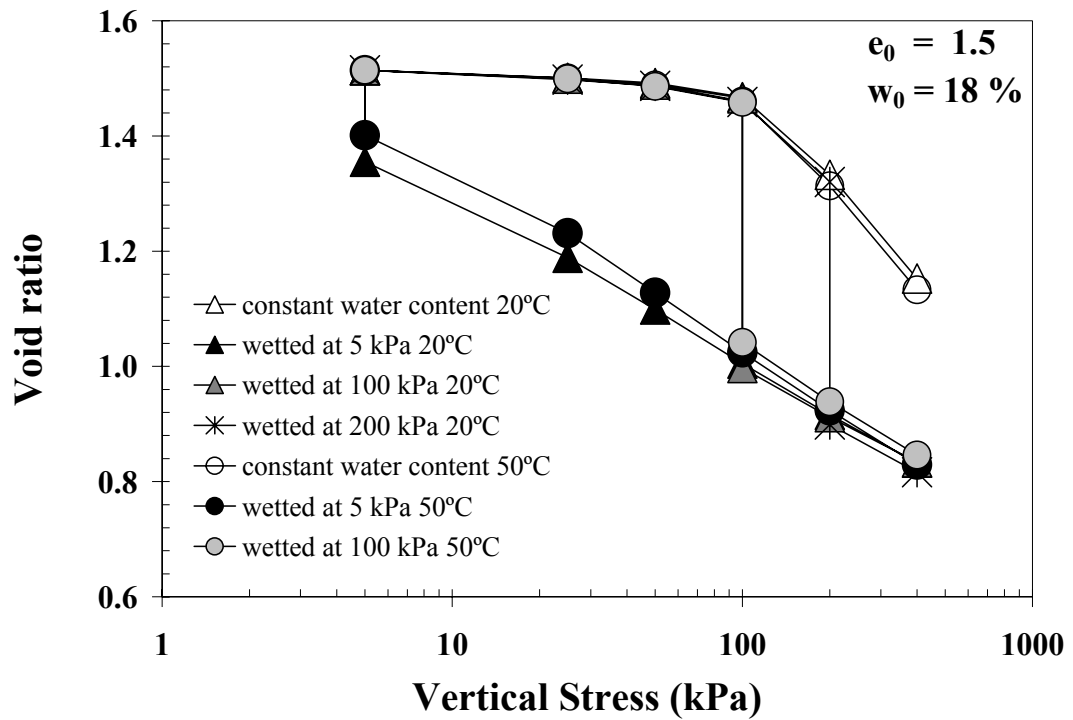


Figure 5.2 Compression curves (samples with  $e_0 = 1.5$  and  $w_0 = 18\%$ , obtained at 20 and 50°C).

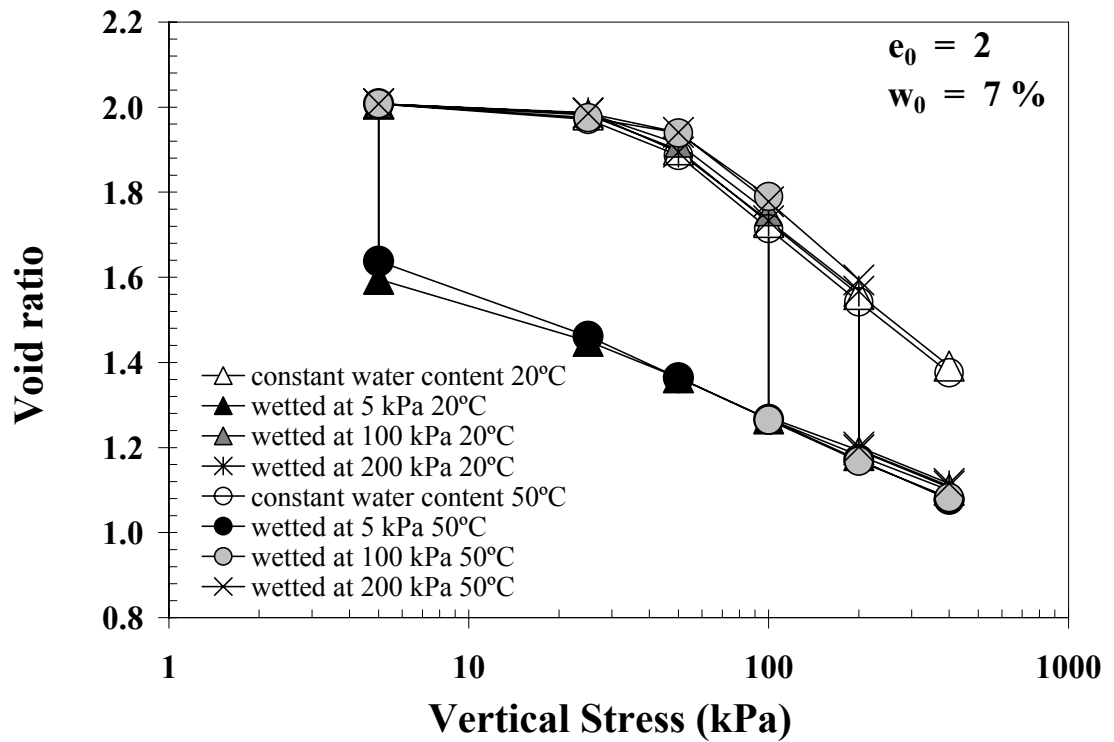
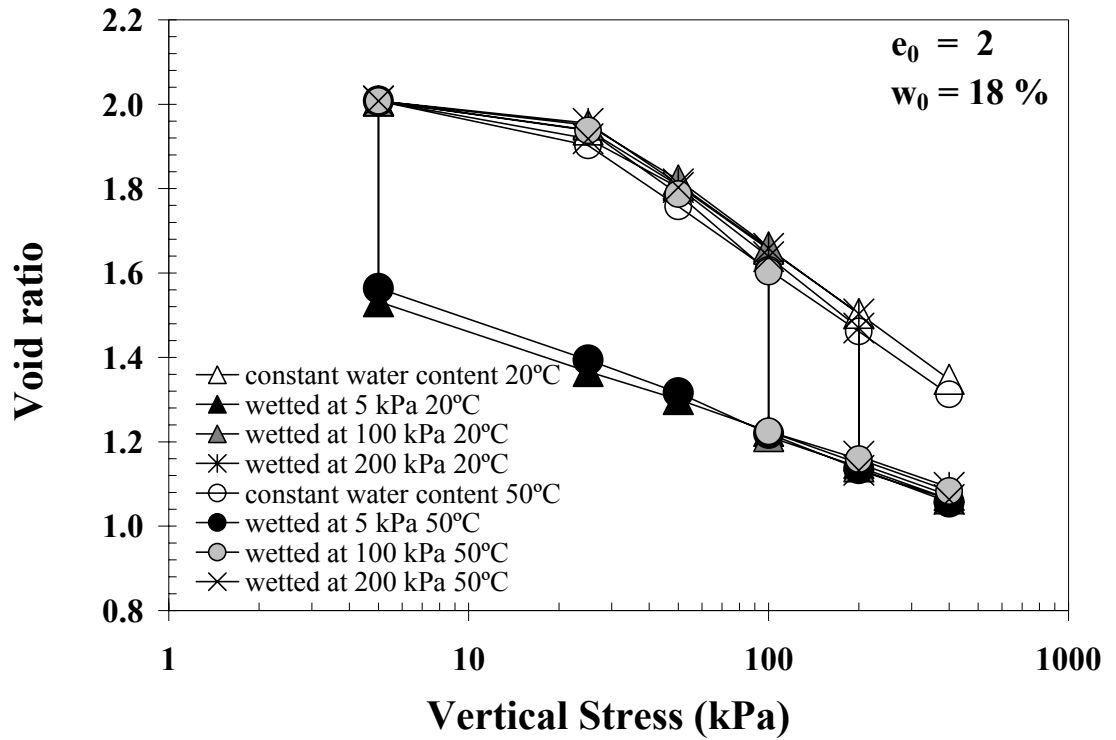
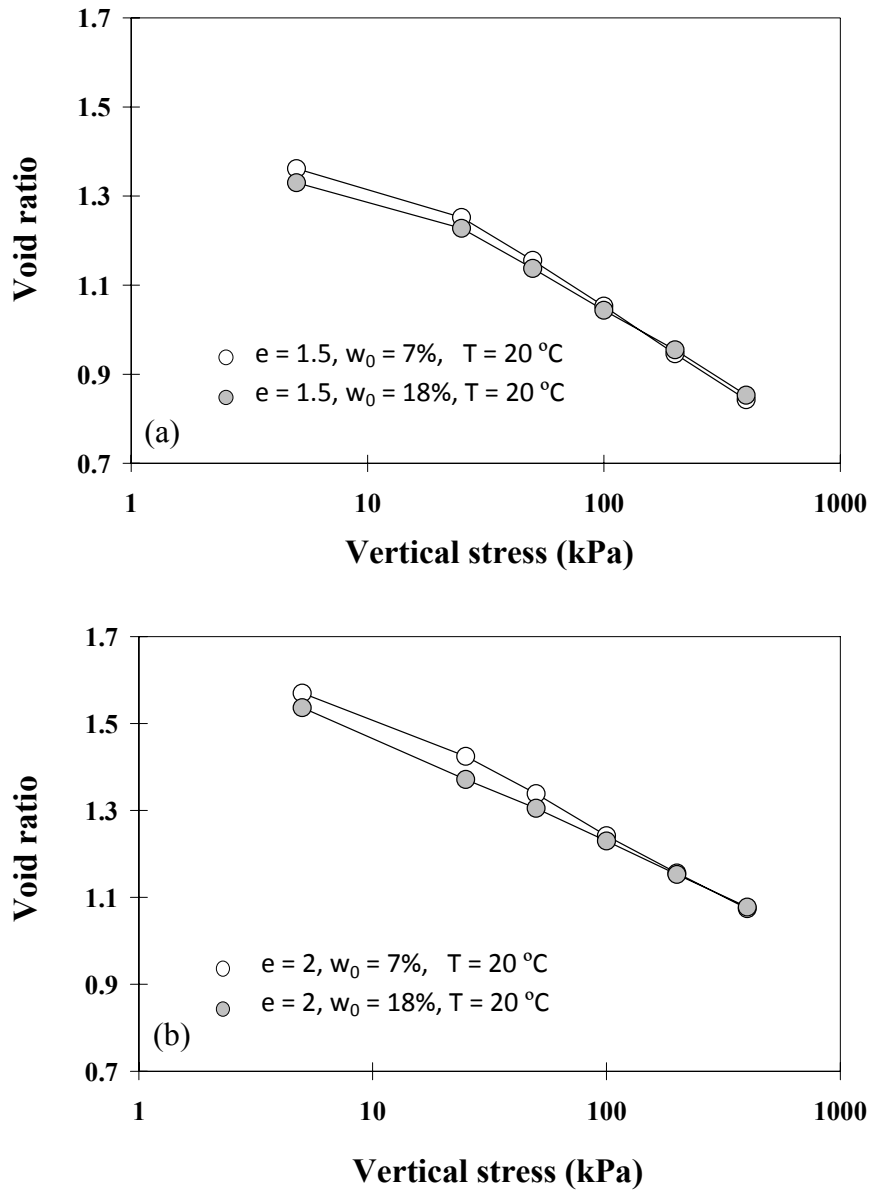


Figure 5.3 Compression curves (samples with  $e_0 = 2$  and  $w_0 = 7\%$ , obtained at 20 and 50°C).



**Figure 5.4** Compression curves (samples with  $e_0 = 2$  and  $w_0 = 18\%$ , obtained at 20 and 50°C).

In order to investigate the influence of initial water-content and initial void ratio on compression behaviour of the material, the soil samples were prepared with initial water contents of 7% and 18% and initial void ratios of 1.5 and 2. It should be acknowledged that soil samples prepared at different compaction water-contents or with different compactive efforts have different soil fabrics. The dry of optimum compacted soils generally tend to exhibit a bimodal PSD. An increase in compaction water-content reduces the volume associated with the larger pores and this will be distributed in smaller pore sizes (Badger and Lohnes, 1973; Ahmed et al., 1974; Garcia Bengochea and Lovell, 1981; Juang and Holtz, 1986). An increase in compaction effort induces the same effect. In this study all the samples are compacted dry of optimum and are expected to exhibit a bimodal PSD. Figure 5.5 compares the saturated normal compression lines for samples compacted with a same initial void ratio but at different initial water contents. From the figure it can be observed that the saturated normal compression lines converge together at higher vertical stresses. The comparison of the normal compression lines of the as-compacted samples is presented in the following sections. The influence of soil fabric on compression behaviour of the samples is not systematically investigated in this research. Therefore no realistic conclusion can be made regarding the influence of soil fabric on compression behaviour of the samples.



**Figure 5.5** Comparison of compression curves for samples compacted at different initial water content (a) samples with initial void ratio of 1.5 (b) samples with initial void ratio of 2.

### 5.3.1 Compressibility behaviour

Figures 5.6 and 5.7 indicate the influence of temperature on soil response for as-compacted samples with initial water-content of 18% and initial void ratios of 1.5 and 2. The results show a softening of the soil response with increasing temperature. From the figures it can be observed that the normal consolidation lines move towards lower stresses with increasing temperature. A similar softening response with increasing temperature was observed when performing a suction-controlled oedometer test (see Chapter 7). The thermal softening response (i.e. reduction of the size of the elasticity domain of the soil with increasing temperature) has also been reported by other authors including Cui et al. (2000), Cekerevac and Laloui (2004), Uchaipichat and Khalili

(2009). From the compression curves, the compressibility parameters were determined: preconsolidation pressure and plastic compressibility parameter ( $\lambda = \Delta e / \Delta \ln P$ ). The preconsolidation pressure (yield stress) was determined from the intersection between the elastic compression slope and the plastic compression slope. From the figures, it can be observed that the slope of the normal consolidation lines,  $\lambda$ , is independent of temperature. The normal consolidation line moves in parallel towards lower stress levels with increasing temperature. It has been reported by many authors that the slope of the compression lines seems to be essentially independent of temperature (e.g. Despax, 1976; Graham et al., 2001; Laloui and Cekerevac, 2003). In the literature, there are only a few contradictory experimental results that report non-parallel consolidation curves at different temperatures (Plum and Ersig, 1969; Tanaka et al., 1997; Sultan et al., 2002).

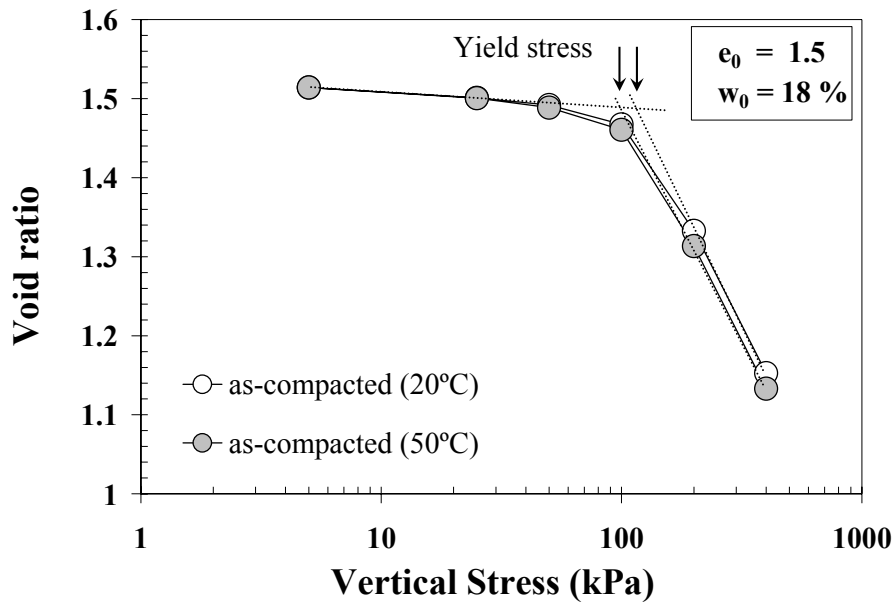


**Figure 5.6** As-compacted compression curves at 20 and 50°C for samples with initial void ratio of 1.5 and initial water-content of 18%.

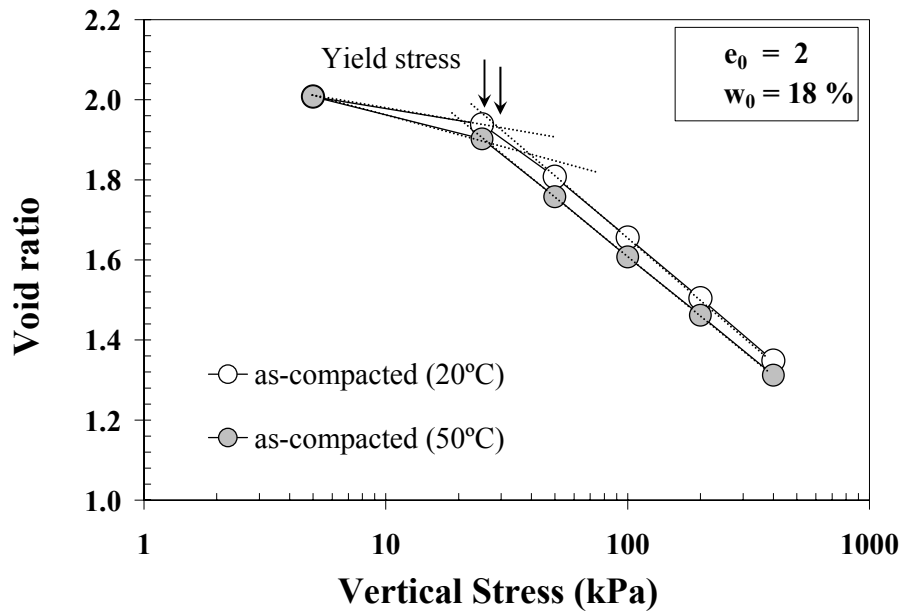


**Figure 5.7** As-compacted compression curves at 20 and 50°C for samples with initial void ratio of 2 and initial water content of 18%.

A similar softening behaviour with increasing temperature was also observed for the as-compacted samples with initial water-content of 7% and initial void ratios of 1.5 and 2. From Figures 5.8 and 5.9, it can be seen that the normal consolidation lines move towards lower stresses with increasing temperature.

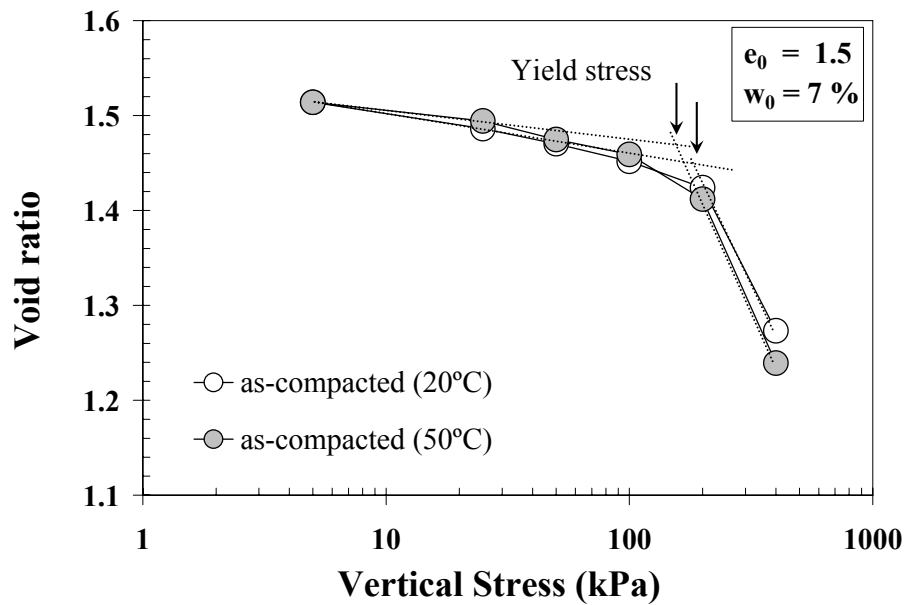


**Figure 5.8** As-compacted compression curves at 20 and 50°C for samples with initial void ratio of 1.5 and initial water-content of 7%.

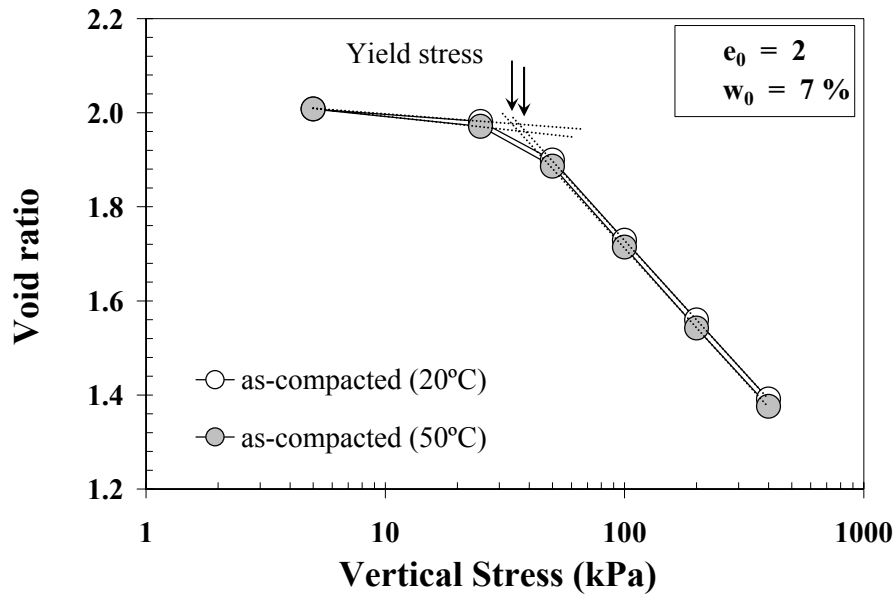


**Figure 5.9** As-compacted compression curves at 20 and 50°C for samples with initial void ratio of 2 and initial water content of 7%.

Preconsolidation pressure of the as-compacted compression curves is the yield stress that separates ‘elastic’ pre-yield from ‘plastic’ post-yield behaviour under oedometric conditions. From Figures 5.6 to 5.9, it can be observed that the yield stress decreases with increasing temperature. Therefore, the elastic domain is reduced as temperature increases, which is representative of thermo-plasticity. According to François (2009), the decrease of the yield stress with temperature may be attributed to the temperature-induced physico-chemical modifications of clay at the microscale. The combinations of several micro-mechanical processes due to heating tend to make the rearrangements of particles easier, reducing the yield limit of the material. Figure 5.10 shows the variation of yield stress with respect to temperature.

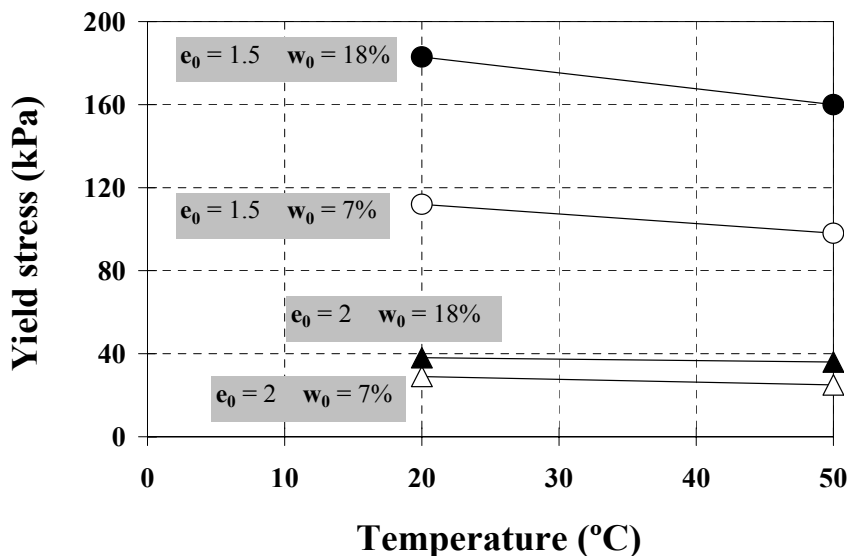


**Figure 5.10** Variation of yield stress with temperature.

Figures 5.11 and 5.12 show the influence of initial water-content on compression behaviour of the as-compacted samples. From the figures it can be observed that, for the samples with the same initial void ratio, yield stress decreases with increasing initial water-content. This behaviour is due to the fact that the samples with a lower initial water-content have a higher matric suction. As suction increases, more voids become air-filled and therefore the number of interparticle contacts influenced by meniscus water increases. The overall stability of the soil skeleton is governed by the number of inter-particle contacts affected by the meniscus water lenses (Wheeler et al., 2003). As mentioned in section 2.2.1, the presence of water menisci at interparticle contact points results in a normal force in their plane of contact, which improves the stability of the soil particles against slippage and therefore compressibility of the soil decreases. Figure 5.13 shows the influence of initial void ratio on compression behaviour of the as-compacted samples. From the figure it can be observed that, for the samples with the same compaction water-content, the yield stress increases with decreasing initial void ratio. This is due to increased compactive effort during sample preparation.

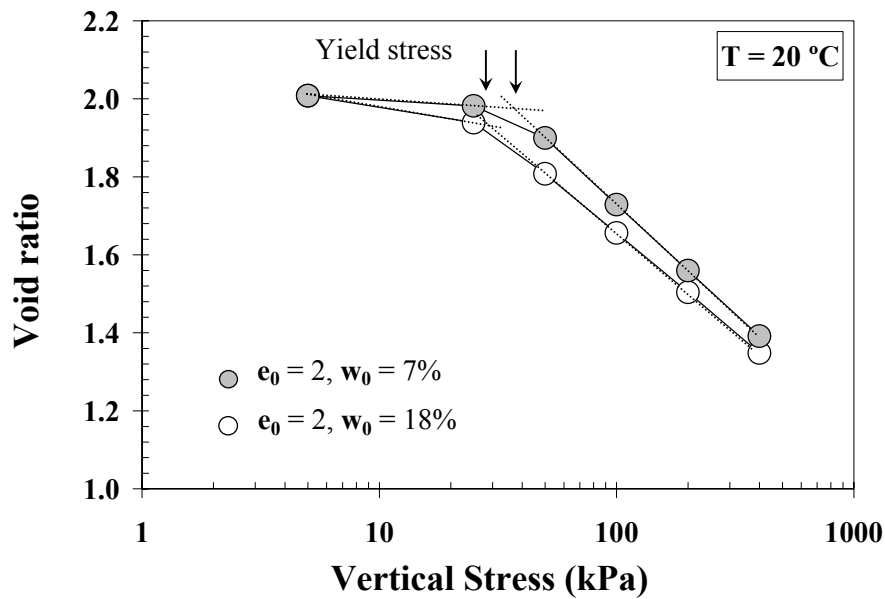


**Figure 5.11** Influence of initial water-content on compression behaviour, As-compacted compression curves at 20°C.



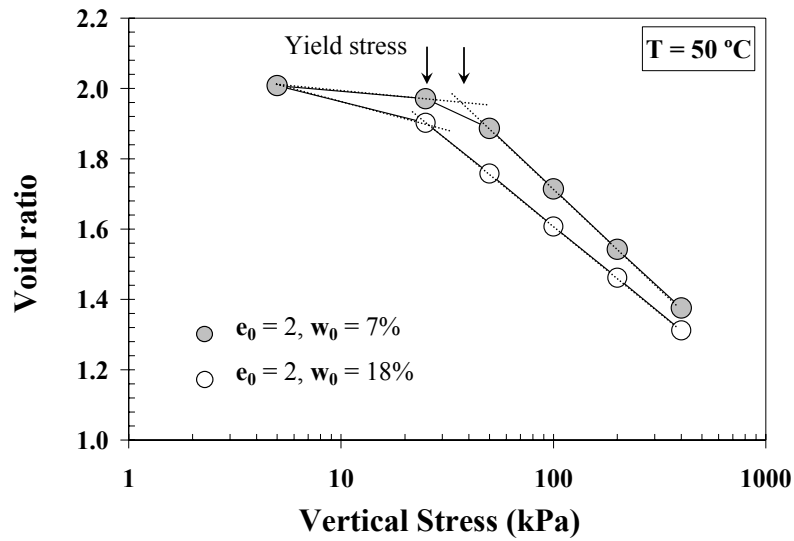


**Figure 5.12** Influence of initial water-content on compression behaviour, As-compacted compression curves at 50°C.

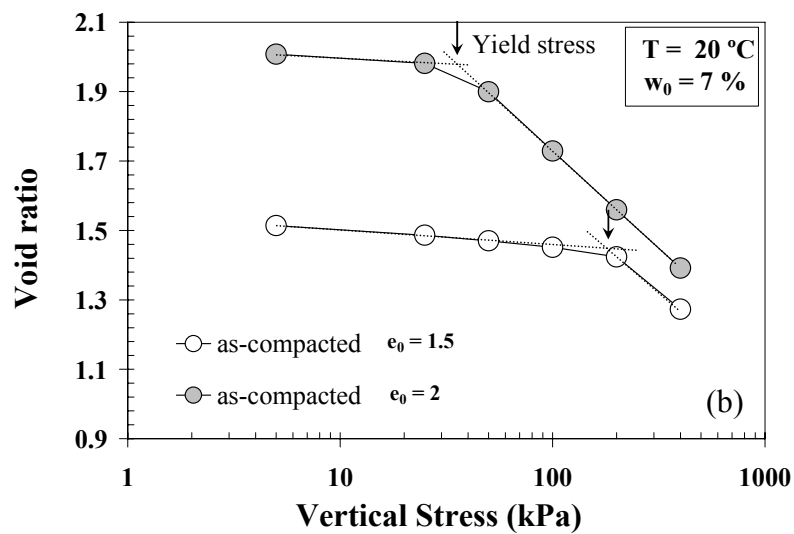
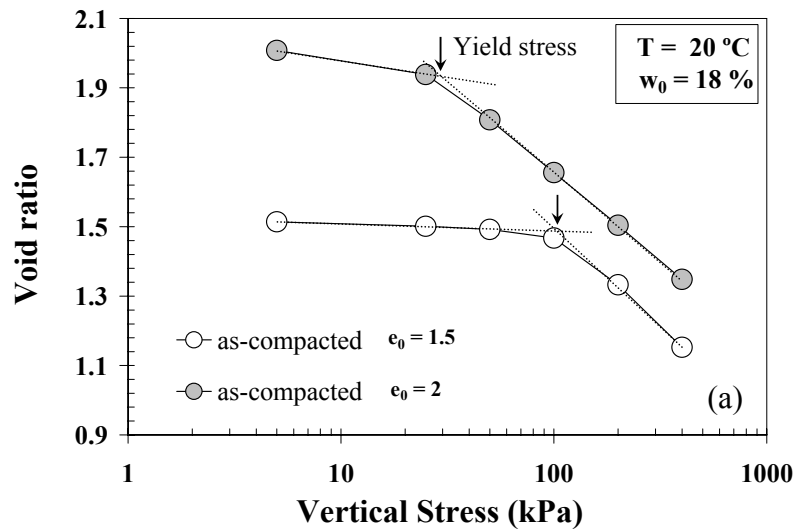


**Figure 5.13** Influence of initial void ratio on compression behaviour at 20°C (a) Samples with initial water content of 18% (b) Samples with initial water content of 7%.

### 5.3.2 Collapse behaviour

From the compression curves (Figures 5.1 to 5.4) it can be observed that the collapse potential (CP) of the samples increases with increasing applied vertical stress up to a maximum value, beyond which the collapse potential decreases for increasing values of vertical stress. Similar behaviour has been reported by other authors (e.g. Sun et al., 2004; Medero et al., 2009; Vilar and Rodrigues, 2011). From the compression curves it can be seen that the maximum wetting-induced collapse occurs at the yield stress. This can be explained by the concept of LC curve proposed by Alonso et al. (1987). Figure 5.14 schematically shows a collapse test performed at four different vertical stresses. At a given suction  $s_1$ , the sample is wetted at stresses:  $P_1$ ,  $P_2$ ,  $P_3$  and  $P_4$ . If the sample is wetted at vertical stress of  $P_1$ , the wetting path is inside the elastic region and therefore small elastic swelling occurs (Figure 5.14b). If the sample is wetted at vertical stress of  $P_2$ , an elastic swelling occurs in the first part of the wetting path before reaching the yield surface. Once the wetting path hits the yield surface, the sample experiences a plastic compression strain which may offset the initial swelling and result in a net collapse (Figure 5.14b). If the sample is wetted at vertical stress of  $P_3$ , the sample does not experience any swelling and only a collapse strain occurs upon wetting. When the stress state reaches the current location of the yield surface, an increase of vertical stress results in an expansion of the yield surface (LC curve shifts to the right due to any plastic deformations). When the stress is beyond the yield stress, hardening occurs. According to Figure 5.14b, if  $\lambda(s) > \lambda(0)$  the maximum wetting induced collapse occurs at the yield stress, beyond which the amount of collapse reduces. However, if  $\lambda(s) < \lambda(0)$  the amount of collapse increases with increasing vertical stress up to the yield stress, beyond which the amount of collapse increases but at a lower rate. From the compression curves performed in this study, it can be observed that the slope of normal consolidation lines in unsaturated condition is bigger than that in saturated condition. Therefore, the maximum collapse occurs at the yield stress.

Lawton et al. (1989) demonstrated that the yield stress of the as-compacted soil is also the vertical stress at which the potential for maximum wetting-induced collapse exists. The authors explained this fact in terms of the vertical stress, dry density and degree of saturation at the time water is added to the specimen. At levels of vertical stress lower than the yield stress, very little compression takes place in the as-compacted soil due to the vertical stress, and the dry density and degree of saturation at all values of vertical stress are approximately the same. Therefore, the potential for wetting-induced collapse

increases with increasing vertical stress. However, if the vertical stress exceeds the level of yield stress, more compression occurs due to the application of the vertical stress, resulting in an increased dry density and a higher degree of saturation. Both these characteristics reduce the potential for wetting-induced collapse. Therefore, the maximum collapse potential for a given compacted condition exists at the yield stress. According to Medero et al. (2003) the amount of collapse decreases for increasing values of vertical stress due to the progressive breakage of meta-stable structure of the soil skeleton under higher loads. At very high stress levels where the soil structure has been broken by compression, the voids are reduced and the collapse becomes negligible. Another reason for the smaller collapse observed at higher stress levels is that increasing compression of the soil at constant water-content generates a progressive reduction of suction from its initial value. The subsequent reduction in suction upon saturation therefore tends to be of smaller magnitude for samples subjected to higher levels of vertical stress.

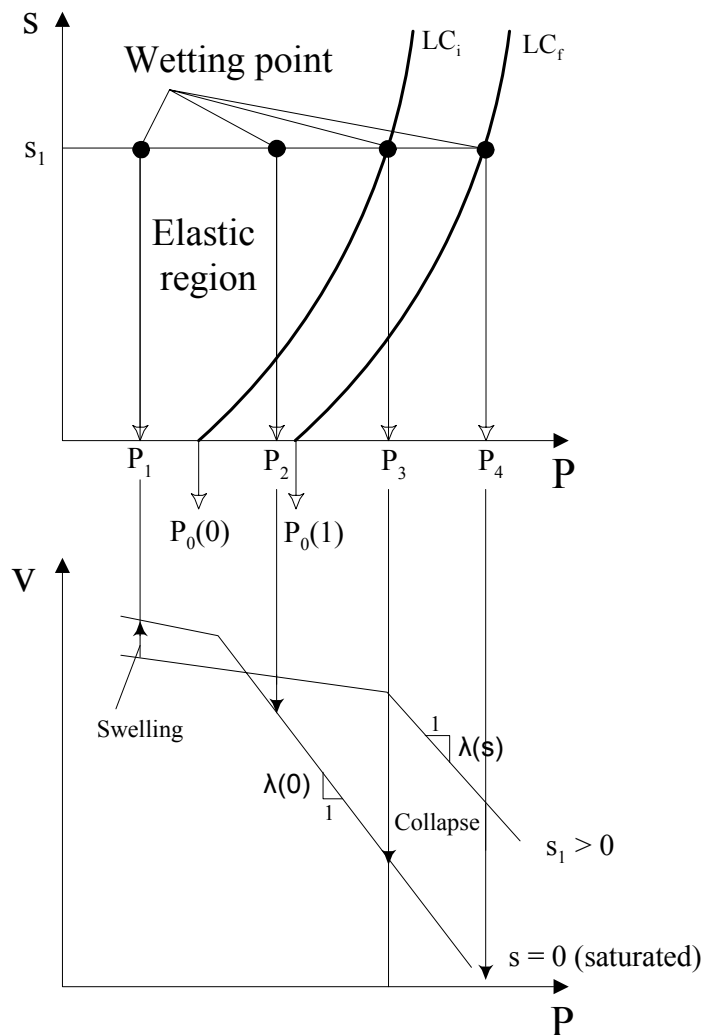


**Figure 5.14** Wetting-induced deformation under loading.

From the compression curves it can be observed that the results of single and double oedometer tests are similar. The results of experiments by Lawton et al. (1989), Basma and Tuncer (1992), also indicate that these two techniques give similar results. Lawton et al. (1989) showed that the collapse deformations obtained from the double oedometer tests for statically compacted clayey sand samples are similar to those measured from single oedometer tests.

The influence of temperature on CP can be seen from the compression curves. The CP of the samples tends to decrease with increasing temperature. Reduction of CP with increasing temperature is attributed to a decrease in matric suction. Reduction of CP with increasing temperature is because of the increased rigidity attained by the soil at larger suction, which tends to compress less than the same soil with lower suction. Therefore, there is a greater volume of voids for deformation when the suction is reduced and the soil reaches a new equilibrium state.

Table 5.3 summarises the maximum CP of the samples at different temperatures and the vertical stress at which maximum collapse occurs (the term critical vertical stress will be used hereinafter to refer to the vertical stress at which maximum collapse occurs). As discussed earlier, the critical vertical stress in as-compacted tests is the yield stress. The yield stress is lower for samples with a higher initial water-content. From the table it can be observed that the maximum CP of samples measured at 20°C is approximately 18%, and it is approximately equal to 17% at 50°C (i.e. 1% reduction in max CP with increasing temperature from 20°C to 50°C). The initial matric suction of the soil samples at different temperatures are reported in Tables 5.1 and 5.2. The results show that the amount of suction is lower at higher temperatures, for the samples prepared with the same void ratio and the same water-content.

**Table 5.3** Maximum collapse potential of samples at different temperatures.

T (°C)	e <sub>0</sub>	w <sub>0</sub> (%)	s <sub>0</sub> (kPa)	Max CP	Critical vertical stress (kPa)
20	1.5	7	914	17.7%	200
20	1.5	18	658	18.5%	100
20	2	7	942	17.9%	37
20	2	18	671	18.9%	25
50	1.5	7	830	16.7%	200
50	1.5	18	591	17.4%	100
50	2	7	864	17.3%	43
50	2	18	610	17.7%	25

The influence of initial water-content on collapse behaviour can be seen from the compression curves. The soil samples with lower initial water-content have higher matric suction, greater resistance against compression and therefore more significant wetting-induced volume changes. As shown in Table 5.3, the maximum CP of samples with initial water-content of 18% are slightly larger than samples with initial water-content of 7%. This behaviour is due to the fact that the initial void ratios of the samples prepared with initial water-content of 18% are slightly higher than those of samples prepared with initial water-content of 7% (see Tables 5.1 and 5.2).

The influence of initial void ratio on collapse behaviour can be seen from the compression curves. Under low levels of vertical stress, CP decreases with decreasing initial void ratio. The lower the initial void ratio, the denser the soil, thus resulting in less collapse upon wetting. Under high levels of vertical stress, the amount of collapse is influenced more by the levels of vertical pressure applied. A dense soil would reduce the relative contribution of the metastable forces in supporting the soil structure. Soil with a higher void ratio is more compressible and, consequently, more deformation occurs due to the vertical pressure applied, and therefore wetting induced volume changes decrease. Table 5.3; however, show that the amount of maximum CP is not influenced to any great extent by the initial void ratio of samples.

## **5.4 Chapter summary**

In this chapter, a series of temperature controlled single and double oedometer tests were conducted on samples with different initial suction values and initial void ratios. From the compression curves, the influence of initial water-content, initial void ratio and temperature on the compressibility and collapse behaviour of the material were studied. The results show that yield stress decreases slightly with increasing temperature. From the compression curves, it was observed that the normal consolidation lines move in parallel towards lower stress levels with increasing temperature. It was therefore concluded that the plastic compressibility parameter is independent of temperature.

The CP of the samples was obtained from the compression curves. The test results show that the collapse deformations obtained from the double oedometer tests are similar to those measured from single oedometer tests. From the test results, it was also observed that CP of samples decreases slightly with increasing temperature (1% reduction in

maximum CP was observed with increasing temperature from 20 to 50°C). The results also show that CP decreases with an increase in initial water-content or a decrease in initial void ratio of samples.

## CHAPTER 6 – TEMPERATURE AND SUCTION INFLUENCES ON OEDOMETER BEHAVIOUR OF KAOLIN CLAY

### 6.1 Introduction

This chapter examines the combined effects of suction and temperature on the mechanical behaviour of kaolin clay under controlled conditions. The tests were performed in a specially designed THM oedometer cell. The original concept of this oedometer cell is based on the design of Romero (1999). The axis translation technique has been used for imposing different matric suction values into the samples. The suction controlled oedometer tests were performed on samples with the same initial conditions as conventional oedometer tests, therefore allowing comparison of results.

### 6.2 Sample preparation and experimental set-up

The soil samples were prepared by mixing deionised water thoroughly into the oven dried clay to obtain a homogenous material, which was then statically compacted into the oedometer ring to obtain the desired initial void ratio. The SWRCs of the samples at different temperatures are presented in Chapter 4. A minimum height to diameter ratio has been selected (20mm/50mm) for the soil samples in order to reduce suction equalisation time. Initial conditions of the samples are presented in Table 6.1. All the samples were prepared with initial void ratio of 1.5 and initial water-content of approximately 52%, as the samples for determination of SWRCs were prepared with the same initial conditions. In this way, the volume reduction in the samples while imposing suction can be compared with the shrinkage behaviour of the material, presented in Chapter 4.

**Table 6.1** Initial condition of soil samples.

Water content: %	51.8
Degree of Saturation: %	91.2
Void ratio:	1.5

The soil samples, for suction-controlled compression tests, were placed over a saturated HAEV ceramic disc, and the loading ram was subsequently placed on top of it. Continuity between soil water and water in the ceramic disc is very important for accurate measurements. Therefore, a thin layer of water was left over the ceramic disc during the setting up process. In this way, ceramic saturation was ensured, preventing the possibility of its de-saturation due to air contact particularly during the setup

operation at high temperatures. The LVDT displacement transducer was connected on top of the loading ram. The pore air pressure and water pressure were applied into the sample and maintained constant to reach the desired suction. The effect of soil water evaporation through the top porous stone connected to the air pressure line and diffusion through the ceramic disc has to be considered in order to obtain a reliable volume change measurement. These two flows act in opposite directions in the water volume change indicator. The diffusion process through the ceramic disc is recorded as a soil water outlet, while the evaporation through the top porous stone is recorded as a water inlet into the sample. After 4 days equilibration time, a constant rate of water volume change ( $10 \text{ mm}^3$  per hour – flow into the sample) at  $50^\circ\text{C}$  was recorded on GDS pressure/volume controller as a balance between the volume of diffused and evaporated water. After equalisation, diaphragm pressure was applied on the soil sample, using standard incremental loading procedure. An equilibration period of 24 hours is adopted to achieve equilibrium for each load increment. The void ratio corresponding to each vertical stress is directly determined by the measurement of height variation (via an LVDT displacement transducer). Table 6.2 shows the initial conditions of the samples at moulding and final condition of each sample after the compression test. When suction was imposed to the moulded samples, the samples volume decreased during the suction equalisation stage, under no applied vertical stress. The volume reduction of samples upon drying was measured and recorded with an LVDT displacement transducer.

**Table 6.2** Initial and final condition of soil samples.

Sample	T( $^\circ\text{C}$ )	* $e_0$	* $w_0$ (%)	* $Sr_0$ (%)	Suction imposed (kPa)	$w_f$ (%)	$e_f$	$Sr_f$ (%)
A1	10	1.50	51.8	91.2	100	33.7	1.01	88.1
A2		1.48	51.4	91.7	300	31.8	1.00	84.0
A3		1.51	51.5	90.0	500	28.8	1.02	74.5
B1	50	1.50	51.6	90.8	100	33.2	0.98	89.4
B2		1.51	51.3	89.7	300	30.1	0.96	82.8
B3		1.49	51.4	91.1	500	28.2	0.99	75.2

\* Initial condition of samples at moulding

### 6.3 Experimental test results and analysis

In order to study the influence of temperature and suction on mechanical behaviour of kaolin clay, an experimental programme was designed using the developed oedometer cell. In total, 6 temperature and suction controlled oedometer tests were performed. Temperature controlled constant suction compression test results at  $10^\circ\text{C}$  and  $50^\circ\text{C}$  are presented in Figures 6.1 and 6.2. The tests were performed at matric suctions of 100,



300, and 500 kPa. The test results are reported in terms of net stress. From the figures it can be observed that the void ratio of the samples decreases from 1.5 to approximately 1.2 during suction equalisation. Clayey soils usually undergo large volume reduction when their water-content is reduced. This reduction in volume is called shrinkage. The higher the imposed suction, the more water is removed from the sample, the more volume reduction upon drying and consequently the lower the void ratio.

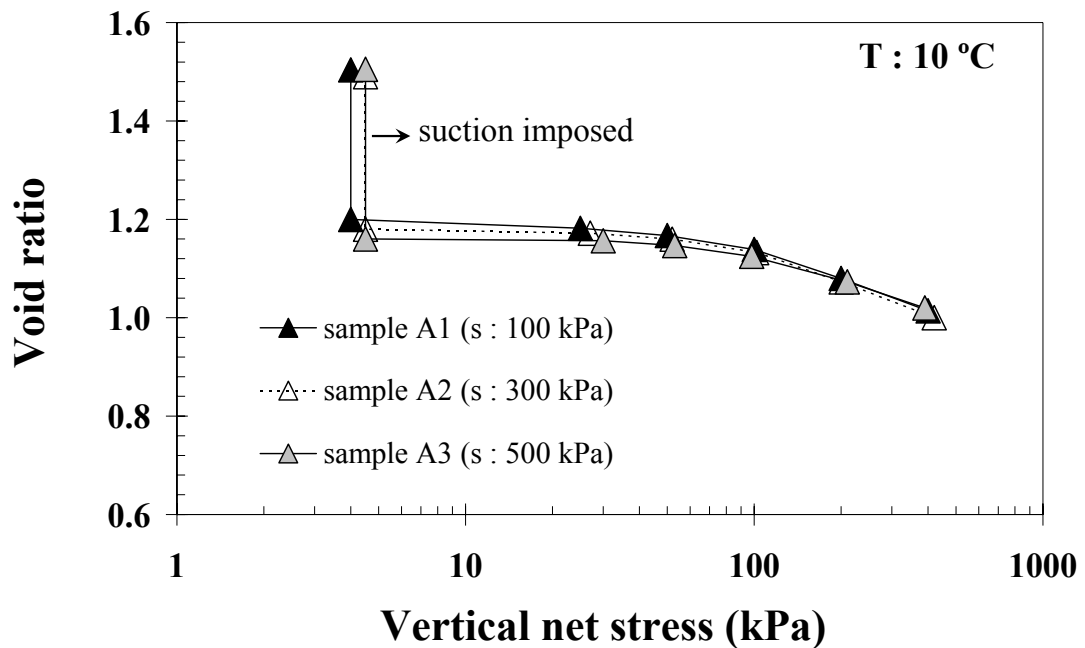


**Figure 6.1** Oedometer compression curves (at 10°C) for suctions of 100, 300, and 500 kPa.

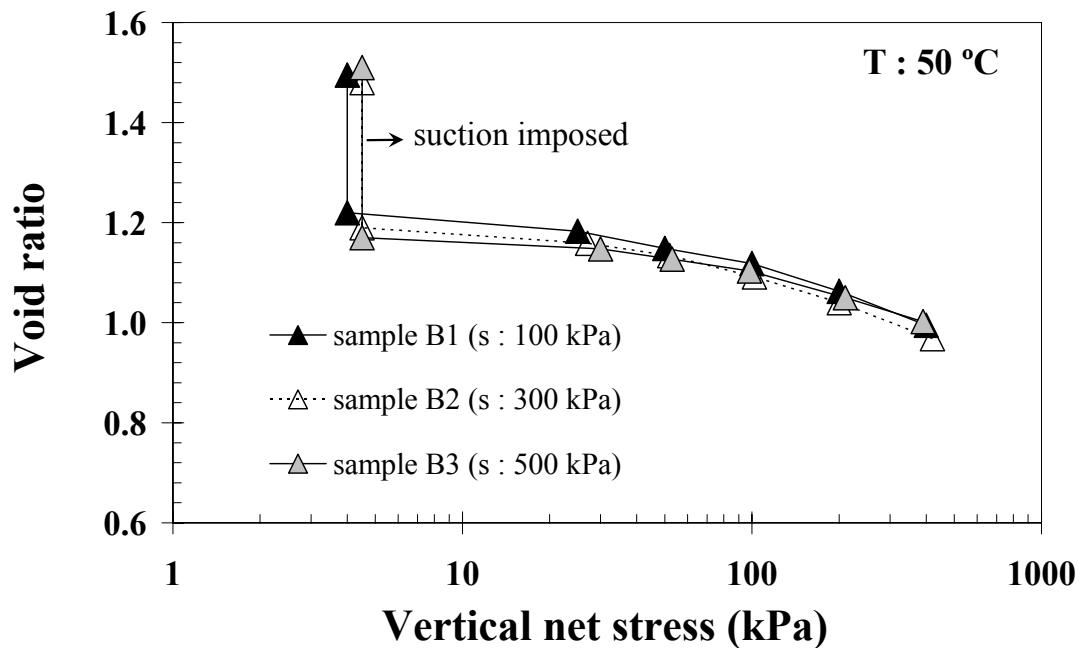


**Figure 6.2** Oedometer compression curves (at 50°C) for suctions of 100, 300, and 500 kPa.

All the soil samples were prepared with the same initial water-content of 52% and initial void ratio of 1.5, however; the void ratio of samples decreased due to impose of suction. Table 6.3 compares the amount of reduction in void ratio of samples when imposing different values of suction.

**Table 6.3** Comparison of reduction in void ratio when imposing suction/wetting the samples.

T (°C)	10			50		
samples condition	*e <sub>0</sub>	*e <sub>1</sub>	Δe/e <sub>0</sub>	*e <sub>0</sub>	*e <sub>1</sub>	Δe/e <sub>0</sub>
suction : 100 kPa	1.50	1.20	20.0%	1.50	1.22	18.7%
suction : 300 kPa	1.48	1.18	20.3%	1.51	1.19	20.2%
suction : 500 kPa	1.50	1.16	23.2%	1.49	1.17	22.1%

\*e<sub>0</sub> = initial void ratio, \*e<sub>1</sub> = void ratio after imposing suction

Figure 6.3 presents the suction-controlled compression curves at 10 and 50°C. Since initial void ratio of the samples varied slightly (referring to Table 6.3), the results of individual tests have been adjusted slightly to show all tests starting from the average initial void ratio. From the figure it can be observed that the normal consolidation lines (NCLs) move forward with increasing matric suction at all temperatures tested, except for the suction value of 300 kPa at 50°C where the normal consolidation line lies close to the one at a suction value of 100 kPa. An increase in suction results in hardening the soil response (suction hardening) and causes an increase in the yield stress. As suction increases, more voids become air-filled and therefore the number of interparticle contacts influenced by meniscus water increases. The overall stability of the soil skeleton is governed by the number of inter-particle contacts affected by the meniscus water lenses (Wheeler et al., 2003). As mentioned in section 2.2.1, the presence of water menisci at interparticle contact points results in a normal force in their plane of contact, which improves the stability of the soil particles against slippage and therefore compressibility of the soil decreases.

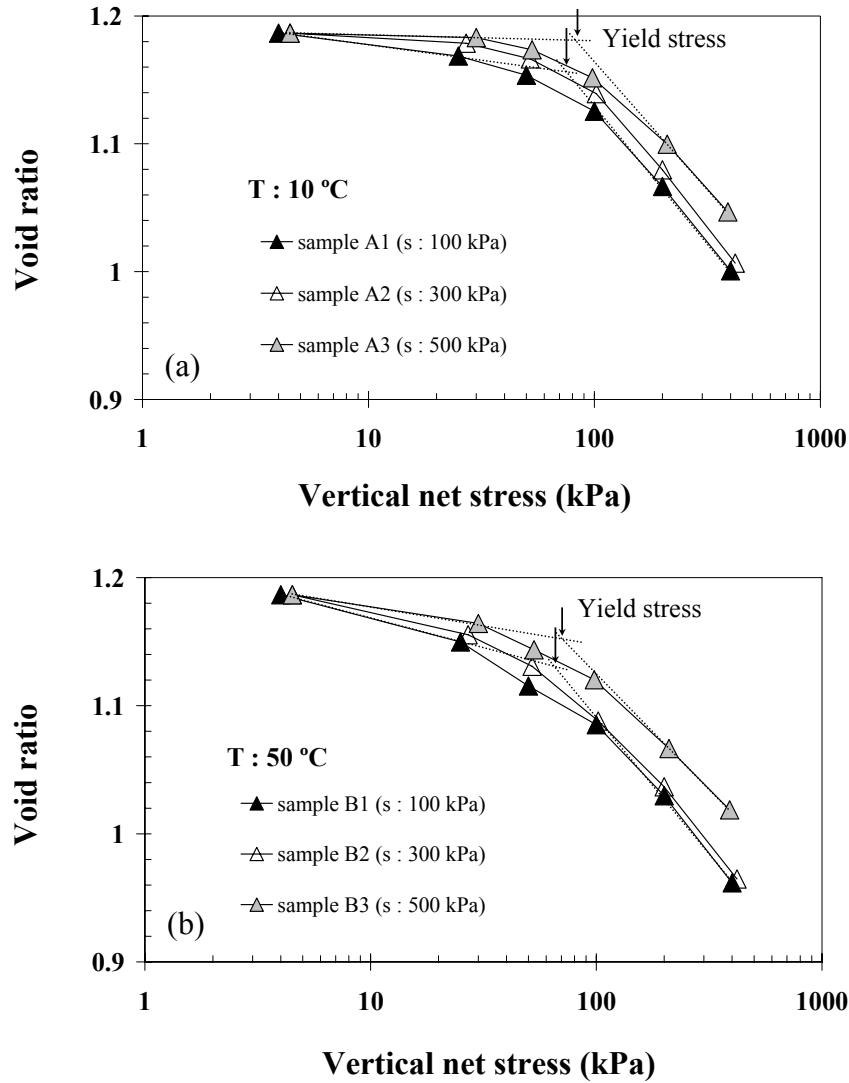


**Figure 6.3** Suction-controlled compression curves for suctions of 100, 300, 500 kPa (a) at  $10^{\circ}\text{C}$  (b) at  $50^{\circ}\text{C}$ .

Figure 6.4 shows the effect of temperature on soil response at suction of 100, 300 and 500 kPa. The results show softening of the soil response with increasing temperature. From the figure it can be observed that the normal consolidation lines (NCLs) move towards lower levels of stress with increasing temperature. The results also show that the yield stress decreases with increasing temperature. Therefore, the elastic domain contracts with increasing temperature (thermal softening). A similar softening in soil response with increasing temperature was observed by other authors (e.g. Cui et al., 2000; Cekerevac and Laloui, 2004; Salager et al., 2008). From the figure it can be observed that the NCLs are almost parallel for the two test temperatures (10 and  $50^{\circ}\text{C}$ ). The slopes of the NCLs (plastic compressibility parameter,  $\lambda$ ) are reported in Table 6.4. This negligible effect of temperature on  $\lambda$  is in agreement with other experimental

evidence, such as the results of Cekerevac and Laloui (2004) on saturated kaolin clay, or Tang et al. (2008) on compacted bentonite in an unsaturated state.

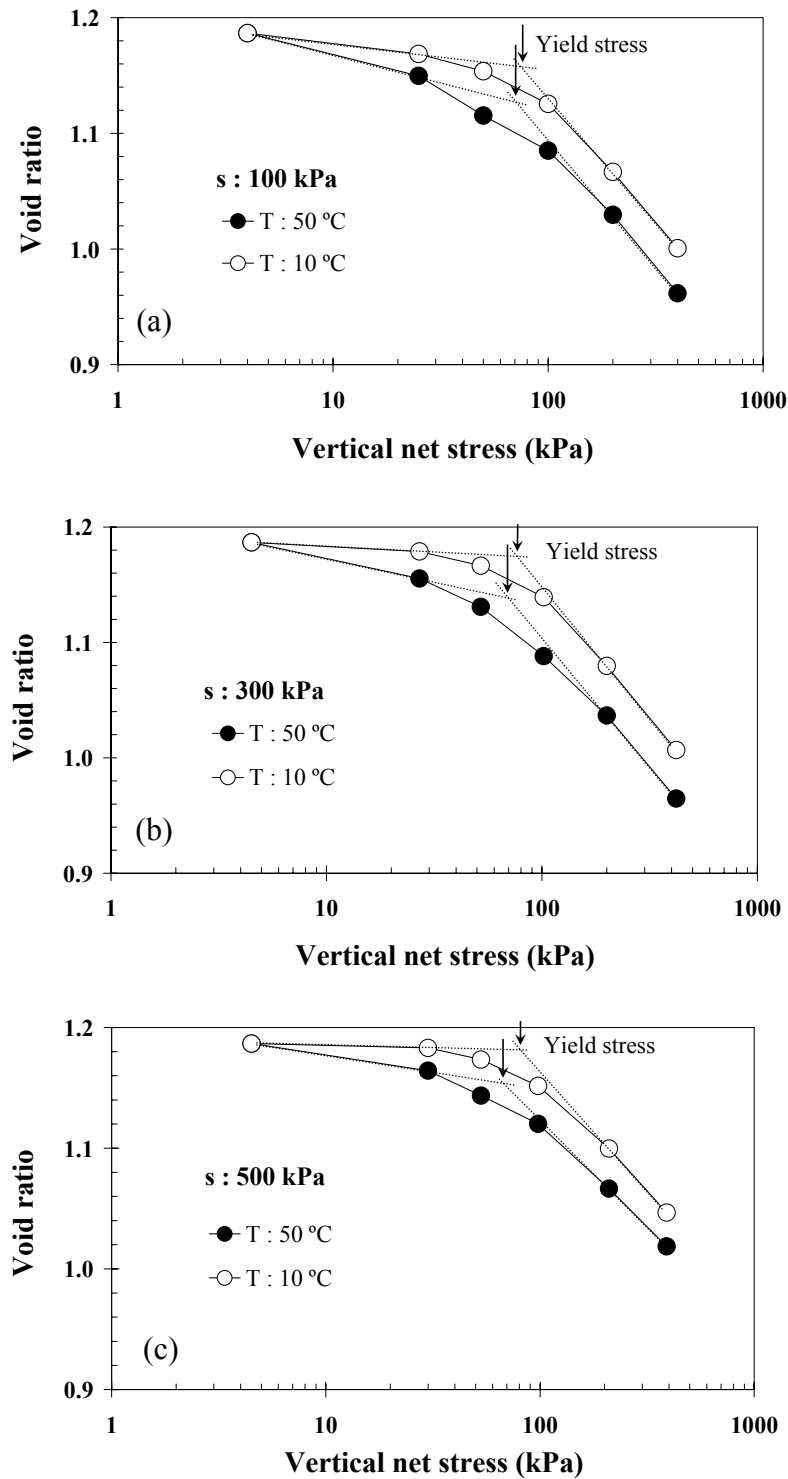


**Figure 6.4** Suction-controlled compression curves at 10 and  $50^\circ\text{C}$  (a) for suction of 100 kPa (b) for suction of 300 kPa (c) for suction of 500 kPa.

**Table 6.4** Compressibility parameters obtained for different tests.

Sample	$\lambda$
A1 (s : 100 kPa – T : 10°C)	0.095
A2 (s : 300 kPa – T : 10°C)	0.098
A3 (s : 500 kPa – T : 10°C)	0.080
B1 (s : 100 kPa – T : 50°C)	0.098
B2 (s : 300 kPa – T : 50°C)	0.097
B3 (s : 500 kPa – T : 50°C)	0.077

Figures 6.5 and 6.6 show variation of the yield stress with respect to suction and temperature. From the figures it can be observed that the yield stress decreases with increasing temperature, and increases with suction. As mentioned in section 2.3.4, the yield line in  $s : p$  space, that separates elastic and plastic regions, has been named LC curve. From Figure 6.5 it can be observed that the LC yield curve tends to shrink when the temperature increases, while it expands when the suction increases. Similar behaviour was observed by other authors including Laloui and Cekerevac (2003), François (2009), Uchaipichat and Khalili (2009). The air-entry values are estimated through the unconfined SWRCs presented in Chapter 4. For suction lower than air entry value, the soil remains saturated and effective stress for saturated state is constant along the 135° line in the  $s : p$  space (for saturated soils effective stress is Terzaghi's stress,  $\sigma' = \sigma_{\text{net}} + \text{suction}$ ).

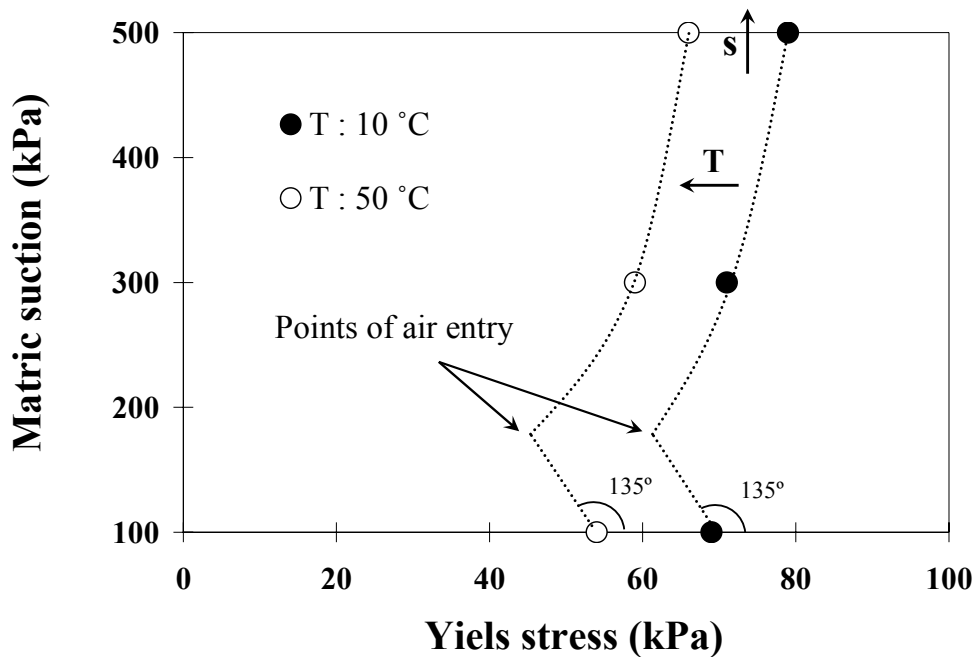


**Figure 6.5** Variation of yield stress with respect to suction.

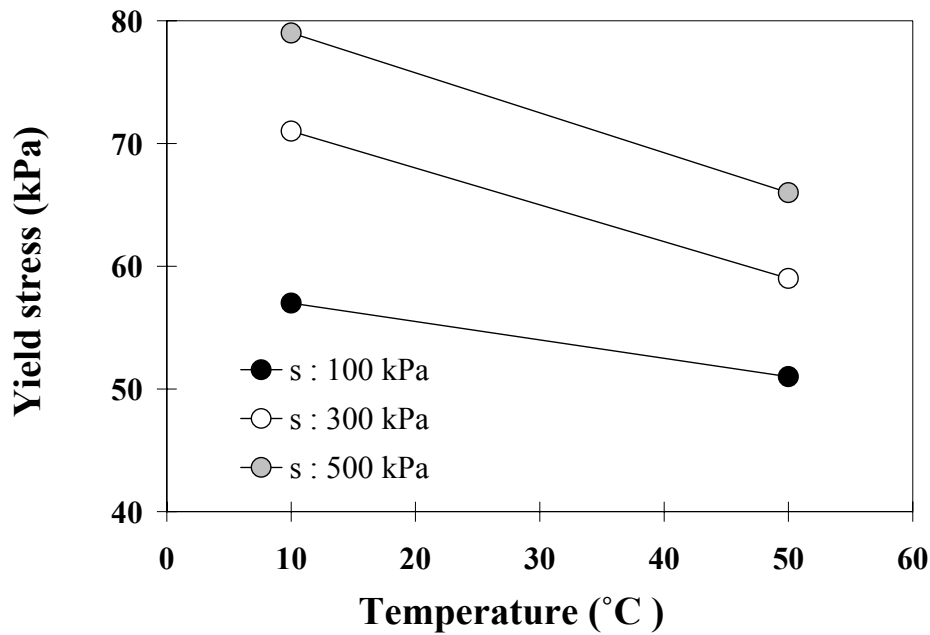


**Figure 6.6** Variation of yield stress with respect to temperature.

#### 6.4 Chapter summary

A series of temperature and suction-controlled oedometer tests has been conducted on kaolin clay samples using a novel oedometer cell. The influence of temperature and suction on the mechanical behaviour of the soil was studied. The results of temperature and suction controlled oedometer tests revealed that suction results in a hardening of the soil response (suction hardening) and causes an increase in the yield stress. The results also showed softening of the soil response with increasing temperature (thermal softening). The yield stress decreased with an increase of temperature and the normal consolidation lines moved in parallel towards lower levels of stress with increasing temperature. The results showed that the plastic compressibility parameters are independent of temperature.

## **CHAPTER 7 – EXPERIMENTAL AND THEORETICAL STUDY OF THERMAL EFFECTS ON SOIL WATER RETENTION CURVES**

### **7.1 Introduction**

The effect of temperature on capillary suction is commonly attributed to the temperature dependence of the surface tension at the air-water interface. Based on the Young-Laplace equation, surface tension is known to decrease with increasing temperature. The capillary pressure would be expected to decrease with increasing temperature if surface tension is the only parameter changing with temperature, as assumed by Philip and de Vries (1957). However, many experimental results on the temperature dependency of soil water retention capacity (e.g. Jury and Miller, 1974; Nimmo and Miller, 1986; Liu and Dane, 1993; Grant and Bachmann, 2002; Villar and Gomez-Espina, 2008) revealed that temperature effects were several times greater than would be predicted from the temperature dependence of the surface tension alone. Additional factors have therefore been proposed by other authors (e.g. Peck, 1960; Hopmans and Dane, 1986; Liu and Dane, 1993) to explain the observed discrepancy, including: thermal expansion of entrapped air, expansion of water, solute effects on the surface tension of water and temperature-induced changes in contact angle.

Peck (1960) and Chahal (1965) developed a theoretical model based on the assumption that the volume of entrapped air in the soil increases with temperature. This assumption gives rise to a higher temperature dependence of capillary pressure than predicted only by variation of the surface tension due to temperature changes. Hopmans and Dane (1986) investigated SWRCs and the corresponding volume of entrapped air at two temperatures and found that the entrapped air volume decreased with temperature. The authors therefore concluded that the observed temperature dependence of capillary pressure cannot be explained by the proposed model by Peck (1960) and Chahal (1965).

Liu and Dane (1993) explained the effect of temperature on SWRCs by assuming that the soil-water pressure to be determined by the continuous water phase only and not by the total water-content. They presumed that an increase in temperature caused entrapped water to become connected with the continuous water phase which results in an additional temperature effect on the capillary pressure. The authors used this theory to clarify the hysteresis in the temperature effect on capillary pressure, which was reported

by Taylor and Stewart (1960), who measured different capillary pressure at the same water-content value during cooling and heating cycles. The experimental results of Taylor and Stewart (1960) show that the slope of the cooling curve ( $\psi$  vs.  $T$  at constant water-content) is generally smaller than that of the heating curve. Liu and Dane (1993) explained this observation by stating that when the temperature increases, some isolated water will be converted to continuous water, but when the temperature decreases there is no reason for part of the continuous water to become isolated. The temperature effect will therefore be smaller during cooling than during heating.

In the present study, it was aimed to determine the temperature dependence of the soil water retention capacity of kaolin clay using vapour equilibrium and axis translation techniques. The experimental results revealed that the influence of temperature on water retention capacity of the soil is greater than would be predicted only from the temperature dependence of the surface tension at the air-water interface. The influence of temperature on additional factors was studied to describe the dependency of soil matric suction on temperature. The factors studied are temperature-induced changes in contact angle and microstructure of the soil sample. Furthermore, the influence of temperature changes on suction was analysed in a cycle of heating and cooling of a compacted kaolin clay sample at constant water-content.

## **7.2 Microstructural analysis**

The role of microstructure on physical and mechanical properties (strength, permeability and compressibility) of clayey soils and on matric suction has been studied by many authors (e.g. Mitchell, 1993; Delage et al., 1996; Djeran-Maigre et al., 1998; Rao and Revanasiddappa, 2005). In this chapter, in order to investigate the effect of temperature on the retention capacity of the soil, pore size distribution (PSD) of the soil samples was obtained at 10 and 25°C using the drying path of the SWRCs. The PSD of a soil sample can be determined from the desorption path of the SWRC (Prapaharan et al. 1985; Romero 1999). The process of injection of a non-wetting liquid (mercury) to penetrate the empty pores (Mercury Intrusion Porosimetry (MIP) test) can be compared to the ejection of water from the pores by applying external air pressure to dry the soil. Assuming the pores in the soil samples are cylindrical in shape, the relationship between the intrusion pressure ( $P_{int}$ ) and the pore radius ( $r_s$ ) and suction ( $u_a - u_w$ ) can be established as follows:

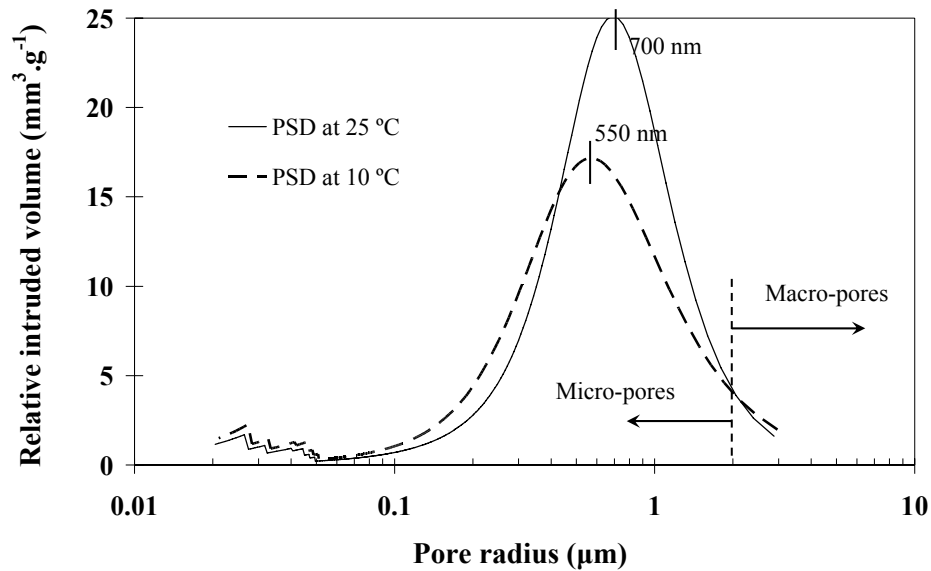


$$P_{\text{int}} = -\frac{2T_{s(\text{Hg})} \cos \beta_{nw}}{r_s} \quad 7.1$$

$$u_a - u_w = \frac{2T_s \cos \beta_w}{r_s} \quad 7.2$$

where  $T_{s(\text{Hg})}$  is the surface tension of mercury,  $\beta_w$  is contact angle of water, and  $\beta_{nw}$  is the contact angle between mercury and pore wall. In this study  $\beta_{nw}$  was taken as  $140^\circ$ . The parameter  $\theta_{nw}$  is usually assumed between  $139^\circ$  to  $147^\circ$  for clayey material according to Diamond (1970), Delage and Lefebvre (1984).  $\beta_w$  was taken equal to zero (as assumed by Romero, 1999). Muñoz (2006) compared the SWRCs of Opalinus clay obtained from the axis translation and vapour equilibrium techniques, and with MIP results. A good agreement was observed between different methods.

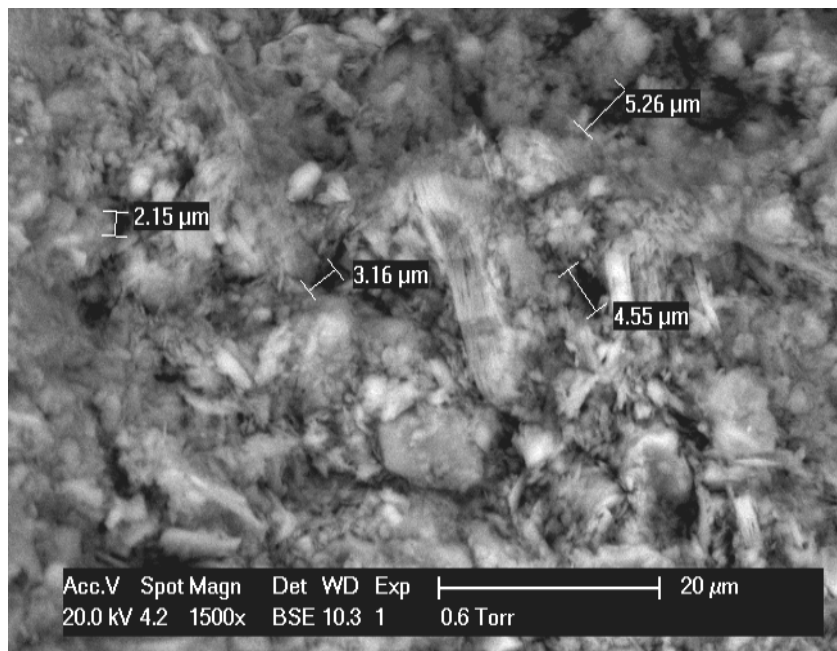
The obtained PSD curves of the soil samples at 10 and  $25^\circ\text{C}$  using drying paths of the SWRCs are shown in Figure 7.1. The soil samples were prepared with initial void ratio of 1.5 and initial water-content of 51.8%. A unimodal PSD (i.e. distribution which only has one peak) was obtained as it was expected, since the soil samples are compacted wet of optimum. As mentioned in section 2.2.3, clay samples compacted dry of optimum generally exhibit a fabric made up of aggregates having a bimodal pore size distribution with relatively larger pores, whereas soils compacted wet of optimum tend to show a more homogenous matrix-dominated fabric with a unimodal pore size distribution. Figure 7.1 is presented in terms of mean pore radius and volume of intruded pores. From the figure it can be observed that the dominant pore radius of the soil sample increases from 550nm at  $10^\circ\text{C}$  to 700nm at  $25^\circ\text{C}$ . Increasing the dominant pore radius of the soil sample with temperature is an additional factor for describing the effect of temperature on the capillary pressure. This fact gives rise to a higher temperature dependence of capillary pressure (based on the Young-Laplace equation) than predicted only by variation of the surface tension due to temperature changes. From Figure 7.1 it can be observed that the samples exhibit a single mode at around 600nm representing intra-aggregate pores. The boundary between the intra-aggregate pores from inter-aggregate pores will be defined in the following pages based on ESEM micrographs.



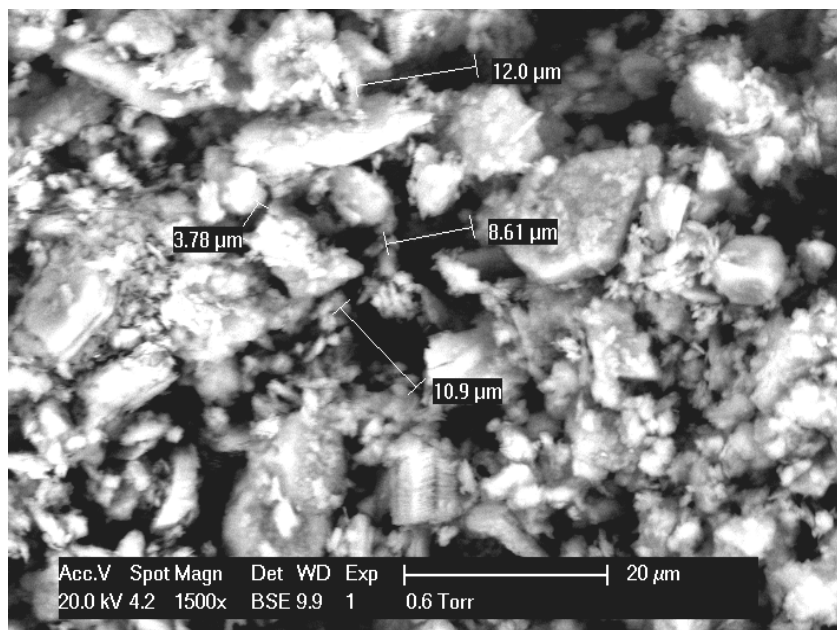
**Figure 7.1** PSD of kaolin clay determined from desorption path of the SWRCs at 10 and 25°C.

Figure 7.2 shows the environmental scanning electron micrograph of a sample of compacted kaolin clay, prepared with initial water-content of 51.8% and initial void ratio of 1.5. The soil sample was dried at room temperature to reach a water-content of 17% (which corresponds to matric suction of 1000 kPa). Figure 7.3 demonstrates the ESEM micrograph of a sample, prepared with initial water-content of 9.4% and initial void ratio of 1.5. The soil sample was wetted (inside a humidification chamber with 100% relative humidity at 25°C) to reach a water-content of 12% (which corresponds to matric suction of 1000 kPa). Figures 7.2 and 7.3 show different fabric of samples compacted on the dry and wet side of optimum. The dry side of optimum aggregates are clearly visible as well as inter-aggregate pores being in the order of tenths of microns. On the other hand, it is difficult to detect the aggregates in the samples compacted on the wet side of optimum and the space between silt particles are filled with the clay fraction that form a relatively uniform matrix. By comparing Figures 7.2 and 7.3, it can clearly be observed that the pores are larger in the case of samples prepared with a lower degree of saturation at the same initial void ratio. As with the shrinkage behaviour of the material studied in Chapter 4, contraction occurs in the soil samples during the drying process. While contraction occurs, the void ratio of the sample decreases and clay particles get closer to each other. As mentioned studied in Chapter 2, soil undergoing the drying process generally shows different mechanical behaviour in comparison with the same value of suction during the wetting process, because of different arrangements of water within the voids and consequently different action of matric suction on the soil skeleton.

In Figure 7.2, the inter-aggregate pores are visible in the ESEM image, whereas intra-aggregate pores are indistinguishable. Inter-aggregate pores correspond to the dark areas in the figure with a typical size of about  $4\mu\text{m}$  in diameter. In this study the pore size with radius of  $2\mu\text{m}$  is considered as a boundary between the inter-aggregate pores and intra-aggregate pores for samples compacted wet of optimum. This is also highlighted in Figure 7.1.



**Figure 7.2** ESEM micrograph, drying path ( $w = 17\%$  and  $s = 1000 \text{ kPa}$ ) - compacted on the wet side of optimum.



**Figure 7.3** ESEM micrograph, wetting path ( $w = 12\%$  and  $s = 1000 \text{ kPa}$ ) - compacted on the dry side of optimum.

In order to compare size of the pores in ESEM micrographs, clay plates (in white) and pores (in black) are highlighted in Figure 7.5. The figure shows the type of pores observed in the micrographs with magnification of 1500 times. From the figure it can clearly be observed that the pores are larger for the sample undergoing the wetting process.

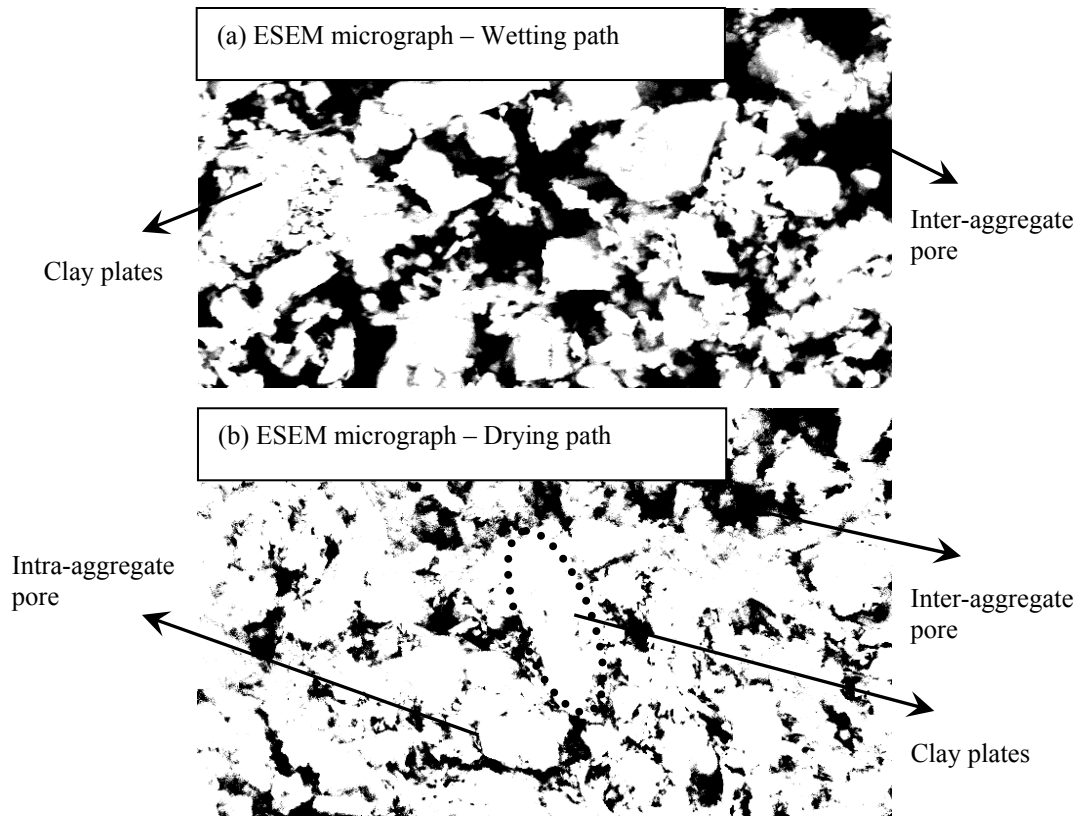


**Figure 7.5** Analysis of pores in ESEM micrographs (a) wetting path (b) drying path.

### 7.3 Temperature-induced changes in contact angle

According to the Young-Laplace equation (Equation 4.3), capillary pressure is dependant on three parameters: ( $T_s$ ) surface tension of water, radius of the capillary tube ( $r_s$ ), and the contact angle between the liquid and the tube ( $\beta$ ). The surface tension at the air-water interface is known to be a function of temperature (Tang and Cui, 2005; Uchaipichat and Khalili, 2009). There are very limited data on temperature dependence of the contact angle of water in porous media.

Many authors, including Tang and Cui (2005) and Uchaipichat and Khalili (2009), only considered the effect of temperature on surface tension of water when calculating matric suction. The effect of temperature on soil microstructure and on the contact angle of water in the soil pores is still controversial. In section 7.2, the influence of temperature on soil microstructure and pores with small radii is studied. In this section, the

temperature dependence of the contact angle ( $\beta$ ) is studied. The results of an experimental study by Poston et al. (1970) on three different refined oils indicated that the contact angle decreases with increasing temperature. However, the changes in contact angle with temperature were small. For instance, the change was  $-0.27^\circ/\text{ }^\circ\text{C}$  for an organic-water glass system. For contact angles between  $0^\circ$  and  $90^\circ$ , a decrease in contact angle results in an increase in the cosine of the contact angle (for instance, if  $\beta$  decreases from  $20^\circ$  to  $10^\circ$ ,  $\cos \beta$  increases 4.5%). The results of studies by Davis (1994), Bradford and Leij (1995) show that contact angle for an air-water-silica system is near zero, and that a decrease in contact angle caused by an increase in temperature is constrained to be small. Increase of  $\cos \beta$  with temperature is an additional factor for describing the effect of temperature on the capillary pressure.

Figure 7.6 shows the captured capillary water at the air-water interface at  $16^\circ$ ,  $28^\circ$  and  $35^\circ\text{C}$ . The figure shows the concave curvature of water inside the capillary tube. The curvature forms an angle ( $\beta$ ) on the inside wall of the capillary tube. The observation from imaging meniscus water at different temperatures suggests that the contact angle ( $\beta$ ) decreases with increasing temperatures. This observation is in agreement with those presented by the other authors (Poston et al., 1970; Bradford and Leij, 1995). From the figure it can also be seen that the concave curvature of water becomes more elliptical with increasing temperature. As the position of the high resolution microscope is changed when capturing the curvature of water inside the capillary tube, the images in Figure 7.6 can only be used for analysis of temperature changes in contact angle.

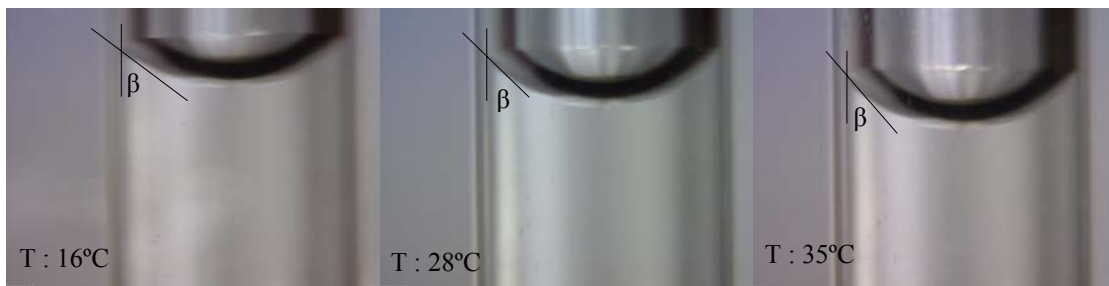


**Figure 7.6** Capillary water at the air-water interface at 16, 28 and  $35^\circ\text{C}$ .

The angle  $\beta$  was determined based on the capillary water images in Figure 7.6 which are reported in Table 7.1. Table 7.1 compares the height of water in a capillary tube (0.4mm inside diameter) at different temperatures using the Young-Laplace equation. The surface tension of water at different temperatures was calculated using Equation 4.4.

**Table 7.1** Comparison of height of water in a capillary tube at different temperatures.

T (°C)	$T_s$ (N/m)	$\beta$ (degree)	$\cos \beta$	H (cm)
16	0.0733	52	0.617	4.5
28	0.0715	45	0.707	5.1
35	0.0704	41	0.755	5.3

In order to gain a better understanding of the experimental results, Figure 7.7 presents schematically the effect of temperature on contact angle of meniscus. By assuming the radius of capillary tubes to be independent of temperature, the water table rises in the capillary tube with the increase in temperature due to the reduction of the contact angle ( $\beta$ ). Figure 7.8 shows the images of capillary water at the air-water interface at 14°, 35° and 40°C. The position of microscope was kept constant in this test. From the figure it can be observed that the water level rose in the capillary tube with increasing temperature. If only considering the effect of temperature on surface tension, it was expected that the water level would fall in the capillary tube with increasing temperature. However, the results of our experiment show that the increase of  $\cos \beta$  with temperature is higher than the reduction of surface tension of water. It should be emphasised that the contact angle of water on a clay surface is clearly different from that on a glass surface; however, this test gives us a general idea of how temperature affects capillary action in pores with small radii in unsaturated soils. In order to determine the precise influence of temperature on matric suction, variation of all three parameters: surface tension, contact angle and radius of capillary tube due to temperature changes, have to be considered in the calculation.

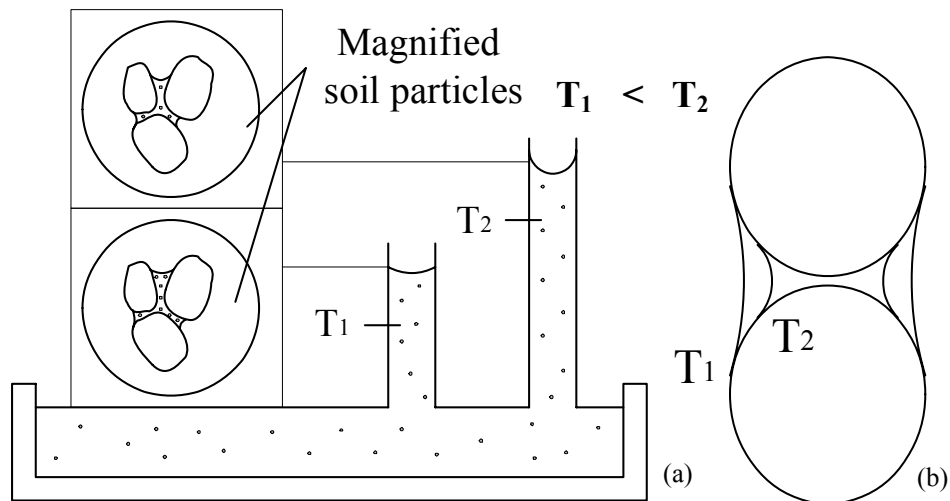


**Figure 7.7** (a) Capillary tubes showing the air-water interface at different temperatures (b) effect of temperature on angle of contact between two identical particles.

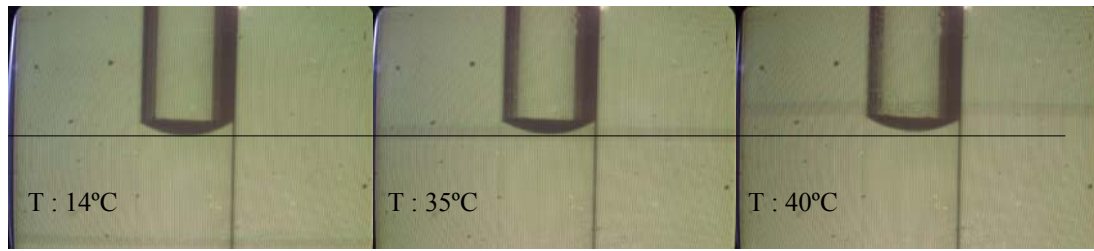


**Figure 7.8** Capillary water at the air-water interface at 14, 35 and 40°C.

#### 7.4 Thermal hysteresis in soil water retention curves

Gardner (1955) presented capillary pressure of a coarse sand at a constant degree of saturation subjected to heating and cooling cycles. The author observed a linear trend in reduction of capillary pressure with increasing temperature (as presented in Figure 7.9a). The results show that for a given water-content, capillary pressure decreases after a cycle of heating and cooling. This behaviour cannot be explained by the theory proposed by Liu and Dane (1993) and further analysis is necessary. Villar and Gomez-Espina (2008) also observed a small hysteresis in measured suction of FEBEX bentonite undergoing heating and cooling process. The results of an experimental study by Faybishenko (1983) on a loam soil indicated a reproducible capillary pressure on a cycle of heating and cooling for a temperature range of 5°C to 20°C. The results presented also suggest that capillary pressure decreases linearly with increasing temperature (as presented in Figure 7.9b).

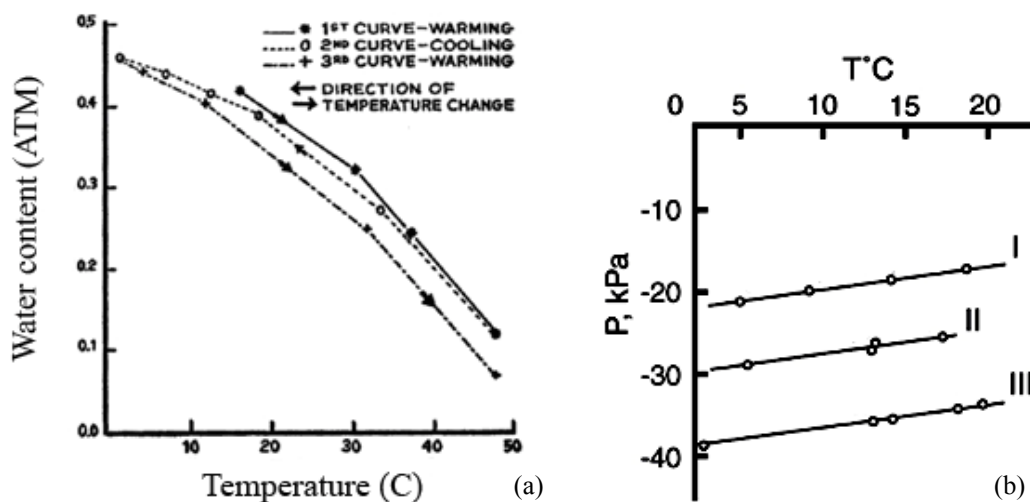


**Figure 7.9** (a) Capillary pressure of a coarse sand presented by Gardner (1955), (b) Capillary pressure of a loam soil measured by Faybishenko (1983).

The SWRCs of kaolin clay at different temperatures reported in Chapter 4 indicate that the relationship between matric suction and temperature is not linear (temperature range

of 10 to 50°C). It was observed that for a given water-content, the rate of suction changes with temperature,  $\Delta s/\Delta T$  decreases with increasing temperature, and that temperature may have a minor effect on matric suction at temperatures higher than 50°C. A similar study was carried out by Villar and Lloret (2004) who obtained SWRCs of compacted bentonite at 20, 60 and 80°C. The results of their experiment showed a reduction in water retention capacity of the soil from 20 to 60°C; however, the difference between samples tested at 60 and 80°C was minor. From these studies, the matric suction of clayey material was shown to be a nonlinear function of temperature.

In this study, a similar experiment to those of Gardner (1995) and Faybishenko (1983) was performed by applying a cycle of heating and cooling to compacted kaolin clay sample. Each sample was placed inside in an isolated system in order to keep the water-content constant during the test. The test results are presented in Figure 7.10. Each point reported on Figure 7.10(b) represents the average suction (variation smaller than 10%) of two samples at a particular temperature. At the end of each stage of temperature increment, two glass jars were opened; and the water-content of the soil samples and the sandwiched filter papers were determined. From Figure 7.10, it can be observed that matric suction at a particular temperature is not totally reversible after a cycle of heating and cooling (i.e. small thermal hysteresis was observed in a cycle of heating and cooling of samples). The results show that while undergoing a cycle of heating and cooling, matric suction decreases slightly at each particular temperature. By comparing points 2 and 4 in Figures 7.10(a) and 7.10(b), it can be seen that even though there is a slight decrease (approximately 2%) in the water-content of the soil samples during the cycle of heating and cooling, the matric suction decreased slightly (approximately 20 kPa). It can therefore be concluded that if the water-content of samples is kept constant, a smaller amount of matric suction would be expected to be measured after a cycle of heating and cooling. On a cycle of heating and cooling, during evaporation and water adsorption, it can be assumed that capillary water in the soil samples will be transmitted to adsorbed water. By considering this assumption it can be concluded that capillary action creates a higher suction potential than adsorption effect. The physical properties of adsorbed water (which is tightly bonded to the soil particle) can be significantly different from the capillary water, which is free water in the pores between the particles under the influence of the menisci.



The difference in capacity of the soil to retain water at different temperatures is due to the fact that the absorption process is basically exothermic in nature (Myers, 1991). The amount of water vapour adsorbed by the soil surface reduces as the temperature increases. From 10 to 25°C the capacity of air around the soil samples to hold water vapour increases from 7.8 to 20 (grWater/kgAir); however, from 25 to 50°C it increases from 20 to 95 (grWater/kgAir). Therefore, from point 2 to 3 (from 25 to 50°C) in Figure 7.10, more evaporation happens within the soil samples and less water absorption. As a result of this, the water-content of the soil samples decreases by increasing the temperature from 25 to 50°C, as expected. From Figure 7.10(a) it can be observed that, during the cooling cycle, some of the evaporated water does not return to the soil samples (water-content in the cooling cycle is less than that during the heating cycle). During the cooling cycle, part of the humidity of the air around the samples becomes water droplets which remain in the glass jar rather than being absorbed by the samples.

It can be seen in Figure 7.10(b) that during heating, total suction decreased (approximately 310 kPa) from 10 to 25°C; and increased (approximately 2100 kPa) from 25 to 50°C. During cooling, total suction decreased (approximately 1980 kPa) from 50 to 25°C; and increased (approximately 85 kPa) from 25 to 10°C. The matric suction showed small variation during the cycle of heating and cooling. During heating the matric suction decreased (approximately 68 kPa) from 10 to 25°C; and increased (approximately 52 kPa) from 25 to 50°C. During cooling, the matric suction decreased (approximately 71 kPa) from 50 to 25°C; and increased (approximately 54 kPa) from 25 to 10°C. The osmotic suction of samples was determined by subtracting matric suction from total suction. From Figure 7.10(b), it can be noted that the osmotic suction of samples changes significantly with temperature. Therefore, the greater influence of temperature on total suction is more likely due to changes in osmotic suction than to changes in matric suction.

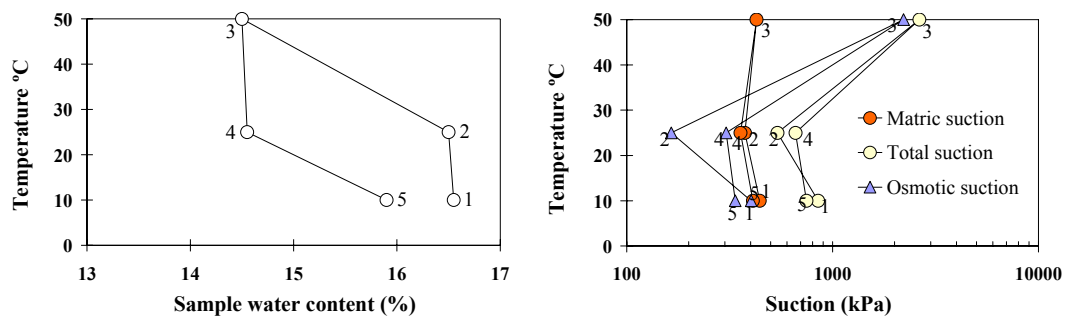


**Figure 7.10** (a) Variation of sample water-content by temperature (b) Measured suction values in a cycle of heating and cooling.

Since the osmotic suction is related to the dissolved salt content in the soil pore water, the osmotic suction changes with changing temperature. The osmotic suction is obtained from the total suction of the salt solution, and it is influenced by the concentration of the solution. Total suction can be calculated using Kelvin's equation, which is temperature dependent. The suction of salt solution may decrease or increase with increasing temperature depending on the type of cation (Arifin and Schanz, 2009). The main ions in the pore-water are  $\text{Na}^+$ ,  $\text{Ca}^{2+}$ ,  $\text{Mg}^{2+}$ ,  $\text{K}^+$  and  $\text{Cl}^-$ , the salt solutions in the pore water are NaCl,  $\text{CaCl}_2$ ,  $\text{MgCl}_2$ , and KCl. In order to gain a better understanding of the influence of temperature on osmotic suction, it is important to investigate the type and magnitude of the cations in the pore water of kaolin clay.

From point 1 to point 2 (see Figure 7.10), soil water-content is fairly constant, and consequently the concentration of dissolved ions in the solution is constant. Therefore, changes in osmotic suction (from 10 to 25°C) are related to changes in relative humidity due to temperature changes. From point 2 to point 3 (see Figure 7.10), as the soil loses water by evaporation (approximately 2% reduction in water-content), the concentration of the dissolved ions increases, and consequently the osmotic component of suction also increases. Osmotic suction may vary significantly with changes in the concentration of dissolved ions (Arifin and Schanz, 2009). In order to be able to undertake a better analysis, it is recommended to measure the osmotic suction of samples at different temperatures using the squeezing technique. Therefore, the osmotic suction measured at different temperatures can be compared with data obtained from subtracting matric suction from total suction.

## 7.5 Chapter summary

In this chapter, the influence of temperature on soil microstructure and contact angle of water is studied to understand the dependency of matric suction with temperature. In order to study the influence of temperature on soil microstructure, PSD of kaolin clay samples were determined from the desorption path of SWRCs. The results showed that the dominant pore radius of the samples increases with increasing temperature. This results in a higher temperature dependence of capillary pressure (based on the Young-Laplace equation) than that predicted only by the variation of the surface tension due to temperature changes. Furthermore, ESEM micrographs of kaolin clay samples are studied after the wetting and drying processes. From ESEM micrographs, it was observed that the pores are larger when the samples are prepared with a low degree of saturation (and followed by wetting process) than samples prepared with a high degree

of saturation (and followed by drying process). The influence of temperature on the contact angle of water was studied by capturing (using a high resolution microscope) images of the concave curvature of water inside a capillary tube at different temperatures. From the captured images, it was observed that the contact angle decreases with increasing temperature. This fact gives rise to a lower temperature dependence of capillary pressure than predicted only by variation of the surface tension due to temperature changes.

The influence of temperature changes on suction was also analysed in a cycle of heating and cooling of samples inside an isolated system, in order to keep the water-content of samples constant. Total and matric suction of samples at different temperatures were measured using the filter paper method. The osmotic suction of samples was determined by subtracting matric suction from total suction. From the results, it was observed that matric suction at a particular temperature is not totally reversible after a cycle of heating and cooling (i.e. small thermal hysteresis was observed in a cycle of heating and cooling of samples). Furthermore, the results showed that total suction changes significantly with temperature, while matric suction changes are small. Therefore it was concluded that the influence of temperature on total suction is more likely due to changes in osmotic suction rather than to changes in matric suction.

## CHAPTER 8 – CONCLUSIONS AND RECOMMENDATIONS

### 8.1 Conclusions

An experimental study of thermal effects on the hydro-mechanical behaviour of kaolin clay has been carried out. The experimental programme involved suction measurements using a range of techniques, and matric suction and temperature controlled experiments to investigate the combined effects of temperature and suction on the hydro-mechanical behaviour of the material. The experimental programme also includes microstructural investigation and study of collapse behaviour at different temperatures. Based on the analysis of the experimental data presented in Chapters 3 to 7, the following conclusions can be drawn.

1. It is shown that temperature has an important influence on filter paper suction measurements and that misleading results can be obtained if temperature is not taken into account in the calibration equation. By performing a series of filter paper calibration tests at different temperatures (using the vapour equilibrium and the axis translation techniques), a unique calibration equation was proposed for Whatman No. 42 filter paper. The proposed calibration equation, in comparison to previous work in the literature, is novel considering that the proposed equation is at the equilibrium condition and that the effect of temperature on filter paper calibration is taken into account (covering a wider range of temperature from 10 to 50°C). Following Marinho (1994b), it was shown that given sufficient time for equalisation, there is only a unique calibration curve for the filter paper regardless of the type of suction.
2. The soil water retention curves (SWRCs) of kaolin clay were obtained at different temperatures using the proposed calibration equation. To the author's knowledge, this thesis presents, for the first time, SWRCs at different temperatures using the filter paper method. The results revealed that the water retention capacity of the soil decreases with increasing temperature. The rate of reduction in suction with increasing temperature ( $\Delta s/\Delta T$ ) was determined from the SWRCs and compared with data reported by other authors. It was observed that the  $\Delta s/\Delta T$  obtained from the experiments, is several times greater than would be predicted from the temperature dependence of the surface tension alone (based on the Young-Laplace

equation). Therefore, it was necessary to study the effect of temperature on additional factors in order to describe the dependency of soil matric suction on temperature.

3. In order to describe the dependency of matric suction on temperature, the microstructure of kaolin clay samples were studied using pore size distribution (PSD) analysis and ESEM tests. The PSD of soil samples was obtained at 10 and 25°C using the drying path of the SWRCs. From analysis of the results, it can be observed that the dominant pore radius of the samples increases with increasing temperature. Increasing the dominant pore radius of the samples with temperature was considered as an additional factor to describe the observed discrepancy of the effect of temperature on soil water retention capacity. This fact gives rise to a higher temperature dependence of capillary pressure than predicted only by variation of the surface tension due to temperature changes.
4. ESEM micrographs were studied for kaolin clay samples after the wetting process and drying process, at known points of the SWRC. The samples for both wetting and drying tests were prepared with the same initial void ratio. From ESEM micrographs, it was observed that the pores are larger when the samples are prepared with a lower degree of saturation, followed by the wetting process, than when samples are prepared with higher degree of saturation followed by the drying process. This is due to the fact that when the soil sample is undergoing drying process, shrinkage occurs in the soil samples and, as a consequence, the void ratio of the samples decreases.
5. The influence of temperature on the contact angle of water was studied by capturing (using a high resolution microscope) images of the concave curvature of water inside a capillary tube at 16, 28, and 35°C. From the images, it was observed that the contact angle decreases with increasing temperature. This fact results in a smaller temperature dependence of capillary pressure than predicted only by variation of the surface tension due to temperature changes.
6. Thermal hysteresis in SWRCs was studied by applying a cycle of heating and cooling on compacted kaolin clay samples inside an isolated system, in order to keep the water-content of samples constant. The filter paper method was used for

measurement of total and matric suction at different temperatures of the heating and cooling cycle. The osmotic suction of samples was determined by subtracting matric suction from total suction. From the results, it was observed that matric suction at a particular temperature (10°C and 25°C) is not totally reversible after a cycle of heating and cooling (i.e. a small thermal hysteresis was observed in a cycle of heating and cooling of samples). Furthermore, the results showed that the total suction varies significantly with temperature, while matric suction changes are small. Therefore it was concluded that the greater influence of temperature on total suction is more likely due to changes in osmotic suction rather than to changes in matric suction.

7. A series of temperature-controlled single and double oedometer tests was conducted on kaolin clay samples with different initial suction values and initial void ratios. From the compression curves, the influence of initial water-content, initial void ratio and temperature on compressibility and collapse behaviour of the material were studied. The results showed that preconsolidation pressure decreased slightly with increasing temperature. It was also observed that the normal consolidation lines move in parallel towards lower stress levels (softening response) with increasing temperature. It was therefore concluded that the plastic compressibility parameter is independent of temperature. The Collapse Potential (CP) of the samples was obtained from the compression curves. The test results show that the collapse deformations obtained from the double oedometer tests are similar to those measured from single oedometer tests. From the test results, it was also observed that CP of samples decreased slightly with increasing temperature (1% reduction in max CP was observed with increasing temperature from 20 to 50°C). The results also show that the CP decreased with an increase in initial water-content and a decrease in initial void ratio of samples.
  
8. A new suction and temperature controlled oedometer cell was designed, developed and calibrated for investigating the thermo-hydro-mechanical behaviour of kaolin clay. The oedometer was used to examine the combined effects of suction and temperature on compressibility and collapse behaviour of the soil. The axis translation technique was used for imposing different matric suction values on the soil samples. Isothermal suction-controlled oedometer tests ( $s$ : 100, 300, 500 kPa) were performed at 10 and 50°C. The results of temperature and suction-controlled

oedometer tests revealed that suction results in a hardening of the soil response (suction hardening) and causes an increase in the yield stress. The results also showed softening of the soil response with increasing temperature (thermal softening). The yield stress decreased with an increase of temperature and the normal consolidation lines moved in parallel towards lower levels of stress with increasing temperature.

## **8.2 Recommendations for future works**

1. In this thesis, the drying path of SWRCs was obtained at 10 and 25°C using the axis translation technique and the filter paper method. The results obtained from both techniques were found to be very similar. The wetting path of SWRC at different temperatures has been obtained only by the filter paper method. The wetting path of SWRC should also be obtained using the axis translation technique. Therefore, it needs to be confirmed that the results of these two techniques are similar (if an appropriate filter paper calibration curve is used, giving enough time to reach suction equalisation, and precise control of temperature).
2. In order to provide a better comparison between different techniques for the measurement of suction, it is recommended to measure total and matric suction using various methods such as high suction tensiometers for matric suction measurement and thermal conductivity sensors and dew point sensors for total suction measurement. It is also recommended to measure osmotic suction using the squeezing technique. The osmotic suction of samples determined by subtracting matric suction from total suction can be compared with the osmotic suction measured using the squeezing technique.
3. In this thesis, the oedometer cell developed was only used for isothermal suction controlled tests at different temperatures. It is recommended to study non-isothermal behaviour of the material under oedometric conditions. There are only a limited number of research papers presenting data on non-isothermal behaviour of unsaturated soils (e.g. Romero et al., 2003; Uchaipichat and Khalili, 2009).

## CHAPTER 9 – REFERENCES

- Abuel-Naga H.M., 2005, *Thermo-mechanical behaviour of soft Bangkok Clay: experimental results and constitutive modelling*, Ph.D. Thesis, Asian Institute of Technology, Bangkok, Thailand.
- Agus S.S., Schanz T., 2003, *The use of a relative humidity sensor for suction measurement of compacted bentonite-sand mixtures*, Proceedings of the Symposium on Geotechnical Measurements and Modelling, Netherlands, 315–320.
- Agus S.C., Schanz T., 2005, *Discussion of paper “Free energy of water suction in filter papers” by R. Bulut and W.K. Wray*, Geotech. Test. J., **28**(4), 517-518.
- Agus S.C., 2005, *An experimental study on hydro-mechanical characteristics of compacted bentonite-sand mixtures*, Ph.D. Dissertation, Bauhaus-University Weimar.
- Agus S.S., Schanz T., Fredlund D.G., 2010, Measurements of suction versus water content for bentonite-sand mixtures. Can Geotech J., **47**, 583-594.
- Alonso E.E., Gens A., Hight D.W., 1987, *Special problem soils. General report*, Proc. 9<sup>th</sup> European Conf. Soil Mech. Dublin, **3**, 1087-1146.
- Alonso E.E., Gens A., Josa A., 1990, *A constitutive model for partially saturated soils*, Géotechnique, **40**(3), 405-430.
- Arifin Y., Schanz T., 2009, *Osmotic suction of highly plastic clays*, Acta Geotechnica, **4**(8), 177-191.
- ASTM standards 2003 D 5333, *Test method for measurement of collapse potential of soils*, Annual Book of ASTM Standards, Philadelphia.
- ASTM Standard 1997 D 5298-94, *Standard Test Method for the Measurement of Soil Potential (Suction) Using Filter Paper*, Annual Book of ASTM Standards, **4.09**, 157-162.
- Al-Tabbaa A., Wood, D.M., 1987, *Some measurements of the permeability of kaolin*, Géotechnique, **37**(4), 499-503.
- Baldi G., Hueckel T., Pellegrini R., 1998, *Thermal volume changes of mineral-water system in low-porosity clay soils*, Can Geotech J., **25**(4), 807-825.
- Bachmann J., Horton R., Grant S.A., van der Ploeg, R.R., 2002, *Temperature dependence of water retention curves for wettable and water-repellent soils*, Soil Sci. Soc. Am. J., **66**, 44-52.
- Bardanis M., Grifiza, S., 2010, *Collapse potential of a compacted weathered serpentinite from Skiros, Greece*. Proceeding of 5<sup>th</sup> International Conference on Unsaturated Soils. Barcelona, 187-192.
- Barden L., Sides G.R., 1971, *Structure of Keuper marl*, Q. JnZ Engng Geol.



- Barden L., McGown A., Collins, K., 1973, *The collapse mechanism in partially saturated soil*, Engineering Geology, **7**(1), 49-60.
- Basma A.A., Tuncer, E.R., 1992, *Evaluation and control of collapsible soils*, Journal of geotechnical engineering Division, **118**, 1491-1504.
- Bastos C.A., Gehling W.Y.Y., Bica A.D., 1998, *Some considerations about the shear strength and erodibility of unsaturated residual soils*. Proc. of 2<sup>nd</sup> International Conference on Unsaturated soils, Beijing: 19-24.
- Benatti J.C.B., Miguel M.G., Rodrigues R.A., Vilar O.M., 2010, *Collapsibility study for tropical soil profile using oedometer tests with controlled suction*. Proceeding of 5<sup>th</sup> International Conference on Unsaturated Soils, Barcelona, 543-548.
- Ben-Rhaim H., Tessier D., Pons C.H., Amara B.H., 1998, *Evolution of the microstructure of interstratified Ca-saturated clays during dehydration: SAXS and HRTEM analysis*, Clay Miner, **33**, 619-628.
- Bishop A.W., 1959, *The principle of effective stress*, Teknisk Ukeblad, **106**(39), 859-863.
- Bishop A., Donald I., 1961, *The experimental study of partly saturated soil in the triaxial apparatus*, 5<sup>th</sup> Int. Conf. on Soil Mechanics and Foundation Engineering, Paris, 13-21.
- Bishop A.W., Blight G.E., 1963, *Some Aspects of Effective Stress in Saturated and Partly Saturated Soils*, Géotechnique, **13**(3), 177-197.
- Bilotta E., Foresta V., Migliaro G., 2008, *The influence of suction on stiffness, viscosity, and collapse of some volcanic ashy soils*, Proceeding of the 1<sup>st</sup> European Conference on Unsaturated Soils, Durham, United Kingdom, 349-354.
- Bizarreta J., de Campos T.M., 2010, *Water Retention Curve and Shrinkage of a Waste from the Paper Industry*, Proceeding of 5<sup>th</sup> International Conference on Unsaturated Soils. Barcelona.
- Bradford S.A., Leij F.J., 1995, *Wettability effects on scaling two and three fluid capillary pressure-saturation relations*, Environ. Sci. Technol, **29**(6), 1446- 1455.
- Brooks R.H., Corey A.T., 1964, *Hydraulic properties of porous media: Hydrology Papers*, Colorado State University.
- Bocking A.L., Fredlund D.G., 1980, *Limitation of the axis translation technique*, Proceeding of the 4<sup>th</sup> International conference on Expansive Soil, **1**, 117-135.
- Bouazza A., Nahlawi H., Murdoch C., Alyward M., 2006, *Temperature monitoring in a green waste landfill cell*, Geoenvironmental Engineering Conference, Japan.
- Bouazza A., Abuel-Naga H.M., Gates W.P., Laloui L., 2008, *Temperature Effects on Volume Change and Hydraulic Properties of Geosynthetic Clay Liners*. The First Pan American Geosynthetics Conference & Exhibition, 102-109.

- Burghignoli A., Desideri A., Miliziano S., 2000, *A laboratory study on the thermo mechanical behaviour of clayey soils*. Can Geotech J., **37**, 764-780.
- Bulut R., Lytton R.L., Warren W.K., 2001, *Suction measurements by filter paper method*, American Society of Civil Engineers, Geotechnical Special Publication, **115**, 243-261.
- Bulut R., Wray W.K., 2005, *Free energy of water-suction in filter papers*, Geotechnical Testing Journal, **28**(4), 355-364.
- Burland J.B., 1965, *Some aspects of the mechanical behaviour of partially saturated soils*, Moisture equilibrium and moisture changes beneath covered areas, Sydney, 270-278.
- Cabarkapa Z., Cuccovillo T., Gunn M., 1999, *Some aspects of the pre-failure behaviour of unsaturated soil*, Proceedings of the Second International Conference on Pre-failure Deformation Characteristics of Geomaterials, Italy, 159-165.
- Cekerevac C., 2003, *Thermal effect on the mechanical behaviour of saturated clays: an experimental and constitutive study*, Ph.D. Thesis. EPFL, Lausanne.
- Cekerevac C., Laloui L., 2004, *Experimental study of thermal effects on the mechanical behaviour of a clay*, International Journal for Numerical and Analytical Methods in Geomechanics, **28**, 209-228.
- Chao K.C., 2007, *Design principles for foundations on expansive soils*, Ph.D. Thesis, Colorado State University.
- Chao K.C., Nelson J.D., Overton D.D, Cumbers J.M., 2008, *Soil water retention curves for remoulded expansive soils*, Proc. 1<sup>st</sup> European Conference on Unsaturated Soils, United Kingdom, 243-248.
- Chahal R.S., 1965, *Effect of temperature and trapped air on matric suction*, Soil Sci., **100**, 262-267.
- Chandler R.J., Gutierrez C.I., 1986, *The filter paper method of suction measurement*, Géotechnique, **36**(2), 265-268.
- Chandler R.J., Crilly M.S., Montgomery-Smith G., 1992, *A low-cost method of assessing clay desiccation for low-rise buildings*, Proceedings Institute of Civil Engineering, **92**, 82-89.
- Chiu C.F., Ng C.W.W., 2003, *A state-dependent elasto-plastic model for saturated and unsaturated soils*, Géotechnique, **53**(9), 809-829.
- Chu T.Y., Mou C.H., 1973, *Volume change characteristics of expansive soils determined by controlled suction testes*. Proc. 3<sup>rd</sup> Int. Conf. Exp. Soils, Haifa, 177-185.
- Clarke E.C.W., Glew D.N., 1985, *Evaluation of the thermodynamic functions for aqueous sodium-chloride from equilibrium and calorimetric measurements*, J. Phys. Chem. Ref. Data, **14**, 489-610.

- Croney D., Coleman J.D., Bridge P., 1952, *The suction of moisture held in soil and other porous materials*. Road Research Technical Paper, 24.
- Croney D., Coleman J.D., 1954, *Soil Structure in Relation to Soil Suction (pF)*, J. Soil Science, **5**(1), 75–84.
- Coleman J.D., 1962, *Stress/Strain Relations for Partly Saturated Soils*, Géotechnique, **12**(4), 348-350.
- Cui Y.J., 1993, *Etude du comportement d'un limon compacté non saturé et de sa modélisation dans un cadre élastoplastique*, Ph.D. Thesis, Ecole Nationale des Ponts et Chaussées. Paris, France.
- Cui Y.J., Delage P., 1996, *Yielding and plastic behaviour of an unsaturated compacted silt*, Géotechnique, **46**(2), 291-311.
- Cui Y.J., Sultan N., Delage P., 2000, *A thermomechanical model for saturated clays*, Can Geotech J., **37**, 607-620.
- Cuisinier O., Laloui L., 2004, *Fabric evolution during hydromechanical loading of a compacted silt*, Int. J. Numer. Anal. Meteorol., **28**(6), 483 – 499.
- Cuisinier O., Mansrouri F., 2005, *Hydro mechanical behaviour of a compacted swelling soil over a wide suction range*, Engineering Geology, **81**, 204-212.
- Cunningham M.R, 2000, *The mechanical behaviour of a reconstituted unsaturated soil*. Ph.D. Thesis, University of London (Imperial College), London, United Kingdom.
- Davis E.L., 1994, *Effect of temperature and pore size on the hydraulic properties and flow of a hydrocarbon oil in the subsurface*, Journal of Contaminant Hydrology, **16**, 55-86.
- Decagon Devices Inc., 2003, *WP4 Dewpoint PotentiaMeter Operator's Manual Version 4*, Pullman, WA, USA.
- De Gennaro V., Delage P., Priol G., Collin F., Cui Y.J., 2004, *On the collapse behaviour of oil reservoir chalk*, Géotechnique **54**(6), 415-420.
- Delage P., Lefebvre G., 1984, *Study of the structure of a sensitive Champlain clay and of its evolution during consolidation*. Can Geotech J., **21**, 21–35.
- Delage P., Suraj De Silva G., De Laure E., 1987, *Un nouvel appareil triaxial pour les sols nonsaturés*, Proceeding of the 9<sup>th</sup> European Conference on Soil Mechanics, Dublin, 25-28.
- Delage P., Audiguier M., Cui Y.J., Howatt M.D., 1996, *Microstructure of a compacted silt*, Can Geotech J., **33**, 150–158.
- Delage P., Howat M., Cui Y.J., 1998, *The relationship between suction and swelling properties in a heavily compacted unsaturated clay*, Engineering Geology, **50**(1), 31-48.

- Delage P., Cui Y.J., 2000, *L'eau dans les sols non saturés*. Éditions Techniques de l'ingénieur, Paris. Traité Construction.
- Delage P., Cui Y.J., De Laure E., 2001, *Récents développement de la technique osmotique de contrôle de succion*. 15<sup>th</sup> Int. Conference on Soil Mechanics and Geotechnical Engineering, Istanbul, 575-578.
- Delage P., Cui Y.J., Antonie P., 2005, *Geotechnical problems related with loess deposits in Northern France*. Proceeding of international conference on problematic soils. Cyprus.
- Delage P., Marcial D., Cui Y. J., Ruiz X., 2006, *Ageing effects in a compacted bentonite: a microstructure approach*, Géotechnique **56**(5), 291 – 304.
- Despax D., 1976, *Influence de la température sur les propriétés mécaniques des argiles saturées*, Ph.D. Thesis, Université de Grenoble, Grenoble.
- Diamond S., 1970, *Pore size distributions in clays*, Clay and Clay minerals, **18**, 7-23.
- Dineen K., Burland J.B., 1995, *A new approach to osmotically controlled oedometer testing*. Proceeding of the 1<sup>st</sup> International Conference on Unsaturated soils, Paris, **2**, 459-465.
- Djeran-Maigre I., Tessier D., Grundberger D., Velde B., Vasseur G., 1998, *Evolution of microstructure and of macroscopic properties of some clays during experimental compaction*, Mar Petrol Geol, **15**, 109–128.
- Elsbury B.R., Daniel D.E., Srader G.A., Anderson D.C., 1990, *Lessons learned from Compacted Clay Liner*, J. Geotechnical Engineering, ASCE, **116**(11), 1641-1660.
- El-Sohby M.A., Elleboudy A.M., 1987, *Swelling and collapsible behaviour of cemented sand upon wetting*. Proc. 9 Eur. Conf. on Soil Mechanics and Foundation Engineering, 553- 556.
- Escario V., Saez J., 1973, *Measurement of the properties of swelling and collapsing soils under controlled suction*. Proceedings of the 3rd International Conference on Expansive Soils, Haifa, 195-199.
- Escario V., Juca J.F.T., 1989, *Strength and Deformation of Partly Saturated Soils*. Proc. of 12<sup>th</sup> International Conf. on Soil Mechanics and Foundation Engineering, 43-46.
- Fawcett R.G., Collis-George N., 1967, *A filter paper method for determining the moisture characteristics of soil*, Australian Journal of Experimental Agriculture and Animal Husbandry, **7**, 162-167.
- Faybishenko B., 1983, *Effect of temperature on moisture content, entropy, and water pressure in loam soils*, Pochvovedenie, **12**, 169-172.
- Feng M., Fredlund D.G. Shuai. F., 2002, *A laboratory study of the hysteresis of a thermal conductivity soil suction sensor*. Geotechnical Testing Journal, **25**, 303-314.

- Fisher R.A., 1926, *On the capillary forces in an ideal soil; correction of formulas by W.B. Haines*, J. Agric. Sci. **16**, 492–505.
- Fleureau J.M., Hadiwardoyo S., Kheirbek-Saoud S., 2004, *Simplified approach to the behaviour of compacted soils on drying and wetting paths*, Proceeding of the third International Conference on Unsaturated Soils, Brazil, **3**, 1147-1154.
- François B., Laloui L., 2008, *A constitutive model for unsaturated soils under non-isothermal conditions*, International Journal of Numerical and Analytical Methods in Geomechanics, **32**, 1955–1988.
- François B., 2009, *Thermo-plasticity of fine-grained various saturation states: application to nuclear waste disposal*, Ph.D. Thesis, EPFL, Switzerland.
- François B., Laloui L., 2010, *An oedometer for studying combined effects of temperature and suction on soils*. Geotechnical Testing Journal, **33**(2), 112-122.
- Fredlund D.G., 1964, *Comparison of soil suction and one dimensional consolidation characteristics of a highly plastic clay*, MSc Thesis, University of Alberta, Edmonton Alta., Canada.
- Fredlund D.G., 1975. *A diffused air volume indicator for unsaturated soils*, Can Geotech J., **12**, 533 -539.
- Fredlund D.G., Morgenstern N.R., 1977, *Stress state variables for unsaturated soils*, Journal of Geotechnical Engineering Division, **103**, 447-466.
- Fredlund D.G., Morgenstem N.R., Widger R.S., 1978, *The shear strength of unsaturated soils*, Can. Geotech. J. **15**(3), 313-321.
- Fredlund D.G., 1979, *Appropriate concepts and technology for unsaturated soils*. Can. Geotech. J. **16**, 121-139.
- Fredlund D.G., 1989, *Negative pore-water pressures in slope stability*, In Simposio Sur americanode Deslizamiento, Columbia, 1-31.
- Fredlund D.G., Wong D.K.H., 1989, *Calibration of thermal conductivity sensors for measuring soil suction*. Geotechnical Testing Journal, **12**(3), 188-194.
- Fredlund D.G., Rahardjo H., 1993, Soil Mechanics for unsaturated soils. John Wille & Sons, New York.
- Fredlund D.G., Xing A., 1994, Equations for the soil water characteristic curve. Can Geotech J., **31**, 521–532.
- Fredlund D. G., Gan J. K-M., 1995, *The collapse mechanism of a soil subjected to one-dimensional loading and wetting*, Genesis and Properties of Collapsible Soils, Kluwer Academic Publishers, 173–205.
- Fredlund D.G., Vanapalli S.K., Xing A., Pufahl D.E., 1995, *Predicting the shear strength for unsaturated soils using the soil water characteristic curve*, Proc. 1<sup>st</sup> Int. Conf. Unsaturated Soils, Paris, 63-69.

- Gallipoli D., Wheeler S.J., Karstunen M., 2003, *Modelling the variation of degree of saturation in a deformable unsaturated soil*, Géotechnique, **53**(1), 105-112.
- Gallipoli D., Gens A., Vaunat, J., Romero, E., 2002, *Role of degree of saturation on the normally consolidated behaviour of unsaturated soils*, Proc. 3<sup>rd</sup> Int. Conf. Unsaturated soils, 113-120.
- Gan J.K.M, Fredlund D.G., Rahardjo H., 1988, Determination of the shear strength parameters of an unsaturated soil using the direct shear test. Can Geotech J., **25**, 500-510.
- Gardner R., 1937, *A Method of Measuring the Capillary Tension of Soil Moisture Over a Wide Moisture Range*. Soil Sci., **43**, 277-283.
- Gardner R., 1995, *Relations of temperature to moisture tension of soil*, Soil Sci., **79**, 257-265.
- Gens A., Alonso E.E., 1992, *A framework for the behaviour of unsaturated expansive clays*, Can. Geo. J., **29**, 1013-1032.
- Getman F.H, Daniels F., 1943, *Outlines of theoretical chemistry*, John Wiley and Sons, 7<sup>th</sup> edition.
- Georgiadis K., 2003, *Development, implementation and application of partially saturated soil models in finite element analysis*, Ph.D. Thesis, University of London, Imperial College, United Kingdom.
- Graham J., Tanaka N., Crilly T. Alfaro M., 2001, *Modified Cam-Clay modelling of temperature effects in clays*. Can Geotech J., **38**, 608-621.
- Grant S.A., Salehzadeh A., 1996, *Calculation of temperature effects on wetting coefficients of porous solids and their capillary pressure functions*, Water Resour. Res., **32**(2), 261-70.
- Grant S.A., Bachmann J., 2002, *Effect of temperature on capillary pressure*. In *Heat and Mass Transfer in the Natural Environment*, Geophysical Monograph 129.
- Gourley C.S., Schreiner H.D., 1995, *Field measurement of soil suction*, Proceeding of the first International Conference on Unsaturated Soils, Paris, **2**, 601-607.
- Haghighi A., Medero G., Woodward P., Laloui, L., 2010, *Effect of temperature on collapse potential of kaolin clay*, Proceeding of 5<sup>th</sup> International Conference on Unsaturated Soils, Barcelona, 543-548.
- Haghighi A., Medero G., Marinho F.A.M., Woodward P., 2011, *Discussion of "Measurements of suction versus water content for bentonite-sand mixture"*, Can Geotech J., **48**(2), 336-337.
- Haghighi A., Medero G., Marinho F.A.M., Mercier B., Woodward P., 2012, *Temperatures effects on suction measurement using filter paper technique*. ASTM Geotechnical Testing Journal, in press.

- Haines W.B., 1923, *The volume changes associated with variations of water content in soil*. Journal of Agricultural Science, **13**, 296-311.
- He L., 1999, *Evaluation of instruments for measurement of suction in unsaturated soils*, MEng Thesis, Nanyang Technological University.
- Hetzel F., Tessier D., Jaunet A.M., Doner H., 1994, *The microstructure of three Na Smectites: The importance of particle geometry on dehydration and rehydration*, Clays Clay Miner, **42**(1), 242-248.
- Hilf J.W., 1956, *An investigation of pore water pressure in compacted cohesive soils*, Technical Memo 654, Denver, Bureau of Reclamation.
- Hillel D., 1998, *Environmental Soil Physics*, Academic Press, London.
- Hird C.C., Srisakthivel S., 2005, *Laboratory investigation of permeability measurement in clay using outflow from unsupported cavities*, Géotechnique, **55**(5), 393-402.
- Hueckel T., Pellegrini R., 1989, *Modelling of thermal failure of saturated clays*, International Symposium on Numerical Models in Geomechanics – NUMOG, 81-90.
- Hueckel T., Pellegrini R., Del Olmo C., 1998, *A constitutive study of thermo-elasto plasticity of deep carbonatic clays*, International Journal of Numerical and Analytical Methods in Geomechanics, **22**, 549-574.
- Hong H.Q., Hu L.M., 2007, *Experimental Study of Electro-Osmosis by Reversing Polarity in Kaolin Clay*, The 1st Sri Lankan Geotechnical Society (SLGS) International Conference on Soil and Rock Engineering, Colombo.
- Houston S.L., Houston W.N., Wagner A.M., 1994, *Laboratory filter paper suction measurements*, Geotechnical Testing Journal, **17**(2), 185-194.
- Hopmans J.W., Dane J.H., 1986, *Temperature dependence of soil hydraulic properties*, Soil Sci. Soc. Am. J., **50**, 4-9.
- Infante Sedano J.A., Vanapalli S.K., Garga V.K., 2007, *Modified ring shear apparatus for unsaturated soils testing*, Geotechnical Testing Journal, **30**(1), 39-47.
- Iyer B., 1990, *Pore water extraction-comparison of saturation extract and high-pressure squeezing*, In: Hoddinott KB, Lamb RO (eds.) Physico-chemical aspects of soil related materials. ASTM STP 1095, Philadelphia, 159-170.
- Jennings J.E., Knight K., 1957, *The additional settlement of foundations due to a collapse of structure of sandy sub-soils on wetting*, Proceeding of International conference on Soil Mechanics and Foundation Engineering. London, 316-319.
- Jennings J.E., Burland J.B., 1962, *Limitations to the use of effective stresses in partly saturated soils*, Géotechnique, **12**(2), 125-144.
- Jennings J.E., Knight K., 1975, *A guide to construction on or with materials exhibiting additional settlement due to collapse of grain structure*, Proc. Regional Conf. for Africa on Soil Mechanics & Foundation Engineering, Rotterdam, 99-105.

Jiang P., Hwang K.S., Mittleman D.M., Bertone J.F. Colvin V.L., 1999, *Template-directed preparation of macroporous polymers with oriented and crystalline arrays of voids*, J. Am. Chem. Soc. **121**, 11630-11637.

Johnston L.N., 1942, *Water permeable thermal radiators as indicators of field capacity and permanent wilting percentage in soils*, Soil Sci., **45**, 123-126.

Josa A., Alonso E.E., Gens A., Lloret A., 1987, *Stress-strain behaviour of partially saturated soils*. Proc. 9 Eur. Conf. Soil Mech. and Found. Eng., 561-564.

Jotisankasa A., Ridley A., Coop M., 2007, *Collapse behaviour of compacted silty clay in suction monitored oedometer apparatus*, J. of Geotechnical and Geoenvironmental Engineering, **133**(7), 867-886.

Jury W.A., Miller E.E., 1974, *Measurement of the transport coefficients for coupled flow of heat and moisture in a medium sand*, Soil Sci. Soc. Am. Proc. **38**, 551-557.

Kassiff G. and Ben Shalom A., 1971, *Experimental relationship between swell pressure and suction*, Géotechnique, **21**, 245-255.

Kawai K., Karube D., Kato S., 2005, *The model of water retention curve considering effects of void ratio*, Proceedings of Asian conference on unsaturated soils, Rotterdam, 329-334.

Kayadelen C., 2008, *The consolidation characteristics of an unsaturated compacted soil*, Environ. Geol. **54**, 325-334.

Khalili N., Khabbaz M.H., 1998, *A Unique Relationship for the Determination of the Shear Strength of Unsaturated Soils*, Géotechnique, **48**, 1-7.

Khoury C., Miller G., 2010, *Effect of Suction Hysteresis on the Shear Strength of Unsaturated Soil Interfaces*, Proceedings of the Fifth International Conference on Unsaturated Soils, Barcelona, 283-288.

Kuntiwattanakul P., Towhata I., Ohishi K., Seko I., 1995, *Temperature effects on undrained shear characteristics of clay*, Soils and Foundations, **35**(1), 147-162.

Knapp R.T., Daily J.W., 1970, *Cavitation*. McGraw-Hill, New York.

Krahn R.L., Fredlund D.G., 1972, *On total, matric and osmotic suction*, Soil Science, **114**, 339-348.

Laloui L., Cekerevac C., 2003, *Thermo-plasticity of clays: an isotropic yield mechanism*, Computer and Géotechnique, **30**, 649-660.

Lamande M., Hallaire V., Curmi P., Peres G., Cluzeau D., 2003, *Changes of pore morphology, infiltration and earthworm community in a loamy soil under different agricultural managements*. Catena, **54**, 637-649.

Lawton E.C., Frigaszy R.J., Hardcastle J.H., 1989, *Collapse of compacted clayey sand*, Journal of Geotechnical Engineering, **115**, 1252-1267.



- Lawton E.C., Fragaszy R.J., Hetherington M.D., 1992, *Review of Wetting-Induced Collapse in Compacted Soil*, Journal of Geotechnical Engineering, **118**(9), 1376-1393.
- Lee R.K.C., Fredlund D.G., 1984, *Measurement of soil suction using the MCS 6000 gauge*, In Proceedings of the 5th International Conference on Expansive Soils, Institution of Engineers, Adelaide, Australia, 50-54.
- Leong E.C., He L., Rahardjo H., 2002, *Factors affecting the filter paper method for total and matric suction measurements*, Geotechnical Testing Journal, **25**(3), 322-333.
- Leong E.C., Tripathy S., Rahardjo R., 2003, *Total suction measurement of unsaturated soils with device using the chilled mirror dew-point technique*, Géotechnique, **53**(2), 173-182.
- Likos W.J., Lu N., 2002, *Filter paper technique for measuring total soil suction*, Transportation Research Record: Journal of the Transportation Research Board, Washington, D.C., 120-128.
- Lim Y.Y., Miller G.A., 2004, *Wetting-Induced compression of compacted Oklahoma soils*, Journal of Geotechnical and Geoenvironmental Engineering, **130**(10), 1014-1023.
- Liu H.H., Dane J.H., 1993, *Reconciliation between measured and theoretical temperature effects on soil water retention curves*, Soil Sci. Soc. Am. J., **57**, 1202-1207.
- Lloret A., Alonso E.E., 1985, *State surfaces for partially saturated soils*, Proc. 11<sup>th</sup> Int. Conf. Soil Mech., San Francisco, 557-562.
- Lloret A., Villar M.V., Sanchez M., Gens A., Pintado X., Alonso, E.E., 2003, *Mechanical behaviour of heavily compacted bentonite under high suction changes*. Géotechnique, **53**(1), 27-40.
- Lourenco S.D.N., Gallipoli D., Toll D., Evans F., Medero G., 2007, *Determination of the soil water retention curve with tensiometers*, In Experimental unsaturated soil mechanics (ed. T. Schanz), 95-102.
- Lourenco S.D.N., Gallipoli D., Toll D., Evans F., Medero G., 2008, *Calibrations of a high-suction tensiometer*. Géotechnique, **58**(8), 659-668.
- Lu N., Likos W., 2004, *Unsaturated soil mechanics*. John Wiley & Sons, New York.
- Maatouk A., Leroueil S., Rochelle P.L.A., 1995, *Yielding and critical state of a collapsible unsaturated silty soil*. Géotechnique, **45**(3), 465-477.
- Marinho F.A.M., 1994a, *Shrinkage behaviour of some Plastic soils*, Ph.D. Thesis, Imperial College, University of London, United Kingdom.
- Marinho F.A.M., 1994b, *Medicao de succao com o methodo do papel filtro*, Proceedings Congresso Brasileiro de Mecanica do solos e Engenharia de Fundacoes, **2**, 516- 522.

- Marinho F.A.M., Chandler R.J., 1995, *Cavitation and the direct measurement of soil suction*, Proceedings of the First International Conference on Unsaturated Soils, Paris, 623-629.
- Marinho F.A.M., Chandler R.J., Crilly M.S., 1995, *Stiffness measurements on unsaturated high plasticity clay using bender elements*, Proceedings of the First International Conference on Unsaturated Soils, Paris, 535-539.
- Marinho F.A.M., Oliveira M., 2005, *The filter paper method revisited*, Geotech. Test. J., **29**(3), 250-258.
- Marinho F.A.M., Take A., Tarantino A., 2008, *Measurement of Matric Suction using Tensiometric and Axis Translation Techniques*, Geotech Geol Eng, **26**(6), 615-631.
- Matyas E.L., Radhakrishna H.S., 1968, *Volume Change Characteristics of Partially Saturated Soils*, Géotechnique, **18**(4), 432-448.
- Medero G.M., Schnaid F., Gehling W.Y.Y., Gallipoli D., 2003, *Analysis of the mechanical response of an artificial collapsible soil*, Proc. From Experimental Evidence towards Numerical Modelling of Unsaturated Soils, Berlin, 135-145.
- Medero G.M., Schnaid F., Gehling, W.Y.Y., 2009, *Oedometer behaviour of an artificial cemented highly collapsible soil*, J. of Geotechnical and Geoenvironmental Engineering, **135**(6), 840-843.
- McKee C.R., Bumb A.C., 1984, *The importance of unsaturated flow parameters in designing a hazardous waste site*, In Hazardous Waste and Environmental Emergencies, Hazardous Materials Control Research Institute National Conference, Houston, Tex, 50-58.
- McQueen, I.S. and Miller, R.F., 1974, Approximating soil moisture characteristics from limited data: Empirical evidence and tentative model. Water Resources Research, 10(3): 521-527.
- Mendes J., Gallipoli D., Toll D., Augarde C.E., Evans F.D., 2008, *A system for field measurement of suctions using high capacity tensiometers*, Advances in Geo-Engineering (eds. Toll D.G., Augarde C.E., Gallipoli D. & Wheeler S.J.), 219-225.
- Mitchell J.K., 1993, *Fundamentals of soil behaviour*, John Wiley & Sons, Inc, New Jersey.
- Mohamed T.A., Faisal H.A., Hashim S., Bujang B.K.H., 2006, *Relationship between shear strength and soil water characteristic curve of an unsaturated granitic residual soil*, American Journal of Environmental Sciences, **2**(4), 142-145.
- Monroy R., 2005, *The Influence of Load and Suction Changes on the Volumetric Behaviour of Compacted London Clay*. Ph.D. Thesis, Imperial College London.
- Monroy R., Ridley A., Dineen K., Zdravkovic L., 2007, *The suitability of osmotic technique for the long term testing of partially saturated soils*, Geotechnical Testing Journal, **30**(3), 220-226.

- Monroy R., Zdravkovic L., Ridley A., 2010, *Evolution of microstructure in compacted London Clay during wetting and loading*, Géotechnique, **60**, 105-119.
- Mualem Y., 1974, *A conceptual model of hysteresis*, Water Resour. Res., **10**, 514-520.
- Mualem Y., 1977, *Extension of the similarity hypothesis used for modelling the soil water characteristics*, Water Resour. Res., **13**(4), 773-780.
- Mualem Y., 1984, *Prediction of the soil boundary wetting curve*. Water Resour. Res., **137**(6), 370-392.
- Multon J.L., Bizot H., Martin G., 1991, *Mesure de l'eau absorbée dans les aliments*, In Techniques d'analyse et de contrôle dans les industries agro-alimentaires. Paris, 1-63.
- Muñoz J.J., 2006, *Thermo-Hydro-Mechanical analysis of soft rock*, PhD. Thesis, Universitat Polytechnic de Catalunya, Barcelona.
- Myers D., 1991, *Surfaces, Interfaces, and Colloids. Principles and Applications*, VCH Publisher Inc., USA.
- Ng C.W.W., Pang, Y.W., 2000, *Influence of stress on soil-water characteristics and slope stability*, Journal of Geotechnical and Geoenvironmental Engineering, **126**(2), 157-166.
- Ng C.W.W., Chiu C.F., Rahardjo H., 2000, *Laboratory study of loosely compacted unsaturated volcanic fill*. In Unsaturated soils for Asia (eds. H. Rahardjo, D. G. Toll and E. C. Leong), Rotterdam, 551-556.
- Nichol C., Smith L. Beckie R., 2003, *Long-term measurement of matric suction using thermal conductivity sensors*, Can Geotech J., **40**, 587-597.
- Nishimura T., Fredlund D.G., 2002, *Hysteresis effects resulting from drying and wetting under relatively dry conditions*, Proceedings of the third International Conference on Unsaturated Soils, Brazil, 301-306.
- Nimmo J.R., Miller E.E., 1986, *The temperature dependence of isothermal moisture vs. potential characteristics of soils*, Soil Sci. Soc. Am. J., **50**, 1105-1113.
- Nuth M., Laloui L., 2007, *New insight into the unified hydro-mechanical constitutive modelling of unsaturated soils*, 3<sup>rd</sup> Asian Conference on Unsaturated Soils, Nanjing, China, 109-125.
- Prashant A., Penumadu D., 2007, *Effect of microfabric on mechanical behaviour of kaolin clay using cubical true triaxial testing*, Journal of Geotechnical and Geoenvironmental Engineering, **133**(4), 433-444.
- Patrick P., Olsen H., Higgins J., 2007, *Comparison of chilled-mirror measurements and filter paper estimates of total soil suction*, Geotechnical Testing Journal, **30**(5), 1-8.
- Peck A.J., 1960, *Change of moisture tension with temperature and air pressure*, Soil Sci. **89**, 303-310.

- Pereira J.H.F., Fredlund D.G., 2000, *Volume change behaviour of collapsible compacted gneiss soil*, Journal of Geotechnical and Geoenvironmental Engineering, **126**(10), 907–916.
- Pereira J.M., Coussy O., Alonso E., Vaunat J., Olivella S., 2010, *Is the Degree of Saturation a Good Candidate for Bishop's  $\chi$  Parameter*, Proceeding of 5<sup>th</sup> International Conference on Unsaturated Soils, Barcelona.
- Peroni N., Tarantino A., 2005, *Measurement of osmotic suction using the squeezing technique*, From Experimental Evidence towards Numerical Modelling of Unsaturated Soil, Springer Proceedings in Physics, Berlin, 159-168.
- Petry T.M., Jiang C.P., 2003, *Evaluation and Utilization of the WP4 Dewpoint Potential Meter Phase I and II*, United States.
- Phene C.J., Hoffmann G.J., Rawlins S.L., 1971, *Measuring soil matric potential in situ by sensing heat dissipation with a porous body: theory and sensor construction*, In Proceedings of Soil Science Society of America, **35**, 27-32.
- Philip J.R., de Vries D.A., 1957, *Moisture movement in porous media under temperature gradients*, American Geophysical Union, **38**(2), 222-232.
- Picornell M., Lytton R.L., Steinberg M., 1983, *Matrix suction instrumentation of a vertical moisture barrier*, Transportation Research Record, **945**, 16-21.
- Poston S.W., Ysrael S., Hossain A.K.M.S., Montgomery E.F., Ramey H.J., 1970, *The effect of temperature on irreducible water saturation and relative permeability of unconsolidated sands*, SPEY, 171-180.
- Pusch R., Schomburg J., 1999, *Impact of microstructure on the hydraulic conductivity of undisturbed and artificially prepared smectite clay*, Eng Geol, **54**, 167–172.
- Plum L., Esrig M.I., 1969, *Some temperature effects on soil compressibility and pore water pressure*, Special report, Report 103, Highway Research Board, Washington.
- Prapaharan S., Altschaeffl A.G., Dempsey B.J., 1985, *Moisture curve of a compacted clay: mercury intrusion method*, J Geotech Eng ASCE, **111**(9), 1139–1143.
- Prashant A., Penumadu D., 2007, *Effect of microfabric on mechanical behaviour of kaolin clay using cubical true triaxial testing*, Journal of Geotechnical and Geoenvironmental Engineering, **133**(4), 433-444.
- Rampino C., Mancuso C., Vinale F., 1999, *Laboratory testing on an unsaturated soil: equipment, procedures, and first experimental results*. Can Geotech J., **36**(1), 1-12.
- Rampino C., Mancuso C., Vinale F., 2000, *Experimental behaviour and modelling of an unsaturated compacted soil*. Can Geotech J., **37**, 748-763.
- Rao S.M., Revanasiddappa K., 2003, *Role of soil structure and matric suction in collapse of a compacted clay soil*, Journal of Geotechnical Testing, **26**, 102-110.

- Rao S.M., Revanasiddappa K., 2005, *Role of microfabric in matrix suction of residual soils*, Engineering Geology, **80**, 60-70.
- Raudkivi A.J., Hutchison D.L., 1974, *Erosion of Kaolinite Clay by flowing water*, Proceedings Royal Society, London, England, 537-544.
- Ridley A.M., 1993, *The measurement of soil moisture suction*, PhD. Thesis. Imperial College, University of London.
- Ridley A.M., Burland W.K., 1993, *A new instrument for the measurement of soil moisture suction*, Géotechnique, **43**(2), 321-32.
- Ridley A.M., Dineen K., Burland J.B., Vaughan P.R., 2003, *Soil matrix suction: some examples of its measurement and application in geotechnical engineering*, Géotechnique, **53**(2), 241-253.
- Rogers C.D.F., 1995, *Types and distribution of collapsible soils*, Proceedings of the NATO Advanced Research Workshop on Genesis and Properties of Collapsible Soils, United Kingdom, 1-17.
- Romero E., 1999, *Characterisation and thermo-hydromechanical behaviour of unsaturated Boom-clay: An experimental study*. PhD. Thesis, Universitat Polytechnic de Catalunya, Barcelona.
- Romero E., Gens A., Lloret A., 2001, Temperature effects on the hydraulic behaviour of an unsaturated clay, Geotechnical and Geological Engineering, **19**, 311-332.
- Romero E., Gens A., Lloret A., 2003, *Suction effects on a compacted clay under non-isothermal conditions*, Géotechnique, **53**(1), 65-81.
- Romero E., Li X.L., 2005, *Thermo-hydro-mechanical tests using vapour and liquid transfer on a clay-based mixture*, Advance Experimental Unsaturated Soil Mechanics, London, 483- 488.
- Romero E., Villar M.V., Lloret A., 2005, *Thermo-hydro-mechanical behaviour of two heavily over consolidated clays*, Engineering Geology, **81**(3), 255-268.
- Romero E., Simms, P.H., 2008, *Microstructure Investigation in Unsaturated Soils: A Review with Special Attention to Contribution of Mercury Intrusion Porosimetry and Environmental Scanning Electron Microscopy*. Geotech Geol Eng, **26**(6), 705-727.
- Romero E., Della Vecchia G., Jommi, C., 2011, *An insight into the water retention properties of compacted clayey soils*. Géotechnique, **61**(4), 313-328.
- Rowe R.K., 2005, *Long term performance of contaminant barrier systems*, Géotechnique, **55**(9): 631-678.
- Sacchi E., Michelot J.L., Pitsch H., Lalieux P., Aranyossy J.F., 2001, *Extraction of water and solutes from argillaceous rocks for geochemical characterisation: methods, processes, and current understanding*, Hydrogeol Journal, **9**, 17-33.

- Sachan A., and Penumadu D., 2007, *Effect of Microfabric on shear behaviour of Kaolin clay*, J. of Geotechnical and Geoenvironmental Engineering, **133**(3), 306 – 318.
- Salager S., Jamin F., El Youssoufi M.S., Saix C., 2006, *Influence de la température sur la courbe de rétention d'eau de milieux poreux*, Compte Rendu de Mécanique, **334**, 393-398.
- Sattler P., Fredlund D.G., 1989, *Use of thermal conductivity sensors to measure matric suction in the laboratory*, Can. Geo. J., **26**, 491-498.
- Salager S., El Youssoufi M.S., Saix C., 2007, *Experimental study of the water retention curve as a function of void ratio*. ASCE Geotechnical special publication.
- Schneider A., 1960, *Neue Diagramme zur Bestimmung der relativen Luftfeuchtigkeit über gesättigten wässerigen Salzlösungen und wässerigen Schwefelsäurelösungen bei verschiedenen Temperaturen*, Holz als Roh- und Werkstoff, **18**, 269–272.
- Seed H.B., Chan C.K., 1995, *Structure and Strength Characteristics of Compacted Clays*, J. Soil Mechanics and Foundation Division ASCE, **85**(5), 87-128.
- Sillers W.S., Fredlund D.G., 2001, *Statistical assessment of soil-water characteristic curve models for geotechnical engineering*. Can Geotech J., **38**(6), 1297-1313.
- Sivakumar V., 1993, *A critical state framework for unsaturated soil*, Ph.D. Thesis, University of Sheffield, United Kingdom.
- Shaw B., Baver L.D., 1939, *An electro thermal method for following moisture changes of the soil institute*, In Proceedings of Soil Science Society of America, **4**, 78-83.
- She H.Y., Sleep B., 1998, *The effect of temperature on capillary pressure-saturation relationships for air-water and tetrachloroethylene-water systems*, Water Resour. Res., **34**, 2587-2597.
- Shuai F., Clements C., Ryland L., Fredlund D.G., 2002, *Some factors that influence soil suction measurement using a thermal conductivity sensor*, Third International Conference on Unsaturated soils, Brazil, 325-329.
- Simms P.H., Yanful E.K., 2001, *Measurement and estimation of pore shrinkage and pore distribution in a clayey till during soil-water characteristic curve tests*, Can. Geotech. J., **38**(4), 741 – 754.
- Sultan N., Delage P., Cui Y.J., 2002, *Temperature effects on the volume change behaviour of Boom clay*, Engineering Geology, **64**, 135–145.
- Sun D.A., Matsuoka H., Xu Y.F., 2004, *Collapse behaviour of compacted clays in suction-controlled triaxial tests*. Geotechnical Testing Journal, **27**, 362-370.
- Taibi S., Ghembaza M., Fleureau J., 2005, *On the suction control techniques in studying the THM behaviour of unsaturated soils*, Int. Symposium: Advanced Experimental Unsaturated Soils Mechanics, Trento, Italy, 69-75.

- Take W.A., Bolton M.D., 2003, *Tensiometer saturation and the reliable measurement of soil suction*, *Géotechnique*, **53**(2), 159 - 172.
- Tarantino A., Mongiovi L., 2001, *Experimental procedures and cavitation mechanisms in tensiometer measurements*. In *Unsaturated soil concepts and their application in geotechnical practice*, 189–210.
- Tarantino A., Mongiovi L., 2003, *Calibration of tensiometer for direct measurement of matric suction*, *Géotechnique*, **53**(1), 137–141.
- Tarantino A., Tombolato S., 2005, *Coupling of hydraulic and mechanical behaviour in unsaturated compacted clay*, *Géotechnique*, **55**(4), 307–317.
- Tarantino A., De Col E., 2008, *Compaction behaviour of clay*. *Géotechnique*, **58**(3), 199–213.
- Tanaka N., Graham J., Crilly T., 1997, *Stress-strain behaviour of reconstituted illitic clay at different temperatures*, *Engineering Geology*, **47**, 339–350.
- Tang A.M., Cui Y.J., 2005, *Controlling suction by the vapour equilibrium technique at different temperatures and its application in determining the water retention properties of MX80 clay*. *Can Geotech J.*, **42**(1), 287–296.
- Tang A.M., Cui Y.J., Barnel N., 2008, *Thermo-mechanical behaviour of a compacted swelling clay*, *Géotechnique*, **58**(1), 45–54.
- Terzaghi K., 1936, *The shearing resistance of saturated soils*, *Proc. 1st Int. Conf. on Soil Mechanics*, Cambridge, 54–56.
- Tessier D., 1984, *Étude expérimentale de l'organisation des matériaux argileux: hydratation, gonflement et structuration au cours de la dessiccation et de la réhumectation*. Ph.D. Thesis, Université de Paris VII, Paris, France.
- Thom R., Sivakumar R., Sivakumar V., Murray E.J., Mackinnon P., 2007. *Pore size distribution of unsaturated compacted kaolin: the initial states and final states following saturation*, *Géotechnique*, **57**(5), 469–474.
- Thakur V.K.S., Sreedeeep S., Singh D.N., 2006, *Laboratory investigations on extremely high suction measurements for fine-grained soils*, *Geotechnical and Geological Engineering*, **24**(3), 565–578.
- Toker N., Germaine J., Sjoblom K., Culligan P. 2004, *A new technique for rapid measurement of continuous soil moisture characteristic curves*, *Géotechnique*, **54**(3), 179–186.
- Toll D.G., 1990, *A framework for unsaturated soil behaviour*. *Géotechnique*, **40**(1), 31–44.
- Toll D.G., Ong B.H., 2003, *Critical-state parameters for an unsaturated residual sandy clay*. *Géotechnique*, **53**(1), 93–103.

- Thu T.M., Rahardjo H., Leong, E.C., 2006, *Effects of Hysteresis on Shear Strength Envelopes from Constant Water Content and Consolidated Drained Triaxial Tests*, Proceedings of the Fourth International Conference on Unsaturated Soils, Arizona, 1212-1222.
- Oberg A., Salfours G., 1997, *Determination of shear strength parameters of unsaturated silts and sands based on the water retention curve*. Geotechnical Testing Journal, **20**, 40-48.
- Olchitzky E., 2002, *Couplage hydromécanique et perméabilité d'une argile gonflante non saturée sous sollicitations hydriques et thermiques*, Courbe de sorption et perméabilité à l'eau, Ph.D. Thesis, École nationale des ponts et chaussées, Paris, France.
- Uchaipichat A., Khalili N., 2009, *Experimental investigation of thermo-hydro-mechanical behavior of an unsaturated silt*, Géotechnique, **59**(4), 339-353.
- van der Raadt P., Fredlund D.G., Clifton A.W., Klassen M.J., 1987, *Soil suction measurement at several silts in western Canada*, Transportation Res. Rec., **1137**, 24-35.
- van Genuchten M.Th., 1980, *A closed-form equation for predicting the hydraulic conductivity of unsaturated soils*, Soil Science Society of America Journal, **44**, 892-898.
- van Olphen, H., 1977, *An Introduction to Clay Colloid Chemistry*, 2nd ed. Wiley Interscience, New York.
- Vanapalli S.K., Fredlund D.G., Pufhal D.E., Clifton A.W., 1996, Model for the prediction of shear strength with respect to soil suction. Can Geotech J., **33**, 379-392.
- Vanapalli S.K., Fredlund D.G., 1997, *Interpretation of undrained shear strength of unsaturated soils in terms of stress state variables*. 3<sup>rd</sup> Brazilian Symposium on Unsaturated Soils, Brazil, 35-45.
- Vanapalli S.K., Sillers W.S., Fredlund M.D., 1998, *The meaning and relevance of residual state to unsaturated soils*, Proceedings of the Canadian Geotechnical Conference. Alberta.
- Vanapalli S.K., Fredlund D.G., Pufhal D.E., 1999, *The influence of soil structure and stress history on the soil-water characteristics of a compacted till*, Géotechnique, **49**(2), 143-159.
- Villar M.V., 2000, *Caracterización termo-hidro-mecánica de una bentonita de Cabo de Gata*, Ph.D. Thesis, Universidad Complutense de Madrid, Madrid, Spain.
- Villar M.V., Lloret A., 2004, *Influence of temperature on the hydro-mechanical behaviour of a compacted bentonite*, Engineering Geology, **26**, 337-350.
- Villar M.V., Gomez-Espina R., 2008, *Effect of temperature on the water retention capacity of FEBEX and MX-80 bentonites*, Proceeding of 5<sup>th</sup> International Conference on Unsaturated Soils, Barcelona, 257-262.
- Villar O.M., Rodrigues R.A., 2011, *Collapse behaviour of soil in a Brazilian region affected by a rising water table*, Can Geotech J., **48**, 226-233.



- Walker S.C., Gallipoli D., Toll, D.G., 2005, *The effect of structure on the water retention of soil tested using different methods of suction measurement*, Proceeding of International symposium on Advance Experimental Unsaturated soil Mechanics, London, 33-39.
- Westermarck S., 2000, *Use of Mercury Porosimetry and Nitrogen Adsorption in Characterisation of the Pore Structure of Mannitol and Microcrystalline Cellulose Powders, Granules and Tablets*. Ph.D. Thesis, Finland: University of Helsinki.
- Wheeler S.J., Karube D., 1995, *Constitutive modelling*, Proceedings of the First International Conference on Unsaturated Soils, Paris, 1323-1350.
- Wheeler S.J., Sivakumar V., 1995, *An elasto-plastic critical state framework for unsaturated soil*, Géotechnique, **45**(1), 35-53.
- Wheeler S.J., Sivakumar, V., 2000, *Influence of compaction procedure on the mechanical behaviour of an unsaturated compacted clay. Part 2: shearing and constitutive modelling*. Géotechnique, **50**(4), 369-376.
- Wheeler S.J., Sharma R.J., Buisson M.S.R., 2003, *Coupling of hydraulic hysteresis and stress-strain behaviour in unsaturated soils*, Géotechnique, **53**(1), 41-54.
- Yesiller N., Hanson J.L., Liu, W.L. 2005. *Heat generation in municipal solid waste landfills*, Journal of Geotechnical and Geoenvironmental Engineering, **131**(11), 1330-1344.
- Yong R.N., Japp R.D., How G., 1971, *Shear strength of partially saturated clays*. Proc. 4<sup>th</sup> Asian Reg. Conf., Bangkok, 183:187.
- Zhou J., Yu J., 2005, *Influences affecting the soil-water characteristics curve*, Journal of Zhejiang University Science, **8**, 797-804.